Etude de la chimie de la fonctionnalisation de l'oxyde de graphène pour concevoir des matériaux à base de l'oxyde de graphène pour des applications antibactériennes

Alexis Pineiro Garcia

PSL UNIVERSITÉ PARIS

THÈSE DE DOCTORAT
DE L'UNIVERSITÉ PSL

Préparée à l'École Nationale Supérieure de Chimie de Paris
Dans le cadre d'une cotutelle avec Instituto Tecnológico de Celaya

Etude de la chimie de la fonctionnalisation de l'oxyde de graphène pour concevoir des matériaux à base de l'oxyde de graphène pour des applications antibactériennes

Study of the chemistry of graphene oxide functionalization to design graphene-based materials for antibacterial applications

Soutenue par
Alexis PIÑEIRO GARCIA
Le 10 02 2021

Ecole doctorale n° 406
Chimie Moléculaire de Paris-Centre

Spécialité
Chimie Moléculaire

Composition du jury :

M. Arturo JIMÉNEZ GUTIÉRREZ Pr, Instituto Tecnológico de Celaya	*Président et rapporteur*
M. Jean-François NIERENGARTEN DR, Université de Strasbourg	*Rapporteur*
Mme Geraldine CARROT Pr, CEA/ Université de Saclay	*Examinatrice*
Mme Anouk GALTAYRIES MdC, Chimie ParisTech/PSL	*Examinatrice*
Mme Cristina CORONADO VELASCO Pr, Instituto Tecnológico de Celaya	*Examinatrice*
M. Ferdinando TRISTÁN LÓPEZ Pr, Instituto Tecnológico de Celaya	*Co-encadrant*
M. Vincent SEMETEY CR, Chimie ParisTech	*Directeur de thèse*
Mme Sofía Magdalena VEGA DÍAZ Pr, Instituto Tecnológico de Celaya	*Co-directrice de thèse*

Chimie Paris ParisTech | PSL

Dédicace

Con todo mi cariño a mi familia:
Fernando Piñeiro Hernández
Gissel García Hernández
Ángel Fernando Piñeiro García
Han sido mi motivación más grande para alcanzar mis sueños.
A ustedes siempre mi agradecimiento y mi amor

Remerciements

First of all, I would like to express my sincere gratitude to my supervisors Professors Sofía Magdalena VEGA-DIAZ and Vincent SEMETEY for their enthusiasm for the project, for their support, encouragement, patience, and guidance during my PhD studies. I would like also to thank to Professor Ferdinando TRISTÁN which encouragement, patience, and guidance helped in the most difficult moments.

I would like to thank to all the people behind this cotutelle, Dr. Cristina CORONADO, Dr. Sofía Magdalena VEGA-DIAZ, Dr. Ferdinando TRISTÁN, Dr. Vincent SEMETEY and Dr. Fethi Bedioui, without their support this cotutelle could not be possible.

I would like to thank to my collaborators in Mexico and France, Dr. David Meses-Rodríguez, Dr. Galdis Judith Labrada-Delgado, Dr. Grégory Lefèvre, many thanks to them which participation in this dissertation enabled us the publications of research articles.

I would like to thank to CONACYT (465629), to the Centre National de la Recherche Scientifique (CNRS) and the Institut de Recherche de Chimie Paris (IRCP) for their financial support during the development of this thesis, and for the visiting research student scholarship at École Nationale Supérieure de Chimie de Paris

To conclude, I cannot forget to thank my family and friends in both sides Mexico and France for all the unconditional support during this wonderful adventure.

Table of Contents

Chapter 4: Graphene Oxide and the Chemical Functionalization by Thiol-ene Michael Addition Reaction

Chapter 5: Quantifying the Functional Groups of Graphene Oxide by Fluorescent Labelling

Chapter 6: Developing Multi- Functional Graphene Oxide Materials For Antibacterial Applications

LIST OF ACRONYMS

AMR	Review on Antimicrobial Resistance
ATR-FTIR	Attenuated total reflectance Fourier-transform infrared spectroscopy
BDE	Bond dissociation energy
DBU	1,8-diazabicyclo[5.4.0]undec-7-ene
DIPEA	*N,N*-Diisopropylethylamine
GL	Graphene Layer
GO	Graphene Oxide
GrO	Graphite Oxide
GO **1**	Graphene oxide functionalized with NHBoc
GO-B	Graphene oxide blanks
GO-CA	Graphene Oxide functionalization with CA in absence of PI
GO-CA-PI	Graphene Oxide functionalized with CA adding PI
GO-DBU	GO functionalized with CA by TEMA adding DBU
GO-DIPEA	GO functionalized with CA by TEMA adding DIPEA
GO-G100	Graphene Oxide functionalization with glycine in GO:G mass ratio 1:1
GO-G150	Graphene Oxide functionalization with glycine in GO:G mass ratio 1:1.5
GO-G200	Graphene Oxide functionalization with glycine in GO:G mass ratio 1:2
GO-G25	Graphene Oxide functionalization with glycine in GO:G mass ratio 1:0.25
GO-G50	Graphene Oxide functionalization with glycine in GO:G mass ratio 1:0.5
GO-LC	Graphene Oxide functionalized with L-cysteine adding PI
GO-MEDA	Graphene Oxide functionalized with MEDA
GO-NEt_3	GO functionalized with CA by TEMA adding NEt_3
Gr	Graphite
GrO	graphite oxide
LC	L-cysteine
MDR	Multi-Drug Resistance
MEDA	2-(Dimethylamino)ethanethiol hydrochloride
NEt_3	Triethylamine
NHBoc	*N*-Boc-ethylenediamine
PI	Photoinitiator
RGO	Reduced Graphene Oxide
RGO **1**	Reduced Graphene Oxide functionalized with NHBoc
RGO **2**	Reduced Graphene Oxide functionalized with CA by TERA
RGO-B	Reduced Graphene Oxide blank experiments
RGO-DBU	Reduced Graphene Oxide functionalized with CA by TEMA adding DBU
RGO-DIPEA	Reduced Graphene Oxide functionalized with CA by TEMA adding DIPEA
RGO-NEt_3	Reduced Graphene Oxide functionalized with CA by TEMA adding NEt_3
ROS	reactive oxygen species
STEM	Scanning transmission electron microscopy
TEMA	Thiol-Michael addition reaction
TER	Thiol-ene reaction
TERA	Thiol-ene radical addition
TEROR	Thiol-epoxy ring opening reaction
XPS	X-ray photoelectron spectroscopy

GENERAL INTRODUCTION

Graphene oxide (GO) is a single carbon layer with a hexagonal array that contains different oxygen functional groups (i.e. epoxides, alcohols and carboxylic acids) throughout its structure as result of a strong graphite oxidation. GO has attracted a great interest since it has a great surface area and chemical versatility as well as interesting optical, electrical, water permeability and molecular sieving properties. In addition, the functional groups of GO allow to increase its stability in polar and non-polar solvents. One of the most important approaches is the functionalization of GO to create novel materials for a wide range of applications. However, the complex chemistry of GO is a limitation since different functional groups can react simultaneously, wasting the possibility to graft more than one molecule in the GO layers.

Generally, GO functionalization has been carried out on epoxide and/or carboxylic acid groups since they constitute the strongest concentration in GO layers. Nucleophiles such as amines have been used for the functionalization on carboxylic acid groups, using coupling agents with the disadvantage of the simultaneous activation of epoxide groups at the same time. During the graphite oxidation, defects arise such as vacancies breaking the aromatic domain and leading to alkene groups formation. This last functional group has been tried to explore, but with the disadvantage of using extreme conditions leading to GO reduction. To explore the chemistry of the graphene oxide, different strategies must be developed to create multi-functionalized graphene materials and particularly, antibacterial materials.

The antibacterial resistance is a worldwide problem that has emerged due to the indiscriminative way in which antibiotics were used in the last decades. The loss of efficiency of the antibiotics has encouraged the research community to propose new strategies for generating novel antibacterial agents that could be efficient, with low cytotoxic effect, easy to obtain and reusable.

In this context, this thesis brings insights and better understanding in the chemical functionalization of GO focusing on the epoxides, carboxylic acids and alkene groups. By exploring new pathways to exploit the GO functionalization, it would be possible to

create GO materials containing different molecules that can improve its performance for a wide range of applications, including the antibacterial activity of GO.

Chapter 1 of this thesis is dedicated to the literature survey which shows the chemical strategies that can be used for the chemical modification of the GO.

Chapter 2 deals with the functionalization of the GO towards the epoxide groups using glycine as model groups. This functionalization carries to the collateral reduction process that involves the use of amino acids until producing reduced graphene oxide (RGO).

Chapters 3 and 4 are dedicated to the study and analysis of the functionalization of the GO towards the alkene groups, applying the photochemical thiol-ene radical addition and the thiol-Michael addition reaction. Both reactions allow to take advantage of the C=C that remains after the graphitic oxidation during the production of GO.

In chapter 5, the quantification of the functional groups of the GO is proposed using selective reactions coupled to fluorescent labelling. The quantification method reported was applied to the epoxides, carboxylic acids and alkene groups of GO which represent the most important functional groups to perform derivatizations.

Finally, chapter 6 introduces to dual functionalization using peptide bond formation and thiol-ene reactions to produce highly positive charged GO materials for antibacterial applications.

CHAPTER 1

LITERATURE SURVEY

1.1 Graphene, graphite oxide and graphene oxide

Since it was obtained by first time by Novoselov and Geim in 2004, graphene has attracted a widespread interest to generate alternative materials with outstanding potentials in many fields, such as nanoelectronics [1], medicine [2], energy technology (for example, fuel cell, supercapacitor, hydrogen storage) [3], sensors [4], and catalysis [5]. Graphene is a 2D carbon material composed of carbon atoms in a honeycomb arrangement with sp^2 hybridization with remarkable electronic, optical, thermal, and mechanical properties [6]. Graphene is considered as the conceptual structure unit of for other carbon materials with sp^2 hybrid such as carbon nanotubes (CNTs), fullerenes and graphite (see Figure 1.1) [7]. In addition, the electronic properties can be preserved in few-layered graphene in a limit of 10 layers. After 10 layers, graphene becomes a 3D graphite structure [7].

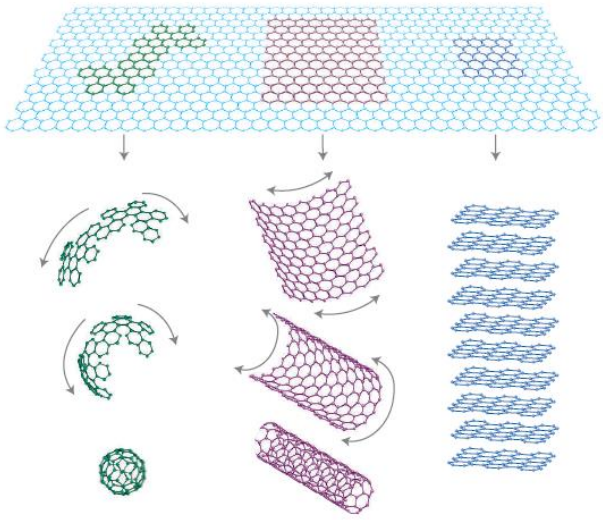

Figure 1.1 Graphene is a 2D building block, mother of all the graphitic forms. Graphene can be wrapped into fullerenes, rolled it into CNTs or stacked it into graphite. Taken from [7].

Graphene can be obtained through several methods and they can be divided into two main categories: the top-down approach and the bottom-up approach [8]. In the top-down approach, the first method to obtain GLs is the mechanical exfoliation through “scotch tape” method where the graphene layers (GLs) are peeled off to obtained high-quality of mono or

few-layered graphene [7]. However, the main drawback of this method is the high cost and low production of GLs. In addition, the top-down approach includes graphite intercalation [9], nanotube slicing [10], pyrolysis [11], graphite oxidation with the subsequent reduction [12], electrochemical exfoliation [13], sonication [14], ball milling and radiation methods have been studied to produce GLs [8]. Except for pyrolysis and graphite oxidation, the rest of the methods produce high quality GLs but with the limitation of the industrialization. On the other hand, the bottom-up approach includes methods such as epitaxial growth on silicon carbide [15], chemical vapor deposition (CVD) [16], dry ice and growth from metal-carbon melts [17,18]. These methods can lead to a production of high-quality GLs but requires conditions which are not suitable for scaling up for production.

Among the methods, the graphite oxidation with the subsequent reduction seems to be a promising approach for the high production of GLs [19]. In this method, oxidizing agents such as nitric acid and sulfuric acid in presence of potassium permanganate or potassium chloride are used to break the sp^2 domain, and insert oxygen functional groups along the carbon lattice [20]. This oxidation reaction leads to graphite oxide (GrO) which consist in a 3D graphite material (over 10 layers), with oxygen functionalities that can be exfoliated using mechanic stirring or sonication (see Figure 1.2) [21]. After the exfoliation, the product consists in a well dispersed brown slurry composed by few-layered graphene sheets with oxygen functional groups; this material is also known as GO [20]. Once GO was produced, the reduction of the GO can be achieved by thermal, chemical of electrochemical methods [22-24]. The GO reduction involves the partial or total elimination of the oxygen functional groups (i. e. C-OH, C-O-C, COOH, etc.) until obtaining GLs. The as obtained material is also called reduced graphene oxide (RGO) or chemically converted graphene oxide (CCGO). The RGO is composed of a GL with a C atomic thickness that contains defects (such as vacancies) product pf the reduction process that GO was undergone. In addition, a minimum quantity of oxygen functional groups can remain after the reduction of GO. However, the defects generated during the reduction of GO produce lower thermal, mechanical, optinc and electronic properties as compared to GLs [21].

Despite that the quality of GLs obtained from chemical methods could be lower as compared to other methods such as CVD or “scotch tape”, the production of the GLs by chemical methods conducts to two conclusions: i) the chemical methods can be scaled up for the bulk production of GO and then GLs and ii) one intermediary during the GLs is the GO

which could be an interesting material since offers the possibility to be tuned for specific applications. In general, GO can be used as a platform for different molecules, from of organic molecules, macromolecules, until other nanomaterials [25]. However, before discussing the chemical pathways in which GO can be modified to enhance its properties, it is necessary to know more about the chemistry of the GO itself.

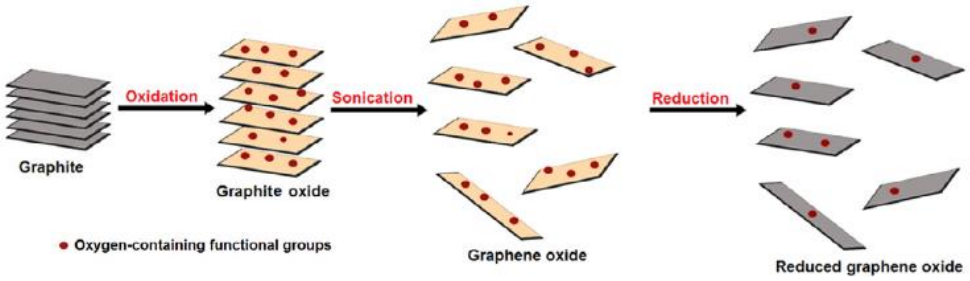

Figure 1.2 Production of reduced graphene oxide layers by graphite oxidation followed to mechanic exfoliation. Taken from [21].

As it was mentioned previously, GO is a GL decorated with oxygen functional groups (i.e., hydroxyl, carbonyl and epoxide groups, etc. see Figure 1.3), and it is synthesized by the graphite oxidation reaction followed by mechanical exfoliation [26]. The chemical structure of the GO is fairly complex and diverse due to the variety of chemical routes to synthesis it [27]. The British chemist B. C. Brodie was the first to study the reactivity of graphite flakes, performing a reaction that involves potassium chlorate and nitric acid [28]. The result was a black slurry that was composed of carbon, hydrogen and oxygen with a higher overall mas in comparison to the graphite flakes. Nearly 40 years later, Staudenmaier proposed a variation of the original Brodie's method, also using potassium chlorate and nitric acid but adding the chlorate in multiples aliquots [29]. The slight change proposed by Staudenmaier allowed to increase the C:O ratios until 2:1 meaning a major oxidation degree as previously described by Brodie. After that, nearly 60 years afterwards, Hummers and Offeman reported a new alternative for the oxidation of graphite using potassium permanganate and sulfuric acid, showing C:O ratio similar to that one obtained by Staudenmaier [30].

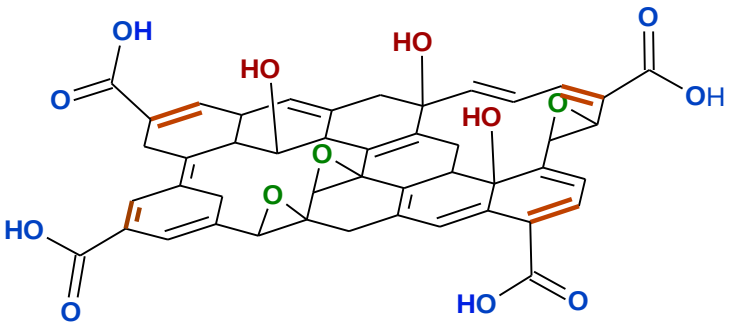

Figure 1.3 Lerf-Klinowsky model of the chemical structure of GO. Epoxy and alcohol groups are mainly in the basal plane whereas carboxylic acid groups at the edges.

Through the years, the Hummer's method has suffered important changes in the reaction conditions to improve the oxidation degree [31]. It becomes evident that not only the different methods that already exist can produce important variation in the chemistry of GO. Some additional parameters that affect the variety and density of functional groups during the GO synthesis are: i) the nature of the pristine graphite and its particle size, ii) oxidizing reagents, iii) temperature and iv) the oxidation time [32-34]. Slight changes in those conditions can lead to a wide density of GO functional groups, and those are the basis for developing graphene-based materials with remarkable properties [35,36].

Since there are different chemical routes that produce a non-stoichiometry GO [33], the chemical structure of the GO has been widely studied by X-Ray photoelectron spectroscopy (XPS) [37], transmission electron microscope (TEM) [38], infrared spectroscopy (FTIR) [37], solid state magnetic resonance (NMAR) [39], and computational simulation [40]. The most accepted GO structure is the Lerf-Klinowsky model shown in Figure 1.3 in which epoxide and hydroxyl groups are in the basal plane, whereas carboxylic acids are at the edges [27,40]. These functional groups are the basis for the chemical functionalization of GO with different molecules, including macromolecules such as polymers, polypeptides, or DNA [8-10]. However, additional oxygen functional groups could be obtained after the oxidation reaction such as ketones, aldehydes, quinone and lactone [41-43].

In addition, the functional groups of GO are important since they make easier the functionalization in comparison with GLs, which have the problem of limited solubility, aggregation sheets and the chemical inertness due to the great sp^2 domain [41-44]. Besides, the GO can be dispersed in a great variety of solvents, including in water, facilitating the functionalization of GO [44]. After the GO oxidation some defects appear throughout the

graphitic lattice such as vacancies and micro graphitic domains, resulting in a combination of sp^2 network with a considerable amount of sp^3 hybridization [45]. This feature allows to obtain a great quantity of alkene groups (C=C) which can be also used for further chemical modifications [46,47].

Therefore, the wide chemistry of GO must be explored to produce new hybrid graphene-based materials with improved dispersion, decreasing aggregation sheets and thus a great surface area would be available. Next sections analyze the base of the GO functionalization, different strategies to active the wide diversity of GO functional groups, and previous studies that exist about applications of GO functionalized materials.

1.2 Functionalization of graphene oxide

The functionalization of GO is an important step because each application demands specific chemical characteristics to have the best performance during the application. The GO functionalization can be performed by covalent or non-covalent bonds [36]. In the non-covalent functionalization electrostatic forces, Van der Waals forces or π-π stacking can take place [48]. For the covalent functionalization, the oxygen functional groups of GO react to form new bonds and new species such as amides, esters, secondary amines, etc. (see Figure 1.4) [35].

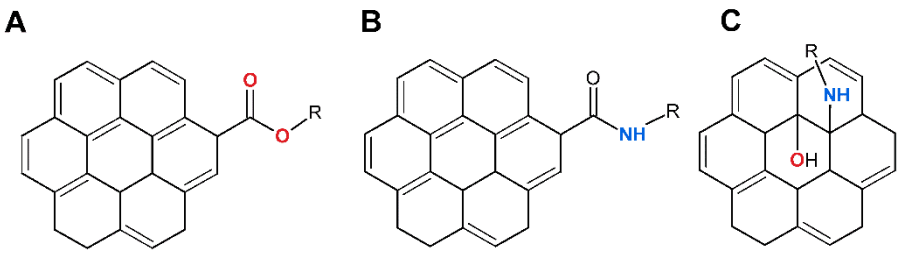

Figure 1.4 Different species can be formed after the covalent functionalization of GO: a) esters, b) amides and c) secondary amines.

Alcohols, epoxides and carboxylic acids are the functional groups commonly used for the deposition of different molecules on GO layers [35,36]. This is because those functionalities represent the major composition in GO [49]. In Figure 1.5 a schematic representation is shown of the activation of epoxides, alcohols, and carboxylic acids. More important, alkene groups also represent an interesting approach for the chemical modification of GO (see Figure 1.5d), as it was mentioned in section 1.1. However, due to the wide variety of functional groups in

GO, orthogonal reactions have not been reported yet, which implies that more than one oxygen functional group of GO can react simultaneously [35,36]. In the next section, it analyzes the chemistry behind each functional group and the required conditions for the GO functionalization.

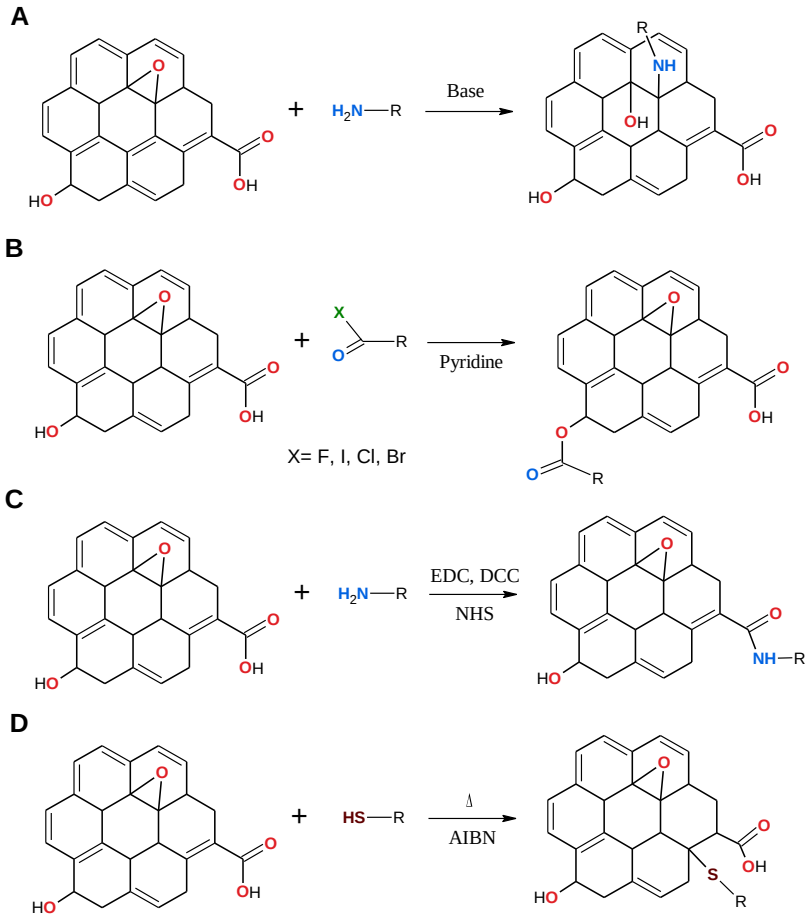

Figure 1.5 Graphene oxide functionalization: a) ring opening reaction, b) nucleophilic attack of the alcohol to ketones, c) peptide bond formation using coupling agents and d) thiol-ene click chemistry.

1.2.1 Functionalization of GO on epoxy and carboxylic acid groups

The covalent functionalization of GO has been extensively reported in the literature throughout epoxides and carboxylic acids, since they constitute the strongest concentration of functional groups in GO layers [49,50]. Primary amines and alcohols have been used for the functionalization on carboxylic acid groups using coupling agents such as thionyl chloride ($SOCl_2$), 1-Ethyl-3-(3-dimethylaminopropyl)-carbodiimide (EDC), *N,N′*-dicyclohexylcarbodiimide (DCC) and 2-(7-aza-1H-benzotriazole-l-yl)-1,1,3,3,-

tetramethyluronium hexafluorophosphate (HATU) (see Figure 1.6) [20, 51]. The resulted functionalized materials have shown enhanced properties for applications in optoelectronics [52], catalysis [53], biodevices [54], drug-delivery vehicles [55], supercapacitors [56], and polymer composites [57].

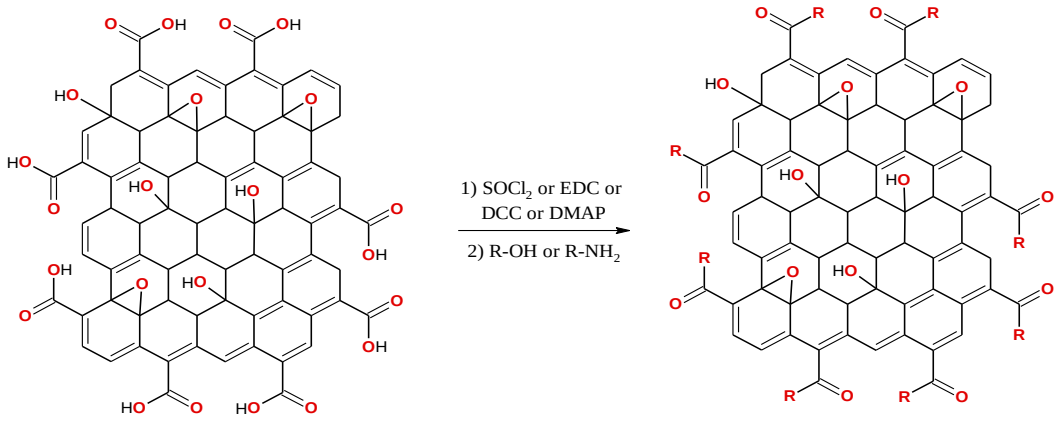

Figure 1.6 Activation of carboxylic acids using coupling agents and adding nucleophiles either amines or alcohols. Adapted from [13].

On the other hand, epoxide groups are susceptible to be attacked by nucleophiles through ring opening reactions [58,59]. This reaction can be easily performed under a wide diversity of reaction conditions. For example, ring opening reactions can be catalyzed using acid or basic conditions or by heating together with a nucleophile such as amines or sulfur compounds [35,36]. Indeed, multiple reactions may be occurred simultaneously due to amines can react with carboxylic acid groups of GO through peptide bond formation [60]. This is because epoxide groups are in part expected to be sterically hindered due to they are probable to be in the GO basal plane, and nucleophiles may more likely react with carboxylic acids in acid–base reactions or, with carbonyl groups located at borders of GO layers [35]. Some examples of ring opening reactions using nucleophiles are reported using hexylamine [61], polyethyleneimine [62], polyallylamine [63], octadecylamine [64], chitosan [65], ethylenediamine [60], and (1-(3-aminopropyl)-3-methylmidazolium bromide [66]. So, nucleophiles can be used for the reaction with carboxylic acids and epoxide groups as well, and therefore it becomes complicated to achieved orthogonal reactions. In the case of diamines, these can attack both sides of GO layers leading to crosslinking layers and together to the simultaneous activation of carboxylic acids and epoxide groups [67], the GO cannot be selective functionalized in a specific functional group.

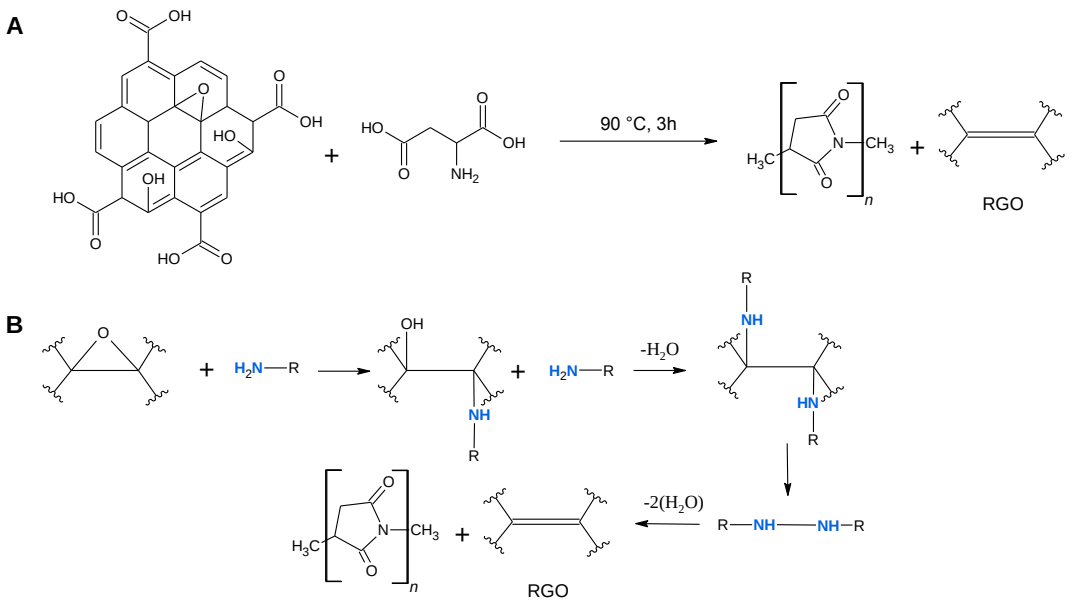

Figure 1.7 Reduction mechanism of GO using L-aspartic acid with the production of polysuccinimide as by-product: a) global reactions and b) mechanism of reduction. Adapted from [72].

Alternatively, amino acids can be used for the functionalization of GO due to open opportunities to have a greener and environmentally friendly reaction, with high availability and low cost [68]. Amino acids have been used extensively for the functionalization of GO under mild conditions, avoiding toxic compounds during the chemical derivatization [68-75]. Amino acids can be used to enhance the GO properties for catalysis, heavy metals elimination from water samples and for the creation of biocompatible materials [69,71,73]. In addition, amino acids are extensively used because they can be used for the reduction of GO (production of RGO) substituting hydrazine as chemical reducing agent and leading to green chemistry [69,70,72]. A wide literature exists about the chemical modification of GO using glycine, L-cysteine, valine, L-aspartic acid, phenylalanine, alanine and L-lysine just to mention a few [68-75]. Amongst the amino acids, glycine arises for GO functionalization or reduction because two interesting sceneries can come out: i) the glycine can produce nucleophilic attack towards epoxide groups and a simultaneous GO reduction [70], and ii) glycine can lead to partial reduction of GO with no traces of glycine in the final material [76]. Despite the reduction mechanism remains unclear, amino acids are extensively used for the reduction of GO, as it was mentioned [69]. It has been suggested that the mechanism is governed by the elimination of epoxide groups as first step [21]. In addition, the reduction process also involves the application of heat to remove the intermediary species and the most stable GO functional groups

[76]. For instance, L-aspartic acid has been used for the chemical reduction of GO and the production of polysuccinimide as by-product [72]. Here, it is pertinent to mention that the proposed mechanism of reduction explained the elimination of epoxide and alcohols from the GO basal plane (see Figure 1.7).

Thus, despite the reduction mechanism can be questioned, the evidence that the reduction was successfully achieved is corroborated in the final electrical properties of the RGO. The increase in the C/O ratio and electrical conductivity are RGO characteristics that have been taken as measure of the restoration of the sp^2 domain [69,70,72].

So, nucleophiles can produce different effects on GO layers: i) attack to the carboxylic acid groups, ii) simultaneous ring opening reactions and iii) reduction of the GO. Therefore, since different effects can be produced with the same nucleophile, it is possible to tune the behavior of the nucleophile to have a preferred functionalization towards a specific functional group or a reduction of GO. The study of the condition reactions can allow the identification of the limit where the functionalization reaction is substituted by a reduction process, or the conditions where the functionalization proceeds towards a specific functional group, for example the epoxide groups.

1.2.2 Functionalization of GO on hydroxyls

The functional groups of GO in the basal plane are mainly hydroxyl and epoxide groups [36]. In the previous section, it was discussed the reactivity of the epoxide groups in presence of nucleophiles, however hydroxyls can be found in a major concentration than epoxide groups, since they can be located at both sides of the GO layers and exist two hydroxyls per epoxide group [35].

According to Figure 1.8, tertiary alcohols of GO can be used to form ester groups *via* nucleophilic attack to α-bromoisobutyryl bromide, to form an initiator for atom transfer radical polymerization (ATRP) [77]. It is worth mentioning that, unlike primary and secondary alcohols, the tertiary alcohols are not prone to esterification with acids, at leat they can be sterically favorable [35]. Thus, ester or ether formation of hydroxyl groups will proceed at all alcohol groups where the reaction is sterically possible. It has been reported that the hydroxyl groups of GO sheets can be cross-linked by condensation with benzene-1,4-diboronic acid, forming boronic esters [78]. This approach yields a functionalized GO and, regardless of the

poor reactivity of tertiary alcohols, the reaction was possible due to the tertiary alcohols were sterically favorable.

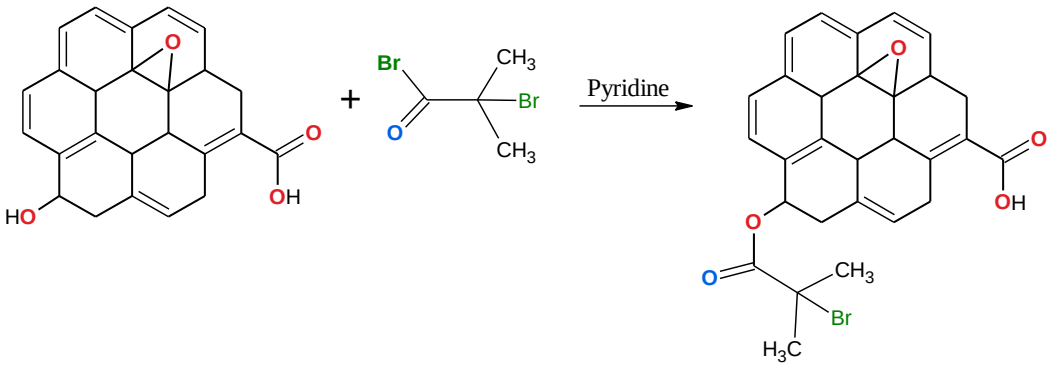

Figure 1.8 Functionalization of the GO through nucleophilic attack of alcohols towards α-bromoisobutyryl bromide. Adapted from [72].

1.2.3 Thiol-ene radical addition

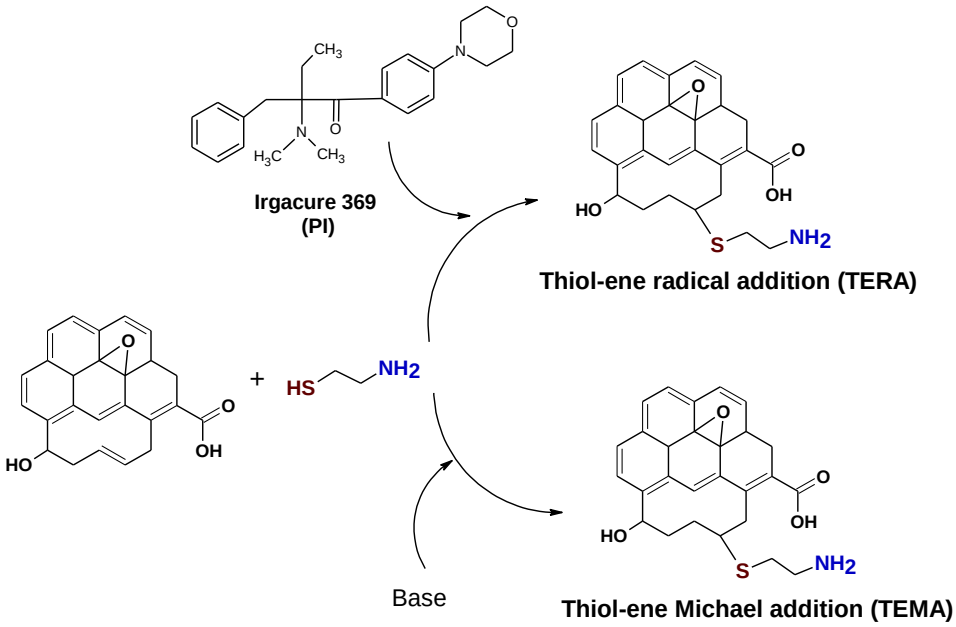

Figure 1.9 Scheme of the GO functionalization using alkene groups by and TEMA where only α,β-unsaturated acids participate.

Thiol-ene click chemistry (TER) is a powerful tool for achieving orthogonal reactions under mild conditions, with high yields and avoiding by-products [79-82]. TER is defined as the addition of a thiol to an alkene bond via "click chemistry", with an anti-Markovnikov orientation [79,80]. After the strong graphite oxidation reaction, a great quantity of defects

arises including vacancies, which reduces the sp^2 domain and more active alkene groups are obtained in GO [83]. As can be seen in Figure 1.9, TER can be applied for the functionalization either by radical addition (TERA) or base catalysts addition (TEMA) [79-81].

The first application of TERA on GO was done by Luong et al. [84], where cysteamine was used in presence of 2,2'-azobis(isobutyronitrile) as thermal radical initiator. Then, different efforts to modified GO by TERA have been reported to produce graphene quantum dots, graphene-based materials decorated with nanoparticles, GO materials for catalysis and depollution as well as the synthesis of amphiphilic particles [85-90]. In all these examples, TERA was carried out using systematically 2,2'-azobis(isobutyronitrile) (AIBN) as thermal radical initiator. The thermal radical initiator allows the production of thiyl radicals (R-S$^{\bullet}$) which attack the unsaturated system of GO. As a consequence of applying thermal initiators, a simultaneous GO reduction can be produced releasing functional groups such as epoxide, that cannot be further used for a second derivatization [48-53]. Alternatively, TERA can be carried out irradiating UV-light in order to produce the R-S• with the disadvantage of low generation of radicals, since the yield of the reactions depends on the bond dissociation energy (BDE) of the S-H [81,82]. Therefore, a PI can be used during the reaction for increasing the production of R-S$^{\bullet}$, and increasing the functionalization degree [91]. The application of TERA under UV-light using a PI possesses several advantages such as reduction in the reaction time, there is no need to heat the system and therefore a minor reduction is observed in the modified GO with TERA being an orthogonal reaction [79,80]. Some reports have been published about photochemical functionalization of GO by TERA in which the mainly approach is the crosslinking in situ on GO layers [92-95]. In these examples, the GO layers were modified with allyl compounds and then the GO sheets were exposed to UV radiation in presence of SH terminated polymers. In addition, some reports have demonstrated the use of the PI for the polymerization *in situ* on GO layers. Darocur 117 and dimethoxyphenyl acetophenone were used for the photochemical functionalization of GO by TER [96,97]. It is worth noting that in all these examples GO was pre-functionalized with allylic halide and then, in a subsequent step, the application of TERA to crosslink the GO layers. This pathway to modified GO considers that the quantity of C=C to be activated by TERA is poor, and a pre-functionalization with allyl compounds could bring a stronger incorporation of the polymer onto GO. Therefore, the photochemical functionalization of GO by TERA can be explored directly on the unsaturated system of GO in order to demonstrate the efficiency of TERA, as a tool to have regioselective and stereoselective functionalization directly on the GO layers.

1.2.4 Thiol-Michael Addition reaction

As mentioned in **section 1.2.3**, GO can be functionalized with thiols by adding a base catalyst which reaction proceeds due to TEMA (see Figure 1.9). Indeed, TEMA is a powerful click reaction that is mostly used in polymer chemistry for coupling α,β-unsaturated acids with thiols [81]. As compared to TERA, the addition of the radical initiator can promote the reaction with a wide range of unsaturated systems. However, TEMA possesses advantages such as high yields, mild condition reactions, a small concentration of base catalyst is needed, rapid reaction rates even in bulk quantities, wide variety of solvents can be used, the reaction is insensitive to ambient oxygen or water, regioselective and this reaction can be used with an enormous range of thiols and alkene molecules [79,80]. Typically, thiol addition on GO has been carried out using thermal radical initiators with the disadvantage of heating during long periods. The thermal treatment can release oxygen functional groups of GO leading to the production of RGO [84,90]. Consequently, the application of base catalyst for the GO functionalization by TEMA is a viable option, since it can take advantage of α,β-unsaturated acids, avoiding heating the reaction and thus, less oxygen functional groups could be removed during the functionalization. However, for the GO functionalization by TEMA, a side reaction can take place that is thiol-epoxide ring opening reaction (TEROR) [59]. Previous studies demonstrated that the functionalization of GO with thiols using base catalysts can occur. Notably, only TEROR was considered during the functionalization of GO and the possible reaction on alkene groups was ignored [98-102]. Since TEMA and TEROR can occur simultaneously under the presence of a base catalyst, there is a need to understand the contributions of both reactions during the GO functionalization from a qualitative and quantitative points of view. Therefore, the study of the functionalization of GO by TEMA can bring insights into the chemical functionalization, and thus answer fundamental questions such as: are the thiol compounds effectively bonded by TEMA or TEROR? What is the dominant reaction? How many molecules can be bonded by TEMA and how many by TEROR?

1.2.5 Non-covalent Functionalization

Non-covalent functionalization of GO has been demonstrated through hydrogen bonding, electrostatic forces, Van der Waals forces or π-π stacking on oxidized or sp^2 domain of GO [20,35,36]. The non-covalent functionalization is an important approach to modify chemically the GO without affecting the sp^2 structure [2]. In the case of the Van der Waals forces or π-π stacking depend on the number of aromatic rings that remain after the graphite

oxidation [103]. The activation energy of this process is reported to be higher than that of physical adsorption processes (5–40 kJ/mol) [104]. The patch of graphitic domains in GO has been used to deposit molecules such as DNA, sulfonated poly(ether-ether-ketone), sulfonated polyaniline and fibroin [105].

The non-covalent functionalization allows to develop stable aqueous GO layers using water-soluble pyrene derivative (1-pyrenebutyrate) [106]. The stabilizer has great affinity towards the graphitic network due to the π-π interactions of the pyrene. Another approach to chemically modify the GO without disrupting the sp^2 network for increasing the aqueous stability is through sodium salt of pyrene-1-sulfonic acid (PyS) (an electronic donor), and the disodium salt of 3,4,9,10-perylenetetracarboxylic diimide bisbenzenesulfonic acid (PDI) (an electronic acceptor) [107]. The negative charges in both molecules favor the repulsive forces in GO layers increasing the water dispersibility of, for example, RGO.

However, the non-covalent functionalization has been extensively used using polymers to improve the mechanic properties of GO. For instance, the preparation of poly(vinyl alcohol) (PVA) nanocomposites with graphene oxide (GO) can increase in 76% the tensile strength and a 62% improvement of Young's modulus, with only 0.7 wt% GO incorporation in the nanocomposite [108]. Nanocomposites of chitosan are produced using sulphonated graphene layers and the highest increase of both, tensile strength and Young's modulus, of 290±7% and 200±7%, respectively [109]. The increase in the mechanical properties were attributed to the H-bonding interaction between chitosan and the sulphonated graphene layers. The H-bonding interactions has been used also for the chemical functionalization of GO using sodium carboxymethyl cellulose (NaCMC) by solution casting [110]. The H-bonding interaction between -OH and -COOH groups of GO with the carboxylate ion of NaCMC was the reason of the composite formation.

So, the non-covalent functionalization appears as an efficient tool for the development of GO composites with increased stable aqueous and mechanical properties, without affecting extended π conjugation of the GO layers.

1.2.6 Applications of the GO functionalization

As it was mentioned in **section 1.1**, the GO is the product of the strong graphite oxidation followed by the mechanical exfoliation. Since the sp^2 domain was disrupted during

the oxidation, GO exhibits lower thermal and electrical properties as compared with GLs [20,21]. However, GO exhibits important physicochemical properties including high intrinsic mobility (200,000 $cm^2 V^{-1} S^{-1}$), good optical transmittance (~97.7%), large specific area (2630 $m^2 g^{-1}$), high Young's modulus (~1.0 TPa), good electrical and thermal conductivity (~5000 $W m^{-1} K^{-1}$) and unmatched pliability and impermeability [103]. Moreover, GO can be dispersed in a great variety of solvents, particularly in water, due to the mixture of oxygen functional groups and sp^2 patch which give to the GO an amphiphilic character [44]. All these properties make GO very attractive to be applied in a wide range of applications ranging from energy, biotechnology, depollution and medicine. For example, GO can be used for biomolecules/enzymes immobilization due to their distinctive characteristics such as biodegradability, notable chemical, and thermal stability, high surface area and pore volume. The oxygen functional groups enable the formation of strong interactions bewteen the enzyme and the GO by elostratic interactions In addition, the covalent functionalization with caboxylic acid groups of GO is one of the most important approaches for the deposition of trypsin [111], bovine serum albumin (BSA) [112], and glucose oxidase [113]. The modification of GO with biomolecules allows to create novel nano-bio-catalyst for applications in de-lignification for biofuels, environmental remediation, food and textile industry, and pulp and paper processing [103].

Another approach are the biosensors which are a promising aplication of GO based materials modified with biomolecules [113]. Single strand-DNA (ss-DNA) modified on golden nanoparticles (Au–DNA) deposited on GO layers allowed the identifcation and quantification of microcystin-LR (MC-LR) (see Figure 1.10) [114]. In this application the fluorescence intensity was decreasing as MC-LR was absorbed in the biosensor

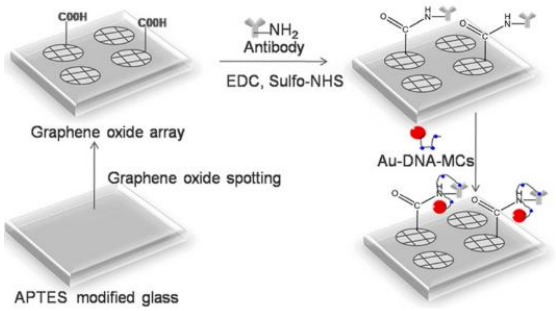

Figure 1.10 Scheme of the development of the GO biosensor based on fluorescence quenching. Taken from [114].

Taking advantage of the electrical properties of the GO, several electronic devices have been fabricated using GO as a starting material for at least one of the components. GO can be expected to be used in the production of transparent conductive films after being deposited on any substrate [115]. The coatings could be applied as flexible electronics, solar cells, liquid crystal devices, chemical sensors, and touch screen devices [116, 117,118]. Previously, GO was used as a transparent electrode for light-emitting diodes (LEDs) and solar cell devices [119].

Given the high surface area, GO has been considered for electrode materials in batteries and double-layered capacitors, as well as fuel cells and solar cells. For example, Li-ion batteries were fabricated using RGO-wrapped Fe_3O_4 anode material, and it was found that the energy storage capacity and cycle stability are increased compared with pure Fe_3O_4 [120]. Besides, caffeic acid has been used with RGO for fabricating electronic gas sensors and super-capacitors for potential sensing and energy storage applications [121]. Another example of GO material for energy storage implies the coupling of TiO_2 particles with RGO [122]. TiO_2 is a cheap and environmentally friendly material with a large cycling ability that can be applied as a cathode material in Li-ion batteries. The TiO_2 can be synthethized through a sol−gel method to obtain highly dispersed and controllable 5 nm in size nanoparticles deposited on RGO. The prepared material exhibited a specific capacity of ∼94 mA h g^{-1} at 59 °C, which is in contrast to a mechanically mixed TiO_2/RGO material that exhibited a specific capacity of ∼41 mA h g^{-1}.

Noncovalently functionalized GO materials are becoming in primising materials for sustainable catalysts and green chemistry with low emissions and high selectivity. GO-based materials are more atractive because their unique chemical properties, high mechanical resistance, and their favorable charge generation and transportation in catalysis and environmental processes [2]. For example, noncovalent magnetic control to reversibly recover GO using iron oxide (Fe_2O_3) was employed, in the presence of magnetic surfactants for the generation of materials for decontamination and water treatment [123]. Because of the noncovalent functionalization, the GO remain unchanged and thus there is no loss of its original properties. This feature allows the GO and magnetic material being reused. In Figure 1.11 is shown a schematic representation of the attraction and repulsion effect in the GO and Fe_2O_3 magnetic particles as a function of the pH. The good dispersion of the magnetic particles in the exfoliated GO sheets increase the surface area available and the mass transfer of reactants toward the active sites during the decontamination [124,125].

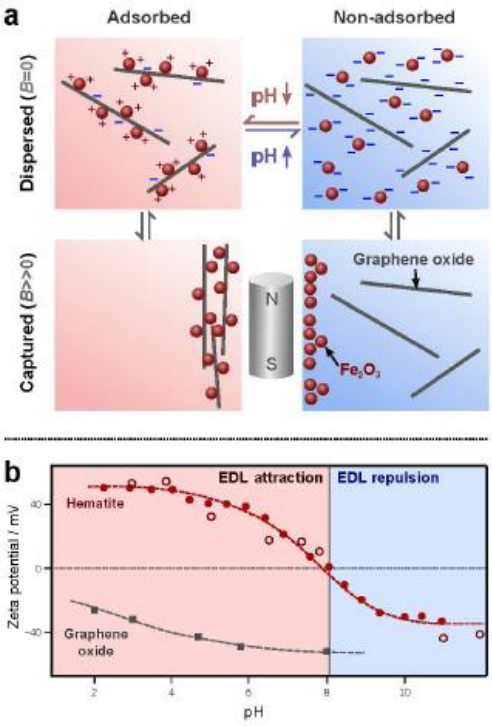

Figure 1.11 a) Scheme representation of the repulsion and attraction forces as a function of the pH. b) Zeta potential of the GO and the Fe_2O_3. Taken from [123].

Another interesting approach of the chemical functionalization of GO is the development of novel materials for medicine and deliver drugs to specific tissues [126]. In this context, the treatment of cancer through near infrarred (NIR) phototherapy has been studied [127]. For this, small size GO sheets show high NIR light absorbance and biocompatibility for potential photothermal therapy. Nanolayers of GO were functionalized with hyaluronic acid (HA) for photothermal ablation therapy of melanoma skin cancer using a NIR laser [128]. In this modifed GO material, HA works as a transdermal delivery carrier of chemical drugs and biopharmaceuticals. The authors reported the photothermal ablation therapy of skin cancer by using GO and GO chemically modified with HA (GO-HA) in SKH-1 mice inoculated with B16F1 cells on both dorsal flanks. The treatment with GO-HA showed that tumor tissues were completely ablated by the photothermal therapy with NIR irradiation.

So, the chemical modification of the GO brings a wide and novel set of materials to be applied in many fields such as energy storage, medicine depollution and catalysis. Given the versatility of the GO, its chemistry can be exploited in order to increase specific properties. In this context, new insights in the chemical functionalization could boost the final characteristics of the GO.

1.3 The rise of antibacterial resistance and the graphene oxide antibacterial activity

Since 1928 when Alexander Fleming discovered the penicillin, people have used it in an indiscriminative way during the next years for the treatment of several diseases [129]. After the introduction of penicillin in the market, more antimicrobial agents were synthetized and extensively used in the society to eradicate bacteria proliferation, fungus and parasites. Nowadays, the excessive consumption of these antimicrobial agents has led to a worldwide problem, which cans affects any one in any part of the world [130,131]. The World Health Organization (WHO) has reported that some bacteria have generated MDR due to the deliberate take of medicines, mainly in the underdeveloped countries, where there is no control in medicine sales [132]. *Escherichia coli* (*E. coli*), *Staphylococcus aureus* (*S. aureus*) and *Mycobacterium tuberculosis* (*M. tuberculosis*) are just some examples of bacteria that have generated MDR [130]. The AMR is an international commission that has encouraged the research community to generate new antimicrobial agents because current drugs have low efficiency to kill bacteria [133]. It has been suggested that in 2050, there will be over 10 million of deaths to a cost of 100 billion dollars annually because of MDR [133,134].

1.3.1 Antibacterial Resistance: Origen and Evolution

Antibacterial resistance has been defined as the loss of efficiency from antibiotics, which allow to bacteria multiply and replicate even at the presence of the antibiotic [135]. Nowadays, the antibacterial resistance has led to an increase in healthcare cost, stay in hospitals and the number of deaths by year [134]. Several factors have contributed to increase antibacterial resistance, such as the overuse of drugs, the sale of antibiotics without a prescription and the lack of new antibiotics [129]. Antibacterial resistance was detected in 1930s with the sulfonamide resistant *Streptococcus pyogenes* (*S. pyogenes*) in military hospitals. Then the resistance to penicillin of *S. aureus* appeared in hospitals in 1940s [136]. *M. tuberculosis* developed resistance to streptomycin after the introduction of the antibiotic to the market [136].

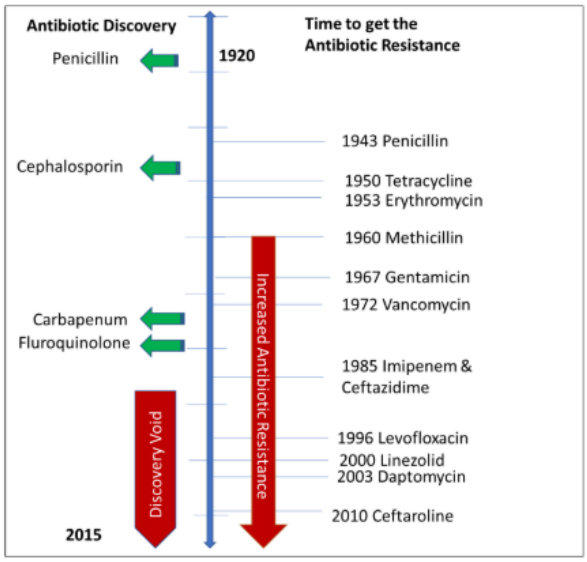

Figure 1.12 Graphical of antibiotic resistance versus time to get the antibiotic. Green arrow history of discovered antibiotic, in right side reported year of antibiotic resistance, red arrow indicates the increase in antibiotic resistance. Taken from [135].

Figure 1.12 contains a time flow highlighting the first time where some antibiotics produce antibacterial resistance [135]. Penicillin produced antibacterial resistance after 20 years of its introduction in the market, whereas Vancomycin resistant *S. aureus* was detected in 2002, 44 years after Vancomycin introduction [137]. Every time that we introduce a new antibiotic, it seems that bacteria need less time to generate the respective resistance, so one important question arises: How is it possible that bacteria generate antibiotic resistance? There are many mechanisms from which bacteria have developed resistance: i) generation of β-lactamases enzymes that destroys the antibiotic before it can affect the bacteria, ii) evacuation of antibacterial agent before it reaches an essential part, iii) developing of mutations in order to eliminate sites where the antibacterial agent can attach to the wall or the membrane and iv) transference of mutagenic materials amongst bacteria to improve the resistance against specific antibiotics [129,136,138]. Amongst these mechanisms, it has been observed that the generation of β-lactamases enzymes in bacteria has increased throughout the years [129]. In Figure 1.13 is possible to observe that between 2000 and 2010, the number of different β-lactamases enzymes detected in bacteria increased three times. These β-lactamases enzymes are the responsible to inhibit β-lactam based antibiotics.

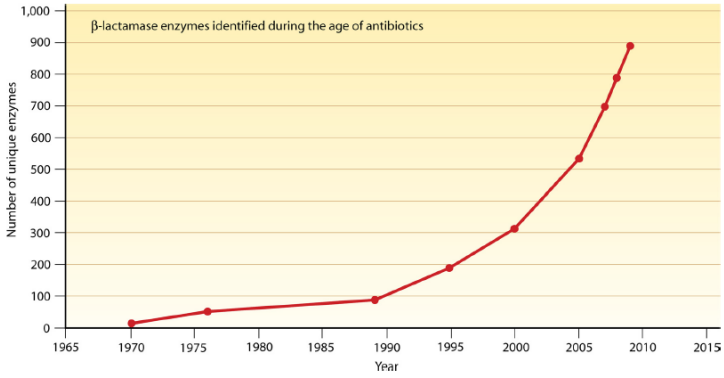

Figure 1.13 Productions of β-lactamases enzymes in bacteria detected since 1970. Taken from [129]

The exchange of genetic material also plays an important role during the antibacterial resistance arising. Indeed, the transfer of free DNA was the mainly reason to *S. pneumoniae* developed resistance against penicillin [139]. Hence, the antibiotic resistance is a natural phenomenon that exists even at the same time of the synthesis of the first antibiotic, but it has increased with the anthropogenic activities. In a globalized world, the emergence of resistance cannot be ignored in any region of the world, since resistant strains accelerates quickly. Only massive global action can prevent a future with untreatable infectious diseases [140]. If new strategies are not considered, all countries will be affected, but the poorest countries will suffer the earliest and the most. Novel antibiotics are developed on β-lactam based antibiotics such as cephalosporin in combination with ceftaroline and ceftolozane [141]. The main problem is that these antibiotics possess limited spectrum of antibacterial activity and, cannot be used to anticipate the challenges that will affront in the next years.

1.3.2 Antibacterial activity of GO

The advantage of GO to kill or inhibit bacteria by comparison with other antibacterial materials are summarized as follows: i) the antibacterial mechanism of GO is affected by both, physical destruction and chemical oxidation, which decrease bacterial resistance, ii) GO has mild cytotoxicity to mammalian cells in low dose, and (iii) in comparison to other carbon nanomaterials, easy processing, large scale production, and low cost of production, guaranteed them as a good antibacterial agent [142].

In the physical mechanism, the GO layers can wrap bacteria isolating them from the environment and inhibiting their proliferation [143]. In addition, the edges of the GO sheets can

also cut the membrane upon contact, leading to leakage of the cytoplasm constituents, and producing the subsequent bacteria death [144]. For instance, Liu et al., studied the impact of the GO size dimension in the antibacterial activity. They found that large GO sheets lead to most cell loss in 1 h incubation. In contrast, the inactivation rate of *E. coli* cells increases continuously when they are incubated with small GO sheets up to 4 h. The concentration of large GO sheets strongly influences their antibacterial activity at relative low GO concentration (<10 μg/ mL) and has less impact at high GO concentration (>20 μg/ mL) [145]. Perreault et al. have reported that the available surface area is important during the antibacterial activity due to a greater GO antibacterial activity can be obtained when GO is graft onto a surface [146]. In this scenery, a greater surface area can be in contact with bacteria as well as the physical and chemical mechanism can occur simultaneously. In addition, Yu et al., illustrated the antibacterial effect of the GO due to the physical contact [147]. They showed that the smallest GO (~ 1μm) has the strongest cutting effect which becomes weaker and weaker with increasing the size of GO. The largest GO (~ 4.5μm) has almost no cutting effect. Moreover, it was proposed that the smallest GO layers have no cell entrapment effect which becomes stronger and stronger with increasing the size of GO. With this, it was proposed a general rule: GO size has an opposite impact on its cutting effect and cell entrapment effect, two of the main physical antibacterial mechanisms of GO.

Another interesting effect of the physical mechanism of GO is the possibility to wrap the bacteria. Akhavan et al., demonstrated that the GO sheets and the RGO layers obtained using melatonin can trap the *E. coli* bacteria within the aggregated sheets [148]. The GO with the oxygen-containing functional groups could better trap the bacteria than the RGO with reduced functional groups. In addition, measuring the glucose consumption of the bacteria, it was found that the bacteria trapped within the aggregated graphene sheets were biologically disconnected from their environment. But, after removing the aggregated graphene sheets from the surface of the bacteria by using sonication, they could be reactivated. The reactivated bacteria consumed the glucose of the suspension and also could proliferate in a culture medium.

On the other hand, the chemical mechanism of GO antibacterial activity consists in the generation of reactive oxygen species (ROS). Different types of ROS, e.g. peroxides, superoxides, and free radicals generate a toxicological effect on cell by the interaction between GO and cell membrane. ROS induce electron transfer between cell membrane and GO, which leads to the reaction followed by membrane damage [149]. Carbon radicals present in GO and

RGO sheets exhibit lipid peroxidation in a three-step reaction [149]. Electron transfer from carbon radicals of GO or RGO to carbon atoms of un- saturated cellular lipid initiates the reaction. This leads to formation lipid peroxide radicals by further electron transfer between unsaturated lipid radical and molecular oxygen and ultimately formation of lipid peroxide and cell membrane disintegration. Thus, the density of functional groups affects the performance of the GO. Liu et al. reported that the antibacterial activity of the Gr, GrO, GO and RGO depends on the concentration of oxygen functional groups [150]. The authors proposed that the sequence of antibacterial activity could be GO > RGO > Gr > GrO. The high antibacterial activity of GO was attributed to a high density of the functional groups and the small size of the sheets. This phenome was explained as small GO sheets have more possibilities to interact with bacteria membrane increasing the membrane stress and the possibility of damage by ROS.

In the literature, the GO and its derivatives have been extensively studied in *E. coli* and rarely in other strains. For example, GO can produce 69.3 % of inhibition of *E. coli* in agar at GO concentrations of 85 μg mL^{-1} and, the 100 % of destruction of bacteria can be achieved at 5 mg mL^{-1} of GO [140]. Other strains have been studied in contact with GO and its derivatives, such as *Listeria monocytogenes* and *Salmonella enterica*. In the case of GLs, they need a concentration as high as 250 μg mL^{-1} to complete inhibit the pathogen growing [151]. The same strains where possible to inhibit their growing with GO and RGO even at a concentration ten times lower (25 μg mL^{-1}) [151]. Additional studies allowed to determine the minimum inhibitory concentration (MIC) of RGO with *E. coli*, *Salmonella typhimurium* and *Enterococcus faecalis* [152]. The MICs value obtained ranging from 1 to 8 μg mL^{-1} while standard drug such as kanamycin showed MICs values from 64 to 128 μg mL^{-1}. GO has been studied also in presence of dental pathogens such as *Streptococcus mutants*, *Porphyromonas gingivalis* and *Fusobacterium nucleatum* [153]. It was found that at concentrations ranging from 20 to 80 μg mL^{-1} produced loss of the integrity of the bacteria membrane and the essential nutrients leaked out. Further studies about GO antimicrobial activity against *Pseudomonas syringae*, *Xanthomonas campestris* and two fungal pathogens such as *Fusarium graminearum* and *Fusarium oxysporum* showed MICs values around 500 μg mL^{-1} [154].

In order to increase the antibacterial activity of GO, several modifications have been proposed using nanoparticles and polymers. The functionalized GO could increase the antibacterial activity as compared with pristine GO due to the synergistic effect created after

the functionalization. In the case of nanoparticles, silver, copper and iron nanoparticles were used for enhancing the antibacterial effect [155]. However, a drawback of GO functionalization with nanoparticles is the increase of bacteria resistance that those metals have produced recently [156]. On the other hand, the GO functionalization with quaternary ammonium salts (QAPs) has been reported as an important step towards graphene-based materials with exceptional antibacterial properties [154]. Chitosan, polyethyleneimine, poly-L-Lysine and polyhexamethylene guanidine hydrochloride are some examples of GO modified with QAPs with increased antibacterial activity [154,156,157]. However, the exact mechanisms with which the functionalization proceeds can be questioned due to the complex chemistry of the polymer and the GO. This item produces an uncertainty if the functionalization was performed by covalent or non-covalent interactions. It is worth mentioning that the functionalization with QAPs can produce an increase in the cytotoxic effect of GO limiting the range of possible applications [158]. Therefore, it is necessary to control and tune the density of QAPs in the final material, or to consider a second functionalization that allows increase in the biocompatibility of the GO. The last one is a possible alternative due to the wide variety of the functional groups that GO possess. Some examples of dual functionalization are reported already although no control during the functionalization was found. In fact, the authors claimed a development of dual functionalization in specific sites of GO, although their evidence can be questioned [159-162].

1.4 Conclusions

Graphene oxide possesses a wide variety of chemical functional groups and important properties, which includes its great surface area. Since the chemistry of the GO represents a challenge for the development of novel materials for a wide range for applications, it is necessary to conduct studies to generate new approaches for selective functionalization. In previous sections, it was discussed the importance of the chemical functionalization of the GO to enhance different properties that allow to expand the field possible applications. In specific, the generation of MDR in recent years demands the generation of alternative materials that could be a possible solution to the antibacterial resistance.

As it was mentioned, the functional groups that have been used are alcohols, epoxide, carboxylic acids and alkene groups. These functional groups represent the basis for the reactivity of the GO. For instance, epoxides and carboxylic acids can react with nucleophiles even at room temperature simultaneously. This problem limits the possibility to modify chemically with multiple molecules since exist multiple competing pathways. Motivated by this idea, in the present thesis it was studied the chemistry of the GO to generate new approaches to perform orthogonal reaction on GO layers.

For this, the chemical functionalization of GO was studied towards basal plane, in specific the epoxide groups. Different conditions must exist in which a nucleophile can lead to ring opening reaction without altering the carboxylic acid groups. More interesting are the alkene groups which seem to be an excellent approach to perform orthogonal reactions on GO layers. The chemistry developed around the GO will allow us to design novel materials based on GO with enhanced antibacterial activity.

In the next chapters, a set of different approaches is presented and discussed for the generation of knowledge around the chemistry of the GO. This thesis can contribute to open the possibility to continue studying the chemistry behind the functionalization of the GO.

BIBLIOGRAPHY

[1] Xuan, Y., Wu, Y. Q., Shen, T., Qi, M., Capano, M. A., Cooper, J. A., & Ye, P. D. (2008). Atomic-layer-deposited nanostructures for graphene-based nanoelectronics. *Applied Physics Letters*, *92*(1), 013101.

[2] Georgakilas, V., Tiwari, J. N., Kemp, K. C., Perman, J. A., Bourlinos, A. B., Kim, K. S., & Zboril, R. (2016). Noncovalent functionalization of graphene and graphene oxide for energy materials, biosensing, catalytic, and biomedical applications. *Chemical reviews*, *116*(9), 5464-5519.

[3] Liu, C., Alwarappan, S., Chen, Z., Kong, X., & Li, C. Z. (2010). Membraneless enzymatic biofuel cells based on graphene nanosheets. *Biosensors and Bioelectronics*, *25*(7), 1829-1833.

[4] Lu, C. H., Yang, H. H., Zhu, C. L., Chen, X., & Chen, G. N. (2009). A graphene platform for sensing biomolecules. *Angewandte Chemie*, *121*(26), 4879-4881.

[5] Qu, L., Liu, Y., Baek, J. B., & Dai, L. (2010). Nitrogen-doped graphene as efficient metal-free electrocatalyst for oxygen reduction in fuel cells. *ACS nano*, *4*(3), 1321-1326.

[6] Terrones, M., Botello-Méndez, A. R., Campos-Delgado, J., López-Urías, F., Vega-Cantú, Y. I., Rodríguez-Macías, F. J., … Terrones, H. (2010). Graphene and graphite nanoribbons: Morphology, properties, synthesis, defects and applications. Nano Today, 5(4), 351–372.

[7] Geim, A. K., & Novoselov, K. S. (2010). The rise of graphene. In *Nanoscience and technology: a collection of reviews from nature journals* (pp. 11-19).

[8] Shams, S. S., Zhang, R., & Zhu, J. (2015). Graphene synthesis: a Review. Materials Science-Poland, 33(3), 566-578.

[9] Lee, H., Kang, J., Cho, M. S., Choi, J. B., & Lee, Y. (2011). MnO 2/graphene composite electrodes for supercapacitors: the effect of graphene intercalation on capacitance. Journal of Materials Chemistry, 21(45), 18215-18219.

[10] Chen, J., Chen, L., Zhang, Z., Li, J., Wang, L., & Jiang, W. (2012). Graphene layers produced from carbon nanotubes by friction. *Carbon*, *50*(5), 1934-1941.

[11] Choucair, M., Thordarson, P., & Stride, J. A. (2009). Gram-scale production of graphene based on solvothermal synthesis and sonication. *Nature nanotechnology*, *4*(1), 30.

[12] Piñeiro-García, A., González-Alatorre, G., Tristan, F., Fierro-Gonzalez, J. C., & Vega-Díaz, S. M. (2018). Simple preparation of reduced graphene oxide coatings for solid phase micro-extraction (SPME) of furfural to be detected by gas chromatography/mass spectrometry. *Materials Chemistry and Physics*, *213*, 556-561.

[13] Parvez, K., Li, R., Puniredd, S. R., Hernandez, Y., Hinkel, F., Wang, S., ... & Müllen, K. (2013). Electrochemically exfoliated graphene as solution-processable, highly conductive electrodes for organic electronics. *ACS nano*, *7*(4), 3598-3606.

[14] Hernandez, Y., Nicolosi, V., Lotya, M., Blighe, F. M., Sun, Z., De, S., ... & Boland, J. J. (2008). High-yield production of graphene by liquid-phase exfoliation of graphite. *Nature nanotechnology*, *3*(9), 563-568.

[15] Sutter, P. (2009). How silicon leaves the scene. *Nature materials*, *8*(3), 171-172.

[16] Mittal, G., Dhand, V., Rhee, K. Y., Park, S. J., & Lee, W. R. (2015). A review on carbon nanotubes and graphene as fillers in reinforced polymer nanocomposites. *Journal of Industrial and Engineering Chemistry*, *21*, 11-25.

[17] Chakrabarti, A., Lu, J., Skrabutenas, J. C., Xu, T., Xiao, Z., Maguire, J. A., & Hosmane, N. S. (2011). Conversion of carbon dioxide to few-layer graphene. *Journal of Materials Chemistry*, *21*(26), 9491-9493.

[18] Amini, S., Garay, J., Liu, G., Balandin, A. A., & Abbaschian, R. (2010). Growth of large-area graphene films from metal-carbon melts. *Journal of Applied Physics*, *108*(9), 094321.

[19] Gilje, S., Han, S., Wang, M., Wang, K. L., & Kaner, R. B. (2007). LETTERS A Chemical Route to Graphene for Device Applications. Nano, 7(11), 3394–3398.
[20] Dreyer, D. R., Park, S., Bielawski, C. W., & Ruoff, R. S. (2010). The chemistry of graphene oxide. Chem. Soc. Rev., 39(1), 228–240.
[21] Thakur, S., & Karak, N. (2015). Alternative methods and nature-based reagents for the reduction of graphene oxide - a review Suman Thakur and Niranjan Karak *. Carbon, 94(June), 224–242.
[22] Stankovich, S., Dikin, D. A., Piner, R. D., Kohlhaas, K. A., Kleinhammes, A., Jia, Y., ... & Ruoff, R. S. (2007). Synthesis of graphene-based nanosheets via chemical reduction of exfoliated graphite oxide. carbon, 45(7), 1558-1565.
[23] Huh, S. H. (2011). Thermal reduction of graphene oxide. *Physics and Applications of Graphene-Experiments*, 73-90.
[24] Sundaram, R. S., Gómez-Navarro, C., Balasubramanian, K., Burghard, M., & Kern, K. (2008). Electrochemical modification of graphene. *Advanced Materials*, *20*(16), 3050-3053.
[25] Karahan, H. E., Wang, Y., Li, W., Liu, F., Wang, L., Sui, X., ... & Chen, Y. (2018). Antimicrobial graphene materials: the interplay of complex materials characteristics and competing mechanisms. *Biomaterials science*, *6*(4), 766-773.
[26] De Silva, K. K. H., Huang, H.-H., Joshi, R. K., & Yoshimura, M. (2017). Chemical reduction of graphene oxide using green reductants. Carbon, 119, 190–199.
[27] Kwan, Y.C.G.; Ng, G.M.; Huan, C.H.A. Identification of functional groups and determination of carboxyl formation temperature in graphene oxide using the XPS O 1s spectrum. Thin Solid Films 2015, 590, 40–48.
[28] Brodie, B. C. (1859). XIII. On the atomic weight of graphite. *Philosophical Transactions of the Royal Society of London*, (149), 249-259.
[29] Staudenmaier, L. (1898). Verfahren zur darstellung der graphitsäure. *Berichte der deutschen chemischen Gesellschaft*, *31*(2), 1481-1487.
[30] Hummers Jr, W. S., & Offeman, R. E. (1958). Preparation of graphitic oxide. *Journal of the american chemical society*, *80*(6), 1339-1339.
[31] Kovtyukhova, N. I., Ollivier, P. J., Martin, B. R., Mallouk, T. E., Chizhik, S. A., Buzaneva, E. V., & Gorchinskiy, A. D. (1999). Layer-by-layer assembly of ultrathin composite films from micron-sized graphite oxide sheets and polycations. *Chemistry of materials*, *11*(3), 771-778.
[32] Sturala, J.; Luxa, J.; Pumera, M.; Sofer, Z. Chemistry of Graphene Derivatives: Synthesis, Applications, and Perspectives. Chem. - A Eur. J. 2018, 24, 5992–6006.
[33] Acik, M.; Lee, G.; Mattevi, C.; Pirkle, A.; Wallace, R.M.; Chhowalla, M.; Cho, K.; Chabal, Y. The Role of Oxygen during Thermal Reduction of Graphene Oxide Studied by Infrared Absorption Spectroscopy. J. Phys. Chem. C 2011, 115, 19761–19781.
[34] Qiao, Q.; Liu, C.; Gao, W.; Huang, L. Graphene oxide model with desirable structural and chemical properties. Carbon N. Y. 2019, 143, 566–577.
[35] Eigler, S.; Dimiev, A.M. Functionalization and Reduction of Graphene Oxide. Graphene Oxide Fundam. Appl. 2016, 175–229.
[36] Gao, W. The Chemistry of Graphene Oxide. In Graphene Oxide; Gao, W., Ed.; Springer International
[37] Dave, K.; Park, K.H.; Dhayal, M. Two-step process for programmable removal of oxygen functionalities of graphene oxide: functional, structural and electrical characteristics. RSC Adv. 2015, 5, 95657–95665.

[38] Erickson, K.; Erni, R.; Lee, Z.; Alem, N.; Gannett, W.; Zettl, A. Determination of the local chemical structure of graphene oxide and reduced graphene oxide. Adv. Mater. 2010, 22, 4467–4472.
[39] He, H., Riedl, T., Lerf, A., & Klinowski, J. (1996). Solid-state NMR studies of the structure of graphite oxide. *The Journal of physical chemistry*, *100*(51), 19954-19958.
[40] Yan, J.A.; Chou, M.Y. Oxidation functional groups on graphene: Structural and electronic properties. Phys. Rev. B - Condens. Matter Mater. Phys. 2010, 82, 21–24.
[41] Feicht, P., Biskupek, J., Gorelik, T. E., Renner, J., Halbig, C. E., Maranska, M., … Eigler, S. (2019). Brodie's or Hummers' Method: Oxidation Conditions Determine the Structure of Graphene Oxide. Chemistry - A European Journal, 25(38), 8955–8959.
[42] Vural, M., Lei, Y., Pena-Francesch, A., Jung, H., Allen, B., Terrones, M., & Demirel, M. C. (2017). Programmable molecular composites of tandem proteins with graphene oxide for efficient bimorph actuators. Carbon, 118, 404–412.
[43] Liu, Z., Dong, N., Jiang, P., Wang, K., Wang, J., & Chen, Y. (2018). Reduced Graphene Oxide Chemically Modified with Aggregation-Induced Emission Polymer for Solid-State Optical Limiter. Chemistry – A European Journal, 24(72), 19317–19322.
[44] Paredes, J.I.; Marti, a; Tasco, J.M.D.; Martı, a Graphene Oxide Dispersions in Organic Solvents Graphene Oxide Dispersions in Organic Solvents. 2008, 24, 10560–10564.
[45] Vacchi, I. A., Guo, S., Raya, J., Bianco, A., & Ménard-Moyon, C. (2020). Strategies for the Controlled Covalent Double Functionalization of Graphene Oxide. *Chemistry – A European Journal*, *24*(23), chem.201905785.
[46] Gómez-Navarro, C., Meyer, J. C., Sundaram, R. S., Chuvilin, A., Kurasch, S., Burghard, M., … Kaiser, U. (2010). Atomic structure of reduced graphene oxide. *Nano Letters*, *10*(4), 1144–1148.
[47] Yan, L., Zheng, Y. B., Zhao, F., Li, S., Gao, X., Xu, B., … Zhao, Y. (2012). Chemistry and physics of a single atomic layer: strategies and challenges for functionalization of graphene and graphene-based materials. *Chem. Soc. Rev.*, *41*(1), 97–114.
[48] Hu K, Gupta MK, Kulkarni DD, Tsukruk V V. (2013) Ultra-Robust Graphene Oxide-Silk Fibroin Nanocomposite Membranes. Adv Mater 25:2301–2307.
[49] Eng AYS, Chua CK, Pumera M (2015) Refinements to the structure of graphite oxide: Absolute quantification of functional groups via selective labelling. Nanoscale 7:20256–20266.
[50] Barua, M., Sreedhara, M. B., Pramoda, K., & Rao, C. N. R. (2017). Quantification of surface functionalities on graphene, boron nitride and borocarbonitrides by fluorescence labeling. *Chemical Physics Letters*, *683*, 459-466.
[51] Eigler, S., & Dimiev, A. M. (2017). Functionalization and reduction of graphene oxide. *Graphene Oxide*, 175-229.
[52] Zhu, J., Li, Y., Chen, Y., Wang, J., Zhang, B., Zhang, J., & Blau, W. J. (2011). Graphene oxide covalently functionalized with zinc phthalocyanine for broadband optical limiting. *Carbon*, *49*(6), 1900-1905.
[53] Hu, X., Mu, L., Wen, J., & Zhou, Q. (2012). Covalently synthesized graphene oxide-aptamer nanosheets for efficient visible-light photocatalysis of nucleic acids and proteins of viruses. *Carbon*, *50*(8), 2772-2781.
[54] Carpio, I. E. M., Mangadlao, J. D., Nguyen, H. N., Advincula, R. C., & Rodrigues, D. F. (2014). Graphene oxide functionalized with ethylenediamine triacetic acid for heavy metal adsorption and anti-microbial applications. *Carbon*, *77*, 289-301.

[55] Wu, H., Shi, H., Wang, Y., Jia, X., Tang, C., Zhang, J., & Yang, S. (2014). Hyaluronic acid conjugated graphene oxide for targeted drug delivery. *Carbon*, *69*, 379-389.
[56] Li, Z. F., Zhang, H., Liu, Q., Liu, Y., Stanciu, L., & Xie, J. (2014). Covalently-grafted polyaniline on graphene oxide sheets for high performance electrochemical supercapacitors. *Carbon*, *71*, 257-267.
[57] Wan, Y. J., Tang, L. C., Gong, L. X., Yan, D., Li, Y. B., Wu, L. B., ... & Lai, G. Q. (2014). Grafting of epoxy chains onto graphene oxide for epoxy composites with improved mechanical and thermal properties. *Carbon*, *69*, 467-480.
[58] Thomas, H.R.; Marsden, A.J.; Walker, M.; Wilson, N.R.; Rourke, J.P. Sulfur-functionalized graphene oxide by epoxide ring-opening. *Angew. Chemie - Int. Ed.* **2014**, *53*, 7613–7618.
[59] Song S, Zhang Y (2017) Construction of a 3D multiple network skeleton by the thiol-Michael addition click reaction to fabricate novel polymer/graphene aerogels with exceptional thermal conductivity and mechanical properties. J Mater Chem A 5:22352–22360.
[60] Kim NH, Kuila T, Lee JH (2013) Simultaneous reduction, functionalization and stitching of graphene oxide with ethylenediamine for composites application. J Mater Chem A 1:1349–1358.
[61] Compton, O. C., Dikin, D. A., Putz, K. W., Brinson, L. C., & Nguyen, S. T. (2010). Electrically conductive "alkylated" graphene paper via chemical reduction of amine-functionalized graphene oxide paper. *Advanced materials*, *22*(8), 892-896.
[62] Halakoo, E., & Feng, X. (2020). Layer-by-layer assembly of polyethyleneimine/graphene oxide membranes for desalination of high-salinity water via pervaporation. *Separation and Purification Technology*, *234*, 116077.
[63] Zhao, Z., Li, Q., Gong, J., Li, Z., & Zhang, J. (2020). Hybrid poly (allylamine hydrochloride)-graphene oxide microcapsules: preparation, characterization and application in textiles with controlled release behavior. *Materials Advances*.
[64] Cao, Y., Fan, D., Lin, S., Mu, L., Ng, F. T., & Pan, Q. (2020). Phase change materials based on comb-like polynorbornenes and octadecylamine-functionalized graphene oxide nanosheets for thermal energy storage. *Chemical Engineering Journal*, *389*, 124318.
[65] Venkataprasanna, K. S., Prakash, J., Vignesh, S., Bharath, G., Venkatesan, M., Banat, F., ... & Venkatasubbu, G. D. (2020). Fabrication of Chitosan/PVA/GO/CuO patch for potential wound healing application. *International Journal of Biological Macromolecules*, *143*, 744-762.
[66] Yang, H., Shan, C., Li, F., Han, D., Zhang, Q., & Niu, L. (2009). Covalent functionalization of polydisperse chemically-converted graphene sheets with amine-terminated ionic liquid. *Chemical Communications*, (26), 3880-3882.
[67] An, Z., Compton, O. C., Putz, K. W., Brinson, L. C., & Nguyen, S. T. (2011). Bio-inspired borate cross-linking in ultra-stiff graphene oxide thin films. *Advanced Materials*, *23*(33), 3842-3846.
[68] Javidparvar AA, Naderi R, Ramezanzadeh B (2020) L-cysteine reduced/functionalized graphene oxide application as a smart/control release nanocarrier of sustainable cerium ions for epoxy coating anti-corrosion properties improvement. J Hazard Mater 389:122135.
[69] Chen, D., Li, L., & Guo, L. (2011). An environment-friendly preparation of reduced graphene oxide nanosheets via amino acid. *Nanotechnology*, *22*(32).
[70] Bose S, Kuila T, Mishra AK, et al (2012) Dual role of glycine as a chemical functionalizer and a reducing agent in the preparation of graphene: an environmentally friendly method. J Mater Chem 22:9696.

[71] Najafi F, Moradi O, Rajabi M, et al (2015) Thermodynamics of the adsorption of nickel ions from aqueous phase using graphene oxide and glycine functionalized graphene oxide. J Mol Liq 208:106–113.
[72] Tran, D. N. H., Kabiri, S., & Losic, D. (2014). A green approach for the reduction of graphene oxide nanosheets using non-aromatic amino acids. *Carbon*, *76*, 193–202.
[73] Huang, Q., Zhou, L., Jiang, X., Zhou, Y., Fan, H., & Lang, W. (2014). Synthesis of copper graphene materials functionalized by amino acids and their catalytic applications. *ACS Applied Materials and Interfaces*, *6*(16), 13502–13509.
[74] Palaniappan N, Cole IS, Kuznetsov AE, et al (2019) Experimental and computational studies of a graphene oxide barrier layer covalently functionalized with amino acids on Mg AZ13 alloy in salt medium. RSC Adv 9:32441–32447.
[75] Mallakpour, S., Abdolmaleki, A., & Borandeh, S. (2014). Covalently functionalized graphene sheets with biocompatible natural amino acids. *Applied Surface Science*, *307*, 533–542.
[76] Kumar, A.; Khandelwal, M. Amino acid mediated functionalization and reduction of graphene oxide-synthesis and the formation mechanism of nitrogen-doped graphene. New J. Chem. 2014, 38, 3457–3467.
[77] Gonçalves, G., Marques, P. A., Barros-Timmons, A., Bdkin, I., Singh, M. K., Emami, N., & Grácio, J. (2010). Graphene oxide modified with PMMA via ATRP as a reinforcement filler. *Journal of Materials Chemistry*, *20*(44), 9927-9934.
[78] Burress, J. W., Gadipelli, S., Ford, J., Simmons, J. M., Zhou, W., & Yildirim, T. (2010). Graphene oxide framework materials: theoretical predictions and experimental results. *Angewandte Chemie International Edition*, *49*(47), 8902-8904.
[79] Hoyle, C. E.; Bowman, C. N. Thiol-Ene Click Chemistry. Angew. Chemie - Int. Ed. 2010, 49 (9), 1540–1573.
[80] Lowe, A. B. Thiol-Ene "Click" Reactions and Recent Applications in Polymer and Materials Synthesis. Polym. Chem. 2010, 1 (1), 17–36.
[81] Nair, D. P.; Podgórski, M.; Chatani, S.; Gong, T.; Xi, W.; Fenoli, C. R.; Bowman, C. N. The Thiol-Michael Addition Click Reaction: A Powerful and Widely Used Tool in Materials Chemistry. Chem. Mater. 2014, 26 (1), 724–744.
[82] Dénès, F.; Pichowicz, M.; Povie, G.; Renaud, P. Thiyl Radicals in Organic Synthesis. Chem. Rev. 2014, 114 (5), 2587–2693.
[83] Shao G, Lu Y, Wu F, et al (2012) Graphene oxide: The mechanisms of oxidation and exfoliation. J Mater Sci 47:4400–4409
[84] Luong, N.D.; Sinh, L.H.; Johansson, L.S.; Campell, J.; Seppälä, J. Functional graphene by thiol-ene click chemistry. Chem. - A Eur. J. 2015, 21, 3183–3186
[85] Huang H, Liu M, Tuo X, et al (2018) A novel thiol-ene click reaction for preparation of graphene quantum dots and their potential for fluorescence imaging. Mater Sci Eng C 91:631–637.
[86] Kanninen P, Luong ND, Sinh LH, et al (2017) Highly active platinum nanoparticles supported by nitrogen / sulfur functionalized graphene composite for ethanol electro-oxidation. Electrochim Acta.
[87] Li J, Cheng Y, Zhang S, et al (2017) Modification of GO based on click reaction and its composite fibers with poly (vinyl alcohol). Compos Part A.

[88] Masteri-farahani M, Modarres M (2017) New Hybrid Nanomaterials Derived from Chemical Functionalization of Clicked Graphene Oxide / Magnetite Nanocomposite with Peroxopolyoxotungstate Species. 10786–10792.
[89] Li Y, Bao L, Zhou Q, et al (2017) Functionalized Graphene Obtained via Thiol-Ene Click Reactions as an Efficient Electrochemical Sensor. ChemistrySelect 2:9284–9290.
[90] Yap PL, Kabiri S, Tran DNH, Losic D (2018) Multifunctional Binding Chemistry on Modified Graphene Composite for Selective and Highly Efficient Adsorption of Mercury. ACS Appl Mater Interfaces 11:6350–6362.
[91] Oberleitner, B.; Dellinger, A.; Déforet, M.; Galtayries, A.; Castanet, A.-S.; Semetey, V. A facile and versatile approach to design self-assembled monolayers on glass using thiol–ene chemistry. Chem. Commun. 2013, 49, 1615.
[92] Eskandari P, Abousalman-Rezvani Z, Roghani-Mamaqani H, et al (2019) Polymer grafting on graphene layers by controlled radical polymerization. Adv Colloid Interface Sci 273:102021.
[93] Rodier BJ, Mosher EP, Burton ST, et al (2016) Polythioether Particles Armored with Modifiable Graphene Oxide Nanosheets. Macromol Rapid Commun 37:894–899.
[94] Liu J, Zhu K, Jiao T, et al (2017) Preparation of graphene oxide-polymer composite hydrogels via thiol-ene photopolymerization as efficient dye adsorbents for wastewater treatment. Colloids Surfaces a Physicochem Eng Asp 529:668–676.
[95] Luo X, Ma K, Jiao T, et al (2017) Graphene Oxide-Polymer Composite Langmuir Films Constructed by Interfacial Thiol-Ene Photopolymerization. Nanoscale Res Lett 12:
[96] Acosta Ortiz R, García Valdez AE, Ku Herrera J de J (2020) Simultaneous reduction in situ and thiol- functionalization of Graphene Oxide during the Photopolymerization of Epoxy/Thiol-ene photocurable systems to prepare polyether-polythioether/reduced graphene oxide nanocomposites. Polym Technol Mater 59:282–293.
[97] Qian X, Jiang S (2018) Modification of graphene with organic/inorganic silicon-based materials and its reinforcement on the UV-curing polyurethane composite coatings. Polym Compos 39:746–754.
[98] Huang, H.; Tian, Y.; Xie, Y.; Mo, R.; Hu, J.; Li, M.; Sheng, X.; Jiang, X.; Zhang, X. Modification of graphene oxide with acrylate phosphorus monomer via thiol-Michael addition click reaction to enhance the anti-corrosive performance of waterborne epoxy coatings. Prog. Org. Coatings 2020, 146, 105724
[99] Nie, L.; Zhang, J.; Wu, Q.; Fei, G.; Hu, K.; Fang, L.; Yang, S. Fabrication of micropatterned gold nanoparticles on graphene oxide nanosheet via thiol-Michael addition click chemistry. Mater. Lett. 2020, 261, 127014
[100] Oz, Y.; Barras, A.; Sanyal, R.; Boukherroub, R.; Szunerits, S.; Sanyal, A. Functionalization of reduced graphene oxide via thiol-maleimide “click” chemistry: Facile fabrication of targeted drug delivery vehicles. ACS Appl. Mater. Interfaces 2017, 9, 34194–34203
[101] Huang, N.; Zhang, S.; Yang, L.; Liu, M.; Li, H.; Zhang, Y.; Yao, S. Multifunctional Electrochemical Platforms Based on the Michael Addition/Schiff Base Reaction of Polydopamine Modified Reduced Graphene Oxide: Construction and Application. ACS Appl. Mater. Interfaces 2015, 7, 17935–17946

[102] Liu, J.; Zhu, K.; Jiao, T.; Xing, R.; Hong, W.; Zhang, L.; Zhang, Q.; Peng, Q. Preparation of graphene oxide-polymer composite hydrogels via thiol-ene photopolymerization as efficient dye adsorbents for wastewater treatment. Colloids Surfaces a Physicochem. Eng. Asp. 2017, 529, 668–676

[103] Adeel, M., Bilal, M., Rasheed, T., Sharma, A., & Iqbal, H. M. (2018). Graphene and graphene oxide: functionalization and nano-bio-catalytic system for enzyme immobilization and biotechnological perspective. *International journal of biological macromolecules*, *120*, 1430-1440.

[104] Liu F, Chung S, Oh G, Seo TS (2012) Three-Dimensional Graphene Oxide Nanostructure for Fast and Efficient Water-Soluble Dye Removal. ACS Appl Mater Interfaces 4:922–927.

[105] Hu, K., Gupta, M. K., Kulkarni, D. D., & Tsukruk, V. V. (2013). Ultra-robust graphene oxide-silk fibroin nanocomposite membranes. *Advanced Materials*, *25*(16), 2301-2307.

[106] Xu, Y., Bai, H., Lu, G., Li, C., & Shi, G. (2008). Flexible graphene films via the filtration of water-soluble noncovalent functionalized graphene sheets. *Journal of the American Chemical Society*, *130*(18), 5856-5857.

[107] Pang, S., Tsao, H. N., Feng, X., & Müllen, K. (2009). Patterned graphene electrodes from solution-processed graphite oxide films for organic field-effect transistors. *Advanced Materials*, *21*(34), 3488-3491.

[108] Liang, J., Huang, Y., Zhang, L., Wang, Y., Ma, Y., Guo, T., & Chen, Y. (2009). Molecular-level dispersion of graphene into poly (vinyl alcohol) and effective reinforcement of their nanocomposites. *Advanced Functional Materials*, *19*(14), 2297-2302.

[109] Layek, R. K., Samanta, S., & Nandi, A. K. (2012). Graphene sulphonic acid/chitosan nano biocomposites with tunable mechanical and conductivity properties. *Polymer*, *53*(11), 2265-2273.

[110] Layek, R. K., Kundu, A., & Nandi, A. K. (2013). High-Performance Nanocomposites of Sodium Carboxymethylcellulose and Graphene Oxide. *Macromolecular Materials and Engineering*, *298*(11), 1166-1175.

[111] Xu, G., Chen, X., Hu, J., Yang, P., Yang, D., & Wei, L. (2012). Immobilization of trypsin on graphene oxide for microwave-assisted on-plate proteolysis combined with MALDI-MS analysis. *Analyst*, *137*(12), 2757-2761.

[112] Shen, J., Shi, M., Yan, B., Ma, H., Li, N., Hu, Y., & Ye, M. (2010). Covalent attaching protein to graphene oxide via diimide-activated amidation. *Colloids and Surfaces B: Biointerfaces*, *81*(2), 434-438.

[113] Sutarlie, L., Ow, S. Y., & Su, X. (2017). Nanomaterials-based biosensors for detection of microorganisms and microbial toxins. *Biotechnology Journal*, *12*(4).

[114] Shi, Y., Wu, J., Sun, Y., Zhang, Y., Wen, Z., Dai, H., ... & Li, Z. (2012). A graphene oxide-based biosensor for microcystins detection by fluorescence resonance energy transfer. *Biosensors and Bioelectronics*, *38*(1), 31-36.

[115] Cai, B., Wang, S., Huang, L., Ning, Y., Zhang, Z., & Zhang, G. J. (2014). Ultrasensitive label-free detection of PNA–DNA hybridization by reduced graphene oxide field-effect transistor biosensor. *ACS nano*, *8*(3), 2632-2638.

[116] Li, S. S., Tu, K. H., Lin, C. C., Chen, C. W., & Chhowalla, M. (2010). Solution-processable graphene oxide as an efficient hole transport layer in polymer solar cells. *ACS nano*, *4*(6), 3169-3174.

[117] Saha, S. K., Bhaumik, S., Maji, T., Mandal, T. K., & Pal, A. J. (2014). Solution-processed reduced graphene oxide in light-emitting diodes and photovoltaic devices with the same pair of active materials. *RSC advances*, *4*(67), 35493-35499.

[118] Matyba, P., Yamaguchi, H., Eda, G., Chhowalla, M., Edman, L., & Robinson, N. D. (2010). Graphene and mobile ions: the key to all-plastic, solution-processed light-emitting devices. *Acs Nano*, *4*(2), 637-642.
[119] Becerril, H. A., Mao, J., Liu, Z., Stoltenberg, R. M., Bao, Z., & Chen, Y. (2008). Evaluation of solution-processed reduced graphene oxide films as transparent conductors. *ACS nano*, *2*(3), 463-470.
[120] Zhou, G., Wang, D. W., Li, F., Zhang, L., Li, N., Wu, Z. S., ... & Cheng, H. M. (2010). Graphene-wrapped Fe3O4 anode material with improved reversible capacity and cyclic stability for lithium ion batteries. *Chemistry of Materials*, *22*(18), 5306-5313.
[121] Bo, Z., Shuai, X., Mao, S., Yang, H., Qian, J., Chen, J., ... & Cen, K. (2014). Green preparation of reduced graphene oxide for sensing and energy storage applications. *Scientific reports*, *4*, 4684.
[122] Li, W., Wang, F., Feng, S., Wang, J., Sun, Z., Li, B., ... & Zhao, D. (2013). Sol–gel design strategy for ultradispersed TiO2 nanoparticles on graphene for high-performance lithium ion batteries. *Journal of the American Chemical Society*, *135*(49), 18300-18303.
[123] McCoy, T. M., Brown, P., Eastoe, J., & Tabor, R. F. (2015). Noncovalent magnetic control and reversible recovery of graphene oxide using iron oxide and magnetic surfactants. *ACS applied materials & interfaces*, *7*(3), 2124-2133.
[124] Le, N. H., Seema, H., Kemp, K. C., Ahmed, N., Tiwari, J. N., Park, S., & Kim, K. S. (2013). Solution-processable conductive micro-hydrogels of nanoparticle/graphene platelets produced by reversible self-assembly and aqueous exfoliation. *Journal of Materials Chemistry A*, *1*(41), 12900-12908.
[125] Zubir, N. A., Yacou, C., Motuzas, J., Zhang, X., & Da Costa, J. C. D. (2014). Structural and functional investigation of graphene oxide–Fe3O4 nanocomposites for the heterogeneous Fenton-like reaction. *Scientific reports*, *4*, 4594.
[126] Yin, P. T., Shah, S., Chhowalla, M., & Lee, K. B. (2015). Design, synthesis, and characterization of graphene–nanoparticle hybrid materials for bioapplications. *Chemical reviews*, *115*(7), 2483-2531.
[127] Yin, P. T., Shah, S., Chhowalla, M., & Lee, K. B. (2015). Design, synthesis, and characterization of graphene–nanoparticle hybrid materials for bioapplications. Chemical reviews, 115(7), 2483-2531.
[128] Jung, H. S., Kong, W. H., Sung, D. K., Lee, M. Y., Beack, S. E., Keum, D. H., ... & Hahn, S. K. (2014). Nanographene oxide–hyaluronic acid conjugate for photothermal ablation therapy of skin cancer. *ACS nano*, *8*(1), 260-268.
[129] Nikaido, H. (2009). Multidrug Resistance in Bacteria. *Annual Review of Biochemistry*, *78*(1), 119–146.
[130] Retrieved from: https://amr-review.org Access: *April 2020*
[131] Davies, J., & Davies, D. (2010). Origins and Evolution of Antibiotic Resistance. *Microbiology and Molecular Biology Reviews*, *74*(3), 417–433.
[132] World Health Organization (WHO) http://www.who.int/news-room/fact-sheets/detail/antibiotic-resistance. Access: *April* 2018.
[133] The Review on Antimicrobial Resistance (AMR) https://amr-review.org/. Access October 16th 2018.
[134] Madkour, A. E., Dabkowski, J. M., Nüsslein, K., & Tew, G. N. (2009). Fast disinfecting antimicrobial surfaces. *Langmuir*, *25*(2), 1060–1067.
[135] Zaman, S. Bin, Hussain, M. A., Nye, R., Mehta, V., Mamun, K. T., & Hossain, N. (2017). A Review on Antibiotic Resistance: Alarm Bells are Ringing. *Cureus*.

[136] Levy, S. B., & Bonnie, M. (2004). Antibacterial resistance worldwide: Causes, challenges and responses. *Nature Medicine*, *10*(12S), S122–S129.
[137] Appelbaum, P. C. (2006). The emergence of vancomycin-intermediate and vancomycin-resistant Staphylococcus aureus. *Clinical Microbiology and Infection*, *12*(SUPPL. 1), 16–23.
[138] Wright, M. O., Hebden, J. N., Allen-Bridson, K., Morrell, G. C., & Horan, T. C. (2012). An American Journal of Infection Control and National Healthcare Safety Network data quality collaboration: A supplement of new case studies. *American Journal of Infection Control*, *40*(5 SUPPL.), S32–S40.
[139] Epstein, F. H., Jacoby, G. A., & Archer, G. L. (1991). New Mechanisms of Bacterial Resistance to Antimicrobial Agents. *New England Journal of Medicine*, *324*(9), 601–612.
[140] Theuretzbacher U. (2011) Resistance drives antibacterial drug development. *Current Opinion in Pharmacology* 11:433–8.
[141] Theuretzbacher, U. (2013). Journal of Global Antimicrobial Resistance Global antibacterial resistance: The never-ending story. *Integrative Medicine Research*, *1*(2), 63–69.
[142] Yousefi, M., Dadashpour, M., Hejazi, M., Hasanzadeh, M., Behnam, B., de la Guardia, M., … Mokhtarzadeh, A. (2017). Anti-bacterial activity of graphene oxide as a new weapon nanomaterial to combat multidrug-resistance bacteria. Materials Science and Engineering C, 74, 568–581.
[143] Akhavan O, Ghaderi E, Esfandiar A (2011) Wrapping bacteria by graphene nanosheets for isolation from environment, reactivation by sonication, and inactivation by near-infrared irradiation. J Phys Chem B 115:6279–6288.
[144] Ji H, Sun H, Qu X (2016) Antibacterial applications of graphene-based nanomaterials: Recent achievements and challenges. Adv Drug Deliv Rev 105:176–189.
[145] Liu S, Hu M, Zeng TH, et al (2012) Lateral dimension-dependent antibacterial activity of graphene oxide sheets. Langmuir 28:12364–12372.
[146] Perreault, F., De Faria, A. F., Nejati, S., & Elimelech, M. (2015). Antimicrobial Properties of Graphene Oxide Nanosheets: Why Size Matters. ACS Nano, 9(7), 7226–7236.
[147] Yu, C. H., Chen, G. Y., Xia, M. Y., Xie, Y., Chi, Y. Q., He, Z. Y., … Peng, Q. (2020). Understanding the sheet size-antibacterial activity relationship of graphene oxide and the nano-bio interaction-based physical mechanisms. Colloids and Surfaces B: Biointerfaces, 191(February), 111009.
[148] Akhavan, O., Ghaderi, E., & Esfandiar, A. (2011). Wrapping bacteria by graphene nanosheets for isolation from environment, reactivation by sonication, and inactivation by near-infrared irradiation. Journal of Physical Chemistry B, 115(19), 6279–6288.
[149] Sengupta, I., Bhattacharya, P., Talukdar, M., Neogi, S., Pal, S. K., & Chakraborty, S. (2019). Bactericidal effect of graphene oxide and reduced graphene oxide: Influence of shape of bacteria. Colloids and Interface Science Communications, 28(October 2018), 60–68.
[150] Liu S, Zeng TH, Hofmann M, et al (2011) Antibacterial activity of graphite, graphite oxide, graphene oxide, and reduced graphene oxide: Membrane and oxidative stress. ACS Nano 5:6971–6980.
[151] Kurantowicz, N., Sawosz, E., Jaworski, S., Kutwin, M., Strojny, B., Wierzbicki, M., ... & Jagiełło, J. (2015). Interaction of graphene family materials with Listeria monocytogenes and Salmonella enterica. Nanoscale research letters, 10(1), 23.

[152] Krishnamoorthy, K., Veerapandian, M., Zhang, L. H., Yun, K., & Kim, S. J. (2012). Antibacterial efficiency of graphene nanosheets against pathogenic bacteria via lipid peroxidation. The journal of physical chemistry C, 116(32), 17280-17287.
[153] He, J., Zhu, X., Qi, Z., Wang, C., Mao, X., Zhu, C., ... & Tang, Z. (2015). Killing dental pathogens using antibacterial graphene oxide. *ACS applied materials & interfaces*, *7*(9), 5605-5611.
[154] Chen, J., Peng, H., Wang, X., Shao, F., Yuan, Z., & Han, H. (2014). Graphene oxide exhibits broad-spectrum antimicrobial activity against bacterial phytopathogens and fungal conidia by intertwining and membrane perturbation. *Nanoscale*, *6*(3), 1879-1889.
[155] Szunerits S, Boukherroub R (2016) Antibacterial activity of graphene-based materials. J Mater Chem B 4:6892–6912.
[156] Lemire JA, Harrison JJ, Turner RJ (2013) Antimicrobial activity of metals: Mechanisms, molecular targets and applications. Nat Rev Microbiol 11:371–384
[157] Shan C, Yang H, Han D, et al (2009) Water-soluble graphene covalently functionalized by biocompatible poly-L-lysine. Langmuir 25:12030–12033.
[158] Li P, Sun S, Dong A, et al (2015) Developing of a novel antibacterial agent by functionalization of graphene oxide with guanidine polymer with enhanced antibacterial activity. Appl Surf Sci 355:446–452.
[159] Vasilev, K., Cook, J., & Griesser, H. J. (2009). Antibacterial surfaces for biomedical devices. *Expert Review of Medical Devices*, *6*(5), 553–567.
[160] Perreault, F., Jaramillo, H., Xie, M., Ude, M., Nghiem, L. D., & Elimelech, M. (2016). Biofouling Mitigation in Forward Osmosis Using Graphene Oxide Functionalized Thin-Film Composite Membranes. *Environmental Science and Technology*, *50*(11), 5840–5848.
[161] Feng, L., Yang, X., Shi, X., Tan, X., Peng, R., Wang, J., & Liu, Z. (2013). Polyethylene glycol and polyethylenimine dual-functionalized nano-graphene oxide for photothermally enhanced gene delivery. *Small*, *9*(11), 1989-1997.
[162] Li, P., Sun, S., Dong, A., Hao, Y., Shi, S., Sun, Z., ... & Chen, Y. (2015). Developing of a novel antibacterial agent by functionalization of graphene oxide with guanidine polymer with enhanced antibacterial activity. *Applied Surface Science*, *355*, 446-452.

CHAPTER 2

REACTION OF GRAPHENE OXIDE WITH GLYCINE: FUNCTIONALIZATION OR REDUCTION?

2.1 Study of the GO functionalization with glycine

In this chapter the study of GO functionalization and reduction using glycine as a model amino acid is performed. As it was mentioned in section 1.2.1, amino acids can be used for functionalization or reduction of GO because they can improve important properties for many applications including biocompatibility, depollution, and catalysis. Indeed, amino acids are important reducing agents because they are environmentally friendly and open new pathways for "green chemistry". However, some questions arise during the functionalization of GO with amino acids including What is the most favorable route when an amino acid is put in contact with GO, the GO functionalization or the GO reduction? Under which conditions we can turn from functionalization to reduction? And even more important, would it be possible to functionalize the GO with amino acids towards the basal plane, in specific, to the epoxide groups without alter the carboxylic acids?

For this purpose, the glycine was tested in different concentrations under basic medium at room temperature. Figure 2.1 shows a scheme of the experimental procedure followed.

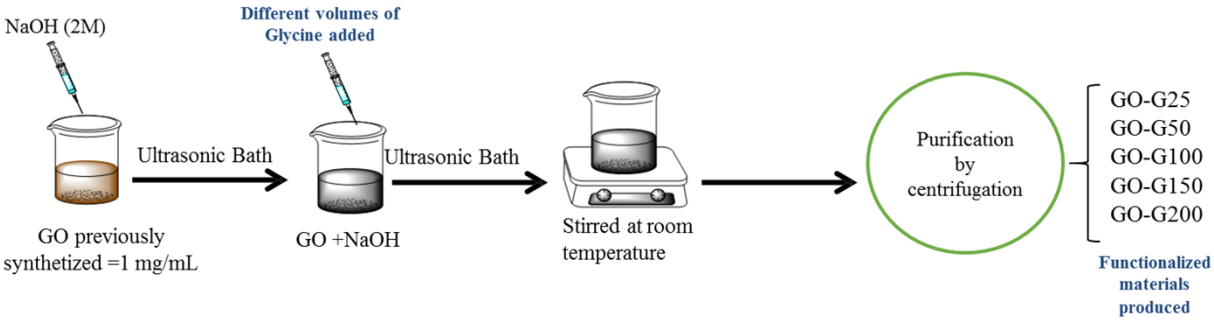

Figure 2.1 Schematic representation of the functionalization/reduction of GO.

The first step of the functionalization/reduction of GO involves the addition of NaOH solution (2 M) to a GO solution using water suspensions. This step allowed the production of sodium carboxylates, which could reduce the interaction between the carboxylic acids of GO and the glycine. After 5 min, a glycine solution was added under the sonication. Different

concentrations of glycine were tested in the final reaction mixture, ranging from 0.25, 0.5, 1, 1.5 and 2 mg/mL. The reaction was performed during for 4 h at room temperature. At the end of this time, each functionalized GO with glycine was washed with ethanol and then with acid water (pH=2, prepared with HCl) by centrifugation. This procedure allowed the removal of basic residues as well as Na^+ from carboxylates formed during the neutralization with NaOH. The obtained materials were labeled GO-G followed by the percentage of mass glycine added (GO-G25, GO-G50, GO-G100, etc.). Finally, the materials were characterized by ATR-FTIR, Raman spectroscopy and XPS. For more details of the methodology see appendix A.1.

2.2 Characterization of the reaction between GO and glycine by ATR-FTIR, Raman spectroscopy and XPS

ATR-FTIR analysis

The first part of the characterization ATR-FTIR is presented in Figure 2.2a, where pristine GO exhibited the bands at 1723 cm^{-1}, 1621 cm^{-1}, 1221 cm^{-1} and 969 cm^{-1} and 1048 cm^{-1} assigned to carboxylic acid groups (OH-C=O) [1], graphitic domains (C=C) [1], the epoxide groups (C-O-C) [2-5], and C-OH for either hydroxyl groups or phenols [1,2]. The band at 1221 cm^{-1} has been attributed to S=O stretching contribution due to sulfated formed after graphite oxidation [6,7]. However, XPS survey results of Figure A1 and Table A1 show that GO lacked S contribution suggesting that, the origin of the band at 1221 cm^{-1} is due to C-O vibration of epoxide groups instead of S=O, as reported elsewhere [2-5].

The ATR-FTIR results of GO-G25 and GO-G50 (Figure 2.2a) exhibited a new band at 1255 cm^{-1} for possible C–N vibrations (bonded to an aromatic ring) [8-11], and a simultaneous decreased at 1221 cm^{-1} and 969 cm^{-1} attributed to epoxide groups [2-5]. This information suggests that, GO-G25 and GO-G50 presented a nucleophilic attack of glycine by ring opening reactions. Moreover, the increase in the intensity of the band of hydroxyl groups at 1048 cm^{-1} confirmed that, ring opening reactions took place, due to this reaction produces an alcohol in the adjacent carbon [12,13]. Besides, GO-G50 presented the symmetric and asymmetric vibration from alkyl chains $–CH_2$ (at 2928 cm^{-1} and 2853 cm^{-1} respectively) and, the strong N atomic percentage (see Figure A1 and Table A1) confirmed the presence of glycine moieties. Notably, the ATR-FTIR of samples GO-100, GO-150 and GO-150 presented the bands of epoxide groups (at 969 cm^{-1}) less intense as compared to pristine GO, as well as a slight increase in the band at 1048 cm^{-1} associated to hydroxyl groups was observed. In addition, GO-100,

GO-150 and GO-150 samples exhibited traces of N atomic contribution in XPS survey (see Figure A1 and Table A1). This information indicates that no glycine was bonded to GO and a partial hydrolysis of epoxide groups was obtained.

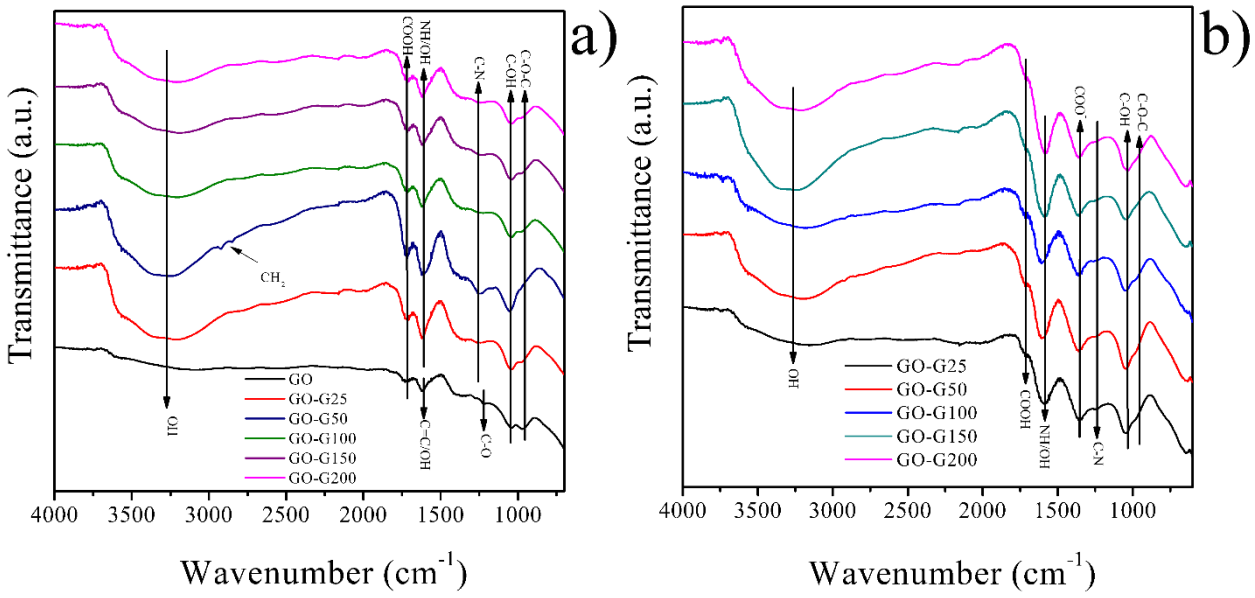

Figure 2.2 GO and GO-G samples characterization: a) ATR-FTIR and b) GO-G samples before the washed step with acid water

On the other hand, in all the GO-G samples no amide bands were detected, which could appear around 1600-1500 cm^{-1} [10,14-16]. The lack of amide groups confirmed that there was no reaction between the glycine and the carboxylic acid groups. This can be attributed to the presence of NaOH that produced the formation of sodium carboxylates [17]. In order to confirm this hypothesis, ATR-FTIR of all the set of experiments GO-G was taken before the washed with acid water, and the results are shown in Figure 2.2b As can be seen in Figure 2.2b, all the samples exhibited an intense band around 1367 cm^{-1} attributed to COO^- species, as well as a low intensity band of the carboxylic acid groups (at 1723 cm^{-1}) [17]. However, the acid washing procedure led to the carboxylic acid band restoration and, a decrease in the intensity of the COO^- band (see Figure 2a) [39]. Thus, these results suggest that the NaOH led in sodium carboxylates and, these species cannot be attacked for a nucleophile because of the resonance of $O=C-O^-$.

Raman spectroscopy characterization

Raman spectroscopy was carried out to follow changes in GO structure due to functionalization or reduction. Figure 2.3 presents Raman spectrum of GO where characteristic *D* and *G* bands were detected at 1364 cm^{-1} and 1600 cm^{-1}, respectively. The *G* band is attributed to graphitic domain whereas *D* band arises for defects on GO layers [17-20]. For the GO-G samples, the Raman information of Figure 2.2b was extracted and the I_D/I_G ratio was calculated in order to observe the whole reduction process (see Table 3.1). The GO-G25 and GO-G50 samples exhibited a downshift in *G* band due to N-type doping [21], whereas GO-G100, GO-G150 and GO-G200 samples the *G* band presented an upshift since less glycine was bonded and predominant oxygen functional groups are in those materials [21,22].

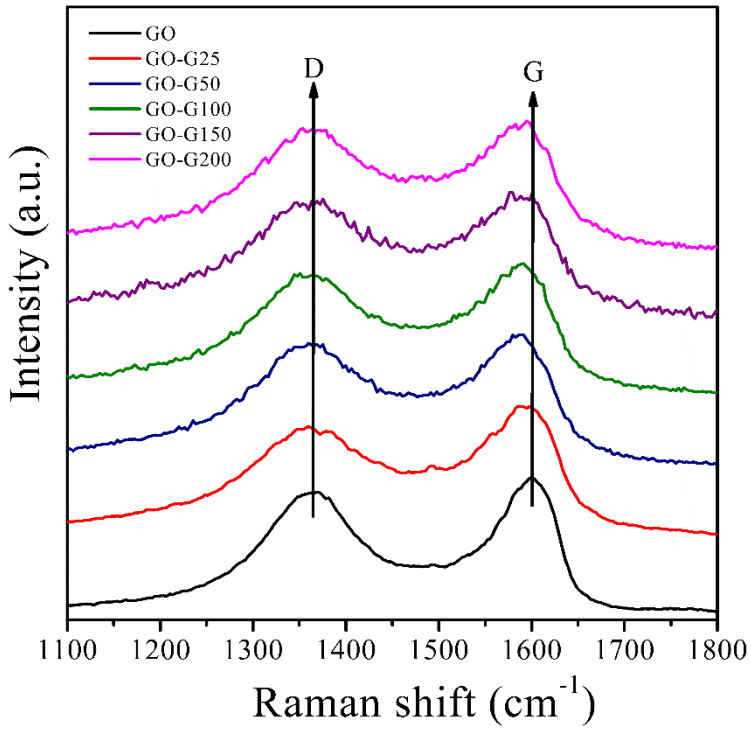

Figure 2.3 GO and GO-G samples characterized by Raman spectroscopy

Besides, GO-G25 and GO-G50 showed an increased in I_D/I_G ratio with the as compared GO, due to slight reduction process that takes place during the functionalization with amine compounds [8,23-25]. Nonetheless, for GO-G100, GO-G150 and GO-G200 the I_D/I_G ratio continues to increase and with the upshift of *G* band, the Raman results suggest that under those conditions, a GO reduction governed the process instead of a functionalization. This conclusion

is supported with the ATR-FTIR where less glycine was bonded to GO for the GO-G100, GO-G150 and GO-G200 samples (see Figure 2.2a).

Table 3.1 Raman information of Figure 2.3

Sample	*G* (cm^{-1})	I_D/I_G
GO	1600	0.903
GO-G25	1595	0.930
GO-G50	1587	0.949
GO-G100	1590	0.972
GO-G150	1593	0.986
GO-G200	1595	0.987

Analysis of XPS information

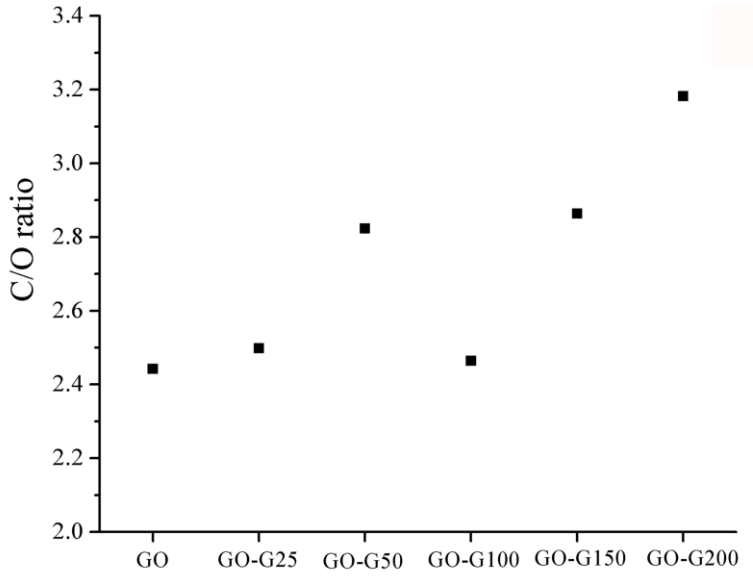

Figure 2.4 C/O atomic ratio obtained from XPS survey of GO and GO-G samples.

The XPS characterization was carried out for the quantitative analyses of elemental composition of the functionalized GO. The relative C/O ratios were calculated (the ratio of the total area of C1s to the total area of O1s), as reported elsewhere [26,27]. As can be seen in Figure 2.4, the C/O ratio increased for the sample GO-G50 which can be attributed to a slight reduction effect of glycine which is consistent with the Raman spectroscopy results (see Figure 2.3). It is worth mentioning that when a functionalization is carried out in GO, a slight increase in C/O ratios has been observed [8,24,25]. This is a constant phenomenon that involves the functionalization of GO when amines are used. Some authors have proposed that the reduction

is governed by the ring opening reaction followed by the elimination of the alcohol group formed in the adjacent carbon [13]. Therefore, GO-G25 and GO-G50 samples exhibited a trend to increase the C/O ratio. However, with higher concentrations of glycine, the C/O ratio decreased and then increased again until a value around 3.2 for GO-G200, which can be attributed to the change in the role of the glycine as reducing agent. Thus, as glycine concentrations increase, it is more probable to have a reduction of GO instead of a functionalization. Previously, the GO reduction using glycine has been published and it was found that glycine can lead a reduction on GO with minimum N contamination in the final material [28]. Hence, the results obtained are consistent with previous studies.

High resolution C1s XPS deconvolution was conducted for GO and GO-G samples using the Lorentzian function after Shirley background correction, as reported elsewhere [13]. In Figure 2.5a, GO was fitted into the following peaks: at 284.2 eV corresponding to C-C/C=C bonds; at 286.2 eV the contributions of epoxide/ether groups; at 287.9 eV the contributions of the carbonyl (C=O); at 289.5 eV the contributions of the carboxylic acid groups (O-C=O) and at 291 eV the π-π* transitions [10,13,24].

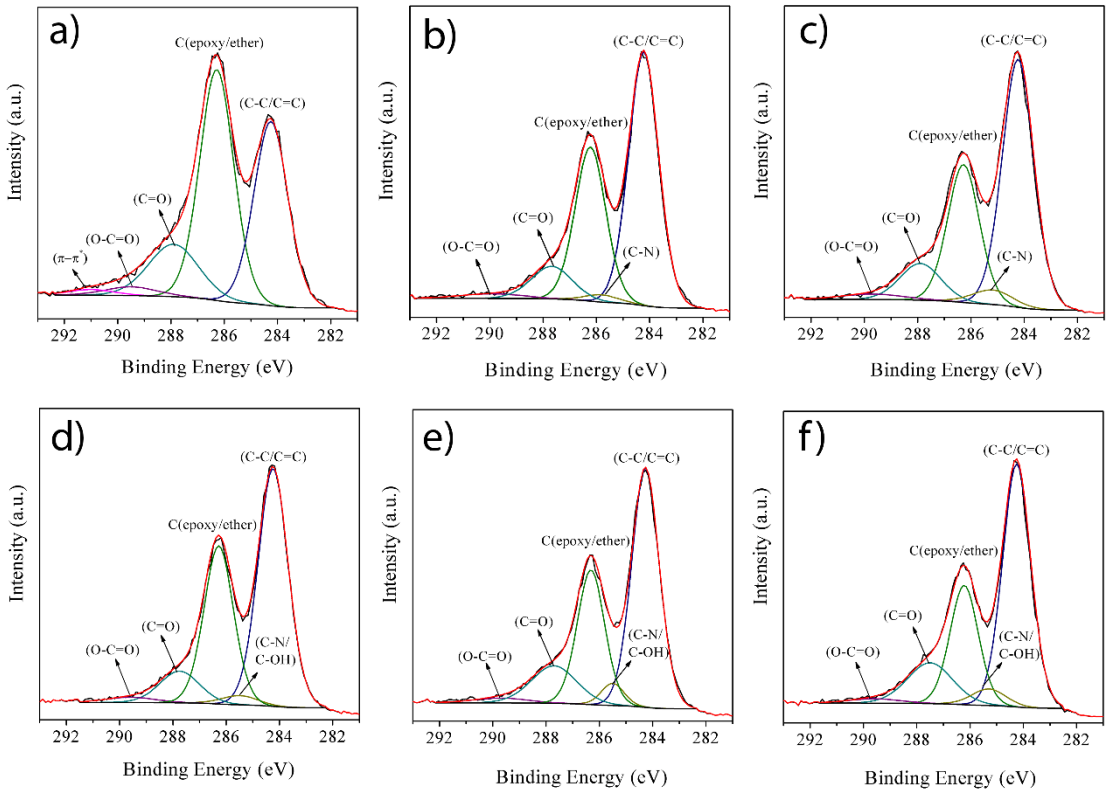

Figure 2.5 De-convoluted C1s XPS spectra of a) GO, b) GO-G25, c) GO-G50, d) GO-G100, e) GO-G150 and f) GO-G200

In the case of the samples GO-G, it was possible to fit a new peak at 285.2 eV, which can be attributed either to C-N and C-OH species [10,13,29]. According to the ATR-FTIR results, low glycine concentrations led a nucleophilic attack on the epoxide groups of GO and thus the peak at 285.2 eV arose because of N-C bonds (see Figure 2.5b and 2.5c). At the same time, the peak at 286.2 eV attributed to epoxide/ether groups decrease in the intensity, confirming the functionalization by ring opening reaction. In addition, samples GO-G100, GO-G150 and GO-G200 were fitted finding a new peak around 285.4 eV (see Figure 2.5d, 2.5e and 2.5f). This can be explained as epoxides partially turned into alcohols because of the basic medium, and thus the peak at 285.5 eV can be attributed to C-OH bonds instead of C-N [3,4]. This information is consistent with the ATR-FTIR where samples GO-G100, GO-G150 and GO-G200 exhibited a slight decrease in the band at 969 cm^{-1}, as compared to GO. Moreover, the GO-G samples were undergone in a change of pH from basic to acid conditions. It has been proposed that a change of pH in GO material from basic to acid conditions, leads in a restoration of oxygen functional groups such as epoxides, alcohols, ketones, aldehydes and carboxylic acids (C-O-C, C-OH, R-C=O, R-(C=O)-R' and O-C=O, which can be generalized as C(O) bonds) of GO in XPS [3]. However, our results did not show a restoration in C(O) bonds, which can be attributed to either functionalization or reduction of GO in presence of glycine. In order to analyze the C(O) bonds, a detailed analysis of the Figure 2.6 was performed by calculating the ratio of the area C(O) bonds to the C=C area, as reported elsewhere [26,27].

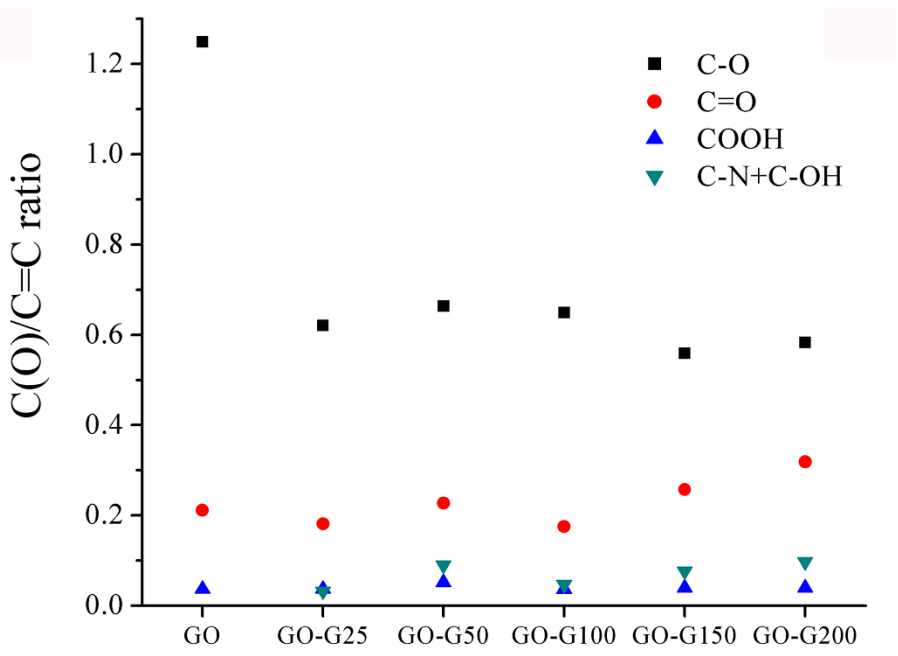

Figure 2.6 Ratio area of C(O) bonds to the C=C bonds

Notably, in Figure 2.6 the contribution of the carbonyls (ketones and aldehydes) and the carboxylic acid groups increased for the GO-G50 sample. This can be attributed to the glycine bonded to GO, as well as the fact that no reaction between carboxylic acid groups of GO with the primary amine of glycine was observed. Furthermore, the Figure 2.6 highlights an increase in the C=O bonds for GO-G100, GO-G150 and GO-G200 samples whereas O-C=O bonds decreased. This information suggests that from ratios 1:1, the glycine reduced the carboxylic acid groups in order to turn them into carbonyl groups.

Table 2.2 Peak area ratio of O-C=O bonds to the C=O bonds in GO and GO-C samples

	Sample					
	GO	GO-G25	GO-G50	GO-G100	GO-G150	GO-G200
O-C=O/C=O	0.174	0.203	0.228	0.209	0.153	0.124

Since the C=O contributions comes from the aldehydes, ketones and carboxylic acid groups, the ratio O-C=O area to C=O was calculated, and the results are presented in Table 2.2. As can be seen in Table 2.2, the GO-G50 sample shows the strongest O-C=O/C=O ratio with respect all the samples due to the presence of covalently bonded glycine. Moreover, the samples GO-G150 and GO-G200 exhibited a trend to decrease the O-C=O/C=O ratio. This information suggests that under basic medium and using GO:G mass ratios from 1:1, the reduction of GO could be governed by the partial hydrolysis of epoxide groups with the subsequent reduction of carboxylic acids to carbonyls. This could be the first step of the whole mechanism of reduction of GO in presence of glycine, since the C/O ratios obtained in this work are around 2.4 to 3.2, so far from the values of 10 obtained in previous studies [9,28,30]. It is worth noting that the chemical reductions of GO using amino acids reported involves the addition of heat to stimulate the reduction [9,28]. This study was performed at room temperature, and this could explain why the C/O ratios around 3.0 were obtained. Some additional studies using amino acids for GO reduction avoid heating the reaction, but long reduction periods are required [31,32]. Therefore, since this study was performed at room temperature, the partial hydrolysis of epoxide groups and the subsequent reduction of carboxylic acids to carbonyls can be associated to the first step of the whole reduction process.

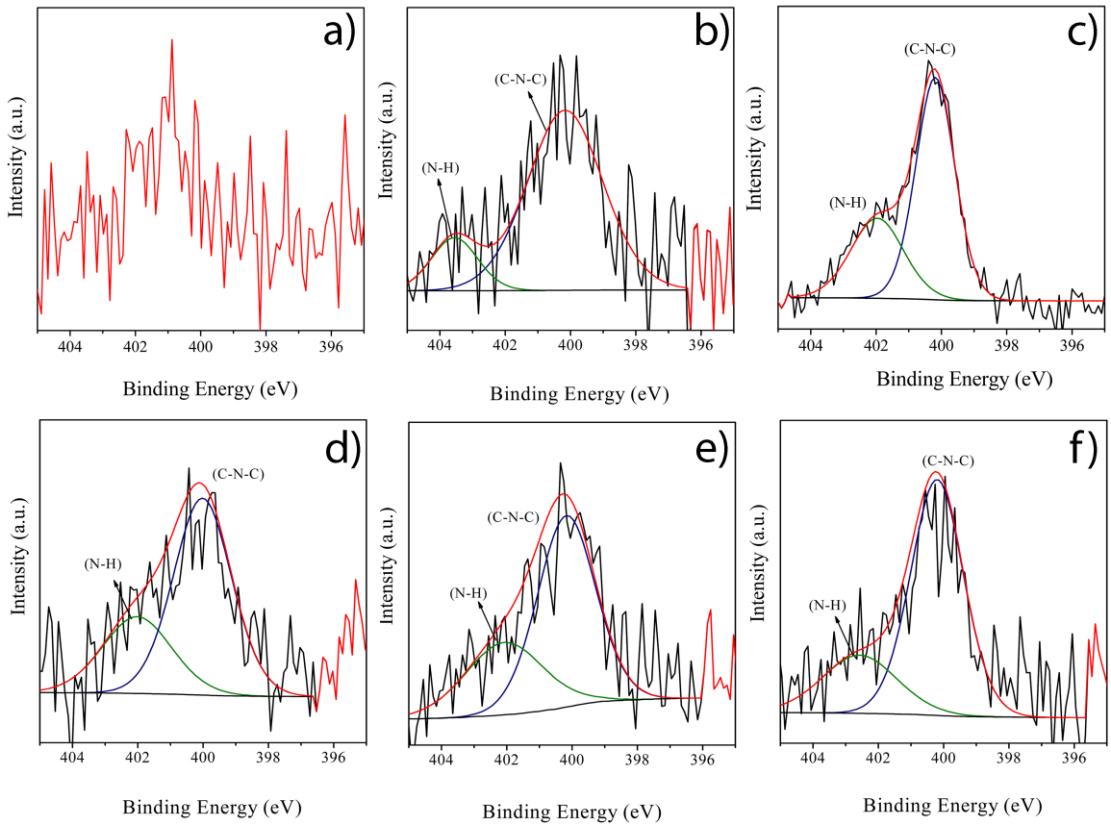

Figure 2.7 N1s XPS spectra deconvolution of: a) GO, b) GO-G25, c) GO-G50, d) GO-G100, e) GO-G150 and f) GO-G200

Glycine can be non-covalently bonded to the GO due to H-bonding and electrostatic forces of some functional groups such as alcohols, carboxylic acids and epoxide groups with the primary amine of glycine [33,34]. Therefore, the N1s deconvolution was performed for GO-G materials, in order to corroborate the covalent bonds formed. In the case of GO, no significant contributions of C-N were detected (see Figure 2.7a), whereas GO-G samples showed the peaks at 400.2 and 401.7 eV attributed to the N-C and N-H bonds of secondary amines [8,9,35,36]. When glycine is adsorbed in a substrate shows an intense peak around 402.5 eV, attributed to -NH_3^+ due to the protonated amino groups of glycine [37]. This information confirms that the glycine was chemically bonded to GO, since GO-G samples exhibit the peak at 401.7 eV less intense as compared to the peak at 400.2 eV. In addition, samples GO-G100, GO-G150 and GO-G200 presented traces of N atomic contribution, which is consistent with previous studies where amino acids have been used for GO reduction [29,32,38]. Since traces of the glycine were detected in GO-G100, GO-G150 and GO-G200 samples, the controlled reduction of the GO led to less contamination of the reducing agent in the final material. Regardless of GO functionalization/reduction with glycine can achieve a stronger N atomic contribution [9], this

work highlights that the reaction conditions could lead to covalent bonds (i.e. GO-G50 sample) or a reduction process instead, with low traces of the reducing agent (i.e. GO-G100, GO-G150, GO-G200 samples).

2.3 Proposed Mechanism of the reduction and functionalization of GO in presence of glycine

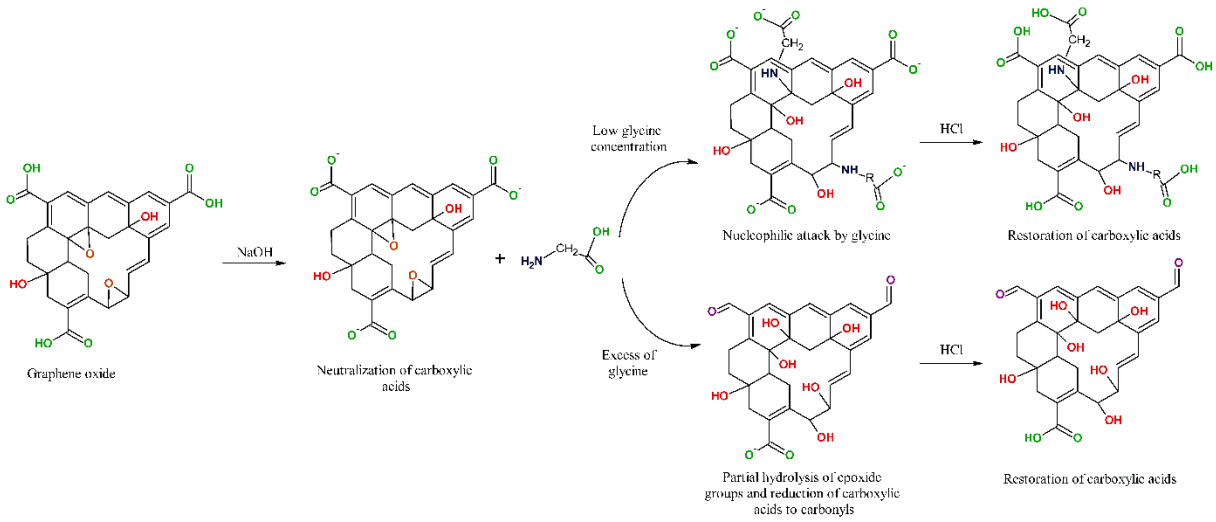

Figure 2.8 Proposed reaction and reduction scheme between GO and glycine under basic medium.

The literature, there are some proposals for the reaction and the reduction of GO using amino acids. However, the exact mechanisms by which the functionalization and the reduction occur remain uncertain [13,30,31]. Most of the mechanism proposed are based in classic chemistry based in homogeneous phase. According to the ATR-FTIR, Raman spectroscopy and XPS results presented here point out that, the GO functionalization with glycine under base medium depends on glycine concentration. As can be seen in Figure 2.8, the first step is a neutralization reaction between the carboxylic acid groups of GO and the NaOH. The second step proceeds once glycine was added to the system, and two sceneries can come out: i) when low concentrations of glycine are used a nucleophilic attack on epoxide groups is carried out and ii) high glycine concentration led to GO reduction. Several authors have proposed that primary amines produce epoxide ring opening reactions and a simultaneous interaction with carboxylic acid groups via electrostatic forces leading, in some cases, to the formation of amides [10,13,14,29]. However, the evidence presented here points out that the glycine did not react with the carboxylic acid groups of GO, when the functionalization was performed (see Figure 2.2a). According to the ATR-FTIR results of Figure 2.2a and Figure A1, the formation

of carboxylates ($O=C-O^-$) probably reduced the interaction of carboxylic acids with the primary amine of glycine. This information is evidence of a selective functionalization on epoxide groups of GO keeping the carboxylic acid groups of GO. Nonetheless, an excess in the glycine concentrations produced a GO reduction, that involves the partial hydrolysis of epoxide groups and the subsequent reduction of carboxylic acids to carbonyls. The reduction of the GO has been proposed using green reductants such as ascorbic acid, proteins, and amino acids [9,28,30,39]. Those reducing agents can produce the elimination of oxygen functional groups of GO leading to C/O ratios from 5 until 10 [39]. For instance, the glutathione can produce the reduction of the GO eliminating epoxides and carboxylic acids [40]. In spite of the lack of a proposed mechanism about how carboxylic acids can be reduced, the evidence showed an increase in the C/O ratios and the electrical conductivity of the RGO. Therefore, it is expected that the carboxylic acids of GO could be reduced until their elimination under de presence of a green reducing agent. The XPS results showed an increase of C=O and a simultaneous decrease of -O-C=O which can be associated to a reduction of carboxylic acids to aldehydes. Here, it was proposed that this could be the first step of the whole mechanism of reduction of GO when glycine is used. Finally, when the GO-G materials were washed with acid water, the increased of H^+ concentration led to the recovery of carboxylic acids moieties of GO [3].

2.4 Conclusions in the study of the functionalization and reduction of GO using glycine

In this chapter, a systematical study of the conditions where the glycine can act as a nucleophile or as a reducing agent was conducted. From this study, the following conclusions were established:

- Low glycine concentrations led to a nucleophilic attack on epoxide groups of GO, keeping most of the carboxylic acid groups of GO. This was possible due to the presence of NaOH, which produces carboxylates on GO and these species cannot be attacked for a nucleophile because of the resonance of $O=C-O^-$. Therefore, this approach of covalent functionalization under basic medium faces the problem of the poor chemical control of GO functionalization.
- When the concentration of glycine was increased, a reduction process was observed instead of a functionalization. The reduction mechanism was governed by the partial hydrolysis of epoxide groups with the subsequent reduction of carboxylic acids to carbonyls. This step could be the first part of the whole mechanism of reduction of GO, when glycine is used.
- This study opens the opportunity to understand the GO interaction with amino acids deeply, given that these compounds have been used for greener GO reduction, and that they can improve important GO properties for applications in depollution, therapeutic and diagnostic agents, as well as drug delivery.

BIBLIOGRAPHY

[1] Acik, M.; Lee, G.; Mattevi, C.; Chhowalla, M.; Cho, K.; Chabal, Y.J. Unusual infrared-absorption mechanism in thermally reduced graphene oxide. Nat. Mater. 2010, 9, 840–845
[2] Yoo, M.J.; Park, H.B. Effect of hydrogen peroxide on properties of graphene oxide in Hummers method. Carbon N. Y. 2019, 141, 515–522
[3] Taniguchi, T.; Kurihara, S.; Tateishi, H.; Hatakeyama, K.; Koinuma, M.; Yokoi, H.; Hara, M.; Ishikawa, H.; Matsumoto, Y. pH-driven, reversible epoxy ring opening/closing in graphene oxide. Carbon N. Y. 2015, 84, 560–566
[4] Krishnamoorthy, K.; Veerapandian, M.; Yun, K.; Kim, S. J. The Chemical and Structural Analysis of Graphene Oxide with Different Degrees of Oxidation. Carbon N. Y. 2013, 53, 38–49
[5] Wang, J.; Salihi, E. C.; Šiller, L. Green Reduction of Graphene Oxide Using Alanine. Mater. Sci. Eng. C 2017, 72, 1–6
[6] Dimiev, A.; Kosynkin, D. V.; Alemany, L.B.; Chaguine, P.; Tour, J.M. Pristine Graphite Oxide. J. Am. Chem. Soc. 2012, 134, 2815–2822
[7] Eigler, S.; Dotzer, C.; Hof, F.; Bauer, W.; Hirsch, A. Sulfur species in graphene oxide. Chem. - A Eur. J. 2013, 19, 9490–9496
[8] Xin, Q.; Li, Z.; Li, C.; Wang, S.; Jiang, Z.; Wu, H.; Zhang, Y.; Yang, J.; Cao, X. Enhancing the CO2 separation performance of composite membranes by the incorporation of amino acid-functionalized graphene oxide. J. Mater. Chem. A 2015, 3, 6629–6641
[9] Bose, S.; Kuila, T.; Mishra, A.K.; Kim, N.H.; Lee, J.H. Dual role of glycine as a chemical functionalizer and a reducing agent in the preparation of graphene: an environmentally friendly method. J. Mater. Chem. 2012, 22, 9696
[10] Huang, Q.; Zhou, L.; Jiang, X.; Zhou, Y.; Fan, H.; Lang, W. Synthesis of copper graphene materials functionalized by amino acids and their catalytic applications. ACS Appl. Mater. Interfaces 2014, 6, 13502–13509
[11] Ouyang, Y.; Cai, X.; Shi, Q.S.; Liu, L.; Wan, D.; Tan, S.; Ouyang, Y. Poly-l-lysine-modified reduced graphene oxide stabilizes the copper nanoparticles with higher water-solubility and long-term additively antibacterial activity. Colloids Surfaces B Biointerfaces 2013, 107, 107–114
[12] Thomas, H.R.; Marsden, A.J.; Walker, M.; Wilson, N.R.; Rourke, J.P. Sulfur-functionalized graphene oxide by epoxide ring-opening. Angew. Chemie - Int. Ed. 2014, 53, 7613–7618
[13] Kim, N.H.; Kuila, T.; Lee, J.H. Simultaneous reduction, functionalization and stitching of graphene oxide with ethylenediamine for composites application. J. Mater. Chem. A 2013, 1, 1349–1358
[14] Liu, Y.; Sajjadi, B.; Chen, W.-Y.; Chatterjee, R. Ultrasound-assisted amine functionalized graphene oxide for enhanced CO2 adsorption. Fuel 2019, 247, 10–18
[15] Lee, J. U.; Lee, W.; Yi, J. W.; Yoon, S. S.; Lee, S. B.; Jung, B. M.; Kim, B. S.; Byun, J. H. Preparation of Highly Stacked Graphene Papers via Site-Selective Functionalization of Graphene Oxide. J. Mater. Chem. A 2013, 1 (41), 12893

[16] Najafi, F.; Moradi, O.; Rajabi, M.; Asif, M.; Tyagi, I.; Agarwal, S.; Gupta, V.K. Thermodynamics of the adsorption of nickel ions from aqueous phase using graphene oxide and glycine functionalized graphene oxide. J. Mol. Liq. 2015, 208, 106–113
[17] Cançado, L.G.; Jorio, A.; Ferreira, E.H.M.; Stavale, F.; Achete, C.A.; Capaz, R.B.; Moutinho, M.V.O.; Lombardo, A.; Kulmala, T.S.; Ferrari, A.C. Quantifying defects in graphene via Raman spectroscopy at different excitation energies. Nano Lett. 2011, 11, 3190–3196
[18] Kudin, K.N.; Ozbas, B.; Schniepp, H.C.; Prud'Homme, R.K.; Aksay, I. a; Car, R. Raman spectra of graphite oxide and functionalized graphene sheets. Nano Lett. 2008, 8, 36–41
[19] Claramunt, S.; Varea, A.; López-Díaz, D.; Velázquez, M.M.; Cornet, A.; Cirera, A. The importance of interbands on the interpretation of the raman spectrum of graphene oxide. J. Phys. Chem. C 2015, 119, 10123–10129
[20] Sadezky, A.; Muckenhuber, H.; Grothe, H.; Niessner, R.; Pöschl, U. Raman microspectroscopy of soot and related carbonaceous materials: Spectral analysis and structural information. Carbon N. Y. 2005, 43, 1731–1742
[21] Liu, H.; Liu, Y.; Zhu, D. Chemical doping of graphene. J. Mater. Chem. 2011, 21, 3335–3345
[22] Guerrero-Contreras, J.; Caballero-Briones, F. Graphene oxide powders with different oxidation degree, prepared by synthesis variations of the Hummers method. Mater. Chem. Phys. 2015, 153, 209–220
[23] Vacchi, I.A.; Guo, S.; Raya, J.; Bianco, A.; Ménard-Moyon, C. Strategies for the Controlled Covalent Double Functionalization of Graphene Oxide. Chem. – A Eur. J. 2020, 26, 6591–6598
[24] Li, Y.; Bao, L.; Zhou, Q.; Ou, E.; Xu, W. Functionalized Graphene Obtained via Thiol-Ene Click Reactions as an Efficient Electrochemical Sensor. ChemistrySelect 2017, 2, 9284–9290
[25] Yi, R.; Yang, R.; Yu, R.; Lan, J.; Chen, J.; Wang, Z.; Chen, L.; Wu, M. Ultrahigh permeance of a chemical cross-linked graphene oxide nanofiltration membrane enhanced by cation-π interaction. RSC Adv. 2019, 9, 40397–40403
[26] Luo, D.; Zhang, G.; Liu, J.; Sun, X. Evaluation criteria for reduced graphene oxide. J. Phys. Chem. C 2011, 115, 11327–11335
[27] Salazar-Aguilar, A.D.; Tristan, F.; Labrada-Delgado, G.J.; Meneses-Rodríguez, D.; Vega-Díaz, S.M. Three-dimensional structure made with nitrogen doped reduced graphene oxide with spherical porous morphology. Carbon N. Y. 2019, 149, 86–92
[28] Kumar, A.; Khandelwal, M. Amino acid mediated functionalization and reduction of graphene oxide-synthesis and the formation mechanism of nitrogen-doped graphene. New J. Chem. 2014, 38, 3457–3467
[29] Xue, B.; Zhu, J.; Liu, N.; Li, Y. Facile functionalization of graphene oxide with ethylenediamine as a solid base catalyst for Knoevenagel condensation reaction. Catal. Commun. 2015, 64, 105–109
[30] Thakur, S.; Karak, N. Alternative methods and nature-based reagents for the reduction of graphene oxide - a review Suman Thakur and Niranjan Karak *. Carbon N. Y. 2015, 94, 224–242

[31] Chen, D.; Li, L.; Guo, L. An environment-friendly preparation of reduced graphene oxide nanosheets via amino acid. Nanotechnology 2011, 22
[32] Mallakpour, S.; Abdolmaleki, A.; Borandeh, S. Covalently functionalized graphene sheets with biocompatible natural amino acids. Appl. Surf. Sci. 2014, 307, 533–542
[33] Wang, M.H.; Guo, Y.N.; Wang, Q.; Zhang, X.S.Y.; Huang, J.J.; Lu, X.; Wang, K.F.; Zhang, H.P.; Leng, Y. Density functional theory study of interactions between glycine and TiO2/graphene nanocomposites. Chem. Phys. Lett. 2014, 599, 86–91
[34] Rossi-Fernández, A.C.; Villegas-Escobar, N.; Guzmán-Angel, D.; Gutiérrez-Oliva, S.; Ferullo, R.M.; Castellani, N.J.; Toro-Labbé, A. Theoretical study of glycine amino acid adsorption on graphene oxide. J. Mol. Model. 2020, 26
[35] Zhang, W.; Zhao, Q.; Liu, T.; Gao, Y.; Li, Y.; Zhang, G.; Zhang, F.; Fan, X. Phosphotungstic Acid Immobilized on Amine-Grafted Graphene Oxide as Acid/Base Bifunctional Catalyst for One-Pot Tandem Reaction. Ind. Eng. Chem. Res. 2014, 53, 1437–1441
[36] Ravi, S.; Zhang, S.; Lee, Y.R.; Kang, K.K.; Kim, J.M.; Ahn, J.W.; Ahn, W.S. EDTA-functionalized KCC-1 and KIT-6 mesoporous silicas for Nd3+ ion recovery from aqueous solutions. J. Ind. Eng. Chem. 2018, 67, 210–218
[37] Tzvetkov, G.; Netzer, F.P. X-ray induced irradiation effects in glycine thin films: A time-dependent XPS and TPD study. J. Electron Spectros. Relat. Phenomena 2010, 182, 41–46
[38] Zhou, W.; Zhuang, W.; Ge, L.; Wang, Z.; Wu, J.; Niu, H.; Liu, D.; Zhu, C.; Chen, Y.; Ying, H. Surface functionalization of graphene oxide by amino acids for Thermomyces lanuginosus lipase adsorption. J. Colloid Interface Sci. 2019, 546, 211–220
[39] De Silva, K. K. H., Huang, H.-H., Joshi, R. K., & Yoshimura, M. (2017). Chemical reduction of graphene oxide using green reductants. Carbon, 119, 190–199.
[40] Pham, T. A., Kim, J. S., Kim, J. S., & Jeong, Y. T. (2011). One-step reduction of graphene oxide with L-glutathione. Colloids and Surfaces A: Physicochemical and Engineering Aspects, 384(1-3), 543-548.

CHAPTER 3

PHOTOCHEMICAL FUNCTIONALIZATION OF GRAPHENE OXIDE BY THIOL-ENE CLICK CHEMISTRY

This chapter is focused on the development of new approaches for GO functionalization using TER as a tool for coupling CA to the unsaturated system of GO. For this, a photoinitiator (PI) was used under UV radiation to promote the R-S• formation and the subsequent functionalization. This functionalization is known as thiol-ene radical addition (TERA) and brings a rapid and selective reaction under mild conditions, avoiding a GO reduction and opening the possibility to develop dual functionalized materials in a second step. Generally, TERA has been used for the functionalization of GO using thermal radical initiator such as AIBN or microwave that implies the use of a great quantity of energy (heat). This could produce a release of some oxygen functional groups in form of CO_2 or CO during the reaction. In the case of AIBN, long reaction times are required for the successful functionalization. Since the functional groups of GO are the basis for the generation of novel materials based on GO, there is an interest to functionalize specific functional groups without alteration of the rest of the GO chemistry. Thus, the use of a PI could bring a simple and alternative pathway for the selective functionalization of GO.

The functionalization of GO by TERA was performed adding Irgacure 369 to promote the photochemical functionalization and adding simultaneously cysteamine (CA) under non-polar solvent (dimethylformamide) (see Figure 3.1). The three solutions were mixed in a beaker and put inside of the UV-chamber during 60 min, under stirring. In order to analyze the impact of the PI during the functionalization, two additional experiments were carried out: i) without adding PI but exposing the reaction mixture to UV light during 60 min and ii) without adding PI and carrying the reaction under darkness and stirring. These experiments are the respective blanks to follow the impact of the UV radiation and then the addition of the PI. Here, it is worth highlight that the reaction proceeded in one hour which is much lower that the time required when thermal radical initiators are used (generally between 12 and 24 h of reaction).

To follow the CA moieties bonded towards the alkene groups of GO, a novel method was proposed to detect the primary amine that remains after the reaction. Figure 3.1b presents a schematic representation of the fluorescent labelling method applied. Using fluorescamine, it is possible to monitor in just a few seconds the CA molecules bonded towards GO when a PI was added to the rection, and in the subsequent experiments in absence of PI and under darkness.

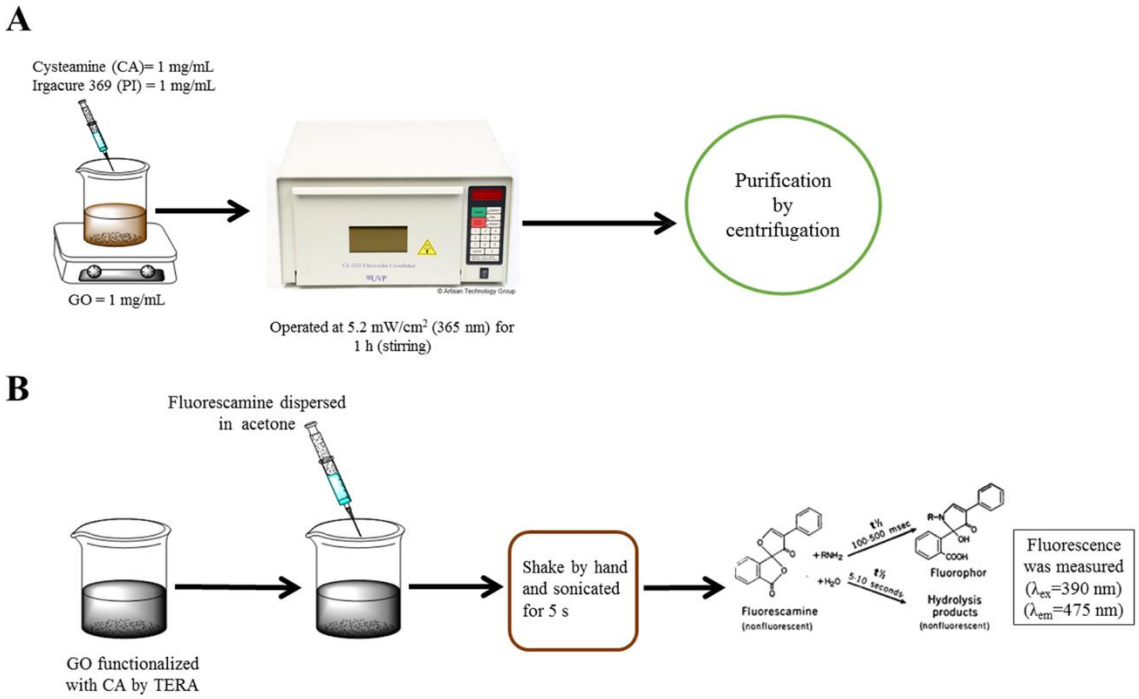

Figure 3.1 a) Scheme of the functionalization of GO with CA using PI as radical initiator and b) fluorescent labelling for the detection of CA moieties using fluorescamine.

As it was mentioned, the functionalization of GO has been carried out using AIBN. Therefore, here it was also compared the GO functionalization using PI and AIBN. The functionalization of GO with CA using AIBN was carried out using the same molar concentration than when PI was used.

Finally, TERA was carried out testing another two thiol compounds: L-cysteine (LC) and 2-(Dimethylamino)ethanethiol hydrochloride (MEDA). The functionalization was conducted as shown in Figure 3.1a.

All the experiments developed in this chapter are summarized in Table 3.1 with the respective conditions and labels. For more details of the experimental procedure see appendix A.1.

Table 3.1 Summary of the reaction conditions for the different samples prepared.

Label	Description	GO (mg/mL)	Thiol[a]	Radical initiator[b]	UV radiation (min)
GO-CA-PI	GO functionalized with CA adding PI	1	CA	PI	60
GO-CA	GO functionalized with CA without PI	1	CA	/	60
GO-B	GO functionalized with CA without PI and under darkness	1	CA	/	/
GO-CA-AIBN	GO functionalized with CA adding AIBN	1	CA	AIBN[c]	/
GO-MEDA	GO functionalized with MEDA adding PI	1	MEDA	PI	60
GO-LC	GO functionalized with LC adding PI	1	LC	PI	60

[a]Thiols were used at concentration of 2 mg/mL giving a final GO : thiol mass ratio 1:1
[b]$3x10^{-5}$ mol of photoinitiator or and thermal initiator were used
[c]Thermal radical initiator was used heating at 70 ºC during 12 h.

The materials presented in Table 3.1 were characterized by Scanning Transmission Electron Microscopy (STEM), ATR-FTIR, UV-spectroscopy, Raman spectroscopy, fluorescent labelling and XPS. The next sections discuss in detail the results obtained from the photochemical functionalization on GO and the advantages as compared to thermal radical initiators.

3.1 Graphene Oxide functionalization by Thiol-ene Radical Addition

TERA involves the formation of radicals, generated by PI subjected to light, that in turn are transferred to CA leading to the formation of R-S•, due to the low S-H bond dissociation energy of CA (see Figure 3.2) [1,2]. The R-S• species are highly reactive, and they can attack C=C of the GO, producing an alkylthiyl radical on GO. Then, the alkylthiyl radical is stabilized by the addition of one hydrogen or another CA molecule through a chain transfer process [3,4]. Notably, after the chemical functionalization a primary amine remains from de CA molecules bonded to the GO. This primary amine can react with fluorescamine to form a fluorophore on GO layers. Through this characterization, the CA moieties are detected rapidly, and the GO functionalization can be followed. The strategy proposed here is a novel and simple method to characterize GO materials with primary amines.

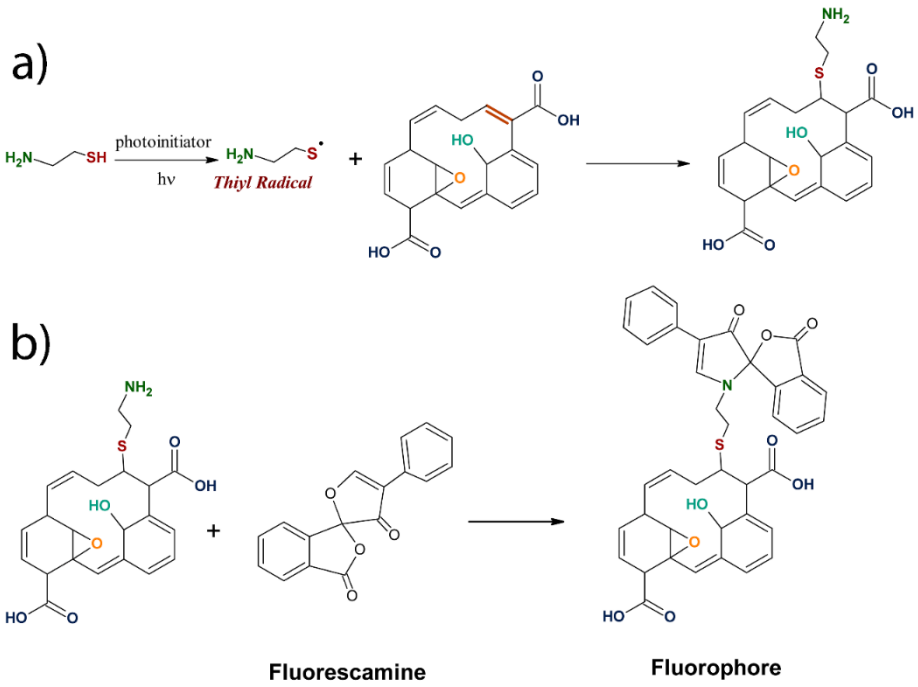

Figure 3.2 a) Reaction of the functionalization of GO with CA by TERA and b) detection of CA on GO by fluorescent labelling.

STEM images

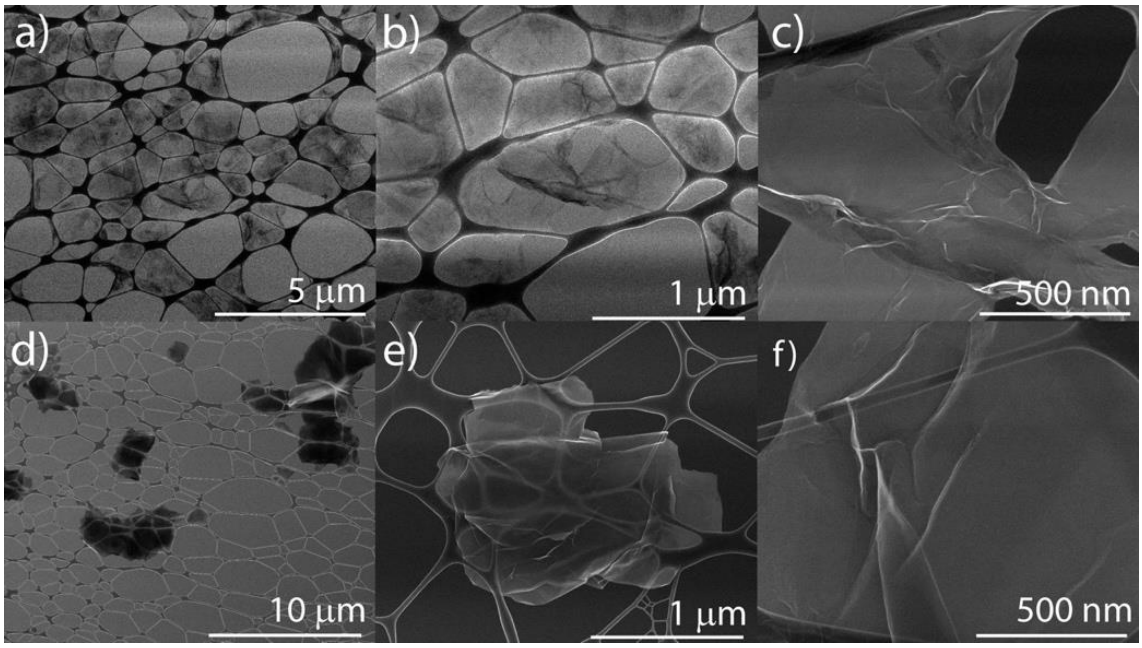

Figure 3.3 STEM images of GO at amplifications: a) 10000x, b) 50000x and c) 100000x. STEM images of GO-CA-PI at amplifications: d) 5000x, e) 40000x and f)100000x.

Figure 3.3 presents STEM images of GO and GO-CA-PI before and after the photochemical functionalization. In Figure 3.3a-3.3c, GO exhibited extended, interconnected, and translucent layers due to low staking. After the chemical functionalization, the GO-CA-PI displays separated structures, that could be formed by stacked sheets functionalized with CA (Figure 3.3d-3.3f). However, no apparent defects on GO layers were detected, suggesting that the mild conditions allowed to preserve the GO layers structure.

ATR-FTIR, Raman spectroscopy, UV-vis spectroscopy, and Fluorescence analysis

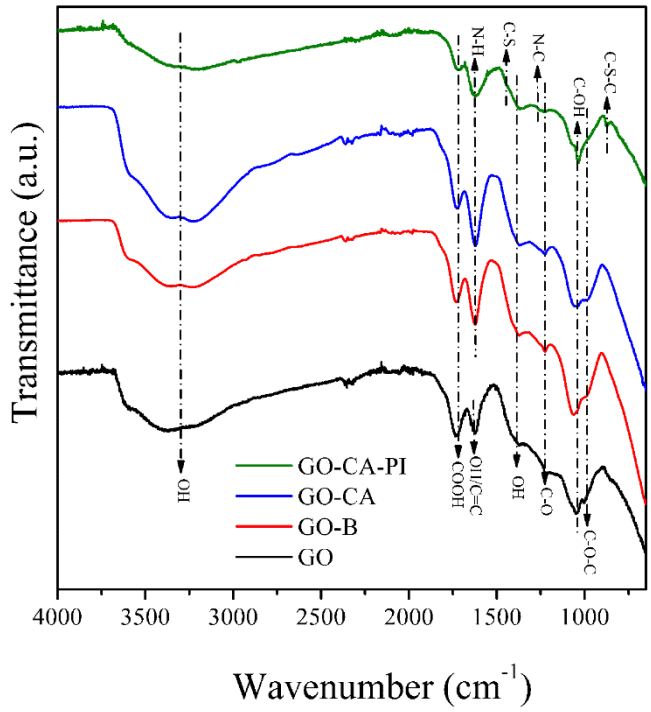

Figure 3.4 ATR-FTIR characterization of the samples GO, GO-B, GO-CA and GO-CA-PI.

The characterization of the chemical species of samples GO-CA-PI, GO-CA, GO-B and GO prepared was carried out by ATR-FTIR, Raman spectroscopy, UV spectroscopy, fluorimetry and XPS. The ATR-FTIR results are presented in Figure 3.4, and GO exhibited the follow bands: O-H stretching vibrations (3312 cm^{-1}), C=O vibrations from carboxylic acid groups (1732 cm^{-1}), C=C bonds and O-H bending vibrations (1622 cm^{-1}), C-O vibrations (1218 cm^{-1}), C-OH vibrations from phenol and alcohol groups (1056 cm^{-1}) and C-O-C asymmetric vibration from epoxy groups (968 cm^{-1}) [5,6]. GO-CA-PI sample showed the most significant changes with two new bands at 1441 cm^{-1} and 710 cm^{-1} attributed to C-S and C-S-C vibrations, respectively [7-9]. This information confirmed the presence of CA moieties bonded on GO.

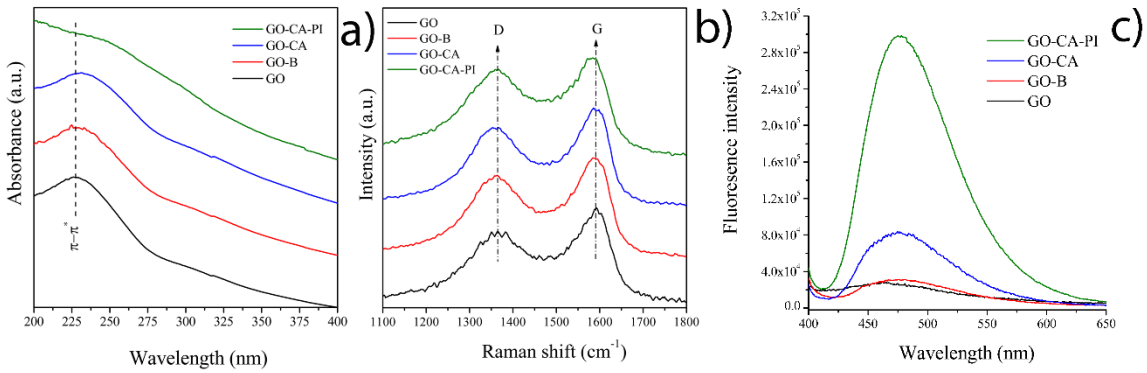

Figure 3.5 Characterization of GO, GO-B, GO-CA and GO-CA-PI samples by: a) UV spectroscopy, b) Raman spectroscopy and b) fluorescence spectrometry (λ_{ex}=390 nm).

UV-Vis spectroscopy characterization was carried out and GO-CA-PI showed a red shift in the broad peak attributed to the plasmon C=C (labeled as π-π*) until 250 nm, as compared to GO (see Figure 3.5a). The change in the maximum position of the plasmon C=C can be attributed to the alkyl chains of CA, which can interact with the GO graphitic domain leading to a red shift, as reported elsewhere [7]. Besides, GO-B preserved the position of the peak at 228 nm confirming that there was no reaction between the GO and CA under darkness by TER.

On the other hand, Figure 3.5b shows the Raman spectrum for the different samples, where GO exhibited the characteristics *D* and *G* band at 1364 cm^{-1} and 1593 cm^{-1}, respectively. D band arises due to the defects in the graphene sheets, in this case due to the change in the hybridization from sp^2 to sp^3 [10,11]. The Raman information was extracted, and the A_D/A_G was calculated for all the samples, and the results are presented in Table 3.2. The change in A_D/A_G allows to observe the contribution of interbands located under *D* and *G* bands, attributed to the introduction of defects such as change in the hybridization from sp^2 to sp^3 [10-12]. GO-CA-PI sample exhibited a blue shift in G band, whereas a slight shift was detected for GO-CA and GO-B samples (see Table 3.2). The blue shift can be attributed to the presence of amine groups from CA on GO layers that produces N-type doping [13,14]. In addition, it was found a similar A_D/A_G ratio in GO and GO-B samples, indicating that minimum defects were introduced in the blank experiment. However, GO-CA showed an increased in A_D/A_G ratio, confirming that UV radiation induced a slight introduction of CA moieties on GO. More important, GO-CA-PI exhibited the strongest A_D/A_G ratio corroborating a higher change in the hybridization by the presence of PI. This information is consistent with the UV spectrum results [10-12].

Table 3.2 Information of Raman spectra of Figure 3.5b

Material	G (cm^{-1})	A_D/A_G
GO	1593	1.15
GO-B	1591	1.16
GO-CA	1589	1.3
GO-CA-PI	1583	1.47

After the functionalization, the free primary amine that resulted from the grafting of CA onto GO can be, as well, detected by fluorescence labelling (Figure 3.2b). Indeed, fluorescamine reacts in picoseconds with primary amines in order to form a fluorophore, with an excitation wavelength (λ_{ex}) of 390 nm and a maximum emission (λ_{em}) in 475 nm [15]. The GO-CA-PI sample exhibited the strongest fluorescence signal, followed by GO-CA>GO-B>GO samples (see Figure 3.5c). GO had the lowest fluorescent contribution meaning that the fluorescence signal of GO-CA-PI and GO-PI came from CA moieties on GO. The sequence of the fluorescence intensity found in the different samples followed the same order that as the UV-vis and Raman spectroscopy results, confirming the photochemical functionalization of GO with CA by TERA.

XPS analysis

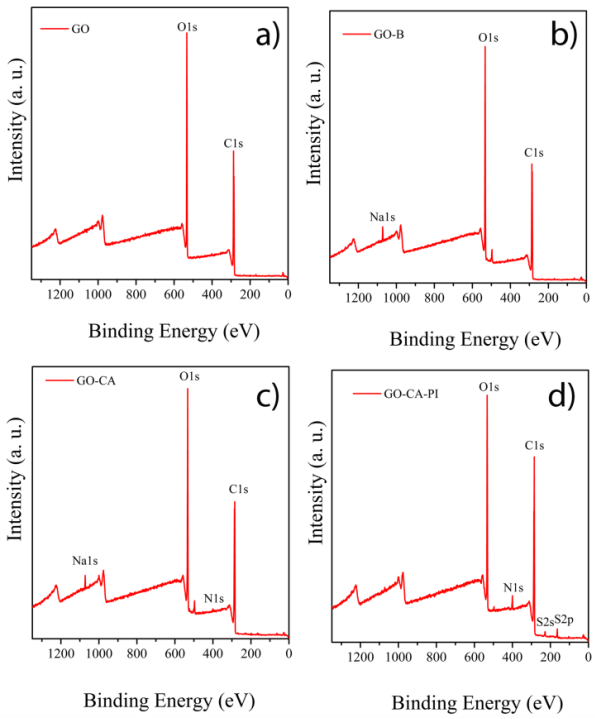

Figure 3.6 XPS survey scan of the samples: a) GO, b) GO-B, c) GO-CA and d) GO-CA-PI.

In order to confirm the presence of CA moieties after the functionalization, XPS characterization was carried out. Figure 3.6 shows the XPS survey results where was possible to detect nitrogen (N) and sulfur (S) contribution in GO-CA and GO-CA-PI samples. Table A2 presents a summary of the survey XPS information and, GO-CA-PI exhibited the strongest S contribution with an atomic percentage around 1.7%, followed by GO-CA>GO-B. This result is consistent with the fluorescence, UV-vis and Raman spectroscopy results. Besides, the low N and S contributions detected for GO-B sample confirmed that no reaction was carried out between GO and CA under darkness.Furthermore, the S2p high resolution XPS deconvolution allowed to confirm the chemical bonds formed after the functionalization. In Figure 3.7, GO-CA and GO-CA-PI were fit in the respective doublet peak at 163.5 eV and 164.8 eV, attributed to $S2p^{3/2}$ and $S2p^{1/2}$ due to C-S-C and C-S bonds [7,8,16,17]. This information confirms that CA was covalently bonded to GO by TER using a PI. It should be highlighted that this functionalization was achieved with just one hour of reaction, whereas classical thermal initiator needs over 12 h of reaction [8,16,18-23].

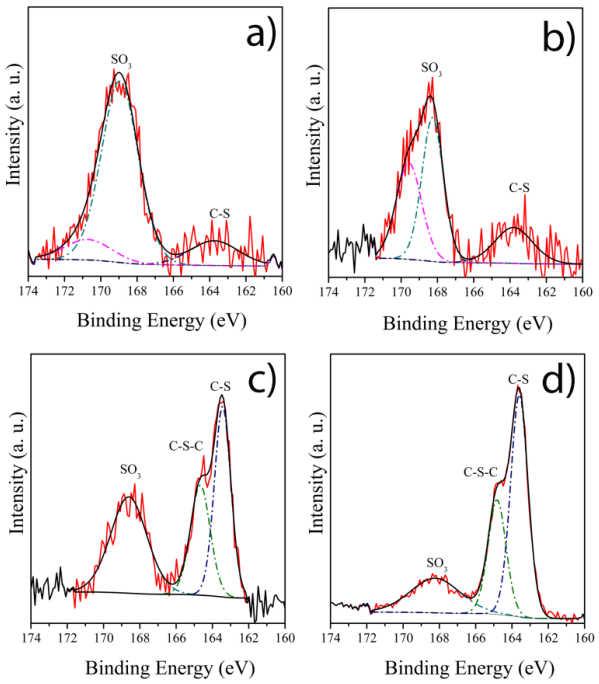

Figure 3.7 S2p deconvolution of XPS high resolution spectrums of a) GO, b) GO-B, c) GO-CA and d) GO-CA-PI.

On the other hand, C/O ratio was calculated to estimate the GO reduction when PI was used. This was calculated as the ratio of the total area of C1s to the total area of O1s, as reported elsewhere [24]. The results are presented in Table 3.3, where GO and GO-B showed similar

C/O ratio, indicating that no reduction was induced. GO-CA and GO-CA-PI exhibited a slight increase in the C/O ratios and suggesting that some oxygen functional groups were lost during the reaction. This can be attributed to the radicals formed from the PI, which could lead in a slight GO reduction. Nevertheless, when thermal initiators are used the C/O ratios observed are around 4.2 until 10.1 values [8,16,18-23]. This information is a clear evidence that the use of PI as radical initiator offers a better control of the functionalization, with short reaction time, while minimizing GO reduction and keeping similar atomic percentage in comparison with classical thermal radical initiators.

Table 3.3 C/O ratios calculated from survey XPS of Figure 3.6

Material	C/O
GO	2.4
GO-B	2.4
GO-CA	2.5
GO-CA-PI	2.8

3.2 GO functionalization with CA using AIBN by TER

When GO has been functionalized by TERA, a thermal radical initiator was used to promote R-S• species [8,16,18-23]. Since the optimal conditions for TERA using AIBN as thermal initiator have been reported [8], this experiment allowed the comparison with PI as radical initiator. GO-CA-AIBN experiment was carried out according to previous reports and, such conditions of GO:CA mass ratio and radical initiator concentration are like the experiment GO-CA-PI presented in this work. As first part, the morphological characterization was conducted, and Figure 3.8 shows STEM images of the functionalized material. GO-CA-AIBN displays a similar behavior that GO-CA-PI where, interconnected, and aggregated layers were detected due to the presence of CA moieties.

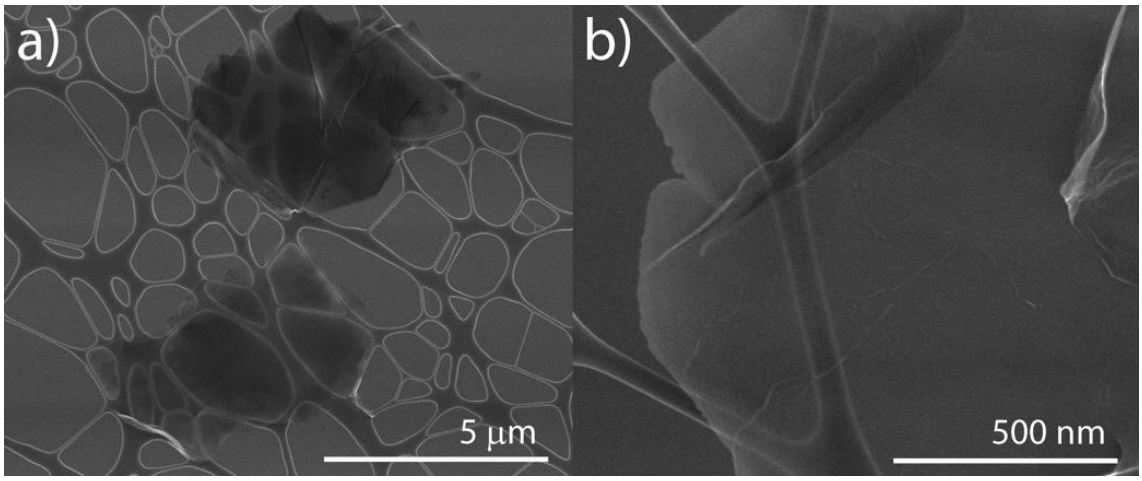

Figure 3.8 STEM images of GO-CA-AIBN at amplifications: a) 10000x, b) 100000x

Figure 3.9 presents the XPS characterization of GO-CA-AIBN where, the XPS survey revealed an atomic percentage of 74.7, 19.2, 2.8 and 2.8 for C, O, N and S, respectively (Figure 3.9a). This represents a C/O ratio of 3.9 which is higher than GO-CA-PI sample, indicating that a stronger GO reduction associated to loss of oxygen was obtained with thermal initiators. It is worth mentioning that the S atomic percentage obtained with AIBN was greater as compared to previous studies [8]. In addition, S2p deconvolution revealed the peaks at 163.5 eV, 164.6 eV and 168.1 eV, attributed to $S2p^{3/2}$ and $S2p^{1/2}$ of C-S and C-S-C bonds, as well as SO_3 moieties (see Figure 3.9b) [7,8,16,17]. The C-S-C bonds detected confirm the GO functionalization with CA using AIBN as thermal initiator.

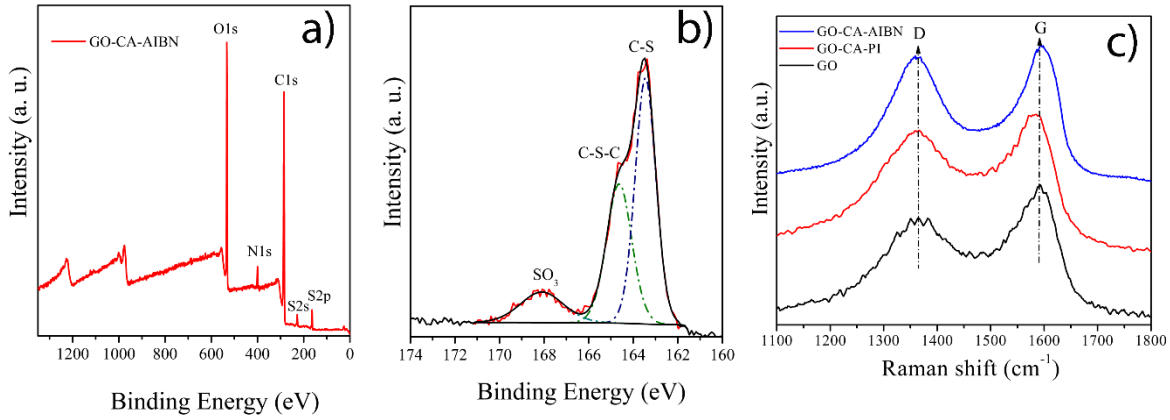

Figure 3.9 a) XPS survey of GO-CA-AIBN, b) S2p deconvolution of XPS high resolution of GO-CA-AIBN and c) Raman spectrum of GO, GO-CA-PI and GO-CA-AIBN

On the other hand, Raman characterization was performed, and the results are presented in Figure 3.9c. Notably, *G* and *D* bands were broader for GO-CA-AIBN than GO and GO-CA-

PI, indicating that a greater functionalization and more defects were introduced [12]. Moreover, the Raman information was extracted from Figure 3.9c and the A_D/A_G ratio was calculated, as can be seen in Table 3.4. The A_D/A_G ratio of GO-CA-AIBN was lower than GO-CA-PI and this can be associated to the strong change in the hybridization from sp^2 to sp^3 [25]. This change is mainly observed with a widening of *G* band and, together to the fact that *D* band was broader, the A_D/A_G ratio can be mitigated [12]. To observe the whole process in GO-CA-AIBN sample, the I_D/I_G ratio was calculated and the results showed a significant difference when compared to the GO-CA-PI sample [26]. The strong intensity of *D* band can be associated to an increase in the oxygen functional groups released.48 This is consistent with the higher C/O ratio of XPS survey calculated for GO-CA-AIBN sample. The low I_D/I_G ratio for GO-CA-PI sample confirmed that the use of PI as radical initiator conducts to an efficient functionalization while minimizing GO defects.

Table 3.4 Information of Raman spectra of Figure 3.9c

Material	G (cm^{-1})	A_D/A_G	I_D/I_G
GO	1593	1.15	0.70
GO-CA-PI	1583	1.47	0.78
GO-CA-AIBN	1595	1.3	0.96

Therefore, considering the XPS information, the use of UV-light coupled with the addition of PI as radical initiator allows the efficient functionalization of GO, minimizing the GO reduction due to the use of mild condition reactions, and opens the possibility to use the rest of oxygen functional groups of GO for further functionalization.

3.3 Functionalization of GO with MEDA and LC by TER

Two additional thiol compounds where tested (MEDA and LC) under the experimental conditions used for GO-CA-PI material. XPS characterization was used to corroborate the functionalization. Figure 3.10 contains the XPS survey scans of GO-MEDA and GO-LC samples and they exhibited a slight N and S atomic contribution.

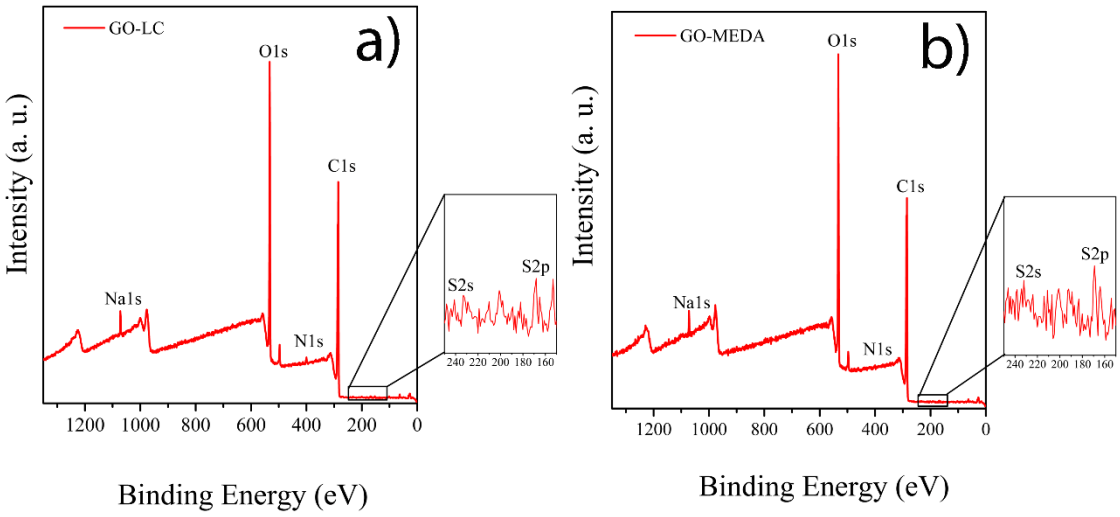

Figure 3.10 XPS survey scan of the samples GO-MEDA and GO-LC

Since low S atomic contribution was found in GO-MEDA and GO-LC samples, XPS high resolution analysis of C, N and S was conducted. In Figure 3.11, the C1s deconvolution of GO-MEDA and GO-LC presented the peak at 284.8 eV, attributed to C-S/C-N bonds possible from MEDA and LC moieties bonded to GO [23,27]. Moreover, the N1s deconvolution of GO-LC showed the peaks at 398.5 eV, 399.7 eV and 401.7 eV attributed to C-N-C, C-N and N-H bonds from secondary and primary amines [28,29]. Furthermore, GO-MEDA exhibited the peaks at 398.5 eV, 400 eV and 402 attributed to secondary and tertiary amines [30,31]. In addition, S2p deconvolution revealed two peaks at 163.5 eV and 168.5 eV attributed to $S2p^{3/2}$ and $S2p^{1/2}$ of C-S bonds [8,32]. So, regardless of the low S and N atomic percentage, it was possible to confirm the chemical functionalization with either MEDA and LC.

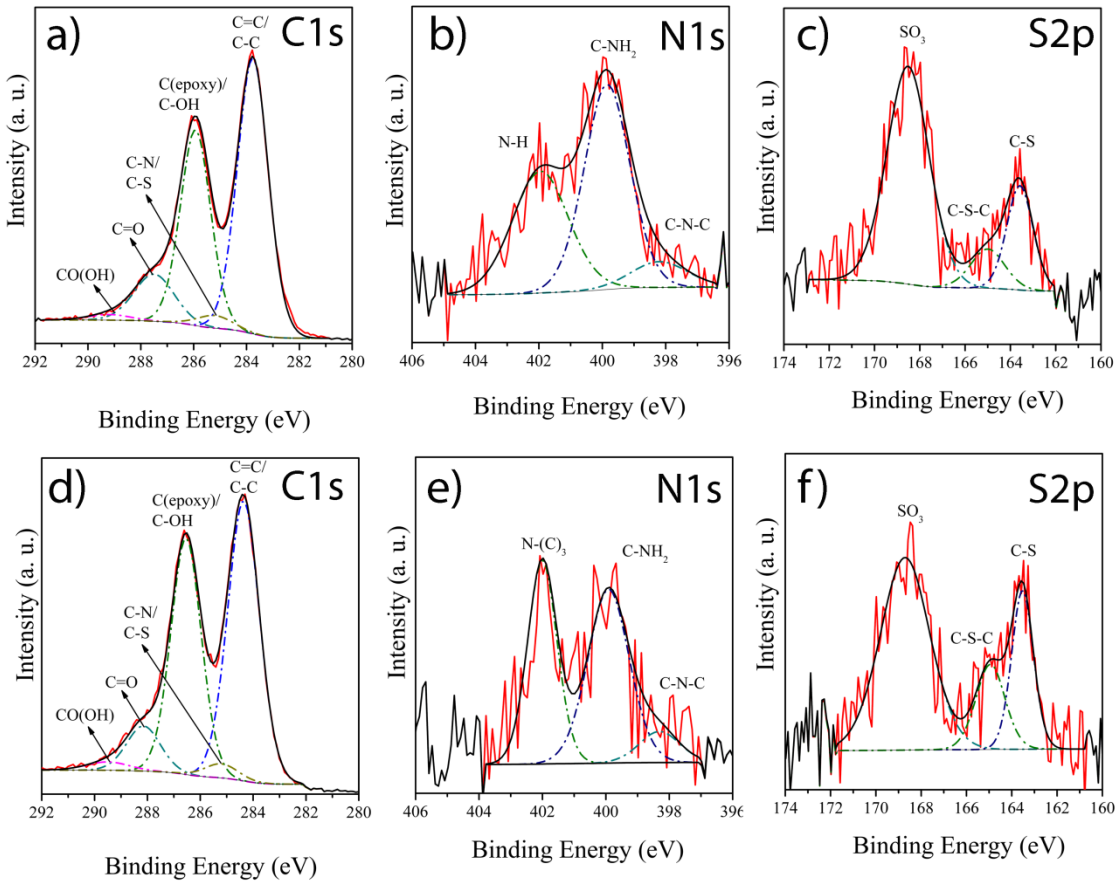

Figure 3.11 Chemical characterization of GO-LC and GO-MEDA. From a) to c) corresponds to the deconvolution XPS high resolution of GO-LC whereas from d) to f) corresponds to GO-MEDA.

As can be seen in Figures 3.10 and 3.11, the functionalization using MEDA and LC presented low contributions, as compared with GO-CA-PI sample. This behavior can be explained as the BDE of S-H bonds that change in different thiols. The BDE can be modified for the type of the alkyl chain i.e., thiol phenols have low BDE and the hydrogen atom can be easily extracted, whereas aliphatic thiols have more difficulty to extract the hydrogen atom [3,4]. The CA molecule can release easier the H atom from the S-H bond than MEDA and LC, due to its low pKa as well as low BDE. This was confirmed by the XPS survey of Figure 3.6, where a stronger sulfur contribution was detected for GO-CA-PI. Moreover, depending on the capability of the thiol to release the hydrogen atom, the change transfer step can be disturbed. Sulfur compounds with low pKa and highly electronegative alkyl chains can easily release the hydrogen atom [4]. In the case of MEDA and LC, the low stability in the radical R-S• can lead to the dissociation via reversible step to obtain the original thiol and alkene group [2].

3.4 Conclusions of the photochemical functionalization of GO using CA

In this chapter, the photochemical functionalization of graphene oxide with cysteamine was discussed, *via* UV-light coupled with a PI as radical initiator. The characterization by ATR-FTIR, UV spectroscopy, fluorescent labelling, XPS and Raman spectroscopy allowed to conclude:

- The efficient GO functionalization keeps most of the oxygen functional groups that can be used for further modification in order to develop multifunctional materials. Therefore, TERA was demonstrated as an orthogonal reaction for the functionalization of GO.
- The functionalization by TER using a PI possesses several advantages as compared to the typical thermal initiator such as high yield achieved in short reaction time, minimum side reactions and GO reduction can be minimized due to the mild reaction conditions used (no heating).
- TERA can be applied for the functionalization of GO with a variety of thiol compounds. However, the functionalization degree depends strongly of the nature of the thiol compound. The chemical structure can help to subtract easily the H atom from the S-H bond.
- Finally, the fluorescamine can be used to monitor the CA moieties bonded to GO by a simple and efficient titration method.

BIBLIOGRAPHY

[1] Dénès, F.; Pichowicz, M.; Povie, G.; Renaud, P. Thiyl Radicals in Organic Synthesis. Chem. Rev. 2014, 114 (5), 2587–2693.
[2] Denisov, E.; Chatgilialoglu, C.; Shestakov, A.; Denisova, T. Rate Constants and Transition-State Geometry of Reactions of Alkyl, Alkoxyl, and Peroxyl Radicals with Thiols. Int. J. Chem. Kinet. 2009, 41 (4), 284–293.
[3] Hoyle, C. E.; Bowman, C. N. Thiol-Ene Click Chemistry. Angew. Chemie - Int. Ed. 2010, 49 (9), 1540–1573.
[4] Lowe, A. B. Thiol-Ene "Click" Reactions and Recent Applications in Polymer and Materials Synthesis. Polym. Chem. 2010, 1 (1), 17–36. [5] Wang, J.; Salihi, E. C.; Šiller, L. Green Reduction of Graphene Oxide Using Alanine. Mater. Sci. Eng. C 2017, 72, 1–6
[5] Stankovich, S.; Piner, R. D.; Nguyen, S. B. T.; Ruoff, R. S. Synthesis and Exfoliation of Isocyanate-Treated Graphene Oxide Nanoplatelets. Carbon N. Y. 2006, 44 (15), 3342–3347.
[6] Marcano, D. C.; Kosynkin, D. V.; Berlin, J. M.; Sinitskii, A.; Sun, Z.; Slesarev, A.; Alemany, L. B.; Lu, W.; Tour, J. M. Improved Synthesis of Graphene Oxide. ACS Nano 2010, 4 (8), 4806–4814.
[7] Li, J.; Cheng, Y.; Zhang, S.; Li, Y.; Sun, J.; Qin, C.; Wang, J.; Dai, L. Modification of GO Based on Click Reaction and Its Composite Fibers with Poly(Vinyl Alcohol). Compos. Part A Appl. Sci. Manuf. 2017, 101, 115–122.
[8] Yap, P. L.; Kabiri, S.; Tran, D. N. H.; Losic, D. Multifunctional Binding Chemistry on Modified Graphene Composite for Selective and Highly Efficient Adsorption of Mercury. ACS Appl. Mater. Interfaces 2018, 11 (6), 6350–6362.
[9] Deng, M.; Huang, Y.; Zhang, X.; Feng, Z.; Gou, J.; Sun, B. Preparation of a Novel Chelating Resin Bearing Amidinothiourea Moieties and Its Removal Properties for Hg(II) Ions in Aqueous Solution. Sep. Sci. Technol. 2016, 6395 (June), 1–10.
[10] Kudin, K. N.; Ozbas, B.; Schniepp, H. C.; Prud'homme, R. K.; Aksay, I. A.; Car, R.; Prud'homme, R. K.; Aksay, I. A.; Car, R.; Prud'homme, R. K.; et al. Raman Spectra of Graphite Oxide and Functionalized Graphene Sheets. Nano Lett. 2007, 8 (1), 36–41.
[11] Claramunt, S.; Varea, A.; López-Díaz, D.; Velázquez, M. M.; Cornet, A.; Cirera, A. The Importance of Interbands on the Interpretation of the Raman Spectrum of Graphene Oxide. J. Phys. Chem. C 2015, 119 (18), 10123–10129.
[12] Cançado, L. G.; Jorio, A.; Ferreira, E. H. M.; Stavale, F.; Achete, C. A.; Capaz, R. B.; Moutinho, M. V. O.; Lombardo, A.; Kulmala, T. S.; Ferrari, A. C. Quantifying Defects in Graphene via Raman Spectroscopy at Different Excitation Energies. Nano Lett. 2011, 11 (8), 3190–3196.
[13] Salazar-Aguilar, A. D.; Tristan, F.; Labrada-Delgado, G. J.; Meneses-Rodríguez, D.; Vega-Díaz, S. M. Three-Dimensional Structure Made with Nitrogen Doped Reduced Graphene Oxide with Spherical Porous Morphology. Carbon N. Y. 2019, 149, 86–92.
[14] Liu, H.; Liu, Y.; Zhu, D. Chemical Doping of Graphene. J. Mater. Chem. 2011, 21 (10), 3335–3345.

[15] Udenfriend, S.; Stein, S.; Böhlen, P.; Dairman, W.; Leimgruber, W.; Weigele, M. Fluorescamine: A Reagent for Assay of Amino Acids, Peptides, Proteins, and Primary Amines in the Picomole Range. Science. 1972, 178 (4063), 871–872.
[16] Luong, N. D.; Sinh, L. H.; Johansson, L. S.; Campell, J.; Seppälä, J. Functional Graphene by Thiol-Ene Click Chemistry. Chem. - A Eur. J. 2015, 21 (8), 3183–3186.
[17] Peng, Z.; Li, H.; Li, Q.; Hu, Y. Microwave-Assisted Thiol-Ene Click Chemistry of Carbon Nanoforms. Colloids Surfaces A 2017, 533 (August), 48–54.
[18] Huang, H.; Liu, M.; Tuo, X.; Chen, J.; Mao, L.; Wen, Y.; Tian, J.; Zhou, N.; Zhang, X.; Wei, Y. A Novel Thiol-Ene Click Reaction for Preparation of Graphene Quantum Dots and Their Potential for Fluorescence Imaging. Mater. Sci. Eng. C 2018, 91 (2017), 631–637.
[19] Masteri-Farahani, M.; Modarres, M. Clicked Graphene Oxide Supported Venturello Catalyst: A New Hybrid Nanomaterial as Catalyst for the Selective Epoxidation of Olefins. Mater. Chem. Phys. 2017, 199, 522–527.
[20] Kanninen, P.; Luong, N. D.; Sinh, L. H.; Flórez-Montaño, J.; Jiang, H.; Pastor, E.; Seppälä, J.; Kallio, T. Highly Active Platinum Nanoparticles Supported by Nitrogen/Sulfur Functionalized Graphene Composite for Ethanol Electro-Oxidation. Electrochim. Acta 2017, 242, 315–326.
[21] Masteri-Farahani, M.; Modarres, M. New Hybrid Nanomaterials Derived from Chemical Functionalization of Clicked Graphene Oxide / Magnetite Nanocomposite with Peroxopolyoxotungstate Species. ChemistrySelect 2017, 2 (33), 10786–10792.
[22] McGrail, B. T.; Mangadlao, J. D.; Rodier, B. J.; Swisher, J.; Advincula, R.; Pentzer, E. Selective Mono-Facial Modification of Graphene Oxide Nanosheets in Suspension. Chem. Commun. 2016, 52 (2), 288–291.
[23] Li, Y.; Bao, L.; Zhou, Q.; Ou, E.; Xu, W. Functionalized Graphene Obtained via Thiol-Ene Click Reactions as an Efficient Electrochemical Sensor. ChemistrySelect 2017, 2 (29), 9284–9290.
[24] Luo, D.; Zhang, G.; Liu, J.; Sun, X. Evaluation Criteria for Reduced Graphene Oxide. J. Phys. Chem. C 2011, 115 (23), 11327–11335.
[25] Kaniyoor, A.; Ramaprabhu, S. A Raman Spectroscopic Investigation of Graphite Oxide Derived Graphene. AIP Adv. 2012, 2 (3), 0–13.
[26] Wu, T.; Wang, X.; Qiu, H.; Gao, J.; Wang, W.; Liu, Y. Graphene Oxide Reduced and Modified by Soft Nanoparticles and Its Catalysis of the Knoevenagel Condensation. J. Mater. Chem. 2012, 22 (11), 4772.
[27] Pirveysian, M.; Ghiaci, M. Synthesis and Characterization of Sulfur Functionalized Graphene Oxide Nanosheets as Efficient Sorbent for Removal of Pb 2+, Cd 2+, Ni 2+ and Zn 2+ Ions from Aqueous Solution: A Combined Thermodynamic and Kinetic Studies. Appl. Surf. Sci. 2018, 428, 98–109.
[28] Kim, N. H.; Kuila, T.; Lee, J. H. Simultaneous Reduction, Functionalization and Stitching of Graphene Oxide with Ethylenediamine for Composites Application. *J. Mater. Chem. A* **2013**, *1* (4), 1349–1358. https://doi.org/10.1039/C2TA00853J.
[29] Zhang, W.; Zhao, Q.; Liu, T.; Gao, Y.; Li, Y.; Zhang, G.; Zhang, F.; Fan, X. Phosphotungstic Acid Immobilized on Amine-Grafted Graphene Oxide as Acid/Base Bifunctional Catalyst for One-Pot Tandem Reaction. *Ind. Eng. Chem. Res.* **2014**, *53* (4), 1437–1441.

[30] Forget, G.; Latxague, L.; Heroguez, V.; Labrugere, C.; Durrieu, M. C. RGD Nanodomains Grafting onto Titanium Surface. In 2007 29th Annual International Conference of the IEEE Engineering in Medicine and Biology Society; IEEE, 2007; pp 5107–5110.
[31] Ravi, S.; Zhang, S.; Lee, Y. R.; Kang, K. K.; Kim, J. M.; Ahn, J. W.; Ahn, W. S. EDTA-Functionalized KCC-1 and KIT-6 Mesoporous Silicas for Nd3+ Ion Recovery from Aqueous Solutions. J. Ind. Eng. Chem. 2018, 67, 210–218.
[32] Chua, C. K.; Pumera, M. Monothiolation and Reduction of Graphene Oxide via One-Pot Synthesis: Hybrid Catalyst for Oxygen Reduction. ACS Nano 2015, 9 (4), 4193–4199.

CHAPTER 4

GRAPHENE OXIDE AND THE CHEMICAL FUNCTIONALIZATION BY THIOL-ENE MICHAEL ADDITION REACTION

In chapter 3, it was found that TER can be applied by adding radical photoinitiators (TERA). This method offers important advantages such as rapid reactions under mild conditions. Since TER is an orthogonal reaction, it is possible to preserve without any important alteration the rest of the oxygen functional groups of GO. However, TER also can be carried out adding base catalysts leading to the coupling reaction between thiols and alkene groups. This reaction is also called thiol-ene Michael addition (TEMA) with the difference that the functionalization proceeds on the α,β-unsaturated acids of GO. This chapter illustrates from a qualitative and quantitative point of view the functionalization of GO with CA by TEMA using different base catalysts. This pathway for the functionalization of GO brings an alternative to selectively deposit thiols towards the α,β-unsaturated acids of GO, preserving its wide chemistry. By exploring different chemical routes in which the GO functionalization can be proceeded in an orthogonal path, it can be developed a multi-functionalized GO using different molecules.

Chapter 3 introduced fluorescamine to selectively label the CA moieties bonded to GO due to the primary amine that remains after the chemical functionalization. This method offers advantages such as short time for the analysis and selective detection of primary amines. Through fluorescamine, it is possible to answer an important question: when a functionalization is performed, how many molecules can be bonded to the GO? In this context, since TEMA and TERA takes place simultaneously, how many molecules can be bonded towards epoxides and α,β-unsaturated acids of GO? These questions can bright insides in the chemical functionalization of the GO using base catalyst and if this rection can offer an important quantity of thiols link on GO layers.

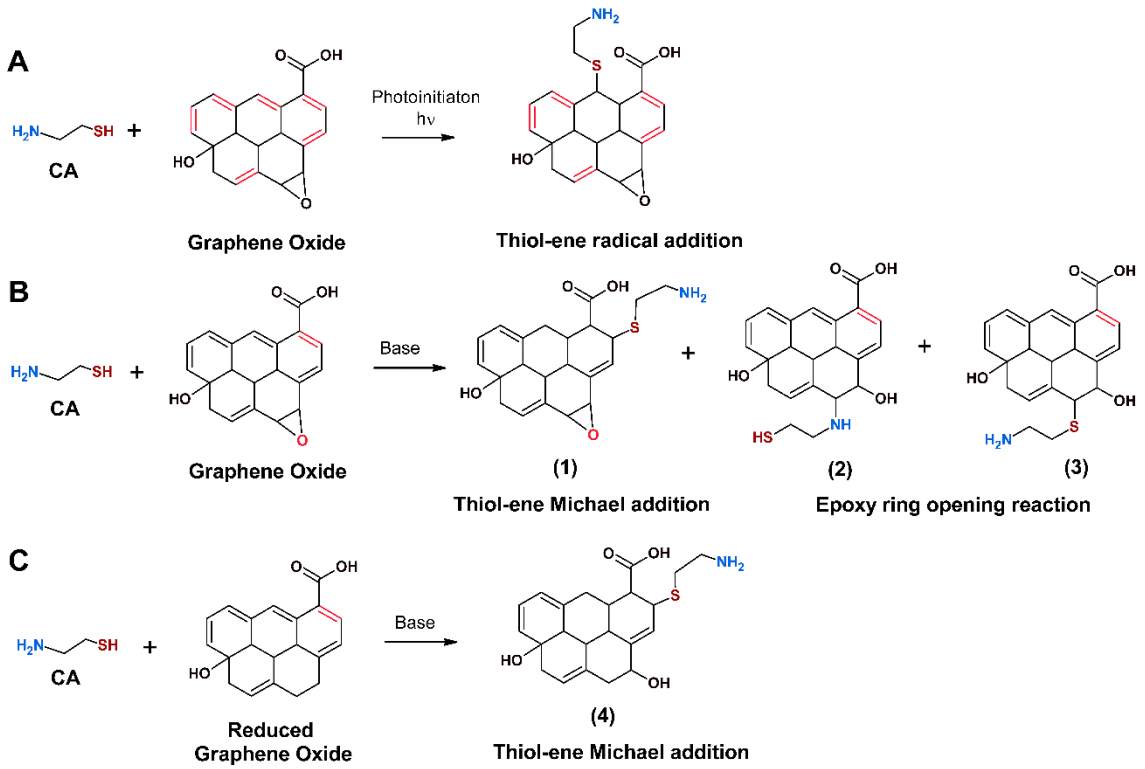

Figure 4.1 a) Functionalization of GO with CA by TERA, b) GO functionalization with CA using a base where three products can be obtained: TEMA **1**, TERA by SH, **2** and epoxy ring opening reaction by NH_2, **3**. c) Functionalization of RGO with CA by TEMA to produce **4**.

Figure 4.1a shows that TERA is a powerful and orthogonal reaction for coupling thiols with a wide variety of unsaturated systems. Alternatively, a base catalyst can be used for the hydrothiolation of α,β-unsaturated acids (Figure 4.1b). In brief, the base catalyst subtracts the hydrogen from the S-H of CA leading to a thiolate anion, which is a strong nucleophile that can attack either alkene (Figure 4.1b, **1**) or epoxide groups (Figure 4.1b, **2**) of GO [1,2]. Since CA molecules have a primary amine group, epoxide ring opening reactions can also occur (Figure 4.1b, **3**). Separately, GO can be thermally reduced to remove the epoxide groups which are susceptible to be attacked by the thiolate anions. The RGO produced is functionalized with CA using a base catalyst to confirm that TEMA takes place (Figure 4.1c, **4**).

According to Figure 4.2, the functionalization of GO with CA by TEMA was proceeded using dispersing GO in DMF, and then adding simultaneously CA and the base catalyst. The base catalyst tested for the chemical functionalization were *N,N*-diisopropylethylamine (DIPEA), triethylamine (NEt_3) and 1,8-diazabicyclo[5.4.0]undec-7-ene (DBU). The final concentration of the base catalyst in the reaction mixture was 100 mM. The reaction was let in ultrasonic bath and then, the mixture was transferred to a beaker wrapped with aluminum foil

for stirring during 4 h. The materials produced in this functionalization were labeled as GO-DIPEA, GO-NEt_3 and GO-DBU. Additionally, a blank experiment was prepared which consisted only in GO and CA without base catalyst (labeled as GO-B). The blank experiment was undergone for the same process as prepared to the GO functionalized using base catalyst.

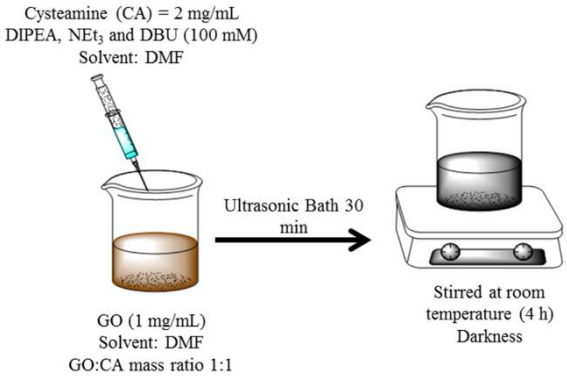

Figure 4.2 Schematic representation of the methodology used to study the GO functionalization by TEMA.

A systematic study of the functionalization between RGO and CA was carried out. The reaction between RGO and CA was performed under the same conditions as in the functionalization using GO, as presented in Figure 4.2. These materials were labeled as RGO-DIPEA, RGO-NEt_3 and RGO-DBU. A similar blank experiment was carried out for the reaction between RGO and CA without the base catalyst. This sample was labeled as RGO-CA. All the experiments developed for this chapter are summarized in Table 4.1 to facilitate their follow-up during the discussion of the results.

Table 4.1 Summary of the reaction conditions for the different samples prepared.

Label	Description	GO (1 mg/mL)[a]	RGO (1 mg/mL)[a]	Base catalyst[b]
GO-DIPEA	GO functionalized with CA adding DIPEA	✓	/	DIPEA
GO-NEt_3	GO functionalized with CA adding NEt_3	✓	/	NEt_3
GO-DBU	GO functionalized with CA adding DBU	✓	/	DBU
GO-B	GO functionalized with CA	✓	/	/
RGO-DIPEA	RGO functionalized with CA adding DIPEA	/	✓	DIPEA
RGO-NEt_3	RGO functionalized with CA adding NEt_3	/	✓	NEt_3
RGO-DBU	RGO functionalized with CA adding DBU	/	✓	DBU
RGO-B	RGO functionalized with CA	/	✓	/

[a]CA was used at concentration of 2 mg/mL
[b]The concentration of the base catalyst was 100 mM in the reaction

In this chapter a simple method for detection and quantification of functionalities inserted onto GO by fluorescent labelling was implemented. The fluorescent method procedure is shown in Figure 4.3a

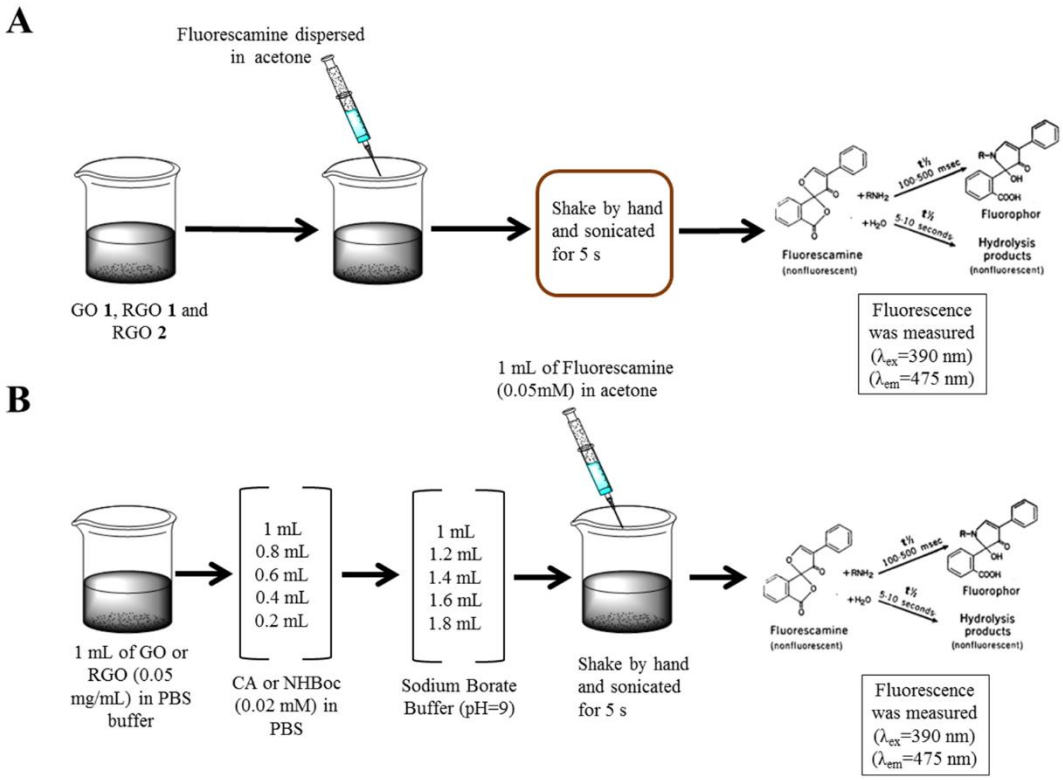

Figure 4.3 Schematic representation of: a) detection of -NH_2 moieties in GO layers and b) preparation of the calibration curve for the quantification of -NH_2 moieties after the chemical functionalization

The detection of -NH_2 moieties in GO layers consisted in a simple titration of a constant volume of the GO functionalized with CA (the pH was adjusted using sodium borate) and then adding fluorescamine. The formation of the fluorophore is quite rapid, and the fluorescence intensity was measured as presented in Figure 4.3a. After that, a calibration curve was built to determine the number of molecules bonded to GO layers. According to Figure 4.3b, a constant volume of GO was taken to add the quenching effect to the calibration curve. Then, different volumes of CA standard (0.02 mM, prepared in PBS) were added with different volumes also of sodium borate buffer (pH~9). Finally, fluorescamine dispersed in acetone was added and the mixture was shaken by hand and then sonicated to eliminate the bubbles. The fluorescence was measured at λ_{ex}=390 nm and λ_{em}=475 nm. This calibration curve was employed for the determination of the number of CA molecules bonded to GO in the different experiments developed for this chapter.

Finally, the functionalized materials were also characterized by STEM and XPS to observe the morphology of the GO layers after the chemical functionalization and corroborate the chemical bonds formed, respectively.

4.1 Study of GO functionalization with CA by TEMA

As first step, XPS characterization was performed to confirm the chemical functionalization. In Figure 4.4, the three materials (GO-DIPEA, GO-NEt_3 and GO-DBU) presented nitrogen (N) and sulfur (S) atomic contributions, because of CA moieties bonded to GO. These CA molecules could be bonded by either TEMA or TEROR. The presence of the base catalyst led to an increase of CA moieties on GO, since the control experiment presented traces of S atomic percentage (GO-B, see Figure A2 and Table A3)

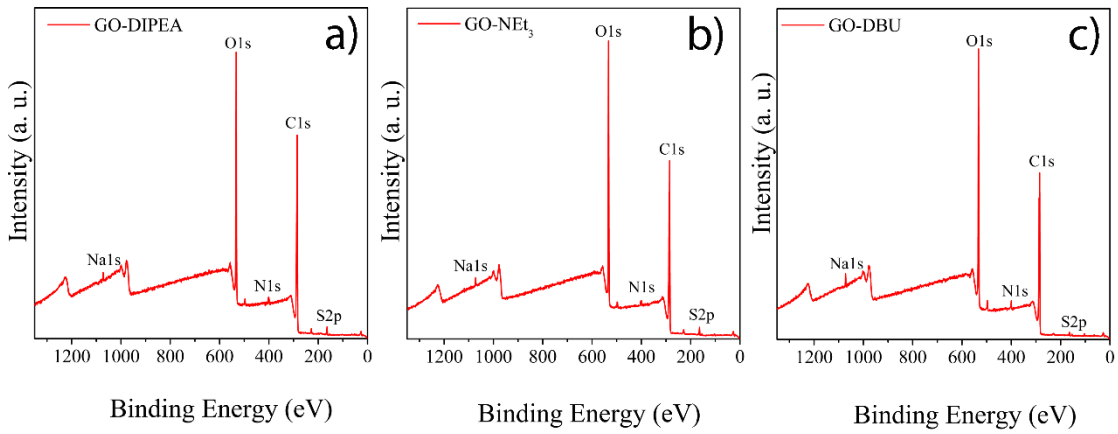

Figure 4.4 XPS survey scan of the samples: a) GO-DIPEA, b) GO-NEt3 and c) GO-DBU.

In addition, the S2p deconvolution of GO-DIPEA, GO-NEt_3 and GO-DBU samples allowed to detect the doublet peak at 163.5 eV and 164.8 eV, attributed to C-S-C and C-S, respectively (see Figure 4.5) [3-5]. XPS information confirmed the successful production of **1** and possible **2** due to the formation of C-S and C-S-C bonds, whereas C-S-C bonds were not detected in blank experiment (see Figure A3).

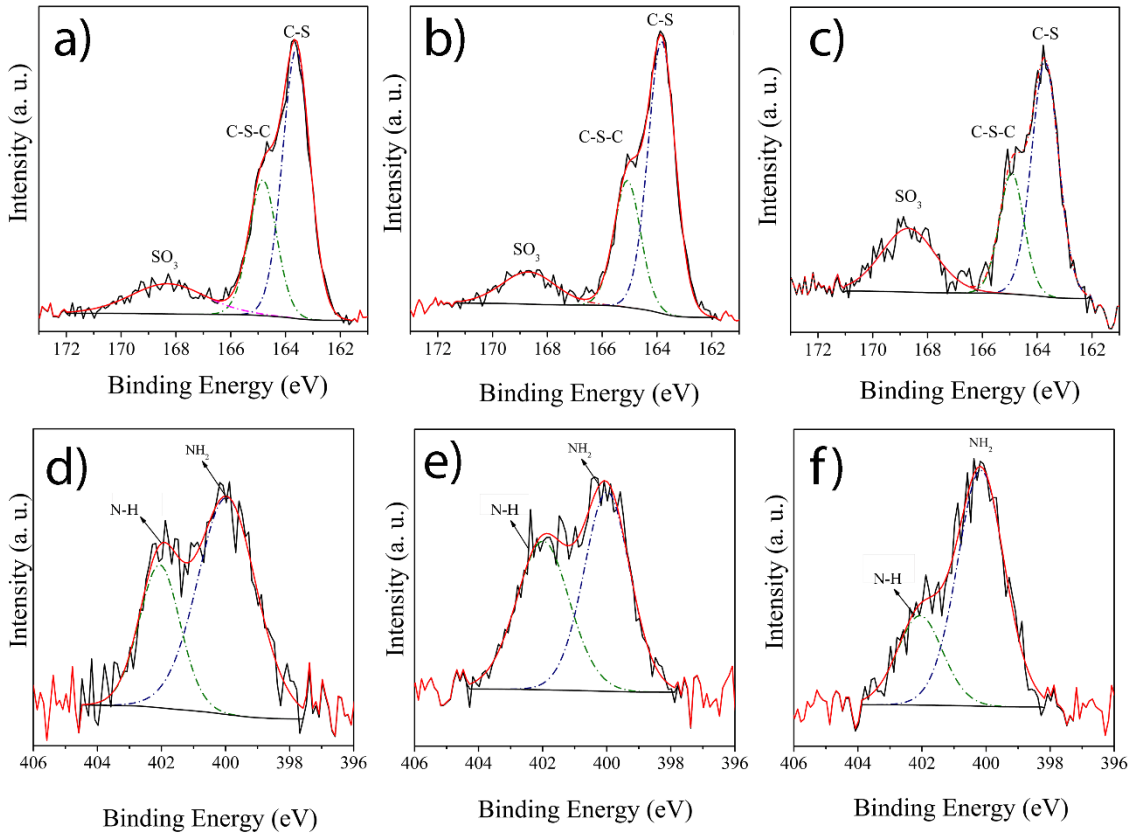

Figure 4.5 S2p deconvolution of a) GO-DIPEA, b) GO-NEt_3 and C) GO-DBU. N1s deconvolution of d) GO-DIPEA, e) GO-NEt_3 and f) GO-DBU.

On the other hand, the CA molecules have two nucleophiles (-NH_2 and -SH) and both can attack epoxides of GO (Figure 4.1b, **2** and **3**). However, the SH of CA has lower pKa than NH_2 and thus, under the presence of a base catalyst, the thiolate anions (S^-) can be easily produced which are stronger nucleophiles than NH_2. N1s deconvolution was carried out to detect possible contributions of secondary amines. GO-DIPEA, GO-NEt_3 and GO-DBU presented two peaks at 399.8 eV and 401.7 eV, attributed to primary amines (-NH_2) and protonated amines (-NH_3^+), respectively (see Figure 4.5) [6-8]. No secondary amines were detected in Figure 4.5 expected around 400.3 eV [9], confirming the absence of **3**. The -NH_2 detected by XPS is consistent with the CA moieties bonded on GO by the thiolate anions. Therefore, N1s XPS deconvolution is consistent with the successful functionalization of GO with CA due to either TEMA or TEROR.

Once the chemical functionalization was confirmed on GO, CA molecules were estimated considering the fluorescent labelling and the S atomic percentage of XPS. Fluorescamine was used for labelling and titration of the CA moieties bonded to GO, and this

compound reacts specifically with primary amine moieties (-NH_2) to form fluorescent pyrrolinone [10]. Therefore, the titration method proposed in this work is able to detect and quantify only products **1** and **3**. Figure 4.6a shows the results of the titrations and highlights that the order of the functionalization was GO-DIPEA > GO-NEt_3 > GO-DBU. In addition, a calibration curve was built at λ_{em}= 475 to quantify the CA moieties bonded to GO (see Figure 4.4b). The quantification was performed taking the fluorescence intensity at λ_{em}= 475 nm from Figure 4.6a and, setting it into the calibration curve (Figure 4.6b). The results are reported in Table 4.2, and remarkably the CA concentration found in the GO functionalized is in a similar order of magnitude to that of some functional groups of GO, such as carbonyl and hydroxy groups and nearby of carboxylic acid [11,12]. This information confirms that a high quantity of CA can be bonded by TEMA coupled to TEROR.

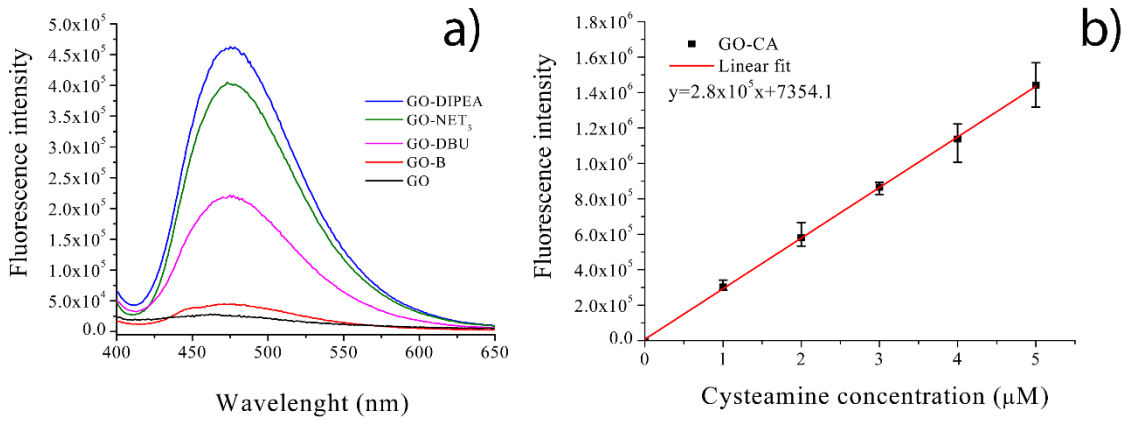

Figure 4.6 a) Fluorescence titrations of CA moieties on the GO functionalized materials (λ_{ex}= 390 nm) and b) calibration curve for quantification of CA moieties bonded.

Table 4.2 Summary of fluorescent labelling and XPS survey for the estimation of CA moieties on GO samples (*n=3*)

Material	CA molecules/mg estimated by fluorimetry (COV)[a]	S atomic percentage from XPS[b]	CA molecules/mg estimated by XPS
GO-DIPEA	$7.7x10^{16}$ (6.8)	1.39	$9.0x10^{16}$
GO-NEt_3	$6.6x10^{16}$ (10.9)	1.32	$8.8x10^{16}$
GO-DBU	$3.6x10^{16}$ (3.5)	0.4	$2.2x10^{16}$

[a]Coefficient of variation (COV) reported as percentage (%)
[b]XPS technique possesses 10% of error

Additionally, XPS survey was used to corroborate the results obtained from the fluorescamine titration. As can be seen in Table A1, the strongest contribution of S was achieved with DIPEA followed by NEt_3 and DBU. This information is consistent with the fluorescent labelling results. The concentration of CA on GO was theoretically estimated taking

the S atomic percentage of XPS (see section A.1). Similar concentrations of CA moieties were found by the XPS survey and fluorescent labelling (see Table 4.2). This information validates the quantification obtained from the titration using fluorescamine. The quantification method was validated using the coefficient of determination (r^2), Limit of Detection (LOD), the Limit of Quantification (LOQ) and the coefficient of variation (COV). The LOD, LOQ and COV were estimated with the following equations:

$$LOD = {}^{3S_a}\!/_{b} \tag{4.1}$$

$$LOQ = {}^{10S_a}\!/_{b} \tag{4.2}$$

$$COV = \frac{C}{S_D} \cdot 100 \tag{4.3}$$

Where S_a is the standard deviation of either *y*-residuals or *y*-intercepts, *b* is the slop of the calibration curve, *C* is the concentration found using the calibration curve, and SD is the standard deviation of *C*. This validation method can be applied in all cases, and it is more applicable when the analysis method does not involve background noise, since the intensity of the signal is too high as compare to the noise [13]. The r^2 obtained in Figure 4.6b was 0.999, which confirms the linearity of the linear adjust. The LOD and LOQ found using this calibration curve were 0.07 and 0.24 μM, respectively. The LOD and LOQ refer to minimum quantity of analyte that can be detected, but not necessarily quantified, and the minimum concentration at which the analyte can be quantitated with acceptable precision and accuracy under the stated conditions of test [14]. The CA molar concentration on GO layers obtained from the Figure 4.6 were 0.98, 0.80 and 0.46 for GO-DIPEA, GO-NEt_3 and GO-DBU, respectively. Finally, the COV value ranged from 3.5 and 10, which is in the same range that the error reported previously for the XPS tool [15]. Therefore, considering this information, the fluorescent method develop in this work can be used for the estimation of CA molecules bonded in GO layers.

Notably, either by fluorescent labelling or XPS, DBU produced the lowest S atomic percentage amongst the catalysts used in this study. However, in XPS a strong N atomic percentage was also detected (see Table A1). This result can be attributed to the behavior of DBU with DMF on GO [16]. Indeed, the hydrolysis of the imidamide can undergo by DMF producing by-products which can interact with GO (Figure 4.7) [16]. However, despite that this

by-product can interact with GO, the fluorescent labelling considers solely the free -NH_2 moieties. Therefore, a higher N atomic percentage with respect the S was found in XPS, but the sequence of the S contribution of the functionalized materials coincides with the fluorescent results.

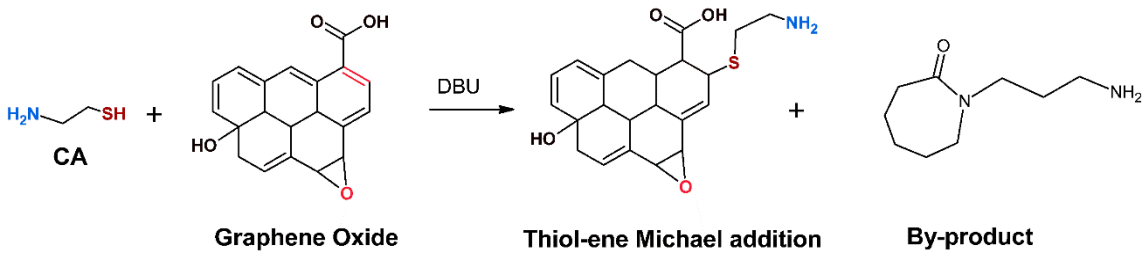

Figure 4.7 Functionalization of GO with CA by TERA using DBU. A possible by-product can be obtained because of the behavior of DBU in presence of DMF and GO.

On the other hand, a deeper analysis of XPS results conducted to estimate the C/O ratio which was calculated as the ratio of the total area of C1s to the total area of O1s (see Table 4.3) [15]. The C/O ratio highlighted that NEt_3 affords to efficient functionalization, associated with a minimum loss of oxygen functional groups on GO. The slight increase in the C/O ratios can be attributed to the functionalization using nucleophiles. Commonly, these reactions involve the partial reduction of GO [17-19]. It has been suggested that the reduction takes place due to an epoxide ring opening reactions, followed by the elimination of the alcohol formed in the adjacent carbon [20,21]. However, the functionalization of GO using base catalysts allows to conserve most of the oxygen functional groups, since similar C/O ratios were obtained as compared to GO.

Table 4.3 C/O ratios calculated from XPS survey of Table A3.

Material	C/O
GO	2.3
GO-B	2.5
GO-DIPEA	2.9
GO-NEt_3	2.7
GO-DBU	2.5

As the addition of DIPEA produced the strongest CA contribution, STEM characterization of GO-DIPEA was performed to observe the morphological changes before and after the functionalization (see Figure 4.8). The GO-DIPEA material showed translucent layers associated to low stacking probably due to the incorporation of CA moieties (Figure 4.8g

to 4.8i). In addition, no significant defects were introduced during the functionalization as compared to GO and GO-B. This information suggests that the mild conditions reactions allowed to preserve the morphology of the GO layers. Therefore, the functionalization proposed in this work conducts to an efficient incorporation of CA in GO, without affecting the structure of the GO.

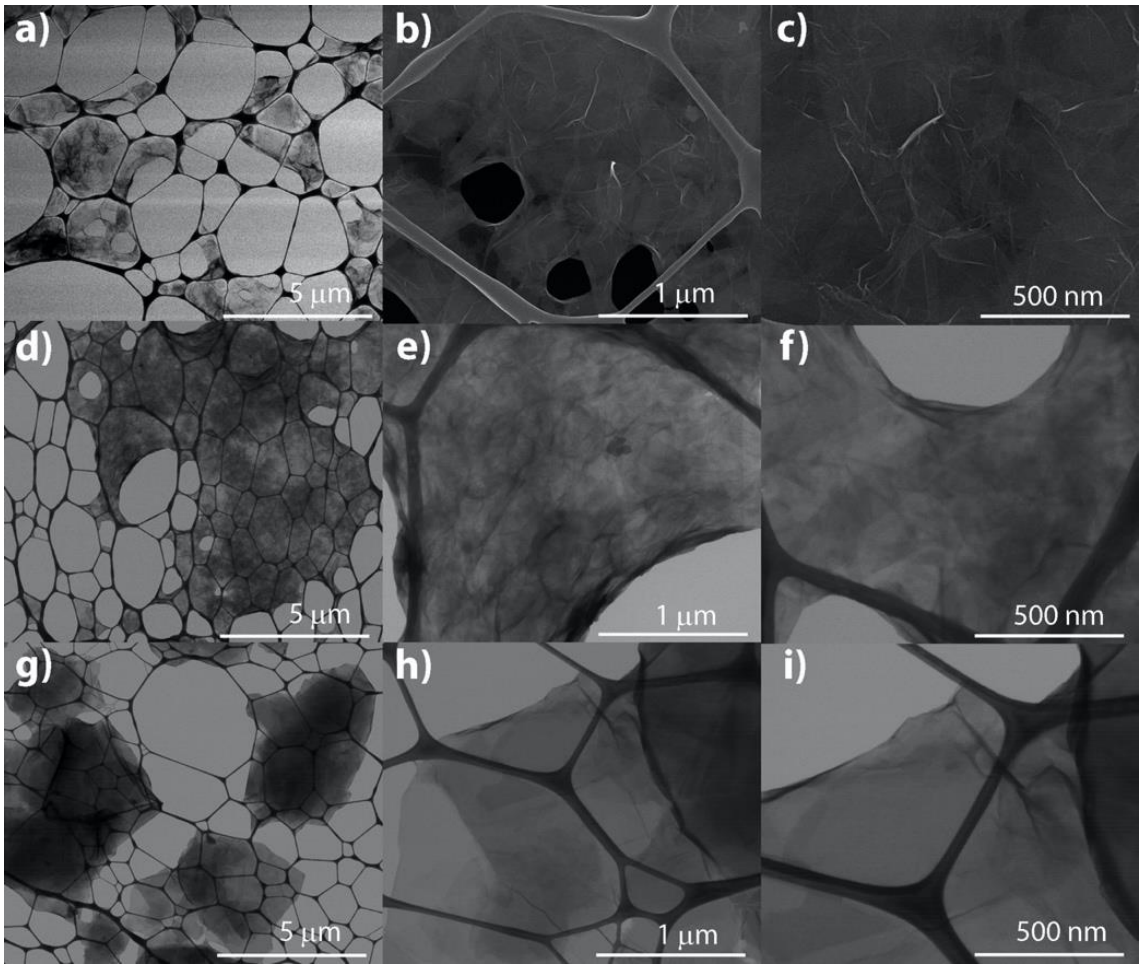

Figure 4.8 STEM images of GO (a to c), GO-B (d to e) and GO-DIPEA (g to i) at amplifications 10,000X, 50,000X and 100,000X.

4.2 Study of RGO functionalization with CA by TEMA

A systematic study was carried out using RGO to study TEMA and TEROR contributions separately (Figure 4.1c). A mild thermal treatment was carried out on GO where epoxide groups were removed, which are susceptible to be activated by the base catalyst.

ATR-FTIR characterization of GO and RGO allowed to detect the decrease in the bands at 1226 cm^{-1} and 946 cm^{-1}, attributed to epoxide groups (Figure 4.9) [22,23]. It is worth noting

that the rest of the functional groups remained after the thermal treatment, such as carboxy/carbonyl (1735 cm^{-1}), alcohol (1385 cm^{-1}) and phenol groups (1046 cm^{-1}) [22,24]. This information suggests that the thermal treatment was sufficiently mild to preserve most of the oxygen functional groups of GO and, just the epoxide groups were removed. It has been reported that at 60 ºC the epoxide groups can be almost eliminated without affecting the rest of the functional groups [25-27]. Therefore, considering the FTIR results it can be assumed that epoxides were almost suppressed.

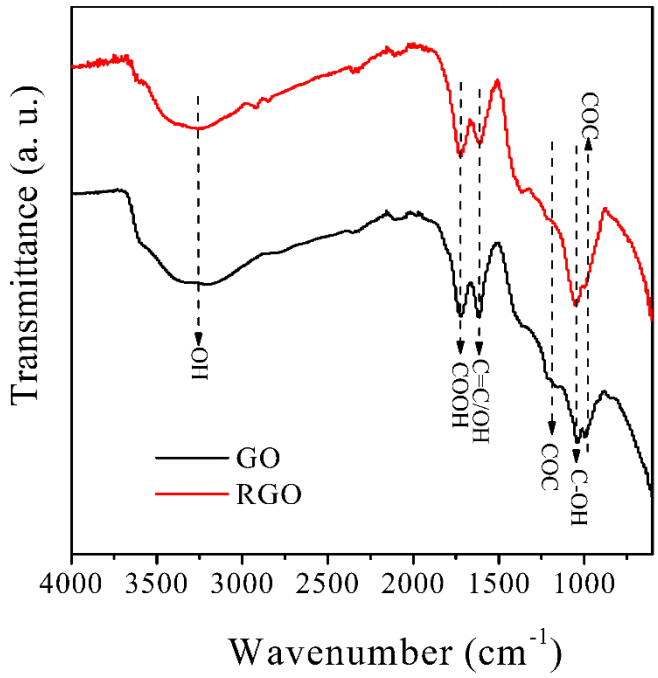

Figure 4.9 ATR-FTIR characterization of the samples GO and RGO.

Once RGO material was obtained, the functionalization with CA under the different base catalysts was carried out. XPS characterization of RGO-DIPEA, RGO-NEt_3 and RGO-DBU allowed to indentify S and N atomic contributions, associated to CA moieties bonded to RGO (see Figure 4.10). Furthermore, in S2p deconvolution the peaks at 163.5 eV and 164.8 eV were detected, which can be attributed to C-S-C and C-S respectively (see Figure 4.11) [3-5]. Since epoxide groups were released during the thermal treatment, the incorporation of CA molecules to GO proceeded by TEMA towards the α,β-unsaturated acids. The lack of the C-S-C peak in RGO-B confirmed that TEMA took place because of the addition of the base catalyst. Furthermore, the N1s deconvolution was conducted and RGO-DIPEA, RGO-NEt_3 and RGO-DBU presented two peaks at 399.8 eV and 401.7 eV, attributed to primary amines ($-NH_2$) and protonated amines (NH_3^+), respectively (see Figure 4.10) [6-8]. The $-NH_2$ bond detected in XPS

supports the production of **4** by TEMA. Therefore, XPS and FTIR results offer evidence that regardless of the elimination of the epoxide groups, CA molecules were bonded on RGO by TEMA towards the α,β-unsaturated acids.

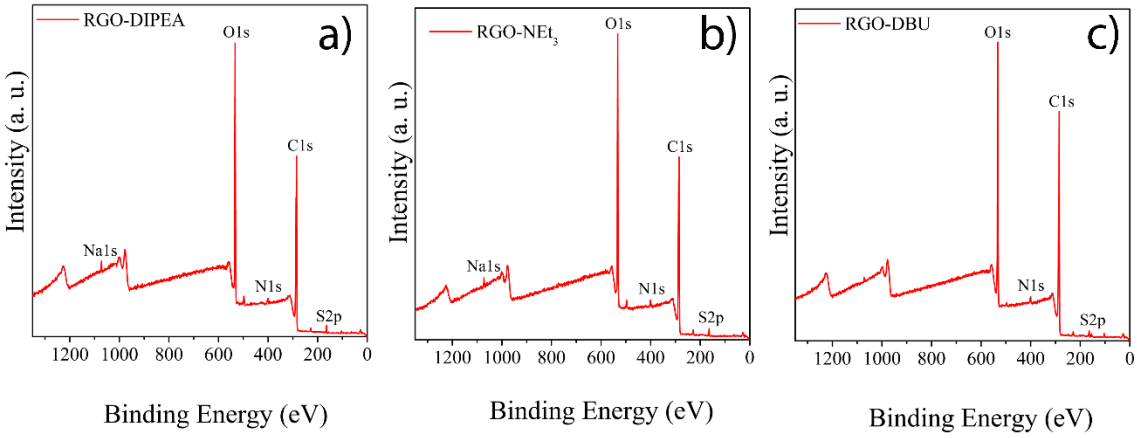

Figure 4.10 XPS survey scan of the samples: a) RGO-DIPEA, b) RGO-Net$_3$ and c) RGO-DBU.

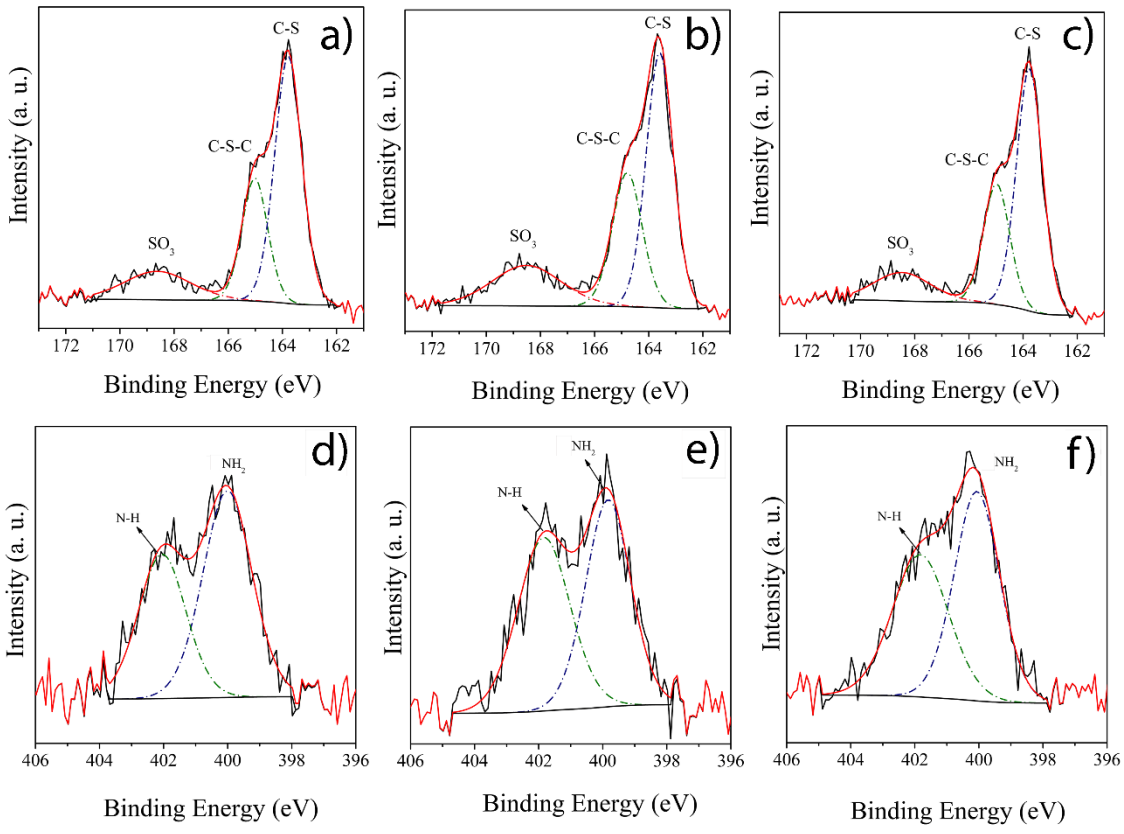

Figure 4.11 S2p deconvolution of a) RGO-DIPEA, b) RGO-Net$_3$ and C) RGO-DBU. N1s deconvolution of d) GO-RDIPEA, e) RGO-Net$_3$ and f) RGO-DBU

As presented previously, the fluorescence titration was applied for the RGO functionalized materials, and Figure 4.12 shows the results.

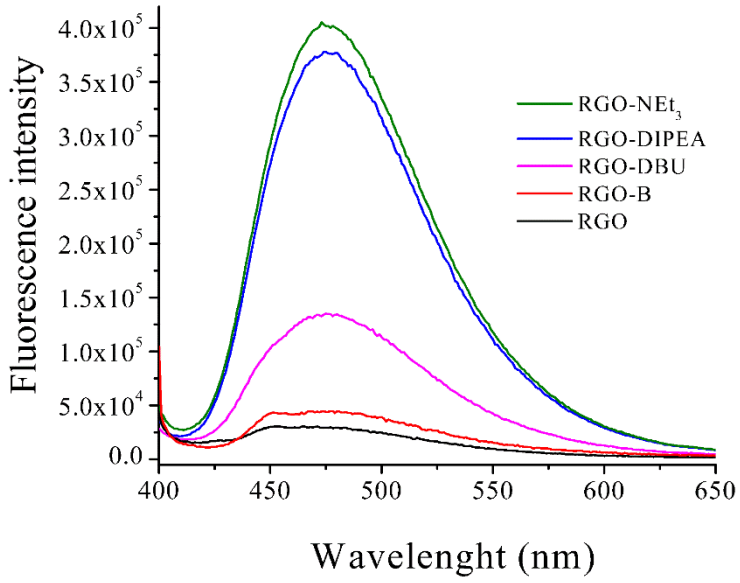

Figure 4.12 Fluorescence titrations of CA moieties bonded to RGO (λ_{ex}= 390 nm).

RGO-NEt_3 exhibited the strongest fluorescence intensity followed by RGO-DIPEA and RGO-DBU. Since similar C/O ratios can be calculated for RGO functionalized materials as compared to the GO functionalized, the quantification was performed taking the fluorescence of Figure 4.12 and setting in the calibration curve (Figure 4.6b). In addition, the previous validation of the fluorescent method allows to apply it for the estimations of the CA molecules in the RGO functionalized materials. Table 4 shows the results where is possible to observe that, the concentration of CA on RGO found was nearby than the GO functionalized materials. The difference of the CA concentration between the functionalization of GO and RGO can be attributed to TEROR. By removing the epoxide groups, the CA molecules can be bonded only through the α,β-unsaturated acids of GO. Taking the CA concentration found in GO-DIPEA and RGO-DIPEA, the TEROR contribution was around $1.5x10^{16}$ CA molecules bounded per mg of GO, which represent 20% of the CA molecules bonded on GO. In the literature, when base catalysts are used, TEROR has been identified as the principal reaction discarding TEMA [28-32]. However, these findings highlight the functionalization towards the α,β-unsaturated acids as the predominant reaction between CA and GO, even more important than the functionalization on epoxides. Hence, as many defects are introduced as long GO structure, it would be possible to increase the molecules bonded by thiol-ene reactions.

Table 4.4 Summary of fluorescent labelling and XPS survey for the estimation of CA on RGO samples (*n=3*)

Material	CA molecules/mg estimated by fluorimetry (COV)[a]	S atomic percentage from XPS[b]	CA molecules/mg estimated by XPS
RGO-DIPEA	$6.2x10^{16}$ (1.5)	0.89	$5.8x10^{16}$
RGO-NEt_3	$6.6x10^{16}$ (4.8)	0.99	$6.2x10^{16}$
RGO-DBU	$2.1x10^{16}$ (3.2)	0.69	$4.6x10^{16}$

[a]COV reported as percentage, %

[b]XPS technique possesses 10% of error

The XPS survey results were taken to corroborate the titration quantification using fluorescamine. The S atomic percentage found in the different samples followed the same order RGO-NEt_3 > RGO-DIPEA > RGO-DBU as obtained with the titration test (Table A3). In the case of RGO, NEt_3 produced an S atomic percentage as high as 0.99, and this represents a difference of 0.33 between GO-NEt_3 and RGO-NEt_3 (see Table A1 and A3). This difference could be attributed to TEROR, which occurs simultaneously during the functionalization on GO. In addition, the quantification of the molecules found with the XPS survey information is like the fluorescent labelling (see Table 4.4). This information allows to validate the titration method proposed in this work as an efficient tool to detect and follow the molecules grafted onto GO layers. For the functionalization of GO and RGO by TEMA, DIPEA and NEt_3 can be used as base catalysts due to the slight difference in the CA moieties that were achieved, whereas DBU produced lower functionalization degree for both GO or RGO (see Table 4.2 and 4.4). As previously explained, DBU and DMF could undergo inside reactions producing by-products which can affect the molecules bonded to GO [16]. The fact that both, GO and RGO, exhibited a stronger N atomic contribution as compared to S confirms that DBU is not an appropriate base catalyst to be used for GO functionalization.

STEM characterization was performed for RGO-NEt_3 due to the highest CA molecules found on RGO by XPS and fluorescent labelling. RGO-NEt_3 exhibited a well-dispersed material and more translucent RGO layers as compared to RGO (Figure 4.13). Since the intercalated water molecules were released after the thermal treatment, RGO sheets presented stacking and became difficult to disperse in DMF in contrast with RGO-NEt_3. This information supports the introduction of CA molecules to RGO. Moreover, similar sizes of the RGO layers were identified before and after the functionalization, indicating that the mild condition reactions produced minimal changes in RGO sheets. Therefore, this work remarks that the addition of CA molecules to the α,β-unsaturated acids of GO was possibly due to TEMA and,

using a base catalyst is possible to produce a high quantity of CA molecules grafted onto GO, without affecting the structure of the layers.

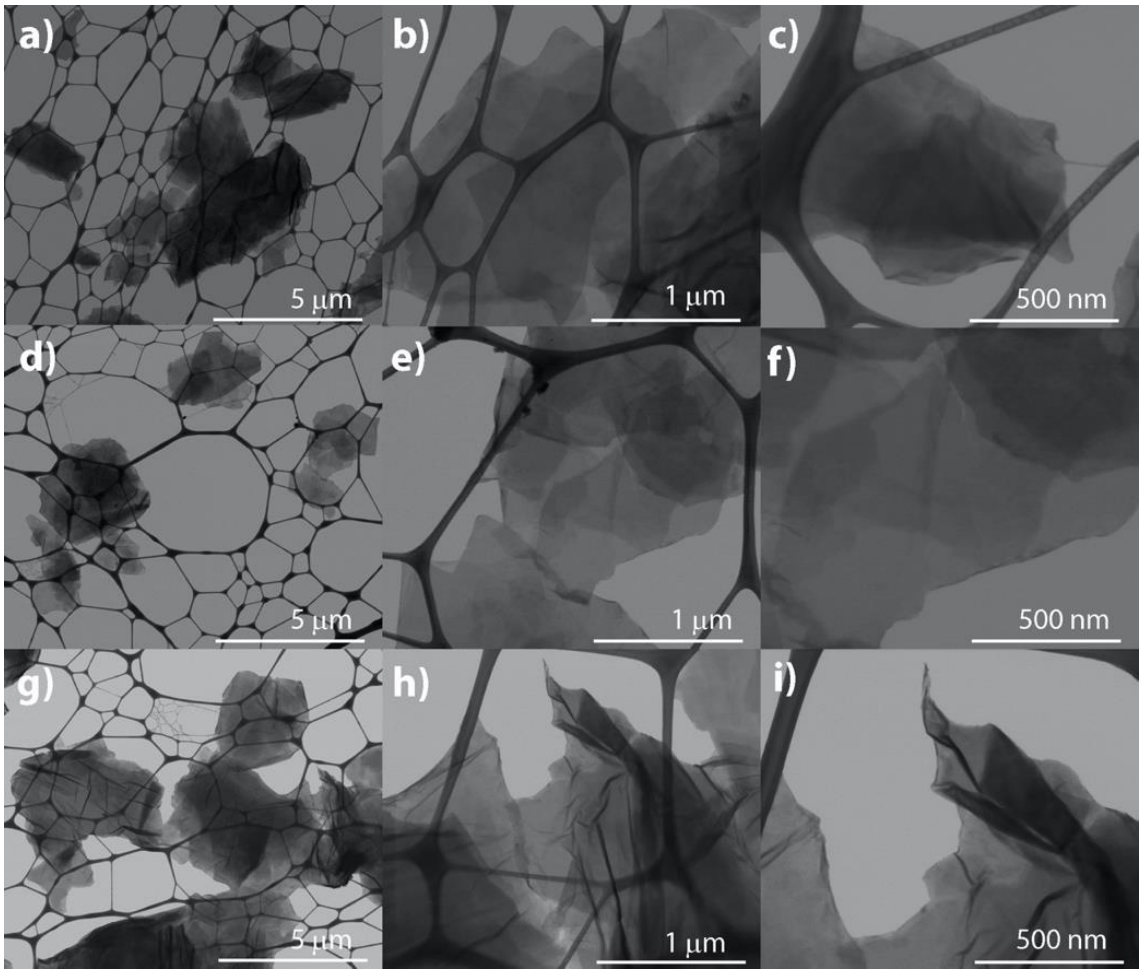

Figure 4.13 STEM images of RGO (a to c), RGO-B (d to e) and RGO-NEt_3 (g to i) at amplifications 10,000X, 50,000X and 100,000X.

In chapter 3, we introduced the photochemical functionalization of GO using Irgacure 369 as radical initiator. The reaction proceeded by TERA and according to XPS results presented (see Table A.2), the S atomic percentage found was around of 1.7, whereas RGO-NEt_3 produced 0.99 (see Table A.2). These results can be explained as TEMA reaction involves solely the α,β-unsaturated acids, whereas through TERA, radicals can attack a wide variety of alkenes groups. Therefore, in this study less CA molecules bonded could be obtained after the chemical functionalization by TEMA as compared to TERA.

4.3 Conclusions of the functionalization of GO and RGO with CA by TEMA

Herein, we systematically studied the functionalization of GO and RGO with CA by TEMA using different base catalysts.

I. In the case of GO, TEMA and TEROR can take place simultaneously during the functionalization using a base catalyst. However, despite the thermal reduction of GO, the functionalization with CA was possible, confirming the coupling reaction between the thiols with α,β-unsaturated acids of GO.

II. The fluorescent labelling using fluorescamine and S atomic percentage allowed to estimate the number of CA molecules bonded to GO and RGO. The CA concentration found was around 10^{16} CA molecules bounded per mg of GO and, RGO exhibited 20% less CA molecules bonded which can be associated to the number epoxide groups on GO ($1.5x10^{16}$ molecules per mg of GO).

III. The fluorescent method was validated by calculating the coefficient of determination, LOD, LOQ and COV which implies that, this method can be used for the quantification of molecules bounded to GO layers after a chemical functionalization.

IV. The functionalization towards α,β-unsaturated acids produced more CA molecules bonded than the ring-opening reactions. This was justified because during the graphite oxidation many defects are introduced breaking the aromatic domain.

V. TEMA produced less S atomic percentage than TERA when GO is functionalized with CA, which can be associated to the nature of the reaction. Whereas TEMA reaction involves solely the α,β-unsaturated acids, the radicals formed in TERA can attack a wide variety of alkenes groups.

VI. This study brings insights in the functionalization of GO by thiol-ene reactions and, opens the opportunity to take advantage of the unsaturated system of GO for functionalization under mild conditions and preserving the chemistry and structure of GO.

BIBLIOGRAPHY

[1] Nair, D.P.; Podgórski, M.; Chatani, S.; Gong, T.; Xi, W.; Fenoli, C.R.; Bowman, C.N. The Thiol-Michael Addition Click Reaction: A Powerful and Widely Used Tool in Materials Chemistry. Chem. Mater. 2014, 26, 724–744

[2] Lowe, A.B. Thiol-ene "click" reactions and recent applications in polymer and materials synthesis. Polym. Chem. 2010, 1, 17–36

[3] Yap, P.L.; Kabiri, S.; Tran, D.N.H.; Losic, D. Multifunctional Binding Chemistry on Modified Graphene Composite for Selective and Highly Efficient Adsorption of Mercury. ACS Appl. Mater. Interfaces 2018, 11, 6350–6362

[4] Piñeiro-García, A.; Vega-Díaz, S.M.; Tristán, F.; Meneses-Rodríguez, D.; Labrada-Delgado, G.J.; Semetey, V. Photochemical Functionalization of Graphene Oxide by Thiol–Ene Click Chemistry. Ind. Eng. Chem. Res. 2020, 59, 13033–13041

[5] Wadekar, P.H.; Khose, R. V.; Pethsangave, D.A.; Some, S. One-Pot Synthesis of Sulfur and Nitrogen Co-Functionalized Graphene Material using Deep Eutectic Solvents for Supercapacitors. ChemSusChem 2019, 12, 3326–3335

[6] Zhang, W.; Zhao, Q.; Liu, T.; Gao, Y.; Li, Y.; Zhang, G.; Zhang, F.; Fan, X. Phosphotungstic Acid Immobilized on Amine-Grafted Graphene Oxide as Acid/Base Bifunctional Catalyst for One-Pot Tandem Reaction. Ind. Eng. Chem. Res. 2014, 53, 1437–1441

[7] Ederer, J.; Janoš, P.; Ecorchard, P.; Tolasz, J.; Štengl, V.; Beneš, H.; Perchacz, M.; Pop-Georgievski, O. Determination of amino groups on functionalized graphene oxide for polyurethane nanomaterials: XPS quantitation vs. functional speciation. RSC Adv. 2017, 7, 12464–12473

[8] Yang, A.; Li, J.; Zhang, C.; Zhang, W.; Ma, N. One-step amine modification of graphene oxide to get a green trifunctional metal-free catalyst. Appl. Surf. Sci. 2015, 346, 443–450

[9] Zhang, X.; Yu, C.; Wang, C.; Wang, Z.; Qiu, J. Chemically converting graphene oxide to graphene with organic base for Suzuki reaction. Mater. Res. Bull. 2015, 67, 77–82

[10] Muz, M.; Ost, N.; Kühne, R.; Schüürmann, G.; Brack, W.; Krauss, M. Nontargeted detection and identification of (aromatic) amines in environmental samples based on diagnostic derivatization and LC-high resolution mass spectrometry. Chemosphere 2017, 166, 300–310

[11] Eng, A.Y.S.; Chua, C.K.; Pumera, M. Refinements to the structure of graphite oxide: Absolute quantification of functional groups via selective labelling. Nanoscale 2015, 7, 20256–20266

[12] Barua, M.; Sreedhara, M.B.; Pramoda, K.; Rao, C.N.R. Quantification of surface functionalities on graphene, boron nitride and borocarbonitrides by fluorescence labeling. Chem. Phys. Lett. 2017, 683, 459–466

[13] Shrivastava, A., & Gupta, V. B. (2011). Methods for the determination of limit of detection and limit of quantitation of the analytical methods. Chronicles of young scientists, 2(1), 21.

[14] Procedures, A. (2000). Methods Validation: Chemistry, Manufacturing, and Controls. Federal Register (Notices), 65, 776.

[15] Luo, D.; Zhang, G.; Liu, J.; Sun, X. Evaluation Criteria for Reduced Graphene Oxide. J. Phys. Chem. C 2011, 115 (23), 11327–11335

[16] Ramírez-Jiménez, R.; Franco, M.; Rodrigo, E.; Sainz, R.; Ferritto, R.; Lamsabhi, A.M.; Aceña, J.L.; Cid, M.B. Unexpected reactivity of graphene oxide with DBU and DMF. J. Mater. Chem. A 2018, 6, 12637–12646

[17] Xin, Q.; Li, Z.; Li, C.; Wang, S.; Jiang, Z.; Wu, H.; Zhang, Y.; Yang, J.; Cao, X. Enhancing the CO2 separation performance of composite membranes by the incorporation of amino acid-functionalized graphene oxide. J. Mater. Chem. A 2015, 3, 6629–6641
[18] Vacchi, I.A.; Guo, S.; Raya, J.; Bianco, A.; Ménard-Moyon, C. Strategies for the Controlled Covalent Double Functionalization of Graphene Oxide. Chem. – A Eur. J. 2020, 24, 6591-6598
[19] Li, Y.; Bao, L.; Zhou, Q.; Ou, E.; Xu, W. Functionalized Graphene Obtained via Thiol-Ene Click Reactions as an Efficient Electrochemical Sensor. ChemistrySelect 2017, 2, 9284–9290
[20] Kim, N.H.; Kuila, T.; Lee, J.H. Simultaneous reduction, functionalization and stitching of graphene oxide with ethylenediamine for composites application. J. Mater. Chem. A 2013, 1, 1349–1358
[21] Thakur, S.; Karak, N. Alternative methods and nature-based reagents for the reduction of graphene oxide. Carbon N. Y. 2015, 94, 224–242
[22] Liu, Y.; Sajjadi, B.; Chen, W.-Y.; Chatterjee, R. Ultrasound-assisted amine functionalized graphene oxide for enhanced CO2 adsorption. Fuel 2019, 247, 10–18.
[23] Krishnamoorthy, K.; Veerapandian, M.; Yun, K.; Kim, S.J. The chemical and structural analysis of graphene oxide with different degrees of oxidation. Carbon N. Y. 2013, 53, 38–49
[24] Taniguchi, T.; Kurihara, S.; Tateishi, H.; Hatakeyama, K.; Koinuma, M.; Yokoi, H.; Hara, M.; Ishikawa, H.; Matsumoto, Y. pH-driven, reversible epoxy ring opening/closing in graphene oxide. Carbon N. Y. 2015, 84, 560–566
[25] Bagri, A.; Mattevi, C.; Acik, M.; Chabal, Y.J.; Chhowalla, M.; Shenoy, V.B. Structural evolution during the reduction of chemically derived graphene oxide. Nat. Chem. 2010, 2, 581–587
[26] Jeong, H.K.; Lee, Y.P.; Jin, M.H.; Kim, E.S.; Bae, J.J.; Lee, Y.H. Thermal stability of graphite oxide. Chem. Phys. Lett. 2009, 470, 255–258
[27] Huh, S.H.; Korea, S. Thermal Reduction of Graphene Oxide. Phys. Appl. Graphene - Exp. 2011, 73–90.
[28] Huang, H.; Tian, Y.; Xie, Y.; Mo, R.; Hu, J.; Li, M.; Sheng, X.; Jiang, X.; Zhang, X. Modification of graphene oxide with acrylate phosphorus monomer via thiol-Michael addition click reaction to enhance the anti-corrosive performance of waterborne epoxy coatings. Prog. Org. Coatings 2020, 146, 105724
[29] Nie, L.; Zhang, J.; Wu, Q.; Fei, G.; Hu, K.; Fang, L.; Yang, S. Fabrication of micropatterned gold nanoparticles on graphene oxide nanosheet via thiol-Michael addition click chemistry. Mater. Lett. 2020, 261, 127014
[30] Oz, Y.; Barras, A.; Sanyal, R.; Boukherroub, R.; Szunerits, S.; Sanyal, A. Functionalization of reduced graphene oxide via thiol-maleimide “click” chemistry: Facile fabrication of targeted drug delivery vehicles. ACS Appl. Mater. Interfaces 2017, 9, 34194–34203
[31] Huang, N.; Zhang, S.; Yang, L.; Liu, M.; Li, H.; Zhang, Y.; Yao, S. Multifunctional Electrochemical Platforms Based on the Michael Addition/Schiff Base Reaction of Polydopamine Modified Reduced Graphene Oxide: Construction and Application. ACS Appl. Mater. Interfaces 2015, 7, 17935–17946
[32] Liu, J.; Zhu, K.; Jiao, T.; Xing, R.; Hong, W.; Zhang, L.; Zhang, Q.; Peng, Q. Preparation of graphene oxide-polymer composite hydrogels via thiol-ene photopolymerization as efficient dye adsorbents for wastewater treatment. Colloids Surfaces A Physicochem. Eng. Asp. 2017, 529, 668–676

CHAPTER 5

QUANTIFYING THE FUNCTIONAL GROUPS OF GRAPHENE OXIDE BY FLUORESCENT LABELLING

In the previous chapters, selective reactions of the GO functionalization were illustrated by exploring ring opening reactions without altering carboxylic acids, and TER for the chemical functionalization of alkene groups that remain after the graphitic oxidation. In chapter 2, it was discussed that the addition of sodium hydroxide can be helpful to reduce the formation of peptide bonds during the ring opening reaction. In chapters 3 and 4 the applications of TER was discussed using two distinct chemical routes: i) adding photoinitiators (reaction conducted by TERA) and ii) using base catalysts (reaction conducted *via* TEMA). In both cases, the functionalization of GO with cysteamine as probe molecule was successfully demonstrated while a reduction effect on GO was minimized.

Notably, chapter 4 helped to answer an important question: how many molecules can be linked towards epoxides and α,β-unsaturated acids of GO? It was possible to answer this question using a novel and simple approach that was the use of fluorescamine to monitor the number of CA molecules linked to GO after the reaction. This method was able to quantify the CA molecules, and thus the question about how many α,β-unsaturated acids of GO do we have available in GO was addressed. To take advantage of the wide diversity of the functional groups of the GO, it is not only necessary to generate new approaches about selective and orthogonal reactions in GO. Also, it is necessary to know the number of molecules that can be grafted onto the GO layers through the different oxygen functional groups. So, the question proposed in the previous chapter can be extended to: what is the density of each oxygen functional group in GO? By knowing the density of the most representative functional groups of GO, it would be possible to anticipate the number of molecules that can be grafted in each functional group. This can conduct us to have a complete knowledge about the chemistry of the GO to design novel GO based materials for specific applications.

Therefore, in this chapter, it is proposed the quantification of different functional groups on GO taking advantage of the fluorescent labelling method proposed in chapter 4 using fluorescamine. This study is focused in three functional groups which are epoxide, carboxylic

acid and alkenes groups. To quantify each functional group, a reaction in the specific functional groups was carried out. Epoxides and carboxylic acids are well known to have a strong density in GO and their chemistry is well-known and relatively easy to apply [1]. In chapter 3 and 4, it was found that the alkene groups of GO represent an important approach for the derivatization of GO using either radical photoinitiator (TERA) or base catalyst (TEMA).

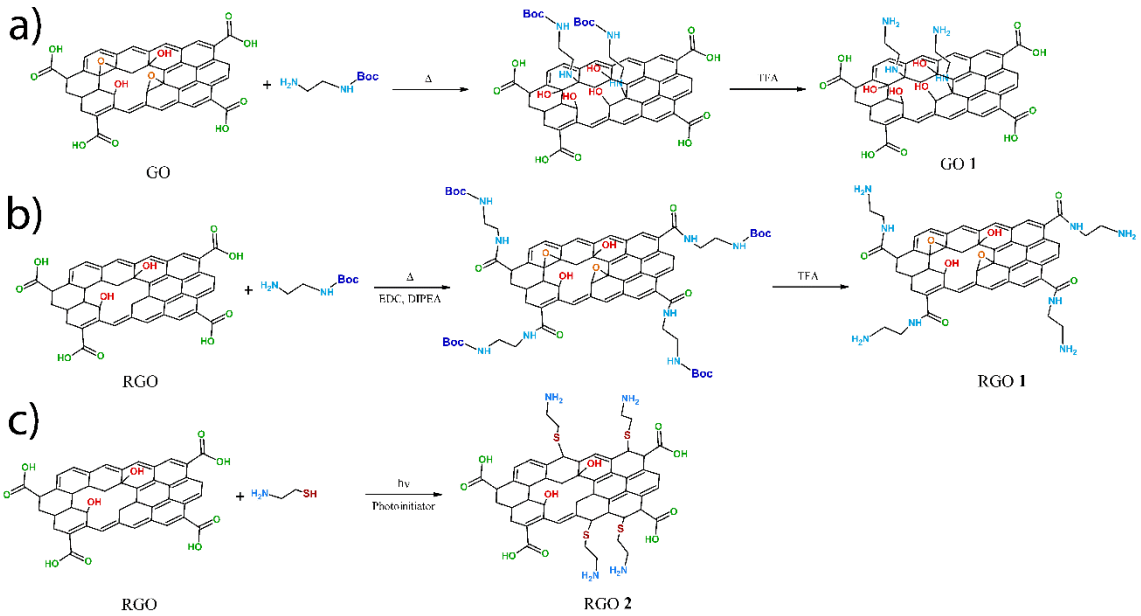

Figure 5.1 a) Functionalization of GO with NHBoc to produce GO **1**, b) reaction to produce RGO **1** and c) production of RGO **2**

Figure 5.1 shows the schematic representation of the reactions conducted in this chapter. To quantify epoxides, GO was reacted with *N*-Boc-ethylenediamine (NHBoc) by nucleophilic attack using DMF as solvent to produce GO **1**. Since the epoxy groups are susceptible to be attacked by nucleophiles, a thermally reduced GO (RGO) was employed for the quantification of carboxylic acids and alkenes. To quantify carboxylic acids, RGO was reacted with NHBoc using coupling agents under DMF solution to produce RGO **1**. For the quantification of alkene groups, RGO was reacted with CA by TERA to produce RGO **2**. Finally, the primary amine from the deprotected NHBoc and CA was labelled using fluorescamine.

To proceed with the GO functionalization shown in Figure 5.1, it was necessary to conduct three different experimental routes that are presented in Figure 5.2. Figure 5.2a shows the schematic representation of the functionalization of GO with NHBoc towards the epoxide groups. The GO (1 mg/mL) dispersed in DMF was bubbled with a constant flow of argon (Ar) and under stirring. After that, the NHBoc (2 mg/mL) was added and the reaction was heated

until 50 ºC keeping the bubbling and the stirring. Then, the system was sealed maintaining the inert atmosphere and the reaction was let for 24 h producing GO **1** material. For the functionalization of RGO with the NHBoc (see Figure 5.2b), RGO (1 mg/mL) dispersed in DMF was bubbled with a constant flow of argon (Ar) and stirring. After that, EDC (20 mM) was added to the system keeping the bubbling and the stirring for another. Thereafter, the NHBoc (2 mg/mL) and 100 µL of DIPEA as base catalyst were added and the reaction was heated until 55 ºC keeping the bubbling and the stirring. The system was sealed maintaining the inert atmosphere and the reaction was let for 48 h producing RGO **1** material. The deprotection of the NHBoc in GO **1** and RGO **1** samples was performed using trifluoracetic acid (TFA), as shown in Figure 5.1a and 5.1b.

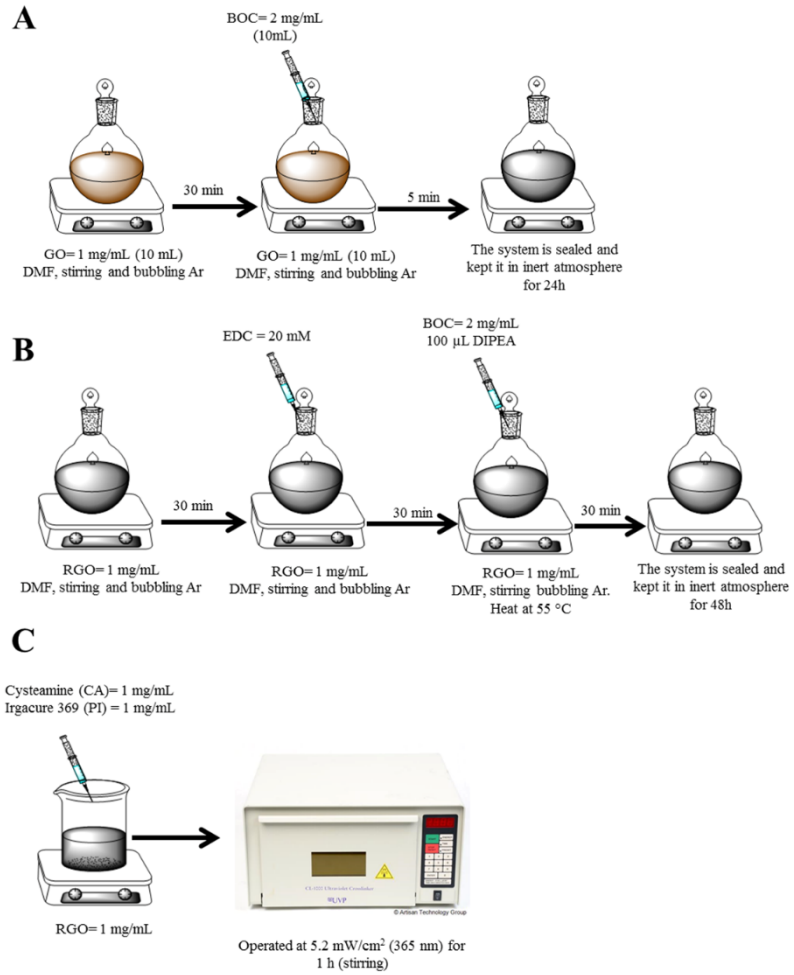

Figure 5.2 Schematic representation of the experimental method followed for: a) functionalization of GO with NHBoc towards epoxide groups, b) functionalization of RGO with NHBoc towards carboxylic acids and c) functionalization of RGO with CA towards alkene groups.

On the other hand, for the functionalization of RGO in the alkene groups, RGO dispersed in DMF was mixed with CA (2 mg/mL) and PI ($2.7x10^{-5}$ mol). Subsequently, the mixture was put inside of the UV-camber during 60 min, under stirring to produce RGO **2**.

Once the materials GO **1**, RGO **1** and RGO **2** were produced, all these functionalized materials possess a primary amine (-NH_2) that remained after the reaction. The detection and quantification were performed using a similar protocol as in chapter 4. Figure 5.3 contains the scheme representation of the titration and quantification of primary amines in the GO functionalized materials.

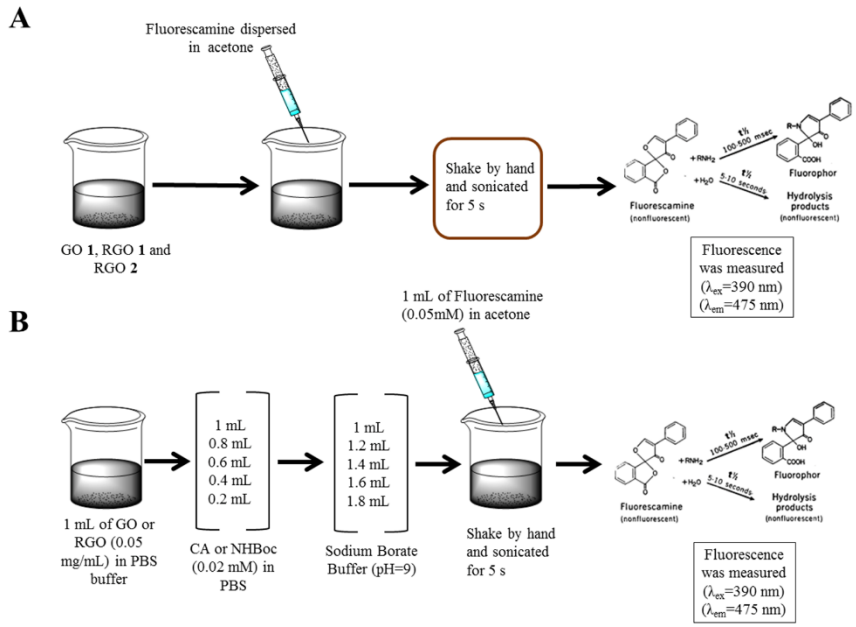

Figure 5.3 Schematic representation of: a) detection of -NH_2 moieties in GO layers and b) preparation of the calibration curve for the quantification of -NH_2 moieties after the chemical functionalization

As presented in chapter 4, the detection of -NH_2 moieties in GO layers consisted in a simple titration of a constant volume of the GO functionalized with CA (the pH was adjusted using sodium borate) and then adding fluorescamine. Here, it is worth mentioning that the -NH_2 moieties detected by fluorescamine come solely from either the NHBoc or CA molecule bonded to GO. The formation of the fluorophore is quite rapid, and the fluorescence intensity was measured and presented in Figure 5.3a. After that, different calibration curves were built to determine the number of NHBoc or CA molecules bonded to GO layers. According to Figure 5.3b, a constant volume of either GO or RGO (for the analysis of RGO **1** and RGO **2**, RGO was

used as a constant volume) was taken to add the quenching effect to the calibration curve. Then, different volumes of either NHBoc or CA standard (0.02 mM, prepared in PBS) were added with different volumes also of sodium borate buffer (pH~9). Finally, fluorescamine dispersed in acetone was added and the mixture was shaken by hand and then sonicated to eliminate the bubbles. The fluorescence was measured at λ_{ex}=390 nm and λ_{em}=475 nm. For the quantification, the fluorescence intensity obtained from the titration test was set into the respective calibration curve. For more details about the experimental procedure, see appendix A.1.

Finally, the functionalized materials were also characterized by FTIR, Raman spectroscopy and XPS to confirm the chemical functionalization after of each chemical rout shown in Figure 5.1.

5.1 Characterization of the functionalized materials by ATR-FTIR, Raman spectroscopy and XPS

The quantification of GO functional groups such as epoxide, carboxylic acids and alkene groups was performed using the chemical routes of Figure 5.1 In order to ensure if the quantification comes from the specific functional group, the characterization of the chemical species was performed in GO **1**, RGO **1** and RGO **2**. Figure 5.4 shows the ATR-FTIR results and GO exhibited the characteristic bands attributed to carboxylic acids (1730 cm^{-1}), skeleton carbon bonds (1624 cm^{-1}), alcohols (1379 and 1046 cm^{-1}) and epoxide groups (1218 and 998 cm^{-1}) [2,3].

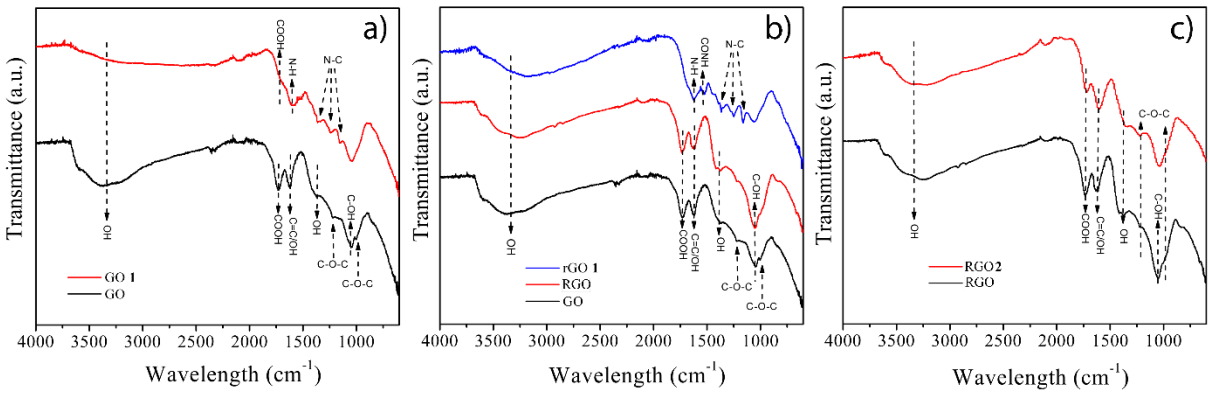

Figure 5.4 ATR-FTIR characterization of GO, RGO, GO **1**, RGO **1** and RGO **2**

After the chemical functionalization on epoxide groups, GO **1** showed new bands at 1592 cm^{-1} 1355 cm^{-1}, 1244 cm^{-1} and 1154 cm^{-1} associated to N-H and N-C bonds for the NHBoc

bonded to GO [4-6], whereas epoxide bands (1218 and 998 cm^{-1}) were suppressed (see Figure 5.4a) [2,3]. In addition, carboxylic acid band (1730 cm^{-1}) was maintained as a shoulder after the chemical functionalization. This information suggests that the functionalization in GO **1** proceeded on epoxide groups. In the case of the chemical functionalization on carboxylic acid groups, a thermal reduction was carried out as first step and, RGO material exhibited a decrease in the bands at 1218 and 998 cm^{-1}, whereas the rest of the groups presented a similar intensity as compared to GO (Fig. 2b). Thus, epoxy groups were almost eliminated of the GO. After the functionalization on carboxylic acid groups, RGO **1** displayed bands attributed to N-C vibrations (1355 cm^{-1}, 1244 cm^{-1} and 1154 cm^{-1}) like GO **1** due to the introduction of NHBoc in the GO [4-6]. However, in the case of RGO **1**, the carboxylic acid band was completely suppressed due to the formation of amide bonds. Indeed, a new band was detected for RGO **1** in Figure 4b at 1526 cm^{-1}, attributed to amide II mode [7,8]. This information suggests the successful functionalization of RGO on carboxylic acid groups.

On the other hand, Fig. 2c presents the ATR-FTIR of RGO **2** which not revealed new bands. Generally, C-S bonds are low intense and thus it became complicated to distinguish those vibrations in ATR-FTIR spectra [9]. Nonetheless, after the functionalization, RGO **2** conserved the oxygen functional groups as compared to RGO, confirming TERA as an orthogonal reaction.

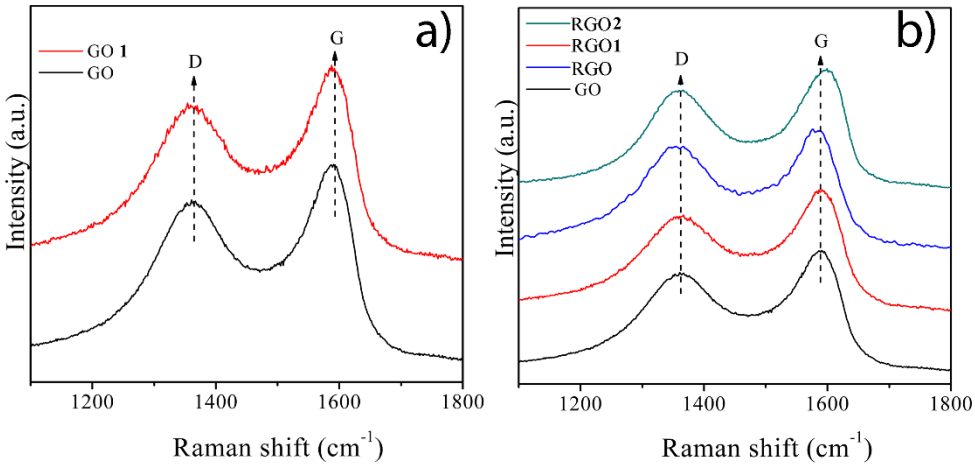

Figure 5.5 Raman spectroscopy characterization: a) GO and GO **1**; b) RGO, RGO **1** and RGO **2**.

Raman spectroscopy characterization was performed to confirm the functionalization in the different samples. In the case of GO **1** and RGO **1,** *G* band presented a downshift of 3 cm^{-1}

and 7 cm^{-1} respectively (see Figure 5a and Figure 5b). The downshift observed in GO **1** and RGO **1** is consistent with a surface N-type doping due to N atoms bonded to the graphitic lattice [10,11]. This information confirmed the functionalization GO **1** and RGO **1** with NHBoc and supports the ATR-FTIR results of Figure 5.4a and 5.4b. Notably, the *G* band RGO **2** material exhibited an upshift of 8 cm^{-1} as compared to RGO (see Figure 5.5). Despite the introduction N and S atoms from CA moieties in RGO structure, the trend of the *G* band was opposite in comparison with GO **1** and RGO **1**. To explain this behavior, the Raman information was subtracted from Figure 5.5b and the A_D/A_G ratio was calculated. In Table 5.1 one can observe that GO and RGO possess similar A_D/A_G ratios confirming the mild thermal reduction that GO was undergone. In addition, the A_D/A_G ratio of RGO **2** was nearby to RGO but lower than RGO **1**. The RGO **1** sample was undergone in an amidation reaction, and thus the long period under stirring could produce an increase in the disorder of RGO layers leading to an increase in *D* band [12]. So, the RGO **1** sample exhibited the greatest A_D/A_G ratio. However, TERA was applied for the functionalization of RGO **2** breaking the C=C bonds and increasing the sp^3 hybridization. Indeed, the width of *G* band was higher as compared to RGO suggesting the increase in *D'* band, which is an interband located under *G* [12,13]. Therefore, the *G* band can present an upshift due to the increase in *D'* band and, due to the area of both bands (*G* and *D* band) increased, the A_D/A_G ratio could be mitigated [14]. Therefore, the upshift in G band of RGO **2** is consistent with the introduction of CA moieties after the functionalization.

Table 5.1 Raman spectroscopy information of Figure 5.5b.

Material	G (cm^{-1})	A_D/A_G
GO	1590	1.20
RGO	1590	1.22
RGO **1**	1583	1.32
RGO **2**	1598	1.23

XPS characterization was conducted to confirm the chemical functionalization of GO **1**, RGO **1** and RGO **2**. In Figure 5.6, all the functionalized materials showed a clear Nitrogen (N) atomic contribution, whereas RGO **2** contains additional sulfur (S) atomic contribution. Moreover, GO and RGO lack of a significant N and S atomic contribution confirming the presence of NHBoc and CA in the functionalized materials (see Figure A2).

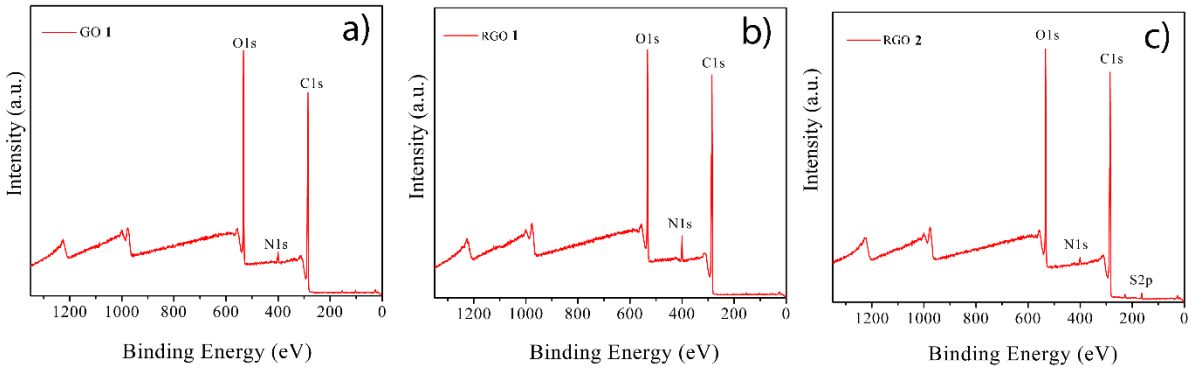

Figure 5.6 XPS survey of GO **1**, RGO **1** and RGO **2**.

The C1s high-resolution XPS deconvolution of GO **1**, RGO **1** and RGO **2** is presented in Figure 5.7. As compared to GO (see Figure A4), GO **1** material was fitted into an additional peak at 285.4 eV attributed to N-C bonds [11,15]. Moreover, RGO **1** exhibited two additional peaks at 285.4 eV and 287.5 eV, attributed to N-C and N-C=O of amide bonds as compared to RGO (see Figure A4) [11,15,16]. The amine and amide bonds identified in C1s deconvolution are consistent with ATR-FTIR results of Figure 5.4b.

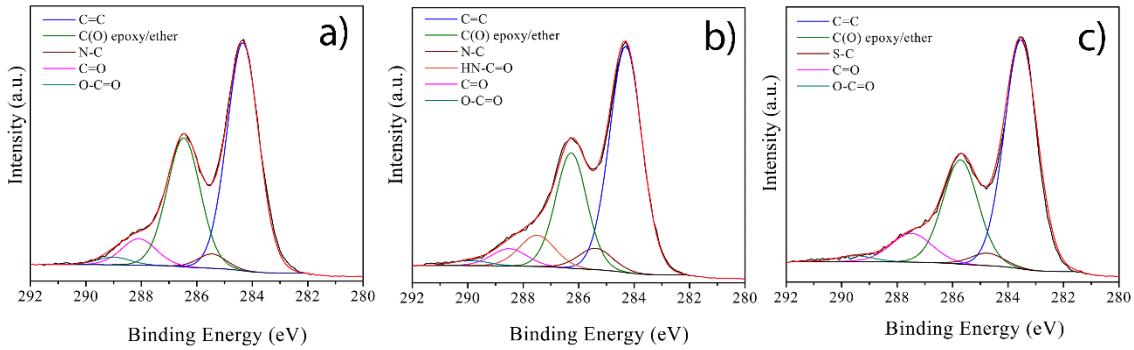

Figure 5.7 High resolution C1s deconvolution of a) GO **1,** b) RGO **1** and c) RGO **2**.

Furthermore, the N1s high-resolution XPS deconvolution of GO **1** presented two peaks at 399.8 eV and 401.8 eV attributed to $-NH_2$ and $-NH^+_3$ bonds, due to the presence of NHBoc once it was deprotected (see Figure 5.8a) [15,17]. Moreover, RGO **1** was possible to fit into three different peaks at 398.5 eV, 399.5 eV and 401.2 eV, associated to $-NH_2$, HN-C=O and $-NH^+_3$, respectively (see Figure 5.8b) [15-17]. When amides are formed on GO, the peaks can be shifted due to the existence of resonance structures as reported elsewhere [18]. This information confirmed the functionalization on epoxide and carboxylic acids in GO **1** and RGO **1** materials.

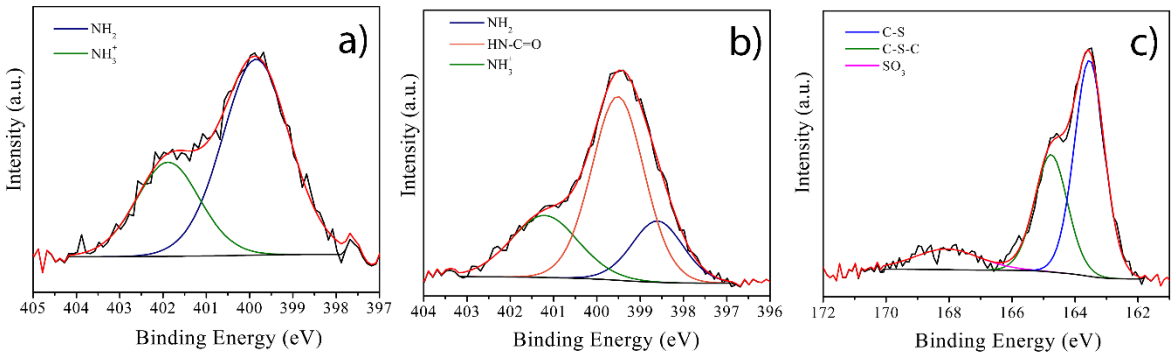

Figure 5.8 N1s high-resolution XPS deconvolution of a) GO **1** and b) RGO **1**. c) S2p high-resolution XPS deconvolution of RGO **2**.

On the other hand, for RGO **2**, the C1s deconvolution presented a new peak at 284.7 which could be associated to C-S bonds (see Figure 5.7c). The S2p deconvolution of RGO **2** confirmed the successful functionalization with CA, since the doublet peak at 163.5 eV and 164.7 eV, attributed to C-S and C-S-C bonds were identified (see Figure 5.8c) [14,19]. Thus, despite that ATR-FTIR presented no significant changes for RGO **2**, XPS analyses allowed to confirm the chemical functionalization. Therefore, ATR-FTIR, the Raman spectroscopy and XPS results offers evidence of the functionalization on epoxide groups, carboxylic acid groups and alkene groups of GO.

5.2 Quantifying epoxides, carboxylic acids and alkene groups of GO

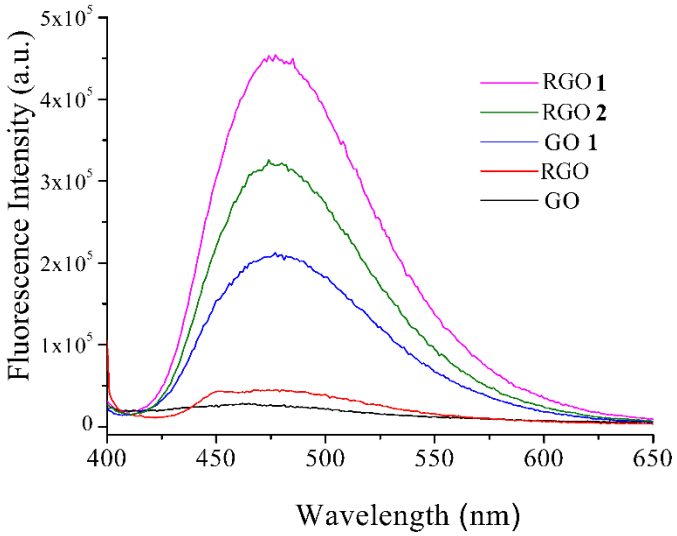

Figure 5.9 Fluorescence characterization of GO, RGO, GO **1**, RGO **1** and RGO **2** (λ_{ex}=390 nm and λ_{em}=475 nm).

After confirming the selective labelling on epoxides, carboxylic acids and alkenes using either NHBoc or CA, the quantification *via* fluorescent titration using fluorescamine and XPS atomic percentage was conducted. Fluorescamine reacts rapidly and specifically with -NH_2 moieties of NHBoc and CA in GO **1**, RGO **1** and RGO **2** to form fluorescent pyrrolinone [20]. The fluorescent titration results are shown in Figure 5.9 and highlight that the strongest contribution corresponds to RGO **1**, followed by RGO **2** and GO **1**. The number of NHBoc molecules grafted to GO **1** and RGO **1** can be associated to the concentration of epoxide and carboxylic acids groups respectively, whereas the CA molecules grafted to RGO **2** to alkenes groups concentration (see Figure 5.1). GO and RGO exhibited a minimum fluorescence signal confirming that no trace of -NH_2 moieties were in the blank materials. The fluorescence intensity was subtracted from Figure 5.9 at λ_{em}=475 nm and set to the respective calibration curve of Figure 5.10.

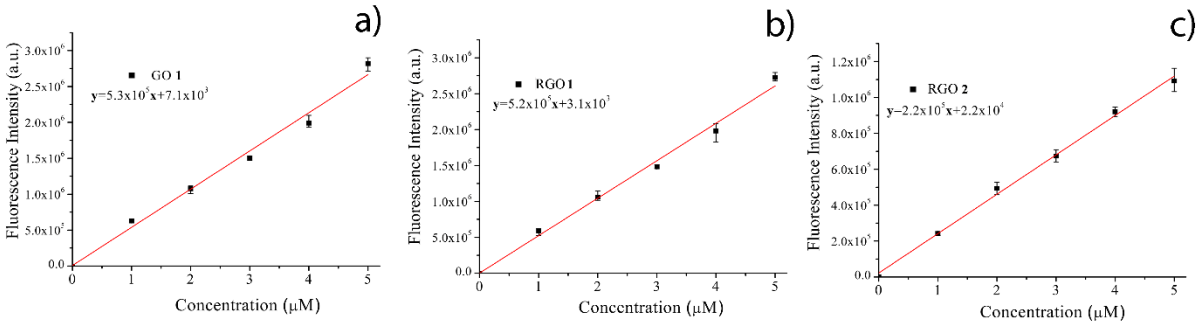

Figure 5.10 Calibration curve for the quantification of: a) epoxide, b) carboxylic acid and c) alkene groups.

The results presented in Table 5.1 show the alkene groups as the functional group with the strongest concentration, followed by carboxylic acids and epoxide groups.

Table 5.1 Summary of fluorescence and XPS results for the estimation of the functional groups of GO (*n=3*)

Functional group	No. of molecules estimated by fluorescent labelling (COV)[ab]	No. of molecules estimated by XPS[b]
Carboxylic acids	$4.2x10^{16}$ (6.8)	$8.7x10^{16}$
Alkenes	$6.6x10^{16}$ (4.2)	$7.1x10^{16}$
Epoxides	$1.9x10^{16}$ (3.5)	$8.6x10^{16}$

[a]COV was reported as percentage, %

[b]Concentration reported per mg of GO or RGO

The literature, the study about concentration of functional groups of GO is fairly limited. However, Eng et al. found that the strongest contribution on GO corresponds to the epoxide groups ($7.8x10^{17}$ molecules per mg of GO) [21]. Additionally, carboxylic acid groups were

reported in a concentration of $1.4x10^{16}$ by Eng et al. [21], whereas Barua et al. reported a concentration of $2.8x10^{18}$ molecules per mg of GO [22]. Both results were obtained from a GO synthesized by modified Hummer's method. Comparing previous reports with the results obtained here, the carboxylic acid groups were found in a concentration of $4.2x10^{16}$ nearby of the results reported by Eng et al. Regardless of the proximity of this result, the epoxide groups concentration was of $1.9x10^{16}$ that represents only 2.4 % of the concentration previously reported by Eng et al. As it was mentioned in section 1.1, the variety and concentration of the functional groups depends on the pristine graphite and its particle size, oxidizing reagents, temperature and the oxidation time [23-25]. Therefore, it is expected that slight changes performed during the GO synthesis conduct to different density of functional groups.

In this study, natural graphite of size ~1 mm was used and given the low dimensions of the initial graphite, the borders are more susceptible to be oxidized and thus, more carboxylic acids groups can be generated [26]. However, a mixture of H_2SO_4/H_3PO_4 was used in order to have a mild oxidation and thus introduce less defects (such as vacancies) in the graphite lattice as reported elsewhere [27]. This could explain the low density of carboxylic acids and epoxide groups concentration found. In addition, alkene groups seem to be an interesting option to carry out chemical modification on GO. Here, the alkene groups concentration was the higher among the functional groups quantified. The origin of this result could be associated to the efficiency of TER, which is a powerful tool for coupling thiols to a wide diversity of unsaturated systems [28].

During the GO synthesis, diverse functional groups arise breaking the aromatic domain and producing a wide range of unsaturated systems [3,29]. The alkenes groups produced are susceptible to be activated by TERA. Indeed, adding the concentration of the carboxylic acids and epoxide in Table 5.1 (giving a total of $6.1x10^{16}$ molecules per mg of GO) and, considering that each functional group break the aromatic domain leading to α,β unsaturated carbonyls or ethers, the obtained value is nearby to the concentration of alkenes. Therefore, as many defects are introduced as long GO structure, it would be possible to increase the molecules bonded by TERA. This information confirms the alkene groups of GO as a promising tool to create multi-functional graphene-based materials *via* orthogonal reactions.

The fluorescent method was validated by estimating the limit of detection (LOD), limit of quantification (LOQ), the coefficient of determination (r^2) and the coefficient of variation (COV). The follow equations show the estimation of the LOD, LOQ and COV

$$LOD = {}^{3S_a}\!/_{b} \quad 5.1$$

$$LOQ = {}^{10S_a}\!/_{b} \quad 5.2$$

$$COV = \frac{C}{S_D} \cdot 100 \quad 5.3$$

Where S_a is the standard deviation of either *y*-residuals or *y*-intercepts, *b* is the slop of the calibration curve, *C* is the concentration found using the calibration curve and SD is the standard deviation of *C*. As discussed in chapter 4, this validation method can be applied in all cases, and it is most applicable when the analysis method does not involve background noise [30]. Table 5.2 contains a summary of the results obtained from the validation method. The r^2 confirmed the linearity of the linear adjust, and thus the fluorescent response is linear to the concentration of either NHBoc or CA. The LOD and LOQ reefer to minimum quantity of analyte that can be detected but not necessarily quantified, and the minimum concentration at which the analyte can be quantitated with acceptable precision and accuracy under the stated conditions of test [31]. The molar concentration found in Table 5.2 were inside of the parameters of the validation method, except for epoxide groups. This can be attributed to the low concentration of epoxide groups in the GO studied here. Since epoxide groups are in the lower concentration, the fluorescent method cannot predict with enough accuracy the epoxide concentration.

Table 5.2 Validation of the fluorescent method

Functional group	LOD (μM)	LOQ (μM)	r^2	COV	C (μM)
Carboxylic acids	0.13	0.44	0.992	6.8	0.86
Alkenes	0.08	0.28	0.996	4.2	0.77
Epoxides	0.16	0.56	0.987	3.5	0.39

In order to corroborate the quantification *via* fluorescent titration, the atomic percentage of XPS survey was analyzed. The atomic percentage found of N in the XPS survey was 2.3% and 4.1% for GO **1** and RGO **1** respectively, whereas RGO **2** possessed 1.0% of S atomic

contribution. According to the XPS results, the NHBoc and CA molecules grafted to GO **1**, RGO **1** and RGO **2** were estimated (see A3) and presented in Table 5.1. The concentration found by XPS was similar to the fluorescent titration results confirming the quantification of the functional groups. The XPS results could be higher than the fluorescent results for two reasons: i) the XPS brings the N atomic contribution from all the species that could be in the samples, including contamination, whereas titration test with fluorescamine only detects and quantifies the $-NH_2$ moieties, and ii) XPS results come from a theoretical estimation using the initial molecules added to the reaction. Despite the slight difference between XPS and fluorescent labelling, the order of magnitude was similar (10^{16}). This information confirmed the reliability of the titration method proposed in this work.

5.3 Conclusions of the quantification of GO functionalities

Herein, it was reported the quantification of epoxide, carboxylic acids and alkene groups of GO *via* fluorescent labelling. Controlled chemistry strategies were used to ensure that the quantification correspond to specific functional groups.

I. Fluorescamine was used to identify rapidly and specifically -NH_2 moieties through the formation of a fluorophore. The highest concentration corresponded to the alkenes groups, and this was attributed to the great quantity of defects introduced in the graphitic lattice during the oxidation reaction. As discussed in chapter 4, as many defects are introduced during the graphite oxidation, more molecules could be bonded towards the alkene groups.

II. The quantification highlights the C=C bonds as an excellent approach for creating multi-functionalized graphene oxide materials. Since TERA is an orthogonal reaction, the rest of the surface chemistry of GO was preserved to be used for dual functionalization.

III. The carboxylic acids and epoxides followed the order of the concentration of the GO functional groups. Despite that those functionalities have been reported with higher concentrations, the mixture of H_2SO_4/H_3PO_4 and the size of the graphite used could explain their low concentration.

IV. Since the structure and chemical composition of the GO strongly depends on the pristine graphite, oxidizing reagents, temperature and the oxidation time, it is necessary to study the characteristics of the pristine GO before its application. Therefore, the quantification of the GO functional groups is an important step for the proper design and functionalization of the GO for specific applications.

V. The fluorescent method proposed in this chapter was validated for the estimation of the concentration of carboxylic acids and alkene groups. Epoxide groups were out of the LOQ due to the low intense fluorescent response obtained. However, this work opens the possibility to monitor and quantify the functional groups of GO, and also the functionalities introduced after a chemical functionalization

BIBLIOGRAPHY

[1] Eigler, S.; Hirsch, A. Chemistry with graphene and graphene oxide - Challenges for synthetic chemists. Angew. Chemie - Int. Ed. 2014, 53, 7720–7738.
[2] Zhang, L.; Dai, F.; Yi, R.; He, Z.; Wang, Z.; Chen, J.; Liu, W.; Xu, J.; Chen, L. Effect of physical and chemical structures of graphene oxide on water permeation in graphene oxide membranes. Appl. Surf. Sci. 2020, 520, 146308.
[3] Yoo, M.J.; Park, H.B. Effect of hydrogen peroxide on properties of graphene oxide in Hummers method. Carbon N. Y. 2019, 141, 515–522.
[4] Ouyang, Y.; Cai, X.; Shi, Q.S.; Liu, L.; Wan, D.; Tan, S.; Ouyang, Y. Poly-l-lysine-modified reduced graphene oxide stabilizes the copper nanoparticles with higher water-solubility and long-term additively antibacterial activity. Colloids Surfaces B Biointerfaces 2013, 107, 107–114.
[5] Mungse, H.P.; Khatri, O.P. Chemically functionalized reduced graphene oxide as a novel material for reduction of friction and wear. J. Phys. Chem. C 2014, 118, 14394–14402.
[6] Xin, Q.; Li, Z.; Li, C.; Wang, S.; Jiang, Z.; Wu, H.; Zhang, Y.; Yang, J.; Cao, X. Enhancing the CO2 separation performance of composite membranes by the incorporation of amino acid-functionalized graphene oxide. J. Mater. Chem. A 2015, 3, 6629–6641.
[7] Kumar, A.S.K.; Jiang, S.J. Chitosan-functionalized graphene oxide: A novel adsorbent an efficient adsorption of arsenic from aqueous solution. J. Environ. Chem. Eng. 2016, 4, 1698–1713.
[8] Zhou, W.; Zhuang, W.; Ge, L.; Wang, Z.; Wu, J.; Niu, H.; Liu, D.; Zhu, C.; Chen, Y.; Ying, H. Surface functionalization of graphene oxide by amino acids for Thermomyces lanuginosus lipase adsorption. J. Colloid Interface Sci. 2019, 546, 211–220.
[9] Li, J.; Cheng, Y.; Zhang, S.; Li, Y.; Sun, J.; Qin, C.; Wang, J.; Dai, L. Modification of GO based on click reaction and its composite fibers with poly(vinyl alcohol). Compos. Part A Appl. Sci. Manuf. 2017, 101, 115–122.
[10] Kumar, A.; Khandelwal, M. Amino acid mediated functionalization and reduction of graphene oxide-synthesis and the formation mechanism of nitrogen-doped graphene. New J. Chem. 2014, 38, 3457–3467.
[11] Liu, F.; Wu, L.; Song, Y.; Xia, W.; Guo, K. Effect of molecular chain length on the properties of amine-functionalized graphene oxide nanosheets/epoxy resins nanocomposites. RSC Adv. 2015, 5, 45987–45995.
[12] Mendoza, M.E.; Ferreira, E.H.M.; Kuznetsov, A.; Achete, C.A.; Aumanen, J.; Myllyperkiö, P.; Johansson, A.; Pettersson, M.; Archanjo, B.S. Revealing lattice disorder, oxygen incorporation and pore formation in laser induced two-photon oxidized graphene. Carbon N. Y. 2019, 143, 720–727
[13] Claramunt, S.; Varea, A.; López-Díaz, D.; Velázquez, M.M.; Cornet, A.; Cirera, A. The importance of interbands on the interpretation of the raman spectrum of graphene oxide. J. Phys. Chem. C 2015, 119, 10123–10129

[14] Piñeiro-García, A.; Vega-Díaz, S.M.; Tristán, F.; Meneses-Rodríguez, D.; Labrada-Delgado, G.J.; Semetey, V. Photochemical Functionalization of Graphene Oxide by Thiol–Ene Click Chemistry. Ind. Eng. Chem. Res. 2020, 59, 13033–13041.
[15] Zhou, F.; Tien, H.N.; Dong, Q.; Xu, W.L.; Li, H.; Li, S.; Yu, M. Ultrathin, ethylenediamine-functionalized graphene oxide membranes on hollow fibers for CO2 capture. J. Memb. Sci. 2019, 573, 184–191.
[16] Cai, N.; Larese-Casanova, P. Application of positively-charged ethylenediamine-functionalized graphene for the sorption of anionic organic contaminants from water. J. Environ. Chem. Eng. 2016, 4, 2941–2951.
[17] Compton, O.C.; Dikin, D.A.; Putz, K.W.; Brinson, L.C.; Nguyen, S.T. Electrically conductive "alkylated" graphene paper via chemical reduction of amine-functionalized graphene oxide paper. Adv. Mater. 2010, 22, 892–896.
[18] Hsiao, M.C.; Liao, S.H.; Yen, M.Y.; Liu, P.I.; Pu, N.W.; Wang, C.A.; Ma, C.C.M. Preparation of covalently functionalized graphene using residual oxygen-containing functional groups. ACS Appl. Mater. Interfaces 2010, 2, 3092–3099.
[19] Yap, P.L.; Kabiri, S.; Tran, D.N.H.; Losic, D. Multifunctional Binding Chemistry on Modified Graphene Composite for Selective and Highly Efficient Adsorption of Mercury. ACS Appl. Mater. Interfaces 2018, 11, 6350–6362.
[20] Udenfriend, S.; Stein, S.; Böhlen, P.; Dairman, W.; Leimgruber, W.; Weigele, M. Fluorescamine: A reagent for assay of amino acids, peptides, proteins, and primary amines in the picomole range. Science (80-.). 1972, 178, 871–872.
[21] Eng, A.Y.S.; Chua, C.K.; Pumera, M. Refinements to the structure of graphite oxide: Absolute quantification of functional groups via selective labelling. Nanoscale 2015, 7, 20256–20266.
[22] M. Barua, M. B. Sreedhara, K. Pramoda and C. N. R. Rao, Chem. Phys. Lett., 2017, 683, 459–466.
[23] Sturala, J.; Luxa, J.; Pumera, M.; Sofer, Z. Chemistry of Graphene Derivatives: Synthesis, Applications, and Perspectives. Chem. - A Eur. J. 2018, 24, 5992–6006.
[24] Acik, M.; Lee, G.; Mattevi, C.; Pirkle, A.; Wallace, R.M.; Chhowalla, M.; Cho, K.; Chabal, Y. The Role of Oxygen during Thermal Reduction of Graphene Oxide Studied by Infrared Absorption Spectroscopy. J. Phys. Chem. C 2011, 115, 19761–19781.
[25] Qiao, Q.; Liu, C.; Gao, W.; Huang, L. Graphene oxide model with desirable structural and chemical properties. Carbon N. Y. 2019, 143, 566–577.
[26] Yan, L.; Zheng, Y.B.; Zhao, F.; Li, S.; Gao, X.; Xu, B.; Weiss, P.S.; Zhao, Y. Chemistry and physics of a single atomic layer: strategies and challenges for functionalization of graphene and graphene-based materials. Chem. Soc. Rev. 2012, 41, 97–114.
[27] Marcano, D.C.; Kosynkin, D. V.; Berlin, J.M.; Sinitskii, A.; Sun, Z.; Slesarev, A.; Alemany, L.B.; Lu, W.; Tour, J.M. Improved synthesis of graphene oxide. ACS Nano 2010, 4, 4806–4814.
[28] Hoyle, C.E.; Bowman, C.N. Thiol-ene click chemistry. Angew. Chemie - Int. Ed. 2010, 49, 1540–1573.
[29] Shao, G.; Lu, Y.; Wu, F.; Yang, C.; Zeng, F.; Wu, Q. Graphene oxide: The mechanisms of oxidation and exfoliation. J. Mater. Sci. 2012, 47, 4400–4409.

[30] Shrivastava, A., & Gupta, V. B. (2011). Methods for the determination of limit of detection and limit of quantitation of the analytical methods. Chronicles of young scientists, 2(1), 21.
[31] Procedures, A. (2000). Methods Validation: Chemistry, Manufacturing, and Controls. Federal Register (Notices), 65, 776.

CHAPTER 6

DEVELOPING MULTI- FUNCTIONAL GRAPHENE OXIDE MATERIALS FOR ANTIBACTERIAL APPLICATIONS

In previous chapters, alternative approaches to functionalize the GO using orthogonal and selective chemical routes were proposed. These new approaches can be used in order to take full advantage of the functional groups of GO to graft different molecules onto specific sites of GO layers. More interestingly, in chapter 5 it was found that the GO synthetized for this thesis possessed more alkene groups than carboxylic acids and epoxides. By knowing the degree of GO functionalities is possible to propose different chemical routes for developing a multi-functionalized GO material [1]. Since the alkene groups of GO are equal to the sum of the concentration of the carboxylic acids and epoxides (see Table 5.1), the GO was functionalized first activating the epoxide and carboxylic acids with 2-(dimethylamino)ethylamine (DMEN) and then alkenes were attacked by 2-(dimethylamino)ethanethiol hydrochloride (MEDA).

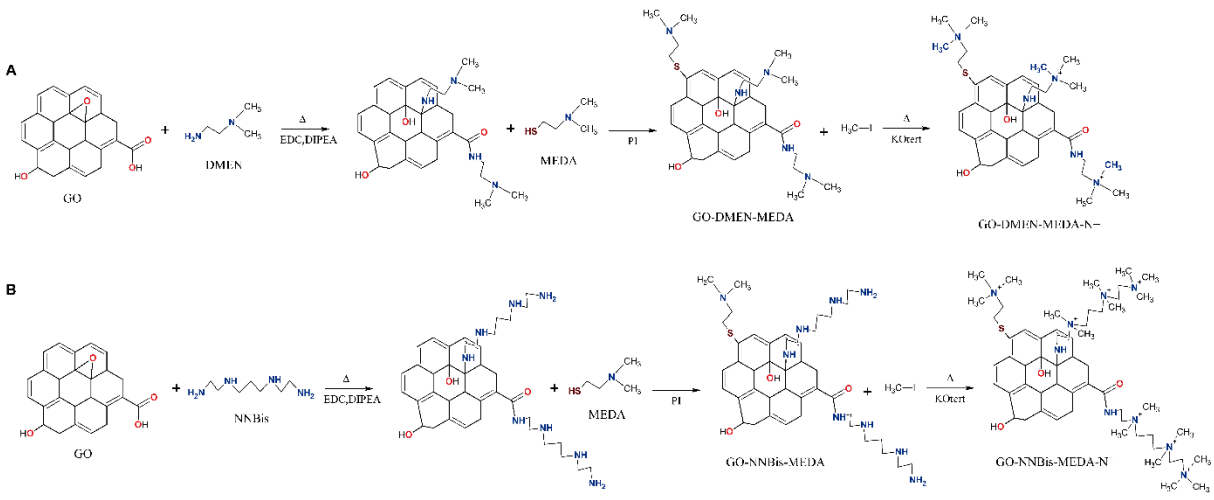

Figure 6.1 Chemical routes for the functionalization of GO: a) first step functionalization with DMEN followed by MEDA and the quaternization and b) a) first step functionalization with NNBis followed by MEDA and the quaternization.

Figure 6.1 shows the set of the reactions used for developing the multi-functionalized GO. With the knowledge generated about the reactivity of GO, it is possible to graft different molecules, even longer molecules, to increase N atoms content through the GO surface. In Figure 6.1b, DMEN was replaced by *N,N′*-Bis(2-aminoethyl)-1,3-propanediamine (NNBis) in the first step of the functionalization. The NNBis can attack either epoxides and carboxylic acids by ring opening reaction and peptide bond formation, respectively. This longer molecule contains more N atoms that can be quaternarized leading to a highly positive charged surface on GO layers. The positive charges generated in the GO surface can increase the antibacterial activity of pristine GO.

To proceed in the generation of GO-DMEN-MEDA-N^+ and GO-NNBis-MEDA-N^+ materials, the experimental method is summarized in Figure 6.2.

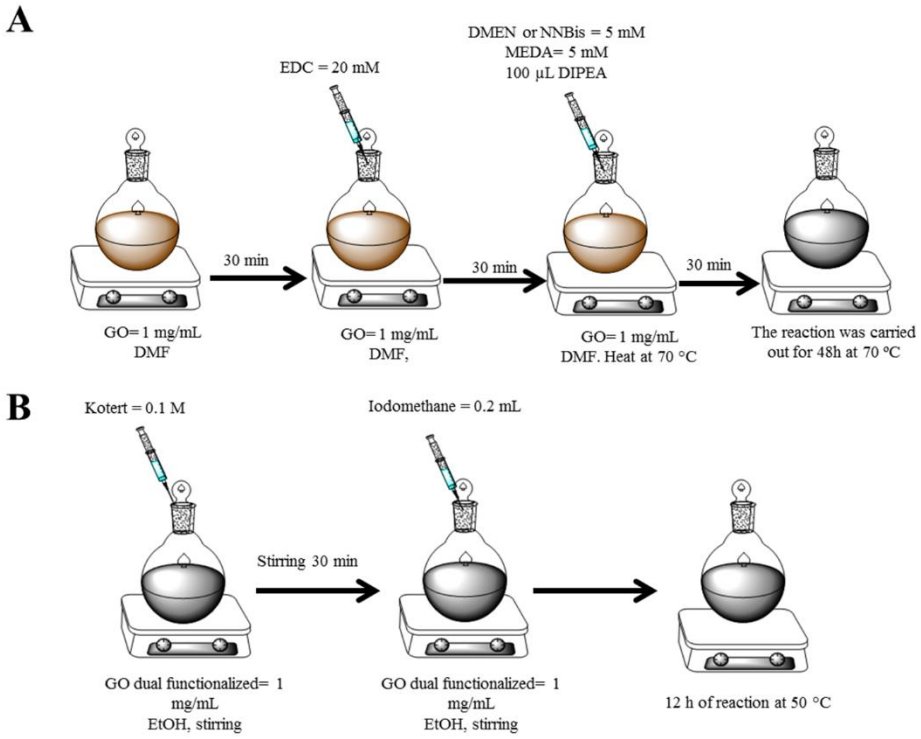

Figure 6.2 Methodology followed for the GO functionalization: a) One pot functionalization using DMEN or NNBis for nucleophilic attack of epoxides and carboxylic acids and MEDA for alkenes functionalization. b) Quaternization of the amines deposited in GO layers using *t*BuOK and iodomethane.

In the first step, the dual functionalization of the GO was carried out, and the methodology is shown in Figure 6.2a. For this, GO dispersed in DMF was mixed with EDC (20

mM) under ultrasonic bath. Then, DMEN or NNBis (5 mM) was added to the functionalization of epoxides and carboxylic acids followed by the addition of MEDA and DIPEA to functionalize the alkenes. These reactions involve the functionalization of epoxides, carboxylic acids and alkenes in solely one step. The reaction was let under stirring at 70 ºC during 48 h. The materials were purified with ethanol and water (18.2 MΩ·cm) by centrifugation. The materials produced correspond to either GO-DMEN-MEDA or GO-NNBis-MEDA. After the dual functionalization, the quaternization of the N atoms was carried out as showed Figure 6.2b. Both materials were dispersed in ethanol (EtOH) and potassium tert-butoxide (*t*BuOK) was added. Iodomethane was used for the alkylation of the amines inserted to GO after the dual functionalization [2]. The reaction was let during 12 h at 50 ºC. The materials produced after the chemical functionalization were labeled as GO-DMEN-MEDA-N^+ and GO-NNBis-MEDA-N^+. These materials were characterized by ATR-FTIR and the antibacterial activity was evaluated in *Escherichia coli* (*E. coli*), following the luminescence response of the bacteria in presence of the functionalized materials.

Classical methods for following the bacteria inhibition are based using UV spectroscopy by OD_{600}. However luminescene has arosen as an alternative technique for different analytical chemical analyses due to its high sensitivity, wide linear range, low cost per test, is relatively simple and inexpensive equipment is necessary [3]. In the case of bacteria assays, the light emitted by luminescence principally relies on the bioluminescent enzyme system which consists of a NAD(P)H:FMN oxidoreductase and a luciferase (eq. (6.1)) [4].

$$\mathrm{NAD(P)H + FMN + H^+ \xrightarrow{NAD(P)H:FMN\ oxidoreductase} NAD(P)^+ + FMNH_2} \qquad 6.1$$

Then bacterial luciferase catalyzes the oxidation of reduced $FMNH_2$ to produce oxidized FMN in the presence of long chain aldehyde (RCHO) and O_2 with the light emission (eq. (6.2)) [5] . The spectral range of the bioluminescence is between 420 nm and 660 nm.

$$\mathrm{FMNH_2 + RCHO + O_2 \xrightarrow{Luciferase} FMN + RCOOH + H_2O + h\nu} \qquad 6.2$$

The light emission is narrowly associated to the cellularmetabolism, and thus light intensity reveals the metabolic status of the bacteria. When luminescent bacteria are exposed to toxic substances, the bacterial luciferase could be inhibited and the light intensity decreases quickly. By measuring the light intensity of the bacteria exposed with inibitory substances and comparing with that of control, the inhibition can be calculated for quantifying the toxicity to

luminescent bacteria. That is the principle of traditional luminescent bacteria inhibition assay, which has been employed as the standard of many countries and regions [4].

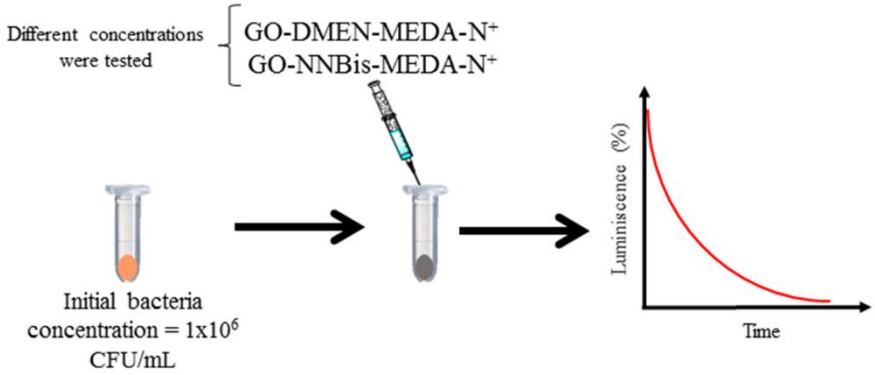

Figure 6.3 Methodology for the evaluation of the antibacterial activity.

The antibacterial activity was evaluated using the methodology presented in Figure 6.3. An initial bacteria concentration of $1x10^6$ CFU/mL was used, and then a solution of the respective positively multi-functionalized GO material was added. The antibacterial activity of the materials was tested in concentrations of 0.05, 0.1 and 0.2 mg/mL and the luminescence was taken as response of the antibacterial inhibition.

6.1 Characterization of the multi-functionalized materials by ATR-FTIR

The synthesis of multi-functionalized GO materials was performed using the chemical routes of Figure 6.1 In order to corroborate the introduction of new molecules in GO layers, ATR-FTIR characterization was carried out. Figure 6.4 shows the results where GO exhibits the characteristic bands attributed to carboxylic acids (1730 cm^{-1}), graphitic domain (1624 cm^{-1}), alcohols (1379 and 1046 cm^{-1}) and epoxide groups (1218 and 998 cm^{-1}) [6,7].

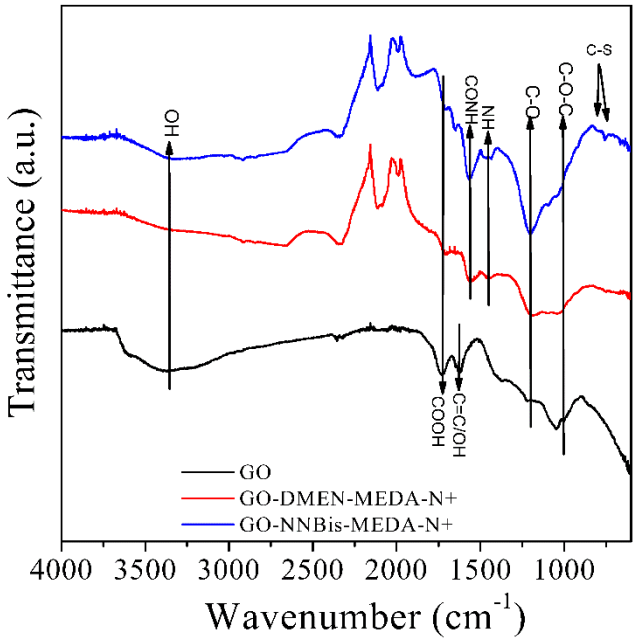

Figure 6.4 ATR-FTIR characterization of GO, GO-DMEN-MEDA-N^+ and GO-NNBis-MEDA-N^+.

After the chemical functionalization, GO-DMEN-MEDA-N^+ and GO-NNBis-MEDA-N^+ showed new bands at 1548 cm^{-1} and 1460 cm^{-1} attributed to N-C and N-H bonds for amide II mode vibrations [8-10], whereas epoxide bands (1218 and 998 cm^{-1}) became in a wide an intense band possible due to the increase of C-OH species after the ring opening reaction [11]. Simultaneously, the carboxylic acids band (1730 cm^{-1}) was shifted to 1710 cm^{-1}. This information confirmed the formation of peptide bonds and the formation of secondary amines due to ring opening reactions [12-14]. Therefore, GO was successfully functionalized with either DMEN or NNBis is the first step.

The second step of the functionalization of GO deals with the deposition of MEDA by thiol-ene Michael addition (TEMA). In the case of GO-DMEN-MEDA-N^+ was not possible to detect the C-S bonds formed after the chemical functionalization. However, GO-NNBis-MEDA-N^+ exhibited minor bands at 806 cm^{-1} and 762 attributed to C-S bonds [15]. Since the condition reactions were the same for both GO-DMEN-MEDA-N^+ and GO-NNBis-MEDA-N^+, it can be assumed that the MEDA could be grafted onto GO layers. Despite this assumption, further spectroscopy evidence is required to corroborate the chemical functionalization of the GO. Unfortunately, due to the pandemic problem that affected the academic activities, the

characterization of these materials is in stand-by and it is expected that at the beginning of the 2021 year, the characterization can be concluded.

6.2 Evaluation of the antibacterial activity of the multi-functionalized GO materials

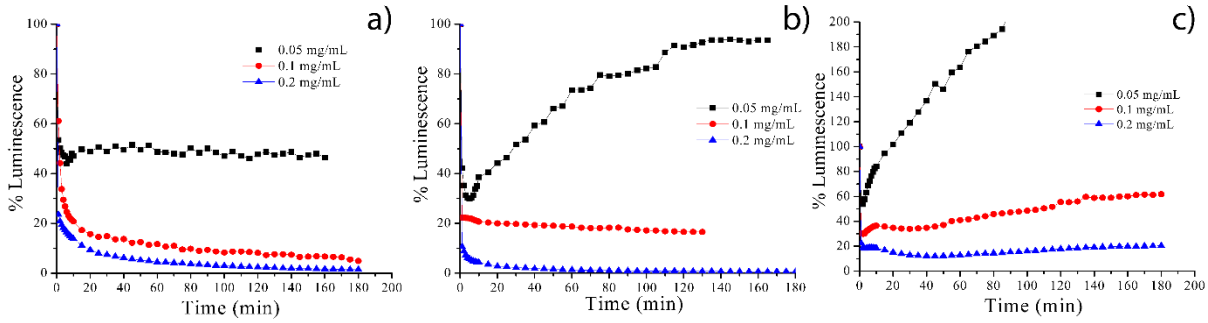

Figure 6.5 Luminescence characterization of: a) GO, b) GO-DMEN-MEDA-N^+ and c) GO-NNBis-MEDA-N^+.

The antibacterial activity of the multi-functionalized GO materials was evaluated in *E. coli* through luminescence characterization. The bacteria *E.coli* MG1655 was used as model bacteria in presence of GO, GO-DMEN-MEDA-N^+ and GO-NNBis-MEDA-N^+. Figure 6.5 shows the results for the antibacterial activity of the three materials under three different concentrations. The GO showed a bacteriostatic effect at concentrations of 0.05 mg/mL since after 2 h, the luminescence response was practically constant. It has been reported that the GO can produce 100% of elimination of *E. coli* at concentrations of 0.085 mg/mL [16,17]. Thus, a lower concentration (see concentration of 0.05 mg/mL in Figure 6.5a) could produce a bacteriostatic effect [18-20]. When the GO concentration increased, a decrease in the luminescence response was detected. From a concentration of 0.1 mg/mL, 80% of bacteria was killed after 15 min of incubation. As it was mentioned, a 0.085 mg/mL of GO concentration leads in 100% of elimination of *E. coli*. Thus, the results obtained in Figure 6.5a were consistent with previous reports, since after 3 h a 95% of bacteria elimination was observed. The 100% of luminescence lost was reached with a concentration of 0.2 mg/mL after 3 h of the test.

In the case of GO-DMEN-MEDA-N^+ and GO-NNBis-MEDA-N^+, both reduced the luminescence response, but then the luminescence increased once again when concentrations of 0.05 mg/mL were used. However, when the concentration of the materials was increased, it

was observed a decrease in the luminescence around 80% after 1 h of incubation. The GO-DMEN-MEDA-N^+ achieved a reduction of 80% of luminescence at 0.1 mg/mL of concentration in 20 min, whereas a concentration of 0.2 mg/mL produced a reduction 95 % of luminesce in the first 10 min. This behavior was better as compared to GO under the same concentration. Interestingly, the maximum luminescence reduction achieved with GO-NNBis-MEDA-N^+ was 80% using a concentration of 0.2 mg/mL, which is less as compared with GO and GO-DMEN-MEDA-N^+ at the same concentrations.

The antibacterial activity of GO in solution has been attributed to a physical contact where the GO layers can cut the bacteria membrane and wrap them [19-23]. The high surface area of the GO layers increases the contact with the bacteria [21,24]. Simultaneously, the chemical mechanism involves the generation of reactive oxygen species which are catalyzed with oxygen functional groups of GO, such as epoxides and carboxylic acids [25]. When the GO is functionalized with positive charges, the mechanism becomes in a synergistic effect between the physical contact and the strong interaction produced between the positive charges of GO and the negative charged membrane bacteria [26-28]. It was expected that GO-DMEN-MEDA-N^+ and GO-NNBis-MEDA-N^+ can exhibit an enhanced antibacterial activity due to the positive charges introduced after the chemical derivatization of GO. The positive charges could be the reason of the improved in the antibacterial activity as compared to GO [29-31]. However, both materials presented no significant enhanced antibacterial activity as compared with pristine GO, in specific GO-NNBis-MEDA-N^+ allowed growing up the bacteria even at concentrations of 0.2 mg/mL. This could be associated to two phenomena: i) the low efficiency in the chemical functionalization, and ii) the change in the morphology of the GO layers after the chemical functionalization. The introduction of molecules of the GO must not alter the physical characteristics of the GO; otherwise, it loses the surface available which is one of the most important features of GO. The first phenomenon is the efficiency of the chemical functionalization of GO with NNBis and MEDA molecules. As it was mentioned previously, it is necessary XPS and Raman spectroscopy characterization to corroborate the presence of peptide bonds, secondary amines, C-S-C bonds and the N^+ generated after the quaternization. The second point is the change in the surface area of the GO after the chemical functionalization which can reduce the contact upon bacteria. To corroborate this, optic microscope was used to observe the possible interactions of GO with *E. coli* MG1655. Since GO-NNBis-MEDA-N^+ produced the worst performance in the luminescence tests presented in Figure 6.5, Figure 6.6 shows the microscope images which were taken in different angles where GO-NNBis-MEDA-

N^+ is in contact with bacteria. As can be seen, the functionalized GO layers presented aggregation that reduced the interaction with bacteria. The green dots represent the bacteria, and it is possible to observe that the black dots, which are functionalized GO, cannot be in full contact with bacteria, since the aggregation of the sheets reduce the available surface area. The aggregation effect that exhibited the GO sheets can be attributed to the elimination of some oxygen functional groups or water molecules [32]. When those are released, the interaction between the basal plane of the GO layers increased and thus, a stacking of the GO sheets is observed [33]. This information suggests that the functionalization with NNBis and MEDA led to a reduction in the surface area and therefore, a decrease of the luminescence was obtained in Figure 6.5. So, the experimental conditions to produce GO-NNBis-MEDA-N^+ must be adjusted to avoid the stacking in the GO layers after the chemical functionalization.

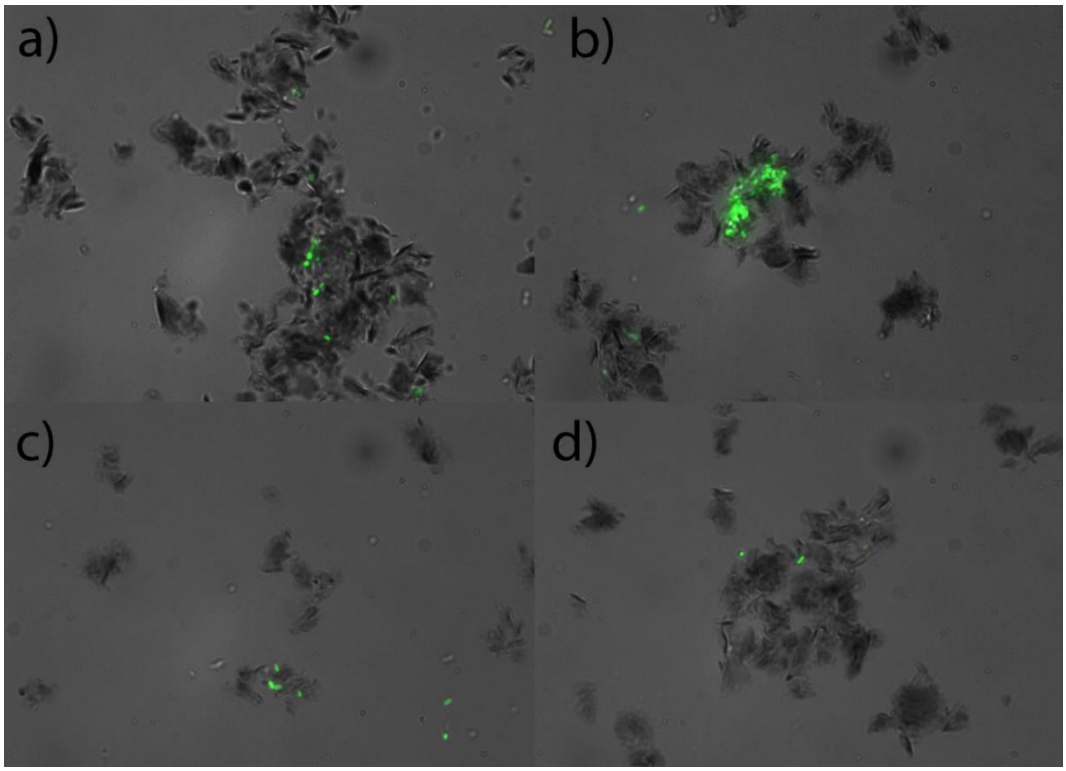

Figure 6.6 Microscope images taken in different positions to evaluate the interaction of GO-NNBis-MEDA-N^+ in presence of *E. coli*. The images were taken for the experiment with a concentration of 0.2 mg/mL of NNBis-MEDA-N^+.

6.3 Conclusions about the synthesis of multi-functionalized GO materials for antibacterial applications

Herein, it was reported the first attempts to develop multi-functionalized graphene oxide materials using the different functional groups of GO for enhancing antibacterial activity. This correspond to the application of the GO chemistry explored during the chapters 2, 3, 4 and 5. The conclusions are listed below.

I. Epoxides, carboxylic acids, and alkenes of GO can be functionalized in one-pot using orthogonal chemical routes. Epoxides are activated by ring opening reactions, whereas carboxylic acids are activated using EDC as coupling agent. The alkenes were modified *via* TEMA. ATR-FTIR results brought partial conclusion about the successful dual functionalization in one-pot experiment. However, additional characterization, in specific XPS and Raman spectroscopy, is required to corroborate the functionalization.

II. The GO-DMEN-MEDA-N^+ exhibited better antibacterial activity as compared to GO at concentrations of 0.2 mg/mL. This could be attributed to the positive charges generated after the chemical functionalization.

III. GO-NNBis-MEDA-N^+ material did not show a significant improvement in the antibacterial activity regardless if NNBis was used during the reaction. NNBis is a longer molecule with more N atoms that can be quaternarized, and thus a higher density of positive charges in GO layers was expected. However, the results presented highlight a poor antibacterial activity due to: i) low insertion of NNBis molecules onto the GO layers, and ii) the change in the morphology of the GO layers after the chemical functionalization. This second point was corroborated by optic microscope characterization where aggregated GO sheets were observed, which reduce the surface area available and the physical contact upon bacteria.

BIBLIOGRAPHY

[1] Avila-Vega, Y. I., Leyva-Porras, C. C., Mireles, M., Quevedo-López, M., Macossay, J., & Bonilla-Cruz, J. (2013). Nitroxide-functionalized graphene oxide from graphite oxide. Carbon, 63, 376-389.

[2] Anderson, E. B., & Long, T. E. (2010). Imidazole-and imidazolium-containing polymers for biology and material science applications. *Polymer*, *51*(12), 2447-2454.

[3] Whitehead, T. P., Kricka, L. J., Carter, T. J. N., & Thorpe, G. H. G. (1979). Analytical luminescence: Its potential in the clinical laboratory. Clinical Chemistry, 25(9), 1531–1546.

[4] Ma, X. Y., Wang, X. C., Ngo, H. H., Guo, W., Wu, M. N., & Wang, N. (2014). Bioassay based luminescent bacteria: Interferences, improvements, and applications. Science of the Total Environment, 468–469, 1–11.

[5] Inouye, S. (1994). NAD(P)H-flavin oxidoreductase from the bioluminescent bacterium, Vibrio fischeri ATCC 7744, is a flavoprotein. FEBS Letters, 347(2–3), 163–168.

[6] Zhang, L.; Dai, F.; Yi, R.; He, Z.; Wang, Z.; Chen, J.; Liu, W.; Xu, J.; Chen, L. Effect of physical and chemical structures of graphene oxide on water permeation in graphene oxide membranes. Appl. Surf. Sci. 2020, 520, 146308.

[7] Yoo, M.J.; Park, H.B. Effect of hydrogen peroxide on properties of graphene oxide in Hummers method. Carbon N. Y. 2019, 141, 515–522.

[8] Ouyang, Y.; Cai, X.; Shi, Q.S.; Liu, L.; Wan, D.; Tan, S.; Ouyang, Y. Poly-l-lysine-modified reduced graphene oxide stabilizes the copper nanoparticles with higher water-solubility and long-term additively antibacterial activity. Colloids Surfaces B Biointerfaces 2013, 107, 107–114.

[9] Mungse, H.P.; Khatri, O.P. Chemically functionalized reduced graphene oxide as a novel material for reduction of friction and wear. J. Phys. Chem. C 2014, 118, 14394–14402.

[10] Xin, Q.; Li, Z.; Li, C.; Wang, S.; Jiang, Z.; Wu, H.; Zhang, Y.; Yang, J.; Cao, X. Enhancing the CO2 separation performance of composite membranes by the incorporation of amino acid-functionalized graphene oxide. J. Mater. Chem. A 2015, 3, 6629–6641.

[11 Lin, Z., Liu, Y., & Wong, C. P. (2010). Facile fabrication of superhydrophobic octadecylamine-functionalized graphite oxide film. *Langmuir*, *26*(20), 16110-16114.

[12] Kumar, A.S.K.; Jiang, S.J. Chitosan-functionalized graphene oxide: A novel adsorbent an efficient adsorption of arsenic from aqueous solution. J. Environ. Chem. Eng. 2016, 4, 1698–1713.

[13] Zhou, W.; Zhuang, W.; Ge, L.; Wang, Z.; Wu, J.; Niu, H.; Liu, D.; Zhu, C.; Chen, Y.; Ying, H. Surface functionalization of graphene oxide by amino acids for Thermomyces lanuginosus lipase adsorption. J. Colloid Interface Sci. 2019, 546, 211–220.

[14] Mungse, H. P., & Khatri, O. P. (2014). Chemically functionalized reduced graphene oxide as a novel material for reduction of friction and wear. *The Journal of Physical Chemistry C*, *118*(26), 14394-14402.

[15] Li, J.; Cheng, Y.; Zhang, S.; Li, Y.; Sun, J.; Qin, C.; Wang, J.; Dai, L. Modification of GO based on click reaction and its composite fibers with poly(vinyl alcohol). Compos. Part A Appl. Sci. Manuf. 2017, 101, 115–122.

[16] Theuretzbacher U. (2011) Resistance drives antibacterial drug development. *Current Opinion in Pharmacology* 11:433–8.
[17] Szunerits, S., & Boukherroub, R. (2016). Antibacterial activity of graphene-based materials. Journal of Materials Chemistry B, 4(43), 6892-6912.
[18] Gurunathan, S., Han, J. W., Dayem, A. A., Eppakayala, V., Park, M. R., Kwon, D. N., & Kim, J. H. (2013). Antibacterial activity of dithiothreitol reduced graphene oxide. Journal of industrial and engineering chemistry, 19(4), 1280-1288.
[19] Akhavan, O., Ghaderi, E., & Esfandiar, A. (2011). Wrapping bacteria by graphene nanosheets for isolation from environment, reactivation by sonication, and inactivation by near-infrared irradiation. *The Journal of Physical Chemistry B*, *115*(19), 6279-6288.
[20] Liu, S., Hu, M., Zeng, T. H., Wu, R., Jiang, R., Wei, J., ... & Chen, Y. (2012). Lateral dimension-dependent antibacterial activity of graphene oxide sheets. *Langmuir*, *28*(33), 12364-12372.
[21] Perreault F, De Faria AF, Nejati S, Elimelech M (2015) Antimicrobial Properties of Graphene Oxide Nanosheets: Why Size Matters. ACS Nano 9:7226–7236.
[22] Ji H, Sun H, Qu X (2016) Antibacterial applications of graphene-based nanomaterials: Recent achievements and challenges. Adv Drug Deliv Rev 105:176–189.
[23] Shi L, Chen J, Teng L, et al (2016) The Antibacterial Applications of Graphene and Its Derivatives. Small 12:4165–4184.
[24] Karahan, H. E., Wang, Y., Li, W., Liu, F., Wang, L., Sui, X., ... & Chen, Y. (2018). Antimicrobial graphene materials: the interplay of complex materials characteristics and competing mechanisms. *Biomaterials science*, *6*(4), 766-773.
[25] Xie, Y., Wu, B., Zhang, X. X., Yin, J., Mao, L., & Hu, M. (2016). Influences of graphene on microbial community and antibiotic resistance genes in mouse gut as determined by high-throughput sequencing. *Chemosphere*, *144*, 1306-1312.
[26] Xiao, L., Sun, J., Liu, L., Hu, R., Lu, H., Cheng, C., ... & Geng, J. (2017). Enhanced photothermal bactericidal activity of the reduced graphene oxide modified by cationic water-soluble conjugated polymer. *ACS applied materials & interfaces*, *9*(6), 5382-5391.
[27] Plachá, D., Muñoz-Bonilla, A., Škrlová, K., Echeverria, C., Chiloeches, A., Petr, M., ... & Fernández-García, M. (2020). Antibacterial Character of Cationic Polymers Attached to Carbon-Based Nanomaterials. *Nanomaterials*, *10*(6), 1218.
[28] Yang, X. N., Xue, D. D., Li, J. Y., Liu, M., Jia, S. R., Chu, L. Q., ... & Zhong, C. (2016). Improvement of antimicrobial activity of graphene oxide/bacterial cellulose nanocomposites through the electrostatic modification. *Carbohydrate polymers*, *136*, 1152-1160.
[29] Liu, P., Xu, G., Pranantyo, D., Xu, L. Q., Neoh, K. G., & Kang, E. T. (2018). pH-sensitive zwitterionic polymer as an antimicrobial agent with effective bacterial targeting. *ACS Biomaterials Science & Engineering*, *4*(1), 40-46.
[30] Lim, M. Y., Choi, Y. S., Kim, J., Kim, K., Shin, H., Kim, J. J., ... & Lee, J. C. (2017). Cross-linked graphene oxide membrane having high ion selectivity and antibacterial activity prepared using tannic acid-functionalized graphene oxide and polyethyleneimine. *Journal of Membrane Science*, *521*, 1-9.
[31] Cai, X., Lin, M., Tan, S., Mai, W., Zhang, Y., Liang, Z., ... & Zhang, X. (2012). The use of polyethyleneimine-modified reduced graphene oxide as a substrate for silver nanoparticles

to produce a material with lower cytotoxicity and long-term antibacterial activity. *Carbon*, *50*(10), 3407-3415.
[32] Huh, S. H. (2011). Thermal reduction of graphene oxide. *Physics and Applications of Graphene-Experiments*, 73-90.
[33] Jeong, H. K., Lee, Y. P., Lahaye, R. J., Park, M. H., An, K. H., Kim, I. J., ... & Lee, Y. H. (2008). Evidence of graphitic AB stacking order of graphite oxides. *Journal of the American Chemical Society*, *130*(4), 1362-1366.

CONCLUSIONS AND PERSPECTIVES

This thesis was dedicated to understanding and generate new approaches for the chemical functionalization of the GO. The approaches were focused in three functional groups: i) epoxides (C-O-C), ii) carboxylic acids (COOH), and iii) alkenes (C=C). Epoxides and carboxylic acids are the oxygen functional groups commonly used for GO functionalization, since the chemistry around those functionalities is very well-known. In the case of alkene groups, these are generated during the graphitic oxidation and those are candidates to be used using appropriate chemical conditions. In this context, thiol-ene click chemistry can bright a new approach to carry out orthogonal reactions, which can conduct in new pathways to graft molecules in specific GO functional group. So, a wide range of molecules can be used for GO functionalization.

In chapter 2, it was studied the functionalization of GO using glycine as probe molecule. With this study was possible to understand the reduction mechanism of the glycine using mild conditions. It was found that the first step of the whole reduction mechanism was govern by the partial hydrolysis of epoxides followed by the reduction of carboxylic acids to carbonyls. Besides, the functionalization of GO with glycine was possible under less mas ratio of glycine with respect the GO. Simultaneously, the carboxylic acids were kept constant and even, a higher OH-C=O contribution was detected in XPS after the functionalization. This result suggests that an orthogonal reaction towards epoxide groups with a minimum interaction of carboxylic acids was succeeded. Therefore, this approach of covalent functionalization under basic medium faces the problem of the poor chemical control of GO functionalization when epoxide groups are reacted.

Chapter 3 and 4 focused on the studied of TER for the functionalization of GO in presence or either, radical initiator or base catalysts. When radical initiators are used the reaction proceeded by TERA, whereas base catalysts conduct to TEMA. These reactions provide efficient GO functionalization keeping most of the oxygen functional groups of GO, which can be used for further modification to develop multi-functional materials. However, it was found that TEMA can lead to a less yield in the functionalization as compared to TERA. This was justified due to TEMA can attack $\alpha-\beta$ unsaturated acids whereas the radical functionalization can activate a wide range of unsaturated systems. In addition, this thesis

introduced the implementation of fluorescamine to detect molecules bonded in GO after the chemical functionalization. This fluorescent labelling method allowed to estimate the number of CA molecules per mass of GO finding that TEMA can graft a higher quantity of molecules onto GO than the reaction on epoxide groups (TEROR).

Since it was possible to quantify the number of CA molecules linked after TEMA, this method can be expanded to quantify to quantify the functional groups GO. In chapter 5 the quantification of oxygen functional groups was proposed following a similar strategy to that presented for the estimation of CA molecules. Remarkably, C=C bonds highlight as an excellent approach for creating multi-functionalized graphene oxide materials, because they represent the higher concentration in the GO analyzed. The carboxylic acids and epoxides followed the order of the concentration of the GO functional groups. Despite that those functionalities have been reported with higher concentrations, the mixture of H_2SO_4/H_3PO_4 and the size of the graphite used could explain their low concentrations. Therefore, it is necessary to study the characteristics of the pristine GO before its application, since the structure and chemical composition of the GO strongly depends on the pristine graphite, oxidizing reagents, temperature, and the oxidation time.

The knowledge generated around the chemistry of GO provides important tools to functionalize using specifically a GO functional group. In chapter 6, it was reported the chemical functionalization of GO with different molecules to develop antibacterial GO-based materials. Epoxides, carboxylic acids, and alkenes of GO can be functionalized in one-pot using orthogonal chemical routes. Two materials were developed, GO-DMEN-MEDA-N^+ and GO-NNBis-MEDA-N^+. GO-DMEN-MEDA-N^+ exhibited better antibacterial activity as compared to GO at the same concentration (0.2 mg/mL). This could be attributed to the positive charges generated after the chemical functionalization. However, GO-NNBis-MEDA-N^+ material did not show a significant improvement in the antibacterial activity regardless if NNBis was used during the reaction. The poor antibacterial activity was attributed to: i) low insertion of NNBis molecules onto the GO layers and ii) the change in the morphology of the GO layers after the chemical functionalization. This second point was corroborated by optic microscope characterization where aggregated GO sheets were observed, which reduce the surface area available and thus the physical interactions.

Perspectives

Here, it was developed different strategies to functionalize the GO and with this information it is possible to create novel materials for a wide range of applications. Each chapter provides novel approaches for the chemical functionalization of GO. However, the studies can be complemented by adding different molecules to understand the behavior of the chemistry of GO face to a wide range of molecules. Therefore, the perspectives are summarized as follows:

I. To study in a deep way the functionalization of GO with amino acids to have a better understand of the behavior of such compounds in the chemistry of GO. Glycine was used as model amino acid, but there is an extensive set of amino acids that can be used for reduction or functionalization of GO.

II. To study the TERA of GO using water-soluble photoinitiator. Chapter 3 demonstrated that TERA can be performed for the photochemical functionalization of GO with CA using Irgacure 369 for the radical formation. Commonly, commercial photoinitators are non-polar which implies that the reaction must be conducted in non-polar solvents. Thus, a water-soluble photoinitiator can be used to functionalize GO and thus, the synthesis of positively charged GO could be performed in solely one-pot reaction. This reaction can reduce the number of steps presented in chapter 6 to developed multi-functionalized GO materials.

III. To develop GO based composite to grow up polymers on the GO surface using TERA or TEMA. In both reactions, CA was used for the analyses as model molecule, but more interesting could be the possibility to grow up *in situ* a polymer in GO layers. TERA and TEMA have the advantage to form polymer networks through a controllable combination of step-growth and chain-growth processes leading to the synthesis and tailorable materials fabrication. Therefore, the direct functionalization of cationic polymers with GO can be substitute by the growing *in situ* of the polymer.

IV. To quantify the oxygen functional groups of GO synthetized by different pathways, varying the initial size and some reaction conditions. This study can help to validate the fluorescent method proposed in chapter 5, and to understand the impact of the reaction conditions to promote specific GO functional group.

V. To complete the characterization of multi-functionalized GO materials presented in Chapter 6. Spectroscopy characterization is missing to have a better understanding

of the functionalization performed. XPS and Raman spectroscopy could allow to confirm the presence of positive charges (N^+) generated after the functionalization. With this information, new experimental conditions could be proposed and tested to enhance the density of positive charges in the final material.

VI. To study the antibacterial activity of the GO-based materials synthetized by additional antibacterial tests such as growth kinetics and solid growth of bacteria, to follow the antibacterial activity of GO and the GO-based materials developed.

VII. To expand the range of molecules that ca be used for the development of highly positive charged GO based materials. The functionalization with cationic imidazoles and polymers can be used for the creation of cationic charged GO materials with remarkable antibacterial activity. However, the functionalization with cationic polymers can be questioned due to the complex chemistry of both, the cationic polymer, and the GO. This problem can be faced with the chemical routes generated in this thesis which can be helpful to control the functionalization with polymers.

APPENDIX

A.1 Materials preparation and synthesis

Chemical reagents

Asbury natural graphite of 1 μm was used for GO synthesis. The reagents used during GO synthesis were sulfuric acid (H_2SO_4), phosphoric acid (H_3PO_4) potassium permanganate ($KMnO_4$), phosphorus pentoxide (P_2O_5), potassium persulfate ($K_2S_2O_8$), hydrogen peroxide (H_2O_2) and hydrochloric acid (HCl), all were analytical grade and purchased from Sigma Aldrich. Other reagents used were glycine (99%), sodium hydroxide (NaOH, 98.7%), 2-benzyl-2-(dimethylamino)-4′-morpholinobutyrophenone (97%) was used as PI, AIBN (99%), CA (≥98%), MEDA (≥95%), *N,N*′-Bis(2-aminoethyl)-1,3-propanediamine (NNBis, 95%), *N,N*-Dimethylethylenediamine (DMEN, 95%), *N,N*-Dimethylformamide (DMF, for HPLC, ≥99.9%), ethanol (EtOH, 96%) potassium tert-butoxide (*t*BuOK, 95%) sodium tetraborate decahydrate (sodium borate, ≥99.5%), phosphate buffered saline tablets (PBS), fluorescamine (≥98%), NEt_3 (≥98%), DBU (98%), NHBoc, (≥98%), N-(3-dimethylaminopropyl)-N′-ethylcarbodiimide hydrochloride (EDC) and dichloromethane (DCM, ≥99.8%) were purchased from Sigma-Aldrich. L-cysteine (LC, 98%), trifluoroacetic acid (TFA, 99%) and DIPEA (99%) were acquired from Alfa Aesar.

Synthesis of GO

GO was synthetized through a modified Hummer's method. In the first step graphite intercalation was carried out, for this H_2SO_4 was heated under stirring until 90 °C, and then of $K_2S_2O_8$ and P_2O_5 was added keeping the stirring. The mixture was cooled at 80 °C and then graphite was added. The reaction was let for 4.5 h keeping the temperature at 80 °C. After that, the mixture was diluted with water (18.2MΩ·cm) and the mixture was let overnight for the precipitation of the graphite. The intercalated graphite was filtered and dried at 40 °C in an oven for 24 h. For the oxidation, the intercalated graphite was added to 7:1 of a mixture of H_2SO_4/H_3PO_4, under bath ice and stirring. Then, $KMnO_4$ was added avoiding that the temperature increased more than 10 °C. Subsequently, the reaction was heated at 65 °C keeping

the stirring for 2 h. Thereafter, the mixture was cooled at 30 ºC and water aliquots were added avoiding that the temperature went up 50 °C. The reaction was let for another 45 min and heated at 65 °C, during this time the mixture turned to violet color. Then, the reaction was cooled at 30 ºC and more water was added. After 2 h, H_2O_2 was added to finish the reaction resulting an intense yellow color. The mixture was let overnight in order to precipitate the GO. In the next day the supernatant was decanted and HCl 10 % v/v was added for the elimination of the impurities. Finally, the GO was washed by centrifugation using a 1:3 mixture or water/methanol until increase the pH at 4.5 approximately. In the final wash, the GO precipitated was dispersed only in water.

Preparation of RGO

The GO was thermally reduced in order to remove the epoxy groups. First, the GO obtained from the oxidation reaction was freeze-dried during 24 h. Then, the freeze-dried GO was put in an oven at 60 °C and 29.5 inHg vacuum pressure during 24 h. The resulting material was dispersed in DMF at the required concentrations using an ultrasonic bath.

GO functionalization with glycine

5 mL of GO suspension in water (1 mg/mL) were dispersed by sonication in 10 mL of NaOH solution (2 M in water) during 5 min. Then, 5 mL of glycine solution in water (0.25, 0.5, 1, 1.5 and 2 mg/mL, each one prepared from a stock solution of glycine of 5 mg/mL), was added systematically to the mixture and sonicated for another 30 min. Subsequently, the mixture was stirred vigorously for 4 h at room temperature. At the end of this time, the mixture was centrifuged at 7600 rpm for 45 min, and the supernatant was removed afterwards. The precipitated GO was purified adding deionized water, centrifuging and removing the supernatant. This procedure was repeated three times. Thereafter, they were washed three times with acid water (pH=2, prepared with HCl) by centrifugation as described above. This procedure allowed the removal of basic residues as well as Na^+ from carboxylates formed during the neutralization with NaOH. The obtained materials were labeled GO-G followed by glycine added (GO-G25, GO-G50, GO-G100, etc.).

All the final materials were obtained as a precipitated after the centrifugation, and a drop of each material was dried on a glass slide in an oven at 40 °C for 4 h. Thereafter, a film of each

material was formed, removed from the glass slide and used as sample in order to perform the characterization.

Photochemical functionalization of GO with CA by TERA

GO (10 mg) was dispersed in 10 mL of DMF using ultrasonic bath until obtaining a well dispersed solution. After that, the GO was kept under sonication another 30 min to exfoliate the GO. On the other hand, two solutions were prepared: the first of CA (10 mg dissolved in 5 mL of DMF) and the second of PI (10 mg dissolved in 5 mL of DMF, this corresponds to $2.7x10^{-5}$ mol). The solutions were deposited in falcon tubes wrapped with aluminum foil and kept at 4 °C until they were used. Subsequently, the three solutions were mixed in a beaker and put inside of the UV-camber during 60 min, under stirring. This experiment was labeled as GO-CA-PI. Two additional experiments were carried out following the same procedure that GO-CA-PI sample: the first without PI (labeled as GO-CA) and the second without PI and carrying the reaction under darkness and stirring (GO-B). These experiments are the respective blanks in order to follow the impact of the UV radiation and then the addition of the PI.

The materials were purified adding 25 mL of ethanol, then they were centrifuged and the supernatant was removed. This wash step was repeated four times. After this, the materials were washed with a solution of NaCl (2 M) with pH~2 (the pH was adjusted using HCl). The solid materials obtained in the step of the purification with ethanol were dispersed with 2 mL of NaCl using an ultrasonic bath. Subsequently, using a microcentrifuge tube of 2 mL the materials were centrifuged for 2 min at 23900 g. The supernatant was removed and enough NaCl solution was added until made them up to 2 mL. This wash step was repeated six times and for each step the ultrasonic bath was used for the materials redispersion. Finally, all the materials were washed with water (18.2MΩ·cm), made them up to 2 mL, centrifuging at 23900 g for 10 min and removing the supernatant. This process was repeated five times. The centrifugation time increased during the wash step with water because the suspensions became more stable as the reaction residues were eliminated. At the end, all the materials were dispersed in 2 mL of water.

Functionalization of GO with CA by TERA using thermal initiator

TER between GO and CA using AIBN was carried out under the reaction conditions described elsewhere.[30] Briefly, GO was dispersed in DMF under ultrasonic bath for 30 min.

Then, the GO was purged with argon gas for 30 min. A mixture containing AIBN ($3.x10^{-5}$ mol) and cysteamine hydrochloride (mass ratio of GO:CA 1:1) was ultrasonicated for 30 min and then added to the GO solution. The reaction mixture was purged for another 30 min with argon and was let for 12 h at 70 °C in oil bath. This experiment was labeled as GO-CA-AIBN and the purification was done as described in the section **Photochemical functionalization of GO with CA by TERA**.

Analysis of Thiol-ene reaction using different thiol compounds

TER was carried out using another two thiol compounds: LC and MEDA. The functionalization and purification were conducted as described in **Photochemical functionalization of GO with CA by TERA** section. All the experiments developed in chapter 3 are summarize in Table 3.1 with the respective conditions and labels.

GO and RGO functionalized with CA by TEMA

The functionalization of GO with CA by TEMA was performed using 10 mg of GO dispersed in 10 mL DMF (GO=1 mg/mL), using ultrasonic bath during 30 min. This procedure allowed the exfoliation of the GO sheets. Then, 5 mL of a solution of CA (CA=2 mg/mL, dispersed in DMF) were mixed with GO, followed by the addition of a base catalyst (DIPEA, NEt_3 or DBU). The final concentration of the base catalyst in the reaction was 100 mM. The reaction was let 30 min under ultrasonic bath and then, the mixture was transferred to a beaker wrapped with aluminum foil, and the solution was stirred at 300 rpm during 4 h. These materials were labeled as GO-DIPEA, GO-NEt_3 and GO-DBU. Additionally, a blank experiment was prepared which consisted in 5 mL of CA (CA=2 mg/mL, dispersed in DMF) and 10 mL of GO in DMF (GO=1 mg/mL) without base catalyst. The blank experiment was undergone to 30 min under ultrasonic bath followed by stirring at 300 rpm during 4 h; this sample was labeled as GO-B.

The reaction between RGO and CA was carried out under the same conditions than the functionalization using GO. These materials were labeled as RGO-DIPEA, RGO-NEt_3 and RGO-DBU. A similar blank experiment was carried out for the reaction between RGO and CA without the base catalyst. This sample was labeled as RGO-CA.

The purification was performed as described in the section **Photochemical functionalization of GO with CA by TERA**. The Table 4.1 in chapter 4 contains a summary of the GO and RGO materials functionalized by TEMA and TERA

Reaction of epoxide groups of GO with NHBoc

10 mL of GO (1 mg/mL) dispersed in DMF was bubbled during 30 min with a constant flow of argon (Ar) and under stirring. After that, 10 mL of NHBoc (2 mg/mL) was added and the reaction was heated until 50 ºC keeping the bubbling and the stirring. After 5 min, the system was sealed maintaining the inert atmosphere and the reaction was let for 24 h producing GO **1** material. Thereafter, the GO 1 was washed first adding ethanol, then centrifuging and removing the supernatant. This wash step was repeated four times. Subsequently, the GO **1** was dispersed in 20 mL of DCM and 1 mL of TFA was added for the deprotection was added. The mixture was let for 2 h under stirring at room temperature. Finally, the purification was performed as described in the section **Photochemical functionalization of GO with CA by TERA**.

Reaction of carboxylic acid groups of GO with NHBoc

In a typical procedure,10 mL of RGO (1 mg/mL) dispersed in DMF was bubbled during 30 min with a constant flow of argon (Ar) and stirring. After that, 10 mL of EDC (20 mM) dispersed in DMF was added to the system keeping the bubbling and the stirring for another 30 min. Thereafter, 10 mL of NHBoc (2 mg/mL) and 100 μL were added and the reaction was heated until 55 ºC keeping the bubbling and the stirring. After 30 min, the system was sealed maintaining the inert atmosphere and the reaction was let for 48 h producing RGO **1** material. The deprotection of the NHBoc and the purification was carried out following the same protocol as described in **Reaction of epoxide groups of GO with NHBoc**.

TERA for the functionalization of RGO with CA

RGO (10 mg) was dispersed in 10 mL of DMF using ultrasonic bath until obtaining a well dispersed solution. After that, the GO was kept under sonication another 30 min to exfoliate the GO. On the other hand, two solutions were prepared: the first of CA (10 mg dissolved in 5 mL of DMF) and the second of PI (10 mg dissolved in 5 mL of DMF, this correspond to $2.7x10^{-5}$ mol). The solutions were deposited in falcon tubes wrapped with

aluminum foil and kept at 4 °C until they were used. Subsequently, the three solutions were mixed in a beaker and put inside of the UV-camber during 60 min, under stirring to produce RGO **2**. The purification was performed as described in the section **Photochemical functionalization of GO with CA by TERA**.

Titration of the synthetized materials with -NH_2 moieties with fluorescamine

1 mL of each functionalized material with -NH_2 moieties (0.05 mg/mL, prepared in PBS buffer) was mixed with 2 mL of sodium borate buffer (pH~9). Then, 1 mL of fluorescamine (0.5 mM dissolved in acetone) was added and the mixture was shaken by hand and then sonicated for 5 s. The fluorescence was measured at 390 nm excitation wavelength (λ_{ex}=390 nm) and emission of 475 nm (λ_{em}=475 nm), as reported previously [1].

Quantification of the synthetized materials with -NH_2 moieties

For the quantification, four calibration curves were built using: i) NHBoc and adding a constant volume of GO (quantification of epoxides), ii) NHBoc and adding a constant volume of RGO (quantification of carboxylic acids), iii) CA and adding a constant volume of RGO (quantification of alkenes) and iv) CA and adding a constant volume of GO (quantification of CA molecules bonded by TEMA). For each calibration curve, 1, 0.8, 0.6, 0.4 and 0.2 mL of either NHBoc or CA standard (0.02 mM, prepared in PBS) were mixed with 1, 1.2, 1.4, 1.6 and 1.8 mL of sodium borate buffer (pH~9). In order to have as much as possible the impact of the quenching in the calibration curve, 1 mL of either GO or RGO solution (0.05 mg/mL, prepared in PBS buffer) was added, followed by the addition of 1 mL of fluorescamine (0.5 mM, dispersed in acetone). The mixture was shaken by hand and then sonicated for 5 s. For the elaboration of each plot, the fluorescence was measured at λ_{ex}=390 nm and λ_{em}=475 nm; each point was repeated by triplicated. The concentration of NHBoc or CA in each sample was found setting the fluorescence obtained from the detection test at λ_{em}=475 nm into the respective calibration curve.

Theoretical estimation of CA on GO and RGO using XPS survey information.

For the production of GO **1** and RGO **1**, 20 mg of NHBoc were used that represents 1.24×10^{-4} mol and thus 7.5×10^{19} molecules. The N atomic contribution detected in XPS for GO **1** and RGO **1** were divided by two since each ethylenediamine molecule provides 2 nitrogen

atoms per molecule. In the case of RGO **1** the N1s spectrum exhibits more peaks for different functional groups. Therefore, N atomic was multiplied for the fraction of area of the amide bonds and then, this value was multiplied for the number of NHBoc molecules. For the GO **1** material, the fraction obtained from the division of the N atomic of XPS was directly multiplied by the initial number of NHBoc molecules.

For the production of RGO **2** and the synthetized materials for the study of TEMA in GO, 10 mg of CA was used which represents $1.29x10^{-4}$ mol and thus $7.80x10^{19}$ molecules. After that, the S atomic contribution detected in XPS was multiplied for the number of CA molecules added to the reaction. However, the S atomic percentage of XPS can also contain the SO_3 moieties inserted to GO graphitic lattice generated during the oxidation reaction. Therefore, in the S2p high resolution XPS, the area percentage of C-S and C-S-C bonds were only considered, and the fraction of both areas was multiplied for the total S atomic percentage. This final atomic percentage was multiplied for the number of CA molecules. Finally, the number of molecules estimated by XPS and fluorescent labelling was normalized per GO or RGO mass.

Synthesis of GO-DMEN-MEDA-N^+ and GO-NNBis-MEDA-N^+ materials

In the first step the dual functionalization of the GO was carried out. For this, 30 mL of GO (1 mg/mL) dispersed in DMF under ultrasonic bath for the dispersion and exfoliation of the GO sheets. Then, 10 mL of EDC (10 mM) were added and let 5 min in ultrasonic bath. After that, 5 mL of either DMEN or NNBis (10 mM) were added for the functionalization of epoxides and carboxylic acids. Subsequently, 5 mL of MEDA (10 mM) were added for the functionalization of alkenes followed with the addition of 100 μL of DIPEA. These reactions involve the functionalization of three different GO functionalities in just one step. The reaction was let under stirring at 70 ºC during 48 h. The material was purified adding ethanol, centrifuging and removing the supernatant, this step was repeated four times. Then, water (18.2 MΩ·cm) was used for the purification by centrifugation. Another four washes were carried out with water. The materials produced correspond to either GO-DMEN-MEDA or GO-NNBis-MEDA. For the quaternization of these materials, both were dispersed in EtOH (20 mL giving a concentration of 1 mg/mL) and then 5 mL of *t*BuOK (10 mM) were added. Finally, 100 μL iodomethane were added. The reaction was let during 12 h at 50 ºC. The materials were purified with water, centrifuging and removing the supernatant. This step was repeated six times.

A.2 Instrumentation

For the photochemical functionalization of GO with CA by TER a UVP CL-1000L Longwave Crosslinker was used and operated at 5.2 mW/cm^2 using UV-lamps of 365 nm. Characterization of chemical species was performed using attenuated total reflection-Fourier transform infrared (ATR-FTIR) conducted in a Nicolet Magna-IR 550 FTIR spectrometer using 50 scans; a Micro-Raman spectrometer confocal Renishaw model DM 2500M operated at laser power of 5%, an exposure time of 3 s and 4 accumulations with a 488 nm laser; a X-Ray photoelectron spectroscopy (XPS) K-ALPHA from Thermo Scientific, with a monochromatic X-ray beam using a k-alpha aluminum line operated at 40 watts irradiating an area of 400 µm^2. Also, it was used a lambda 800 UV-Vis spectrometer from Perkin Elmer and all the samples were prepared in water at concentrations of 0.05 mg/mL. For the fluorescence characterization a FluoroMax (Jobin-Yvon/Horiba) was used; all the samples were prepared at concentrations of 0.05 mg/mL with sodium borate as buffer with 5 mM of fluorescamine. STEM images were taken in a UHR-SEM model DUAL Beam Helios Nanolab 600 from FEI.

A.3 Additional information of XPS characterization

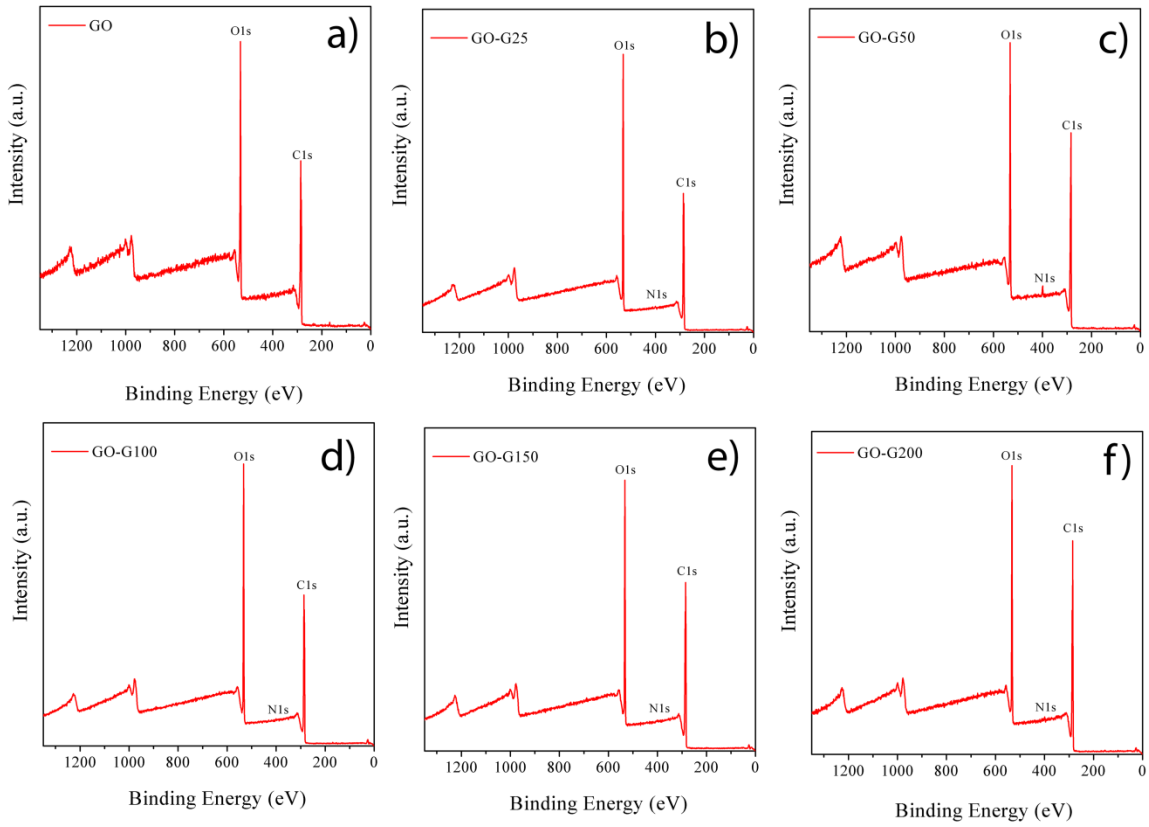

Figure A1. XPS survey scan for GO and GO-G samples

The Figure A1 contained the XPS survey information of the GO-G materials where only the GO-G50 exhibits a strong N atomic contribution. The XPS information was subtracted from the Figure A1 and is presented in Table A1. This information allows to estimate the C/O ratios by dividing the total C 1s area to the O 1s area.

Table A1. XPS survey information obtained from Figure A1

Sample	Element	Position	FWHM	Area	At %
GO	C 1s	286.08	4.12	132190.5	70.82
	O 1s	532.08	2.55	159595.2	29.18
GO-G25	C 1s	286.08	4.06	465921.8	71.15
	O 1s	532.08	2.16	546486.9	28.48
	N 1s	401.8	1.5	2434.63	0.37
GO-G50	C 1s	284.08	3.46	301886.78	72.38
	O 1s	532.08	2.55	313369.5	25.64
	N 1s	399.08	2.49	14795.4	1.97
GO-G100	C 1s	287.08	3.96	534376.6	70.93
	O 1s	533.08	2.3	635281.43	28.78
	N 1s	400.08	0.93	2156.44	0.29
GO-G150	C 1s	285.08	3.98	498222.6	74
	O 1s	533.08	2.34	509867.4	25.85
	N 1s	400.08	2.43	4720.6	0.16
GO-G200	C 1s	285.08	3.66	412409.25	75.84
	O 1s	533.08	2.32	379624.71	23.83
	N 1s	399.08	2.34	7952.74	0.33

The Table A2 contains the XPS information of Figure 3.5 for the detection of CA moieties in the GO-CA materials after the application of TERA.

Table A2. XPS survey information obtained from Figure 3.5

Sample	Element	Position	FWHM	Area	At %
GO	C1s	287.08	4.22	550043	70.10
	O1s	533.08	2.37	678753	29.52
	S2p	170.08	3.47	5023	0.38
GO-B	C1s	287.08	4.22	558498	69.74
	O1s	533.08	2.28	687591	29.39
	S2p	169.08	2.37	3159	0.24

	Na1s	1072.08	2.07	49399	0.72
GO-CA	C1s	285.08	4.15	608584	70.44
	O1s	533.08	2.38	712482	28.15
	N1s	400.08	3.91	8226	0.53
	S2p	163.08	2.05	3559	0.25
	Na1s	1072.08	1.92	46697	0.63
GO-CA-PI	C1s	285.08	3.52	581357	71.67
	O1s	533.08	2.51	577241	25.85
	N1s	400.08	2.29	32342	2.22
	S2p	164.08	2.36	23333	1.72
	Na1s	1072.08	1.84	7356	0.11

The Figure A2 shows the XPS survey of the blanks for the study of TEMA in the functionalization of GO with CA.

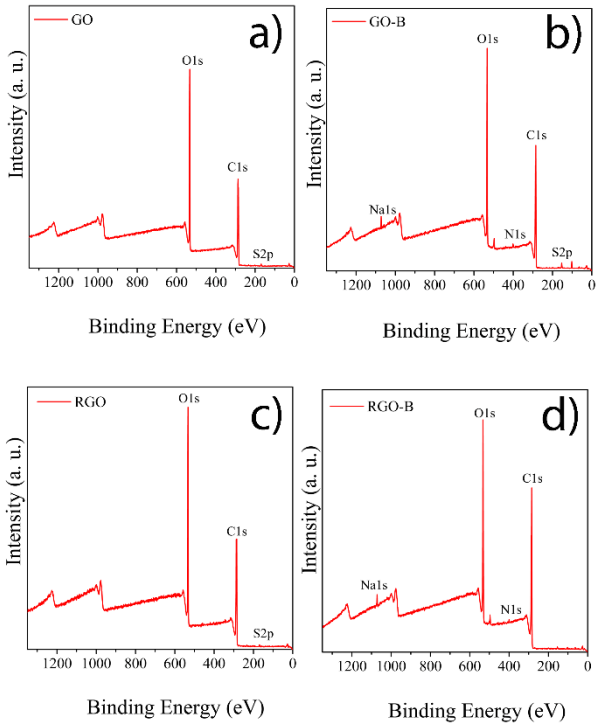

Figure A2. XPS survey scan of the samples: a) GO, b) GO-B, c) RGO and d) RGO-B.

The Figure A2 reveals that GO and RGO only contains traces of S atomic percentage attributed to sulfates (SO_3) introduced into the graphitic lattice.

The XPS survey information was subtracted from Figures 4.2 and A2 and is presented in Table A3.

Table A3. XPS survey information extracted from Figure 4.2 and Figure A2

Sample	Element	Position	FWHM	Area	At %
GO	C1s	287.08	4.51	454206	69.40
	O1s	533.08	2.39	574785	29.97
	S2p	169.08	2.63	6905	0.63
GO-B	C1s	285.08	4.03	593362	70.34
	O1s	533.08	2.53	502715	28.34
	N1s	401.08	2.64	10940	0.85
	Na1s	1072.08	1.65	28712	0.47
GO-DIPEA	C1s	285.08	3.53	529767	71.96
	O1s	533.08	2.45	536038	24.85
	N1s	401.08	3.79	20692	1.56
	S2p	164.08	2.35	17185	1.39
	Na1s	1072.08	1.75	14347	0.23
GO-NEt_3	C1s	285.08	3.99	622207	71.09
	O1s	533.08	2.44	671644	26.19
	N1s	400.08	4.26	18293	1.16
	S2p	164.08	2.21	19414	1.32
	Na1s	1072.08	1.80	18031	0.24
GO-DBU	C1s	285.08	3.95	575191	70.19
	O1s	533.08	2.47	663147	27.62
	N1s	400.08	1.79	19582	1.33
	S2p	164.08	0.4	5503	0.4
	Na1s	1072.08	0.46	32180	0.46

The Figure A3 presents the Sp2 deconvolution of the XPS results of Figure A2. In the GO was detected sulfates that can be produced in GO during the oxidation. The low intensity of the peak C-S confirmed that in absence of base catalyst TEMA cannot proceed in GO.

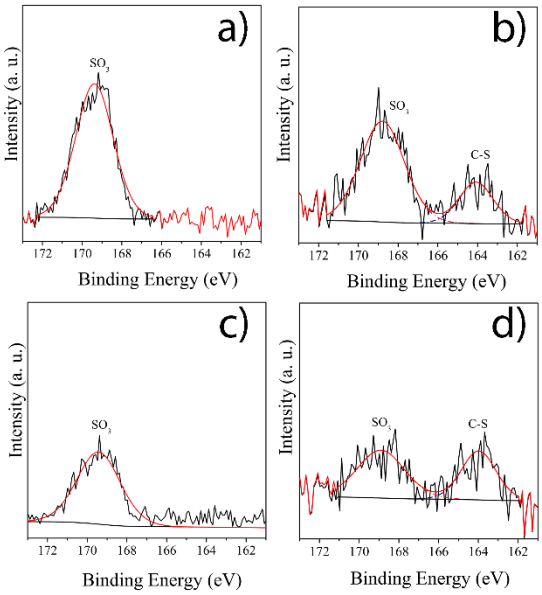

Figure A3. S2p deconvolution of XPS high resolution spectrums of a) GO, b) GO-B, c) RGO and d) RGO-B.

Table A4 presents a summary of the XPS survey information for the RGO materials functionalized by TEMA using different base catalysts.

Table A4. XPS survey information extracted from Figure 4.8 and Figure A2

Sample	Element	Position	FWHM	Area	At %
RGO	C1s	285.08	4.50	622913	74.24
	O1s	533.08	2.45	610897	24.85
	N1s	401.08	2.72	8561	0.57
	S2p	169.08	2.42	4757	0.34
RGO-B	C1s	285.08	3.96	586719	73.64
	O1s	533.08	2.56	586915	25.14
	N1s	400.08	3.03	9883	0.69
	Na1s	1072.08	2.19	35797	0.53
RGO-DIPEA	C1s	285.08	3.87	501578	71.02
	O1s	533.08	2.50	554345	26.79
	N1s	400.08	3.77	11955	0.94
	S2p	164.08	1.81	10558	0.89
	Na1s	1072.08	1.75	21995	0.37
RGO-NEt$_3$	C1s	285.08	3.90	465556	70.80
	O1s	533.08	2.37	513818	26.67
	N1s	400.08	3.58	14240	1.20
	S2p	164.08	2.24	10892	0.99
	Na1s	1072.08	1.85	19004	0.34
RGO-DBU	C1s	285.08	3.15	680798	73.00
	O1s	533.08	2.50	684325	25.04
	N1s	400.08	3.17	18989	1.33
	S2p	164.08	2.04	10808	0.69
	Na1s	1072.08	1.82	10498	0.13

Figure A4 shows the C1s deconvolution of the GO and RGO materials used during the development of this work.

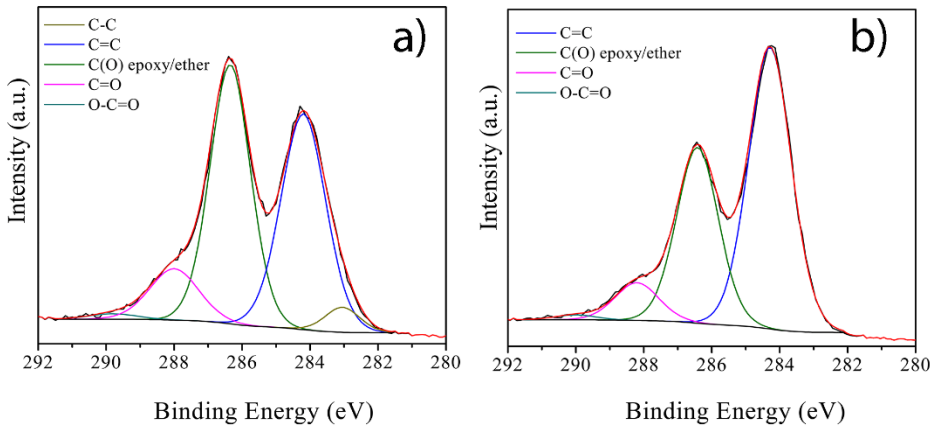

Figure A4 High resolution C1s deconvolution of a) GO and b) RGO.

Résumé de la thèse en Français

INTRODUCTION GÉNÉRALE

L'OG est une couche de carbone avec arrangement hexagonal qui contient différents groupes fonctionnels oxygène (c'est-à-dire des époxydes, des alcools et des acides carboxyliques) à travers sa structure suite à une réaction d'oxydation du graphite. L'OG a suscité un grand intérêt car il possède une grande surface, une polyvalence chimique mais aussi des propriétés optiques, électriques, de perméabilité à l'eau et de tamisage moléculaire intéressantes. De plus, les groupes fonctionnels de OG permettent d'augmenter la stabilité de OG dans différents solvants. L'une des approches les plus importantes est la fonctionnalisation de l'OG pour créer de nouveaux matériaux pour une large gamme d'applications. Cependant, la chimie complexe de l'OG est une limitation puisque différents groupes fonctionnels peuvent réagir simultanément, limitant la possibilité de greffer plus qu'une molécule dans les feuillets de l'OG.

D'une manière générale, la fonctionnalisation OG a été réalisée sur des groupements époxyde et/ou acide carboxylique car ils sont présents en grand nombre dans les feuillets de l'OG. Des nucléophiles tels que des amines ont été utilisés pour la fonctionnalisation sur des groupes acide carboxylique en utilisant des agents de couplage avec l'inconvénient de l'activation simultanée de groupes époxyde en même temps. Au cours de l'oxydation du graphite, des défauts apparaissent tels que des lacunes brisant le domaine polyaromatique et conduisant à la formation de groupes alcènes. Ce dernier groupe fonctionnel peut être activé par irradiation de la lumière UV afin de produire des radicaux thiyle avec l'inconvénient d'une faible génération de radicaux, car le rendement des réactions dépend du l'énergie de dissociation de la liaison S-H. Pour faire face à ce problème, un photoinitiateur (PI) peut être utilisé lors de la réaction pour augmenter la production de radicaux thiyle et ainsi augmenter le degré de fonctionnalisation. Afin d'explorer la chimie de l'oxyde de graphène, différentes stratégies doivent être développées pour créer des matériaux de graphène multi-fonctionnalisés et en particulier des matériaux antibactériens.

La résistance antibactérienne est un problème mondial qui est apparu en raison de une façon dont les antibiotiques ont été utilisés au cours des dernières décennies. La perte d'efficacité des antibiotiques a stimulé la recherche pour proposer de nouvelles stratégies

et générer de nouveaux agents antibactériens qui pourraient être efficaces, à faible effet cytotoxique et faciles à obtenir.

Dans ce contexte, cette thèse apporte un éclairage et une meilleure compréhension de la fonctionnalisation chimique de OG en se concentrant sur les époxydes, les acides carboxyliques et les groupes alcènes. Ainsi, il serait possible de créer des matériaux à base de OG multi-fonctionnalisés qui peuvent améliorer ses performances pour un large éventail d'applications, y compris l'activité antibactérienne de OG.

Le chapitre 1 de la thèse est dédié à l'étude de la littérature, qui nous conduit aux stratégies chimiques utilisables pour la modification chimique du OG.

Le chapitre 2 de la thèse traite de la fonctionnalisation du OG vers les groupes époxydes en utilisant la glycine comme groupes modèles. Cette fonctionnalisation porte sur processus de réduction collatérale qui implique l'utilisation d'acides aminés jusqu'à la production d'oxyde de graphène réduit (OGR).

Les chapitres 3 et 4 sont consacrés à l'étude et à l'analyse de la fonctionnalisation de l'OG *via* les groupes alcènes, en utilisant la réaction thiol-ene par activation photochimique et la réaction d'addition thiol-Michael. Les deux réactions permettent de profiter des C=C qui subsiste après l'oxydation graphitique lors de la production de l'OG pour le fonctionnaliser efficacement avec de forts rendements.

Dans le chapitre 5, la quantification des groupes fonctionnels de l'OG est proposée à l'aide de réactions sélectives couplées à un marquage fluorescent (fluorescamine). La méthode de quantification rapportée a été appliquée aux époxydes, acides carboxyliques et groupes alcènes de OG.

Enfin, le chapitre 6 présente la double fonctionnalisation utilisant la formation de liaisons peptidiques et la réaction thiol-ène pour produire des matériaux à base d'OG chargés positiveent pour des applications antibactériennes.

CHAPITRE 1

Oxyde de Graphène : Fonctionnalisation et Activité Antimicrobienne

1.1 Graphène, oxyde de graphite et oxyde de graphène

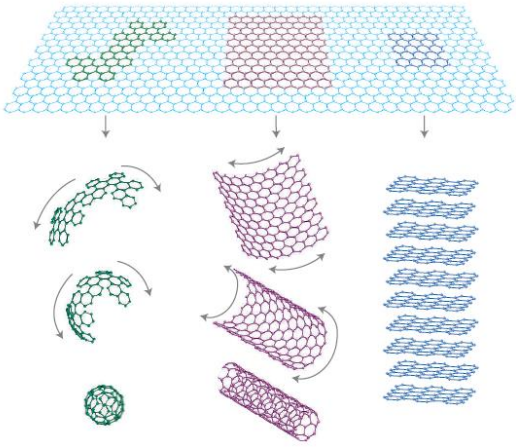

Figure 1.1 Le graphène est feuillet 2D, à la base de toutes les formes graphitiques : fullerènes qui sont matériaux 0D, des nanotubes de carbone (CNT, matériaux 1D) ou empilé dans du graphite (3D).[7]

Depuis qu'il a été obtenu pour la première fois par Novoselov et Geim en 2004, le graphène a suscité un intérêt général pour générer des matériaux alternatifs avec des potentiels exceptionnels dans de nombreux domaines, tels que la nanoélectronique,[1] la médecine,[2] la technologie énergétique,[3] les capteurs,[4] et catalyse.[5] Le graphène est un matériau de carbone 2D composé d'atomes de carbone dans un arrangement en nid d'abeille avec une hybridation sp^2 ainsi que des propriétés électroniques, optiques, thermiques et mécaniques remarquables.[6] Le graphène est considéré comme l'unité de structure conceptuelle des autres matériaux de carbone avec hybride sp^2 tels que les nanotubes de carbone (CNT), les fullerènes et même le

[1] Xuan, et al. *Applied Physics Letters*, 2008, *92*(1), 013101.
[2] Georgakilas, et al. *Chemical reviews*, 2016, *116*(9), 5464-5519.
[3] Liu, C., et al. *Biosensors and Bioelectronics*, 2010, *25*(7), 1829-1833
[4] Lu, C., et al. *Angewandte Chemie*, 2009, *121*(26), 4879-4881.
[5] Qu, L., et al. *ACS nano*, 2010, *4*(3), 1321-1326.
[6] Terrones, M., et al. *Nano Today*, 2010, 5(4), 351–372.

graphite (voir Figure 1.1).[7] Par ailleurs, les propriétés électroniques peuvent être conservées dans du graphène à quelques couches dans une limite de 10 couches. Après 10 couches, le graphène devient une structure de graphite 3D.[7]

Pour produire des feuillets de graphène (GLs), l'oxydation du graphite, suivie d'une réduction semble une approche prometteuse pour la production efficace des GLs.[8] Dans ce procédé, des agents oxydants tels que l'acide nitrique et l'acide sulfurique en présence de permanganate de potassium ou de chlorure de potassium sont utilisés pour briser le domaine sp^2 et insérer des groupes fonctionnels oxygène le long du réseau carboné.[9] Cette réaction d'oxydation conduit à l'oxyde de graphite (OGr) qui consiste en un matériau graphite 3D (sur 10 couches), avec des fonctionnalités oxygène qui peuvent être exfoliées par agitation mécanique ou sonication.[10] Après l'exfoliation, le produit consiste en une suspension brune bien dispersée composée de quelques feuilles de graphène en couches avec des groupes fonctionnels oxygène ; ce matériau est également connu sous le nom d'oxyde de graphène (OG).[9] Une fois l'OG produit, la réduction de l'OG peut être obtenue par des méthodes thermiques, chimiques ou électrochimiques.[11,12,13]

La structure chimique de l'OG a été largement décrite, mais la structure de l'OG la plus acceptée est le modèle de Lerf-Klinowsky dans lequel les groupes époxyde et hydroxyle sont dans le plan basal tandis que les acides carboxyliques sont aux bords.[14] Ces groupes fonctionnels sont à la base de la fonctionnalisation chimique de GO avec différentes molécules, y compris des macromolécules telles que des polymères, des polypeptides ou de l'ADN.[8] Cependant, des groupes fonctionnels oxygène supplémentaires pourraient être obtenus après la réaction d'oxydation tels que les cétones, les aldéhydes, la quinone et la lactone.[15]

Par conséquent, la chimie large de l'OG peut être explorée pour produire de nouveaux matériaux hybrides à base de graphène avec une dispersion améliorée, une agrégation réduite

---

[7] Geim, A. K., & Novoselov, K. S. *Nanoscience and technology: a collection of reviews from nature journals* 2010, (pp. 11-19).
[8] Gilje, S, et al. *Nano*, 2007, 7(11), 3394–3398.
[9] Dreyer, D. R., et al. *Chem. Soc. Rev*., 2010, 39(1), 228–240.
[10] Thakur, S., & Karak, N. Carbon, 2015, 94(June), 224–242.
[11] Stankovich, S., et al. Carbon, 2007, 45(7), 1558-1565.
[12] Huh, S. H. *Physics and Applications of Graphene-Experiments*, 2011, 73-90.
[13] Sundaram, R. S., et al. *Advanced Materials*, 2008, *20*(16), 3050-3053.
[14] Kwan, Y.C.G. et al. *Thin Solid Films,* 2015, 590, 40–48
[15] Feicht, P., et al. *Chemistry - A European Journal,* 2019, 25(38), 8955–8959.

et une plus grande surface disponible. Cette thèse propose de nouvelles approches pour la fonctionnalisation chimique de GO.

1.2 Fonctionnalisation de l'oxyde de graphène

La fonctionnalisation des OG peut être réalisée par des liaisons covalentes ou non covalentes.[8] Dans la fonctionnalisation non covalente des forces électrostatiques, des forces de Van der Waals ou empilement π-π peuvent avoir lieu.[16] Pour la fonctionnalisation covalente, les alcools, les époxydes et les acides carboxyliques sont les groupes fonctionnels couramment utilisés pour le dépôt de différentes molécules sur les couches d'OG.[8] En effet, ces fonctionnalités représentent la composition principale de l'OG.[17] La figure 1.2 montre une représentation schématique de l'activation d'époxydes, d'alcools et d'acides carboxyliques. Plus important encore, les groupes alcènes représentent également une approche intéressante pour la modification chimique de l'OG (voir Figure 1.2d).

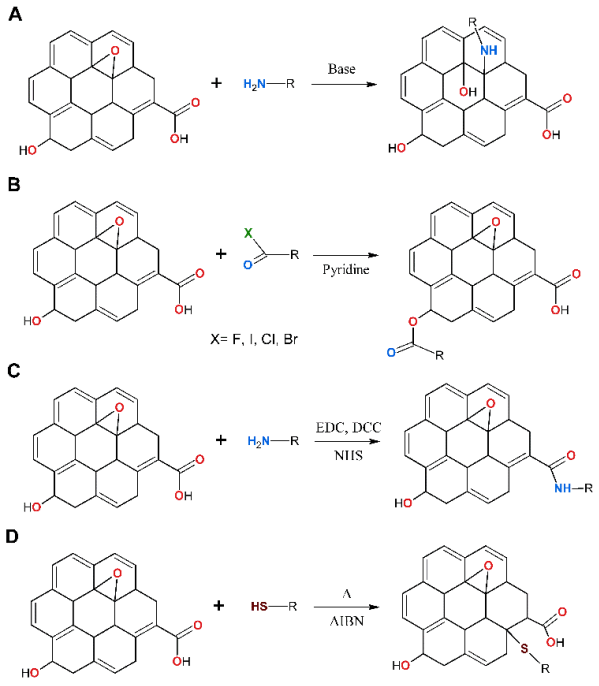

Figure 1.2 Fonctionnalisation de l'oxyde de graphène : a) réaction d'ouverture de cycle, b) attaque nucléophile de l'alcool vis-à-vis de carbonyles activés (ex. chlorures d'acyle), c) formation de liaisons peptidiques à l'aide d'agents de couplage et d) Réaction thiol-ene.

[16] Hu K, et al. *Adv Mater,* 2013, 25:2301–2307.

[17] Eng AYS, et al. *Nanoscale*, 2015, 7:20256–20266.

1.2.1 Fonctionnalisation de GO sur les groupes époxy et acide carboxylique

La fonctionnalisation covalente des OG a été largement rapportée dans la littérature à travers les époxydes et les acides carboxyliques, car ils constituent la plus forte densité de groupes fonctionnels sur les feuillets de l'OG.[17] Des nucléophiles tels que des amines et des alcools ont été utilisés pour la fonctionnalisation sur des groupes acide carboxylique à l'aide d'agents de couplage. D'autre part, les groupes époxyde sont susceptibles d'être attaqués par les nucléophiles par des réactions d'ouverture de cycle.[18] Cette réaction peut être facilement réalisée dans diverses conditions. Par exemple, les réactions d'ouverture de cycle peuvent être catalysées en utilisant des conditions acides ou basiques ou en chauffant conjointement avec un nucléophile tel que des amines ou des composés soufrés.[8] En effet, plusieurs réactions peuvent se produire simultanément car les amines peuvent réagir avec les groupes acides carboxyliques de l'oxyde de graphène à travers la formation de liaisons peptidiques.[19]

1.2.2 La réaction thiol-ène

La réaction thiol-ène (RTE) est un outil puissant pour réaliser des réactions orthogonales dans des conditions douces, avec des rendements élevés et en évitant les sous-produits.[20] La RTE est défini comme l'addition d'un thiol à une liaison alcène avec une orientation anti-Markovnikov.[20] La réaction thiol-ène répond à la définition de chimie « click ». La RTE peut être obtenu en ajoutant un générateur de radicaux (réaction thiol-ène radicalaire, RTER) ou par l'addition des catalyseurs basiques. [20] Ce dernier est également connu sous le nom de réaction de thiol-ène par addition de Michael (AM). Après la réaction d'oxydation du graphite, une grande quantité de défauts apparaît, y compris des lacunes, ce qui réduit le domaine sp^2 et plus de groupes alcènes sont obtenus sur l'OG.[21] La première application de la RTER sur l'OG a été réalisée par Luong et al.,[22] où la cystéamine était utilisée en présence de 2,2'-azobis(isobutyronitrile) (AIBN) comme initiateur de radicaux thermique. L'initiateur de radicaux thermique permet la production de radicaux thiyle (R-S$^{\bullet}$) qui attaquent le système non saturé de l'OG. En raison de l'utilisation d'initiateurs activables par voie thermique (T > 70°C), une réduction simultanée de l'OG peut être produite en perdant des groupes fonctionnels tels que les époxydes, qui ne peuvent pas être utilisés pour une seconde dérivatisation.[22]

---

[18] Song S, Zhang Y. *J Mater Chem A*, 2017 5:22352–22360.
[19] Kim NH, et al. *J Mater Chem A,* 2013 1:1349–1358.
[20] Hoyle, C. E.; Bowman, C. N. *Angew. Chemie - Int. Ed.* 2010, 49 (9), 1540–1573.
[21] Shao G, et al. *J Mater Sci,* 2012 47:4400–4409
[22] Luong, N.D, et al. *Chem. - A Eur. J.* 2015, 21, 3183–3186

Alternativement, nous avons montré que la RTER peut être réalisée par voie photochimique et qu'un photoinitiateur (PI) peut être utilisé pendant la réaction pour augmenter la production de R-S$^{\bullet}$ et ainsi accroitre le degré de fonctionnalisation.[23] L'application de la RTER sous lumière UV à l'aide d'un PI présente plusieurs avantages tels que la réduction du temps de réaction, il n'y a pas besoin de chauffer le système et donc une réduction moindre est observée dans l'OG modifié.[20] Par conséquent, la fonctionnalisation photochimique de l'OG par la RTER peut être explorée directement sur le système insaturé de l'OG. Sans étape de pré-fonctionnalisation, il peut être démontré l'efficacité de l RTER en tant qu'outil pour avoir une fonctionnalisation régiosélective et stéréosélective directement sur les couches de l'OG.

1.2.3 Réaction de thiol-ène pour l'addition de Michael

L'AM est une réaction click puissante qui est principalement utilisée en chimie des polymères pour coupler des acides α, β-insaturés avec des thiols.[20] Par rapport à la RTER, l'ajout de l'initiateur radicalaire peut favoriser la réaction avec une large gamme de systèmes insaturés. Cependant, l'AM possède des avantages tels que des rendements élevés, des réactions dans des conditions douces, une petite concentration de catalyseur de base est nécessaire, des vitesses de réaction rapides même en grandes quantités, une grande variété de solvants peut être utilisée, la réaction est insensible à l'oxygène ambiant ou à l'eau, régiosélective et cette réaction peut être utilisée avec une vaste gamme de thiols et de molécules d'alcène.[20] L'étude de la fonctionnalisation de l'OG par l'AM peut apporter des éclairages sur la fonctionnalisation chimique et ainsi répondre à des questions fondamentales telles que : les composés thiols sont-ils effectivement liés aux OG par AM ou réaction d'ouverture de cycle thiol-époxide (ROCE) ? Quelle est la réaction dominante ? Combien de molécules peuvent être liées par l'AM et combien par la ROCE ?

1.3 La montée de la résistance antibactérienne et l'activité antibactérienne de l'oxyde de graphène

Depuis 1928, date à laquelle Alexander Fleming a découvert la pénicilline, les antibiotiques ont été utilisés de façons souvent inappropriées au cours des années suivantes pour le traitement de plusieurs maladies. Après l'introduction de la pénicilline sur le marché, davantage d'agents antimicrobiens ont été synthétisés et largement utilisés dans la société pour éradiquer la

[23] Oberleitner, B., et al. *Chem. Commun.,* 2013, 49, 1615.

prolifération des bactéries, les champignons et les parasites.[24] De nos jours, la consommation excessive de ces agents antimicrobiens a conduit à un problème de résistance aux antibiotiques au niveau mondial. L'organisation mondiale de la santé (OMS) a signalé que certaines bactéries ont généré une résistance aux médicaments (RM) en raison de la prise délibérée de médicaments, principalement dans les pays sous-développés, où il n'y a pas de contrôle des ventes de médicaments.[24] Il a été suggéré qu'en 2050, il y aura plus de 10 millions de décès pour un coût de 100 milliards de dollars par an à cause de la résistance aux antibiotiques.[25]

1.3.1 Activité antibactérienne de GO

L'OG a été proposé comme un agent antibactérien alternatif car il peut interagir physiquement et chimiquement avec différents micro-organismes. Le mécanisme antibactérien de l'OG peut être par contact physique ou chimique comme le montre la figure 1.3.[26]

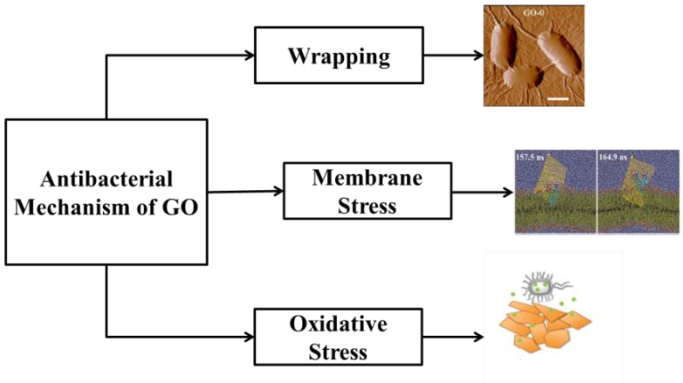

Figure 1.3 Différents mécanismes antibactériens de l'OG contre les bactéries.[28]

Dans le mécanisme physique, les couches de l'OG peuvent envelopper les bactéries en les isolant de l'environnement et en inhibant leur prolifération.[27] De plus, les bords des feuilles d'OG peuvent également couper la membrane au contact, ce qui entraîne une fuite des constituants du cytoplasme et la mort ultérieure des bactéries.[28] D'autre part, le mécanisme chimique de l'activité antibactérienne OG consiste en la génération de ROS. Il a été suggéré

[24] World Health Organization (WHO) http://www.who.int/news-room/fact-sheets/detail/antibiotic-resistance. Access: *April* 2018.

[25] The Review on Antimicrobial Resistance (AMR) https://amr-review.org/. Access October 16th 2018.

[26] Perreault F, et al. *ACS Nano*, 2015, 9:7226–7236.

[27] Akhavan O, et al. *J Phys Chem B*, 2011, 115:6279–6288.

[28] Ji H, et al. *Adv Drug Deliv Rev,* 2016, 105:176–189.

que l'adsorption d'O_2 dans les défauts de OG conduit à la formation de ROS. Les ROS libérés endommagent ensuite irréversiblement différents constituants de la membrane bactérienne.[29]

[29] Shi L, et al. *Small*, 2016 12:4165–4184.

CHAPITRE 2

RÉACTION DE L'OXIDE GRAPHÈNE AVEC LA GLYCINE : FONCTIONNALISATION OU RÉDUCTION?

Dans ce chapitre, l'étude de la fonctionnalisation et de la réduction de l'OG en utilisant la glycine comme acide aminé modèle a été réalisée. Comme il a été mentionné dans la section 1.2.1, les acides aminés peuvent être utilisés pour la fonctionnalisation ou la réduction de l'OG car ils peuvent améliorer des propriétés importantes pour de nombreuses applications, y compris la biocompatibilité, la dépollution et la catalyse. En effet, les acides aminés sont des agents réducteurs importants car ils sont respectueux de l'environnement et ouvrent de nouvelles voies pour la « chimie verte ». Cependant, certaines questions se posent lors de la fonctionnalisation de OG avec des acides aminés dont : quelle est la réaction la plus favorable lorsqu'un acide aminé est mis en contact avec l'OG : la fonctionnalisation de l'OG ou la réduction de l'OG ? Dans quelles conditions peut-on passer de la fonctionnalisation à la réduction ? Et plus important encore, serait-il possible de fonctionnaliser l'OG avec des acides aminés dans le plan basal, en particulier, aux groupements époxydes sans altérer les acides carboxyliques ?

Dans ce but, la glycine, a été testée à différentes concentrations en milieu basique à température ambiante. Dans la figure 2.1, est présenté un schéma de la procédure expérimentale suivie.

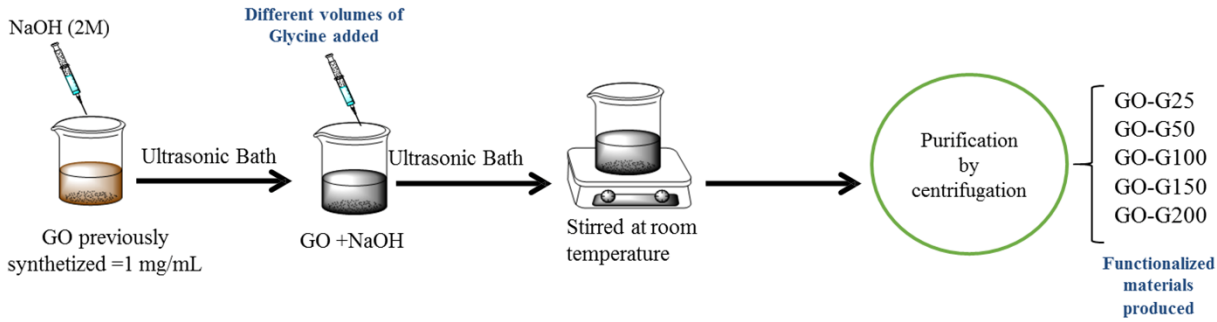

Figure 2.1 Représentation schématique de la fonctionnalisation / réduction de OG

Résultats

Les résultats infrarouges de OG-G25 et OG-G50 (Figure 2.2) ont montré une nouvelle bande à 1255 cm^{-1} pour les vibrations C – N de la glycine liée à un cycle aromatique. En outre, une diminution simultanée des bandes à 1221 cm^{-1} et 969 cm^{-1} attribuées aux groupes époxyde.[30] Ces informations suggèrent que GO-G25 et GO-G50 ont présenté une attaque nucléophile de la glycine par des réactions d'ouverture de cycle. Notamment, les résultats infrarouge des échantillons GO-100, GO-150 et GO-150 présentaient les bandes de groupes époxydes (à 969 cm^{-1}) moins intenses par rapport à l'OG, ainsi qu'une légère augmentation de la bande à 1048 cm^{-1} associée à des groupes hydroxyles.

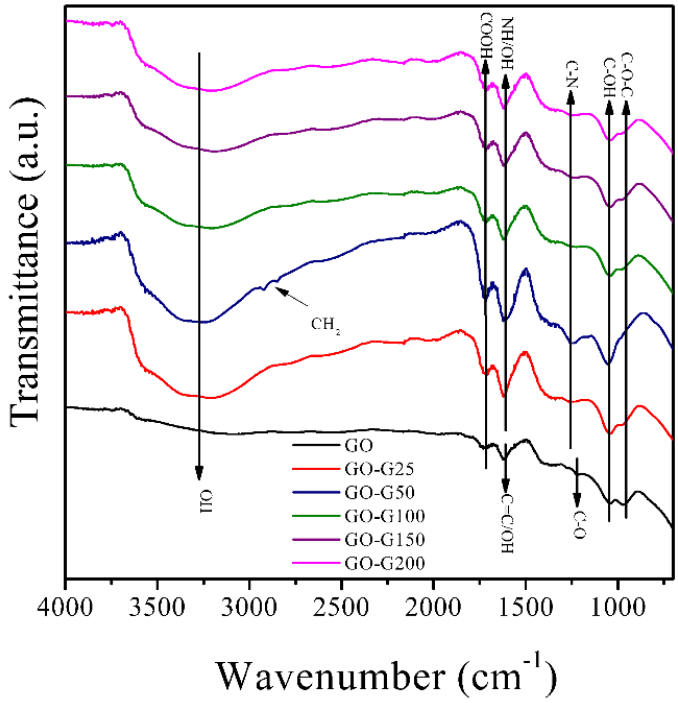

Figure 2.2 Caractérisation des échantillons GO et GO-G par ATR-FTIR.

La caractérisation par spectroscopie Raman a permis de confirmer la présence de groupements glycine dans les échantillons GO-G25 et GO-G50, car ceux-ci présentaient un rétrogradage en bande G de 5 cm^{-1} et 13 cm^{-1}, respectivement (voir Figure 2.3). Ce comportement est attribué à un dopage de type N dû à des molécules à N atomes proches de l'OG.[31] Les échantillons GO-G100, GO-G150 et GO-G200 de la bande G ont présenté un décalage vers le haut car moins de glycine était liée et les groupes fonctionnels oxygène

[30] Bose, S.; et al. *J. Mater. Chem*. 2012, 22, 9696

[31] Liu, H. et al. *J. Mater. Chem.* 2011, 21, 3335–3345

prédominants sont dans ces matériaux, comme on peut le voir sur la figure 2.3.[31] Ces informations et les résultats infrarouge indiquent que sous une faible concentration en glycine une fonctionnalisation a eu lieu, une réduction de l'OG a été observée.

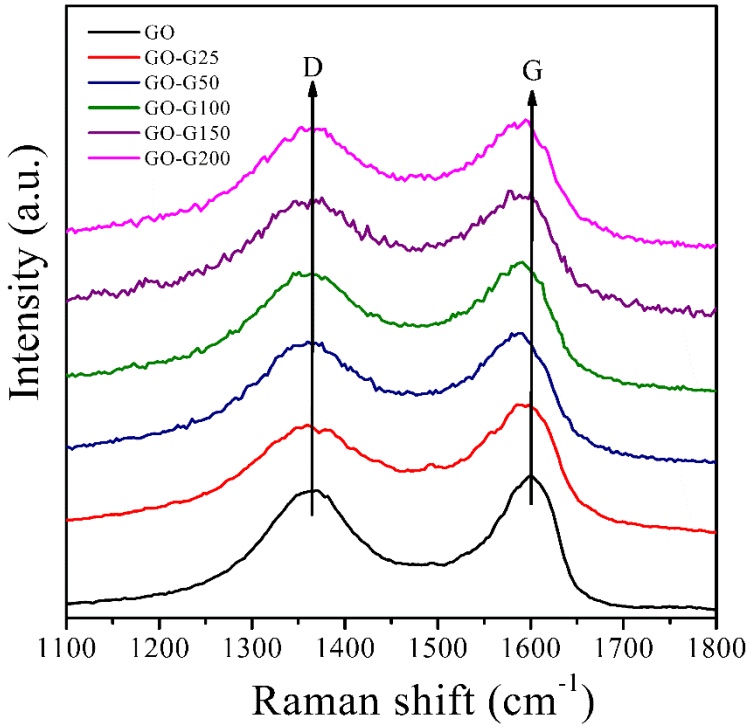

Figure 2.3 Caractérisation des échantillons GO et GO-G par spectroscopie Raman.

Une déconvolution C1s XPS haute résolution a été réalisée pour les échantillons GO et GO-G (Figure 2.4). Dans le cas des échantillons GO-G, il a été possible d'observer un pic à 285,2 eV, qui peut être attribué aux espèces C-N et C-OH.[32] D'après les résultats infrarouge, de faibles concentrations de glycine ont conduit une attaque nucléophile sur les groupes époxyde de l'OG et se traduisant également par l'apparition du pic à 285,2 eV caractéristique des liaisons N-C (voir figures 2.4b et 2.4c).[30] De plus, les échantillons GO-G100, GO-G150 et GO-G200, il a été observé un pic autour de 285,4 eV (voir les figures 2.4d, 2.4e et 2.4f). Cela peut s'expliquer par le fait que les époxydes sont partiellement transformés en alcools à cause du milieu basique et ainsi, le pic à 285,5 eV peut être attribué à des liaisons C-OH au lieu de C-N.[33]

[32] Huang, Q.; et al. *ACS Appl. Mater. Interfaces* 2014, 6, 13502–13509
[33] Taniguchi, et al. *Carbon N. Y.* 2015, 84, 560–566

Sur la figure 2.4, il est possible d'observer que les contributions C = O ont augmenté pour les échantillons GO-G100, GO-G150 et GO-G200. Le groupe C = O provient des groupes aldéhydes, cétones et acides carboxyliques. Pour observer plus de détails sur le changement de la proportion de C = O et O-C = O, l'aire des pics C = O à O-C = O a été calculée et les résultats sont présentés dans le tableau 2.1. Comme on peut le voir dans le tableau 2.1, l'échantillon GO-G50 présente le rapport O-C = O / C = O le plus fort par rapport à tous les échantillons en raison de la présence de glycine liée de manière covalente. De plus, les échantillons GO-G150 et GO-G200 ont montré une tendance à diminuer le rapport O-C = O / C = O. Cette information suggère que dans un milieu basique et des rapports massiques OG : G de 1 : 1, la réduction de l'OG pourrait être régie par la réduction des acides carboxyliques en carbonyles. Cela pourrait être la première étape de tout le mécanisme de réduction de l'OG en présence de glycine, puisque les rapports C / O obtenus dans ce travail sont de l'ordre de 2,4 à 3,2, donc loin des valeurs de 10 obtenues dans les études précédentes.[30]

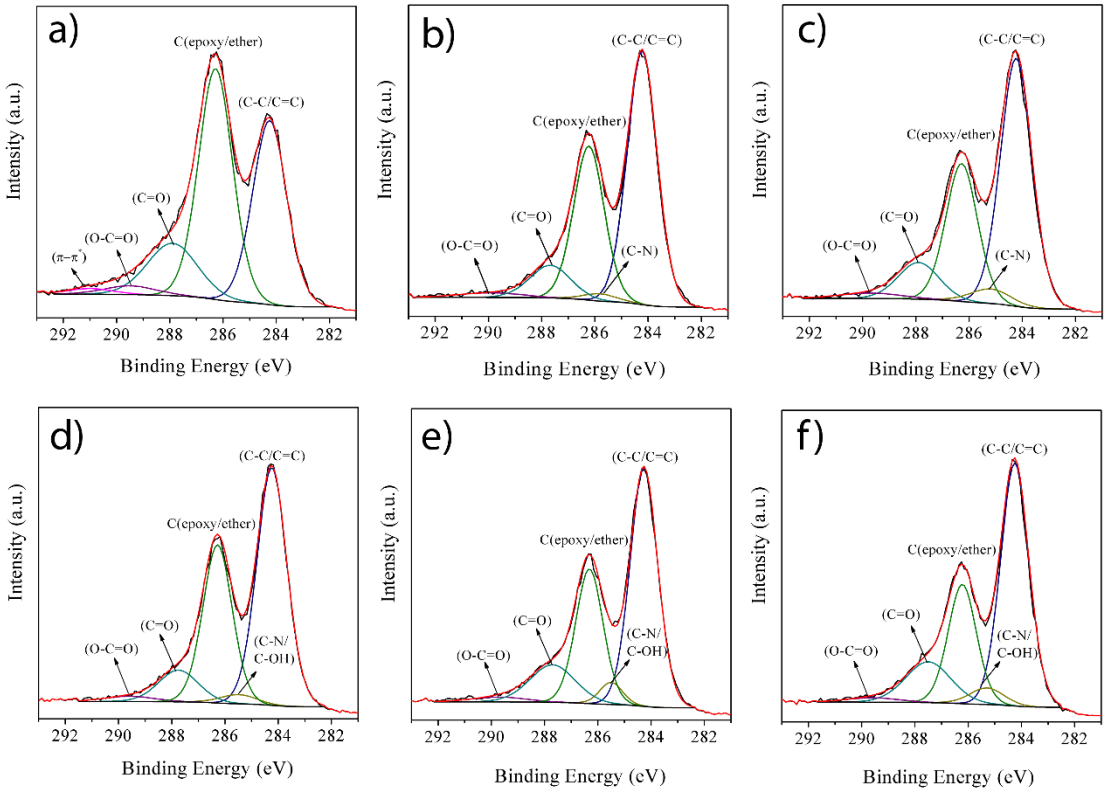

Figure 2.4 Déconvolution C1s XPS haute résolution pour les échantillons: a) GO, b) GO-G25, c) GO-G50, d) GO-G100, e) GO-G150 and f) GO-G200

Tableau 2.1 Rapport de surface de pic des liaisons O-C = O aux liaisons C = O dans les échantillons GO et GO-C

	Échantillons					
	GO	GO-G25	GO-G50	GO-G100	GO-G150	GO-G200
O-C=O/C=O	0.174	0.203	0.228	0.209	0.153	0.124

Conclusions

Une étude systématique des conditions dans lesquelles la glycine peut agir comme nucléophile ou comme agent réducteur a été menée. Il a été constaté que de faibles concentrations de glycine conduisaient à une attaque nucléophile sur les groupes époxyde de l'OG. Dans ces conditions, les acides carboxyliques de l'OG ont été préservés grâce à la présence de NaOH qui produit des carboxylates sur l'OG. Par conséquent, il était possible d'avoir une fonctionnalisation covalente sur l'OG en conservant les acides carboxyliques des OG pour une seconde fonctionnalisation. Ceci représente un avantage pour la double fonctionnalisation dans des sites spécifiques conduisant à un meilleur contrôle de la chimie des OG. De plus, lorsque la concentration de glycine a été augmentée, un processus de réduction a été observé au lieu d'une fonctionnalisation. Lorsque la réduction a eu lieu, le mécanisme était régi par l'hydrolyse partielle des groupes époxyde et la réduction des acides carboxyliques en carbonyles. Cela pourrait être la première étape de tout le mécanisme de réduction de l'OG lorsque la glycine est utilisée.

CHAPITRE 3

FONCTIONNALISATION PHOTOCHIMIQUE DE L'OXIDE GRAPHÈNE PAR THIOL-ENE CLICK CHEMISTRY

Ce chapitre se concentre sur le développement de nouvelles approches pour la fonctionnalisation des OG, en utilisant la réaction thiol-ène (RTE) comme un outil pour coupler cystéamine (CA) aux insaturations de l'OG. La RTE peut être obtenu en utilisant un générateur de radicaux (réaction de thiol-ène radicalaire, RTER). Pour cela, un photoinitiateur (PI) a été utilisé sous rayonnement UV pour favoriser la formation de R-S$^{\bullet}$ et la fonctionnalisation ultérieure entre le OG et la CA. Cette fonctionnalisation apporte une réaction rapide et sélective dans des conditions douces, évitant une réduction de l'OG et ouvrant la possibilité de développer des matériaux à double fonctionnalisation dans un second temps.

La fonctionnalisation de l'OG par RTER a été réalisée en utilisant 2-Benzyl-2-(dimethylamino)-4′-morpholinobutyrophenone pour favoriser la fonctionnalisation photochimique et en ajoutant simultanément la cystéamine comme molécule modèle (CA). Les trois solutions ont été mélangées dans un bêcher et placées à l'intérieur de la chambre UV (360 nm) pendant 60 min, sous agitation (GO-CA-PI). Afin d'analyser l'impact du PI lors de la fonctionnalisation, deux expériences supplémentaires ont été réalisées : i) sans ajout de PI mais en exposant le mélange réactionnel à la lumière UV pendant 60 min (GO-CA) et ii) sans ajout de PI et en réalisant la réaction à l'obscurité et sous agitation (GO-B). Ces expériences constituent des contrôles afin de suivre les impacts respectifs du rayonnement UV et PI sur l'OG.

Résultats

Une caractérisation par spectroscopie UV-Vis a été réalisée et GO-CA-PI a montré un décalage vers le rouge dans le pic large attribué au plasmon C = C (marqué comme π-π*) jusqu'à 250 nm, par rapport à l'GO (voir Figure 3.1a). Le changement de la position maximale du pic C = C peut être attribué aux chaînes alkyles de CA, qui peuvent interagir avec le domaine

graphitique GO conduisant à un décalage vers le rouge, comme rapporté ailleurs.[34] Par ailleurs, GO-B a conservé la position du pic à 228 nm confirmant qu'il n'y avait pas de réaction entre l'OG et le CA dans l'obscurité par RTE.

La caractérisation par spectroscopie Raman a confirmé la fonctionnalisation par RTE puisque l'échantillon GO-CA-PI présentait un décalage vers le bleu dans la bande *G*, alors que les expériences à blanc (GO-CA et GO-B) ne présentaient aucun changement significatif (Figure 3.1b). Le décalage vers le bleu peut être attribué à la présence de groupes amine des CA sur l'OG qui produit un dopage de type N.[31]

Après la fonctionnalisation, l'amine primaire libre résultant du greffage de CA sur l'OG peut être détectée par marquage par fluorescamine et suivi par fluorescence (Figure 3.1c). L'échantillon GO-CA-PI a présenté le signal de fluorescence le plus fort, suivi par les échantillons GO-CA> GO-B> GO. La séquence de l'intensité de fluorescence retrouvée dans les différents échantillons suivait le même ordre que les résultats de spectroscopie UV-vis et Raman, confirmant la fonctionnalisation photochimique de OG avec CA par RTER.

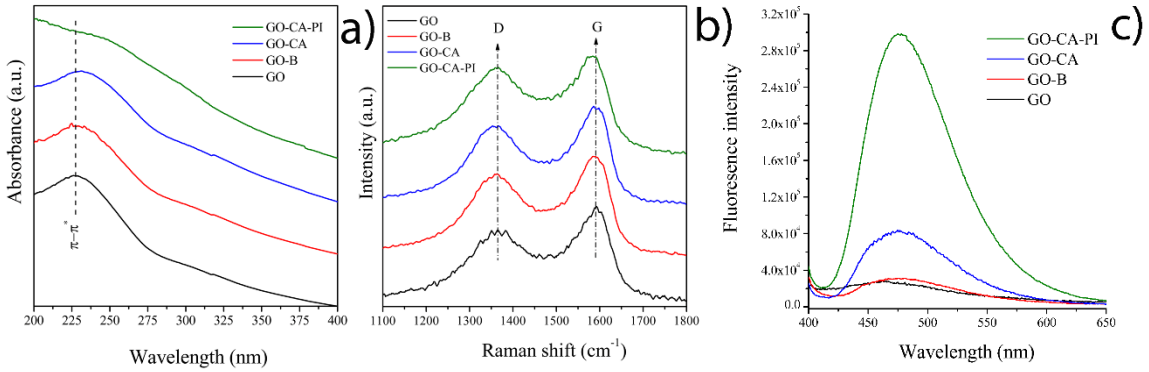

Figure 3.1 Caractérisation des échantillons GO, GO-B, GO-CA et GO-CA-PI par : a) spectroscopie UV, b) spectroscopie Raman et b) spectrométrie de fluorescence (λ_{ex} = 390 nm).

Enfin, la déconvolution XPS haute résolution S2p a été réalisée pour confirmer les liaisons chimiques formées après la fonctionnalisation. Dans la figure 3.2, GO-CA et GO-CA-PI ont été observés les pics à 163,5 eV et 164,8 eV, attribué à $S2p^{3/2}$ et $S2p^{1/2}$ en raison de la présence des liaisons C-S-C et C-S.[35] Ces informations confirment que CA a été lié de manière covalente à l'OG par RTE à l'aide du PI. Il faut souligner que cette fonctionnalisation a été

[34] Li, J.; et al. *Compos. Part A Appl. Sci. Manuf.* 2017, 101, 115–122.
[35] Peng, Z.; et al. *Colloids Surfaces A* 2017, 533, 48–54.

réalisée en une heure seulement de réaction, alors que l'initiateur thermique classique nécessite plus de 12 h de réaction.[36]

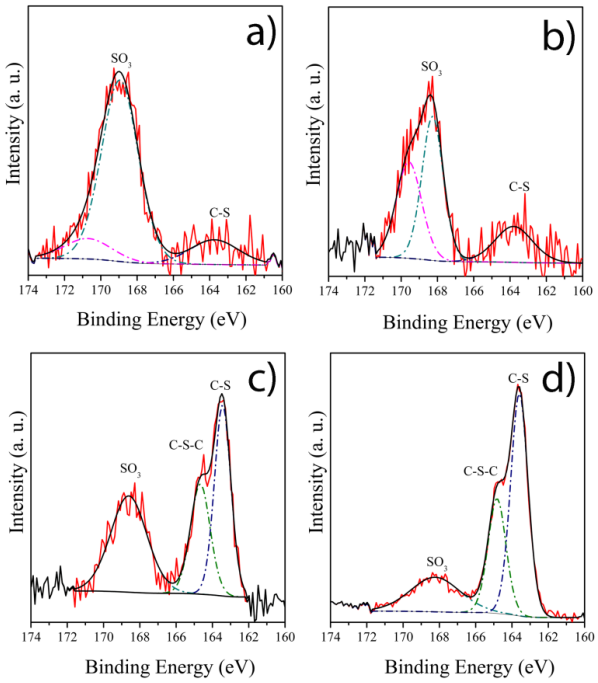

Figure 3.2 Déconvolution S2p des spectres XPS haute résolution de : a) GO, b) GO-B, c) GO-CA et d) GO-CA-PI.

Conclusions

Dans le présent chapitre, la fonctionnalisation photochimique de l'oxyde de graphène avec la cystéamine a été discutée, couplée via un PI comme initiateur de radicaux. La caractérisation par ATR-FTIR, spectroscopie UV-vis, marquage fluorescent, spectroscopie XPS et Raman a confirmé l'efficacité de la fonctionnalisation de l'OG tout en évitant la réduction de l'OG. Par conséquent, la RTER peut être considéré comme une réaction orthogonale pour la fonctionnalisation de l'OG. Cette réaction possède plusieurs avantages par rapport à l'initiateur thermique comme l'AIBN tels qu'un rendement élevé obtenu en un temps de réaction court, des réactions secondaires minimales et une réduction de OG peuvent être minimisées en raison des conditions de réaction douces utilisées (pas de chauffage). Enfin, la fluorescamine peut être utilisée pour quantifier les fragments CA liés à l'OG.

[36] Yap, P. L.; et al. *ACS Appl. Mater. Interfaces* 2018, 11 (6), 6350–6362.

CHAPITRE 4

OXYDE GRAPHÈNE ET FONCTIONNALISATION CHIMIQUE PAR THIOL-ÈNE POUR l'ADDITION DE MICHAEL

Dans le chapitre 3, il a été montré que la réaction thiol-ène (RTE) peut être appliqué en ajoutant des photoinitiateurs radicalaires (RTER). Cette méthode offre des avantages importants tels que des temps de réaction rapides dans des conditions douces. Cependant, la RTE peut également être réalisée en ajoutant des catalyseurs basiques conduisant à la réaction de couplage entre les thiols et les groupes alcène. Cette réaction est également connu sous le nom de réaction de thiol-ène par addition de Michael (AM) à la différence que la fonctionnalisation se déroule sur des systèmes α,β-insaturés de l'OG. Ce chapitre illustre d'un point de vue qualitatif et quantitatif la fonctionnalisation de OG avec (cystéamine) CA par l'AM en utilisant différentes bases. Cette voie de fonctionnalisation de l'OG apporte une autre alternative pour lier sélectivement des thiols sur les acides α,β-insaturés de l'OG.

La figure 4.1a montre RTER qui est une réaction puissante et orthogonale pour coupler des thiols avec une grande variété de systèmes insaturés. En variante, un catalyseur basique peut être utilisé pour la thiolation d'acides α,β-insaturés (figure 4.1b). L'anion thiolate qui est un nucléophile puissant qui peut attaquer les groupes alcène (Figure 4.1b, **1**) mais également l'époxyde (Figure 4.1b, **2**) de OG. Puisque les molécules de CA ont un groupe amine primaire, des réactions d'ouverture du cycle époxyde peuvent également se produire (figures 4.1b, **3**). L'OG peut être également thermiquement réduit (oxyde de graphène réduit, OGR) pour éliminer les groupes époxyde qui sont susceptibles d'être attaqués par les anions thiolate. Ainsi l'OGR produit peut être fonctionnalisé avec CA en utilisant une base pour catalyser la réaction d'AM (Figure 4.1c, **4**).

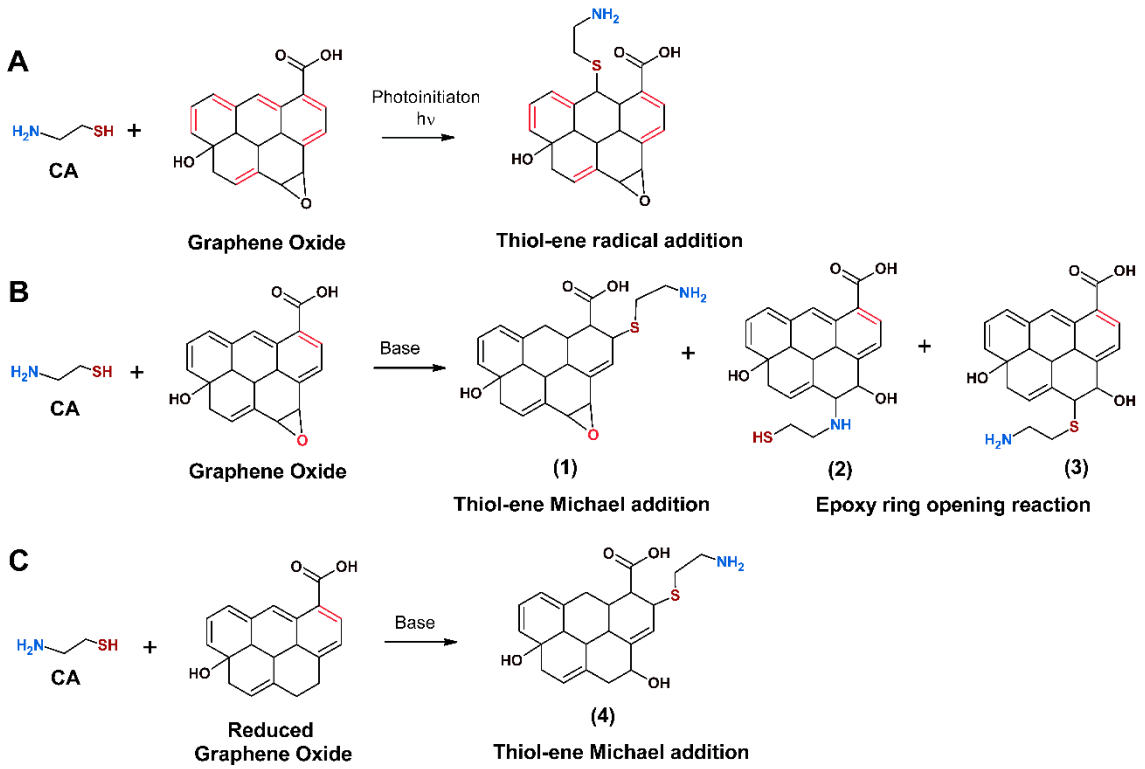

Figure 4.1 a) Fonctionnalisation de l'OG avec la CA par RTER, b) Fonctionnalisation de l'OG avec la CA en utilisant une base ; trois produits peuvent être obtenus via l'AM 1, la RTER par SH, 2 et la réaction d'ouverture du cycle époxy par NH_2, 3. c) Fonctionnalisation de l'OGR avec la CA par l'AM pour produire 4**.**

La fonctionnalisation de l'OG avec la CA par l'AM a été réalisée en utilisant la dispersion de l'OG dans le DMF puis en ajoutant simultanément laCA et le catalyseur de base. Les bases testées pour la fonctionnalisation chimique étaient la *N,N*-diisopropyléthylamine (DIPEA, GO-DIPEA), la triéthylamine (NEt_3, GO-NEt_3) et le 1,8-diazabicyclo [5.4.0] undéc-7-ène (DBU, GO-DBU). Une étude systématique de la fonctionnalisation entre l'OGR et la CA a été réalisée (RGO-DIPEA, RGO-NEt_3, RGO-DBU). La réaction entre l'OGR et laCA a été réalisée dans les mêmes conditions que la fonctionnalisation à l'aide de l'OG.

Le chapitre 3 a introduit la fluorescamine pour marquer sélectivement l'amine primaire des CA liées à l'OG. Cette méthode offre des avantages tels qu'un temps court pour l'analyse et la détection sélective des amines primaires. Grâce à la fluorescamine, il est possible de répondre à une question importante : lorsqu'une fonctionnalisation est effectuée, combien de molécules peuvent être liées à l'OG ?

Résultats

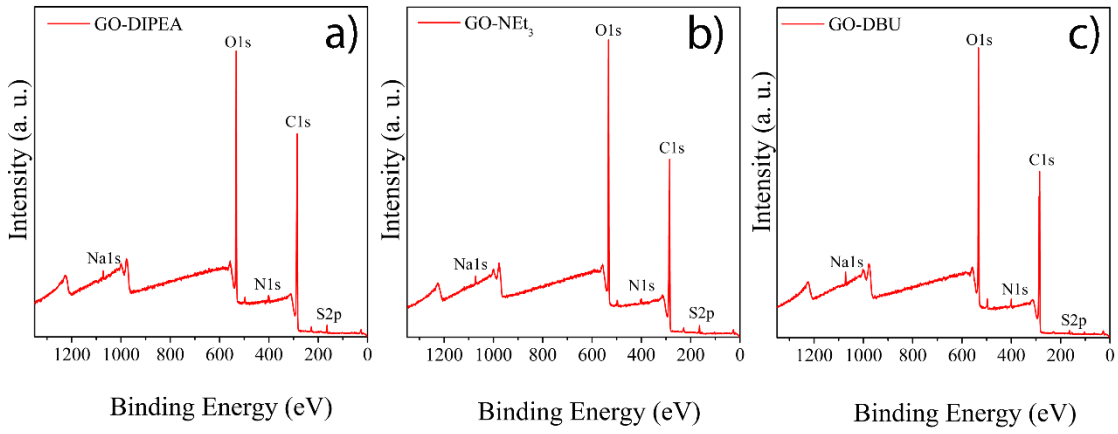

Figure 4.2 Sondage XPS des échantillons : a) GO-DIPEA, b) GO-NEt_3 et c) GO-DBU.

La fonctionnalisation de l'OG avec la CA a été confirmée par caractérisation XPS. Sur la figure 4.2, les trois matériaux (GO-DIPEA, GO-NEt_3 et GO-DBU) ont présenté des contributions atomiques d'azote (N) et de soufre (S) confirmant la liaison de la CA à l'OG via l'AM ou la ROCE.

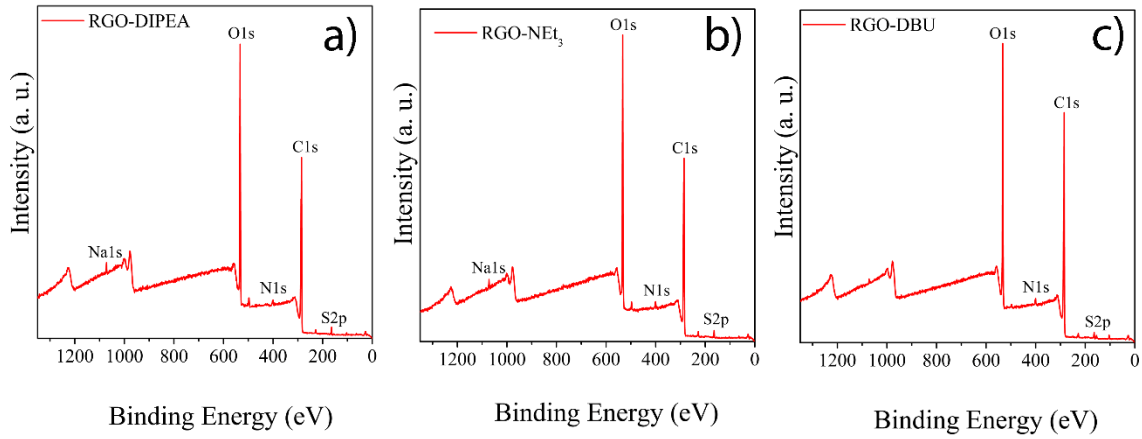

Figure 4.3 Sondage XPS des échantillons : a) RGO-DIPEA, b) RGO-NEt_3 et c) RGO-DBU.

De la même manière, la fonctionnalisation de l'OGR avec la CA en présence de bases a présenté des contributions atomiques S et N, associées à des groupements CA liés à l'OGR (voir Figure 4.3). Cette information confirme que malgré l'élimination de l'époxyde, la fonctionnalisation de l'OGR a été réalisée par l'anion thiolate formé par suite de l'ajout de la base.

Les molécules de CA ont été estimées par un marquage fluorescent. La fluorescamine a été utilisée pour le marquage et la quantification des groupements CA liés à l'OG, et ce composé

réagit spécifiquement avec les groupements amine primaire (-NH_2) pour former un adduit fortement fluorescent.[37] La figure 4a montre les résultats des titrages et met en évidence que, l'ordre de la fonctionnalisation était GO-DIPEA> GO-NEt_3> GO-DBU. De plus, une courbe d'étalonnage a été construite à λ_{em} = 475 pour quantifier les groupements de CA liés à l'OG (voir Figure 4.4b). La quantification a été effectuée en prenant l'intensité de fluorescence à λ_{em} = 475 nm de la figure 4.4a et en la plaçant dans la courbe d'étalonnage (figure 4.4b). Les résultats figurent dans le tableau 4.1. Remarquablement, la concentration de CA trouvée dans les OG fonctionnalisés est dans un ordre de grandeur similaire à celui des groupes fonctionnels de l'OG, tels que les groupes hydroxyles et acide carboxyliques.[38] Ces informations confirment qu'une grande quantité de CA peut être liée par l'AM.

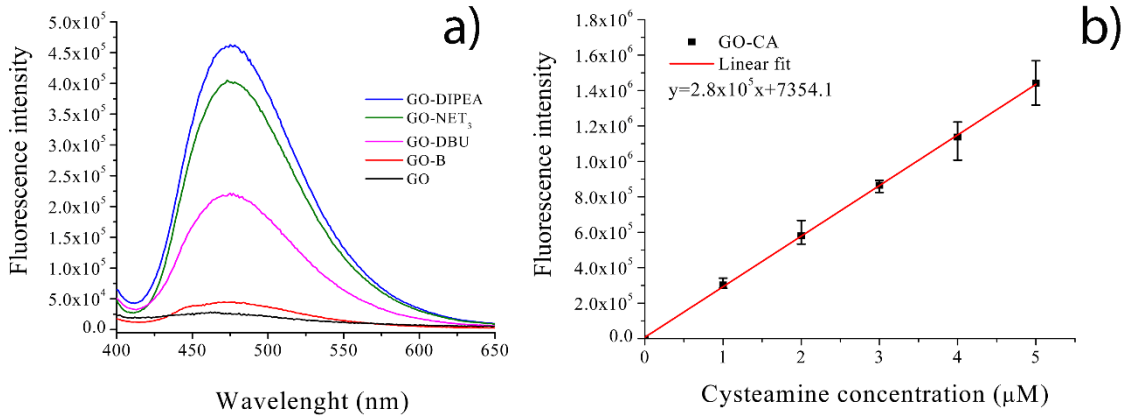

Figure 4.4 a) Titrages de fluorescence des fragments CA sur les matériaux fonctionnalisés d'OG (λ_{ex} = 390 nm) et b) courbe d'étalonnage pour la quantification des fragments CA liés.

Tableau 4.1 Résumé du marquage fluorescent et de l'enquête XPS pour l'estimation des fractions CA sur les échantillons d'OG (n = 3)

Échantillon	Molécules CA / mg de GO
GO-DIPEA	$7.7x10^{16}$
GO-NEt_3	$6.6x10^{16}$
GO-DBU	$3.6x10^{16}$

Conclusions

Ici, il a été systématiquement étudié la fonctionnalisation d'OG et d'OGR avec la CA par l'AM en utilisant différentes bases. Les résultats XPS ont permis de confirmer la

[37] Muz, M.; et al. *Chemosphere* 2017, 166, 300–310

[38] Eng, A.Y.S.; Chua, C.K.; Pumera, M. *Nanoscale* 2015, 7, 20256–20266

fonctionnalisation de l'OG et de l'OGR avec la CA. Malgré la réduction thermique de l'OG, la fonctionnalisation avec laCA a été possible confirmant la réaction de couplage entre les thiols avec les acides α,β-insaturés de l'OG. Le marquage fluorescent à l'aide de fluorescamine a permis d'estimer le nombre de molécules CA liées à l'OG. La concentration de la CA trouvée était d'environ 10^{16} molécules de CA liées par mg d'OG. Cette étude apporte un éclairage sur la fonctionnalisation de l'OG par des réactions thiol-ène et, ouvre l'opportunité de tirer parti du système insaturé de l'OG pour la fonctionnalisation dans des conditions douces et en préservant la chimie et la structure de l'OG.

CHAPITRE 5

QUANTIFIER LES GROUPES FONCTIONNELS D'OXIDE GRAPHÈNE PAR ÉTIQUETAGE FLUORESCENT

Dans les chapitres précédents, les réactions sélectives de la fonctionnalisation d'OG ont été illustrées en explorant les réactions d'ouverture de cycle sans altérer les acides carboxyliques et, la RTE pour la fonctionnalisation chimique des groupes alcènes qui restent après l'oxydation graphitique. Le chapitre 4 a notamment permis de répondre à une question importante : combien de molécules peuvent être liées aux époxydes et aux acides α, β-insaturés de l'OG ? Pour répondre à cette question, une approche nouvelle et simple a consisté à utiliser la fluorescamine pour quantifier le nombre de molécules cystéamine (CA) liées à l'OG après la réaction. Par conséquent, dans ce chapitre, il est proposé la quantification de différents groupes fonctionnels des OG en tirant parti de la méthode de marquage fluorescent proposée au chapitre 4 utilisant la fluorescamine. Cette étude se concentre sur trois groupes fonctionnels qui sont les groupes époxydes, acides carboxyliques et alcènes. Pour quantifier chaque groupe fonctionnel, une réaction dans les groupes fonctionnels spécifiques a été réalisée. Pour quantifier les époxydes, l'OG a été mis à réagir avec la *N*-Boc-éthylènediamine (NHBoc) par attaque nucléophile pour produire GO **1** (Figure 5.1a). Puisque les groupes époxydes sont susceptibles d'être attaqués par des nucléophiles, un OG thermiquement réduit (OGR) a été utilisé pour la quantification des acides carboxyliques et alcènes. Pour quantifier les acides carboxyliques, OGR a été mis à réagir avec NHBoc en utilisant des agents de couplage pour produire RGO **1** (Figure 5.1b). Pour la quantification des groupes alcène, l'OGR a été mis à réagir avec la CA par RTER pour produire RGO **2** (Figure 5.1c). Enfin, l'amine primaire du NHBoc déprotégée et de la CA a été quantifiée à l'aide de fluorescamine.

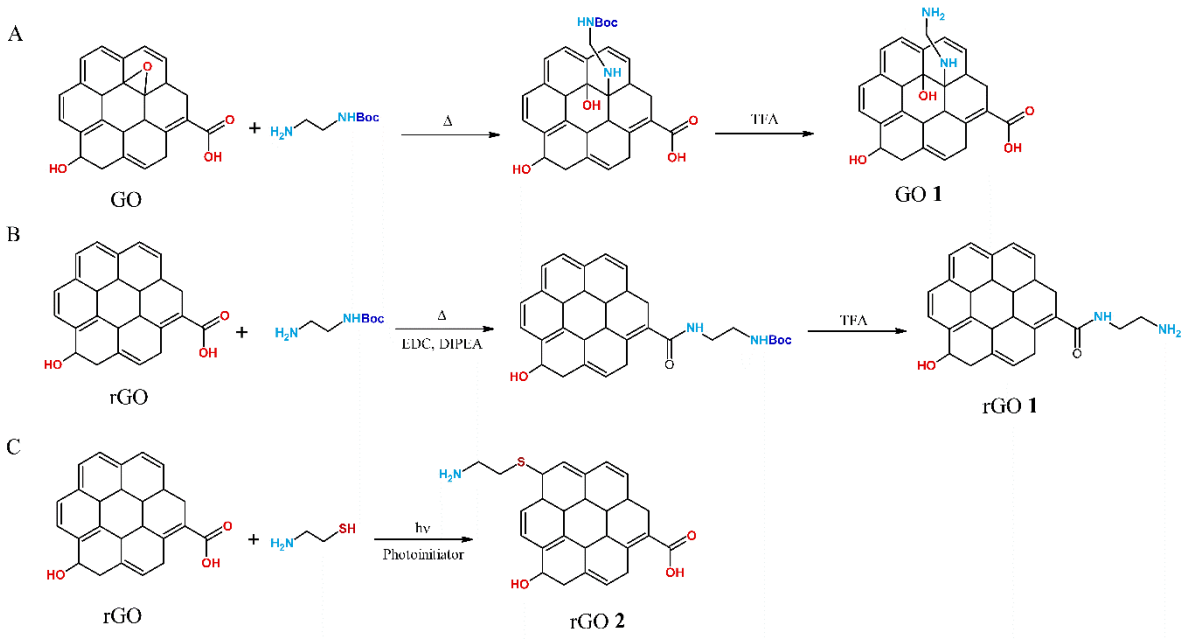

Figure 5.1 a) Fonctionnalisation d'OG avec BocDA pour produire GO **1**, b) réaction pour produire rGO **1** et c) production de rGO **2**

Résultats

La caractérisation XPS a été réalisée pour confirmer la fonctionnalisation chimique de GO **1**, RGO **1** et RGO **2**. Sur la figure 5.2, tous les matériaux fonctionnalisés ont montré une contribution atomique claire d'azote (N), alors que RGO **2** contient une contribution atomique supplémentaire de soufre (S).

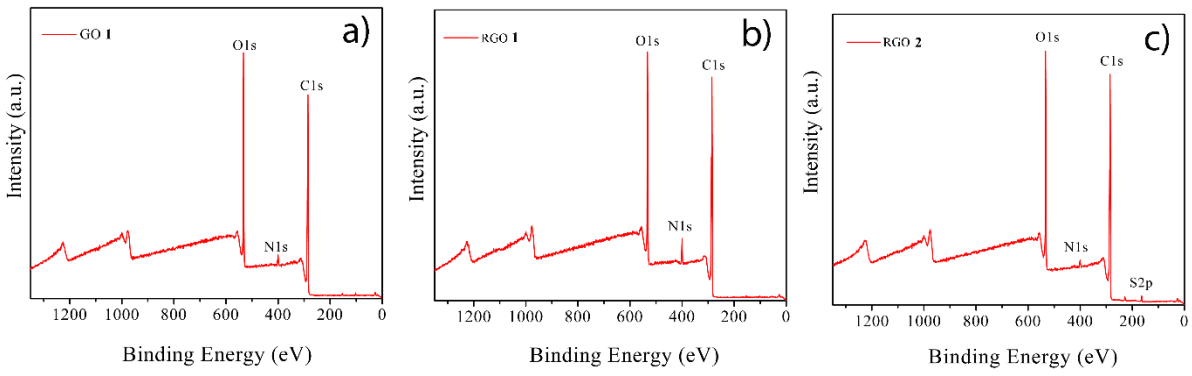

Figure 5.2 Enquête XPS de GO **1**, RGO **1** et RGO **2**.

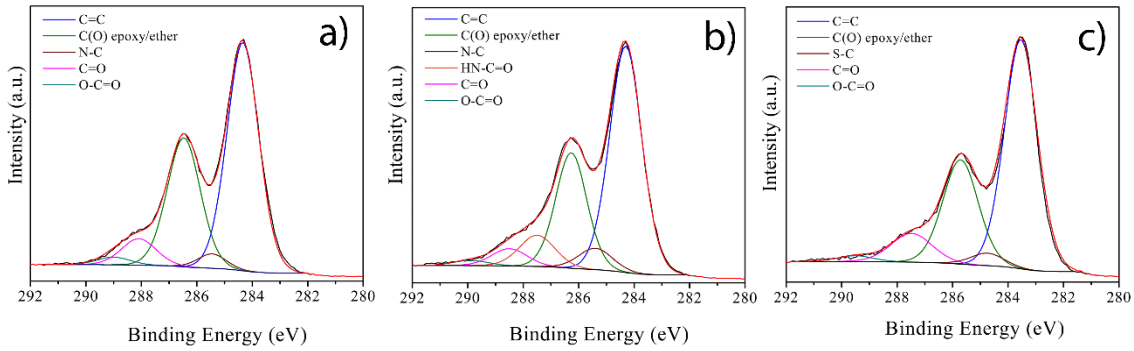

Figure 5.3 Déconvolution C1s haute résolution de : a) GO **1**, b) RGO **1** et c) RGO **2**.

La déconvolution XPS haute résolution C1s de GO **1**, RGO **1** et RGO **2** est présentée à la figure 5.3. Pour le matériau GO **1**, un pic à 285,4 eV a été observé et attribué aux liaisons N-C.[39] De plus, RGO **1** présentait deux pics supplémentaires à 285,4 eV et 287,5 eV, attribués à N-C et N-C = O des liaisons amide.[40]

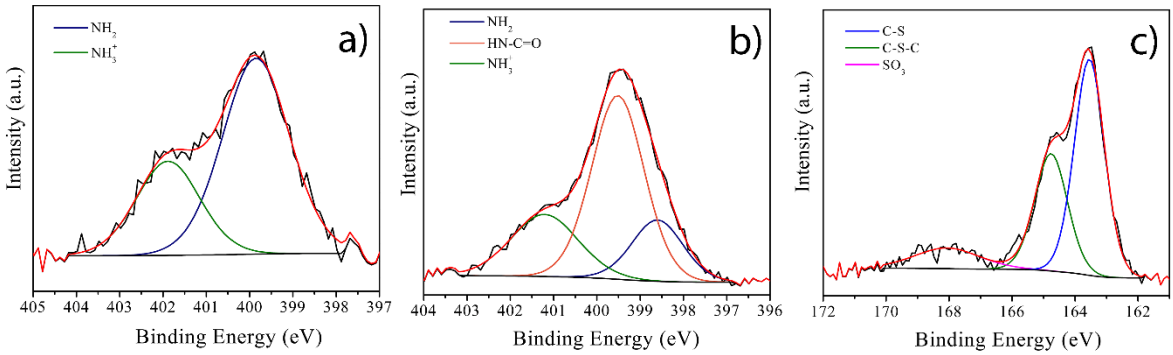

Figure 5.4 Déconvolution XPS haute résolution N1s de : a) GO **1** et b) RGO **1**. c) Déconvolution XPS haute résolution S2p de RGO **2**.

De plus, la déconvolution XPS haute résolution de N1 de GO **1** présentait deux pics à 399,8 eV et 401,8 eV attribués aux liaisons $-NH_2$ et $-NH_3^+$, en raison de la présence de NHBoc une fois déprotégé (voir Figure 5.4a).[39] De plus, pour RGO **1**, trois pics sont observés à 398,5 eV, 399,5 eV et 401,2 eV, associés respectivement à $-NH_2$, HN-C = O et $-NH_3^+$ (voir Figure 5.4b).[39] Ces informations confirment la fonctionnalisation sur l'époxyde et les acides carboxyliques dans les matériaux GO **1** et RGO **1**. Dans le cas de RGO **2**, la déconvolution C1s révèle un nouveau pic à 284,7 qui pourrait être associé à des liaisons C-S (voir Figure 5.7c). La

[39] Piñeiro-García, A.; et al. *Ind. Eng. Chem. Res.* 2020, 59, 13033–13041.
[40] Zhou, F.; et al. *J. Memb. Sci.* 2019, 573, 184–191.

déconvolution S2p de RGO **2** a confirmé la fonctionnalisation avec la CA, puisque les deux pics à 163,5 eV et 164,7 eV, attribué aux liaisons C-S et C-S-C ont été identifiés (voir figure 5.8c).[39] Ainsi, les analyses XPS ont permis de confirmer la fonctionnalisation chimique.

Après avoir confirmé le marquage sélectif sur les époxydes, les acides carboxyliques et les alcènes en utilisant soit le NHBoc ou la CA, la quantification à l'aide de fluorescamine a été réalisée. Les résultats présentés dans le tableau 5.1 montrent que les groupes alcène sont présents à de fortes concentrations, suivi des acides carboxyliques et des groupes époxyde. Dans cette étude, du graphite naturel de taille ~ 1 mm a été utilisé et étant donné les faibles dimensions du graphite initial, les bordures sont plus susceptibles d'être oxydées et ainsi, plus de groupes acides carboxyliques peuvent être générés.[41] Cependant, un mélange de H_2SO_4 / H_3PO_4 a été utilisé afin d'avoir une oxydation douce et donc d'introduire moins de défauts (tels que des lacunes) dans le réseau graphite comme rapporté ailleurs.[42] Cela pourrait expliquer la faible densité des acides carboxyliques et la concentration en groupes époxyde trouvée. Les groupes alcènes semblent être une option intéressante pour effectuer des modifications chimiques sur l'OG car la concentration en groupes alcènes est la plus élevée parmi les groupes fonctionnels quantifiés. L'origine de ce résultat pourrait être associée à l'efficacité de la RTE, qui est un outil puissant pour coupler les thiols à une grande diversité de systèmes insaturés.[43]

Tableau 5.1 Résumé des résultats de fluorescence et XPS pour l'estimation des groupes fonctionnels de GO (*n = 3*)

Groupe fonctionnel	Nombre de molécules estimé par marquage fluorescent
Acides carboxyliques	4.2×10^{16}
Alcènes	6.6×10^{16}
Époxydes	1.9×10^{16}

Conclusions

Il a été rapporté la quantification de l'époxyde, des acides carboxyliques et des groupes alcènes de l'OG *via* un marquage fluorescent. La concentration la plus élevée correspond aux groupes alcènes et cela est attribué à la grande quantité de défauts introduits dans le réseau graphitique lors de la réaction d'oxydation. Bien que les acides carboxyliques et les époxydes fonctionnalités aient été rapportées avec des concentrations plus élevées, le mélange de H_2SO_4 / H_3PO_4 et la taille du graphite utilisé pourraient expliquer la faible concentration observé. La

[41] Yan, L.; et al. *Chem. Soc. Rev*. 2012, 41, 97–114.

[42] Marcano, D.C.; et al. *ACS Nano* 2010, 4, 4806–4814.

[43] Hoyle, C.E.; Bowman, C.N. *Angew. Chemie - Int. Ed*. 2010, 49, 1540–1573.

structure et la composition chimique de l’OG dépendent fortement du graphite vierge, des réactifs oxydants, de la température et du temps d'oxydation. Par conséquent, la quantification des groupes fonctionnels de l’OG est une étape importante pour la bonne conception et la fonctionnalisation de l’OG pour des applications spécifiques.

CHAPITRE 6

DÉVELOPPER DES MATÉRIAUX D'OXIDE DE GRAPHÈNE MULTIFONCTIONNELS POUR LES APPLICATIONS ANTIBACTÉRIENNES

Dans les chapitres précédents, des approches alternatives pour fonctionnaliser le GO en utilisant des voies chimiques orthogonales et sélectives ont été proposées. En connaissant précisément la composition des feuilles d'OG, il est possible de proposer différentes stratégies chimiques pour développer des matériaux à base d'OG multi-fonctionnalisés et notamment antimicrobiens. Pour ce faire, l'OG a été fonctionnalisé en activant d'abord les époxydes et les acides carboxyliques avec de la 2-(diméthylamino)éthylamine (DMEN) puis, les alcènes ont été attaqués par le 2-(diméthylamino)éthanethiol (MEDA) (voir figure 6.1).

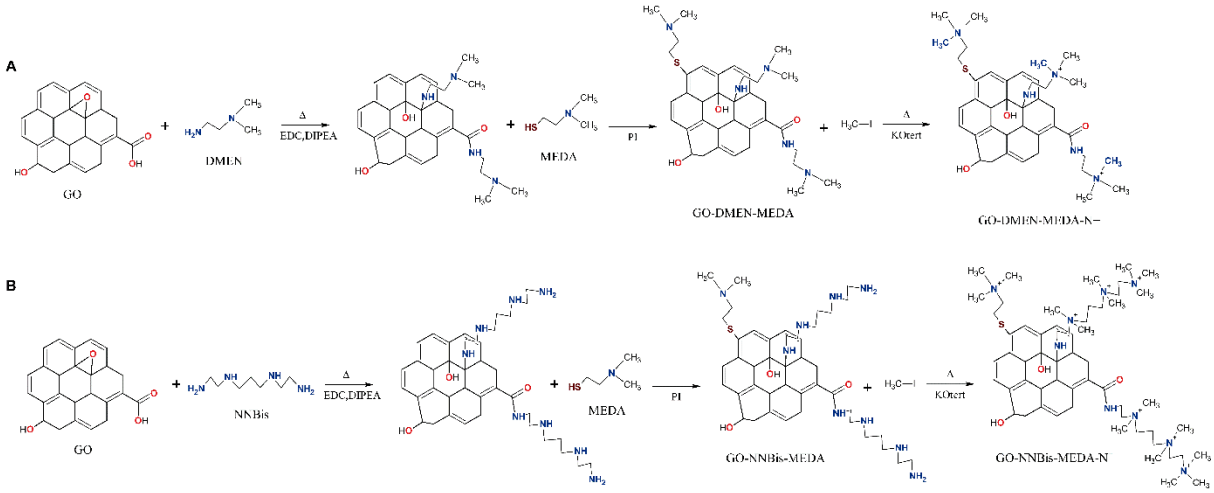

Figure 6.1 Voies chimiques pour la fonctionnalisation d'OG : a) première étape de fonctionnalisation avec DMEN suivie de MEDA et de quaternarisation et b) a) première étape de fonctionnalisation avec NNBis suivie de MEDA et de quaternarisation.

La figure 6.1 montre l'ensemble des réactions utilisées pour développer l'OG multi-fonctionnalisé antimicrobien. Grâce aux connaissances générées sur la réactivité de l'OG, il est possible de greffer différentes molécules, voire des molécules plus longues, pour augmenter la teneur en atomes d'azote à travers la surface de l'OG. Sur la figure 6.1b, le DMEN a été

remplacé par la *N,N′*-Bis (2-aminoéthyl)-1,3-propanediamine (NNBis) dans la première étape de la fonctionnalisation. Les NNBis peuvent attaquer les époxydes et les acides carboxyliques par réaction d'ouverture de cycle et formation de liaisons peptidiques, respectivement. Cette molécule plus longue contient plus d'azotes qui peuvent être quaternarisés ensuite conduisant à une surface chargée hautement positive sur les couches d'OG. Les charges positives générées sur la surface d'OG peuvent augmenter l'activité antibactérienne de l'OG.

Les matériaux produits dans ce chapitre sont illustrés à la figure 6.1 et ils ont été étiquetés comme GO-DMEN-MEDA-N^+ et GO-NNBis-MEDA-N^+. Ces matériaux ont été caractérisés par ATR-FTIR et l'activité antibactérienne a été évaluée chez *Escherichia coli* (*E. coli*), par la mesure de la bioluminescence des bactéries en présence des matériaux fonctionnalisés.

Pour suivre l'inhibition des bactéries nous avons choisi la bioluminescence en raison de sa sensibilité élevée. L'activité antibactérienne a été évaluée en utilisant la méthodologie présentée à la figure 6.3. Une concentration initiale de bactéries de 1 x 10^6 CFU / ml a été utilisée, puis une solution du matériau à base d'OG multi-fonctionnalisé positivement a été ajoutée. L'activité antibactérienne des matériaux a été testée à des concentrations de 0,05, 0,1 et 0,2 mg / ml et la luminescence a été mesurée comme une réponse à l'inhibition antibactérienne.

Résultats

La synthèse de matériaux à base d'OD multi-fonctionnalisés a été réalisée en utilisant les voies chimiques de la figure 6.2. Afin de vérifier l'introduction de nouvelles molécules dans les couches GO, une caractérisation ATR-FTIR a été réalisée. Après la fonctionnalisation chimique, GO-DMEN-MEDA-N^+ et GO-NNBis-MEDA-N^+ ont montré de nouvelles bandes à 1548 cm^{-1} et 1460 cm^{-1} attribuées aux liaisons N-C et N-H pour les vibrations en mode amide II,[44] tandis que les bandes des époxydes (1218 et 998 cm^{-1}) ont décru en raison de l'ouverture du cycle.[45] Simultanément, la bande des acides carboxyliques (1730 cm^{-1}) a été déplacée à 1710 cm^{-1}. Ces informations ont confirmé la formation de liaisons peptidiques et la formation d'amines secondaires dues à des réactions d'ouverture de cycle. Par conséquent, le GO a été fonctionnalisé avec succès avec les DMEN et NNBis. La deuxième étape de la

[44] Ouyang, et al. *Colloids Surfaces B Biointerfaces* 2013, 107, 107–114.
[45] Mungse, H.P.; Khatri, O.P. *J. Phys. Chem. C* 2014, 118, 14394–14402.

fonctionnalisation de l'OG a consisté à greffé le MEDA par addition de thiol-ène Michael (AM). Dans le cas de GO-DMEN-MEDA-N^+, il n'a pas été possible de détecter les liaisons C-S formées après la fonctionnalisation chimique. Cependant, GO-NNBis-MEDA-N^+ présentait des bandes mineures à 806 cm^{-1} et 762 cm^{-1} attribuées aux liaisons C-S.[46]

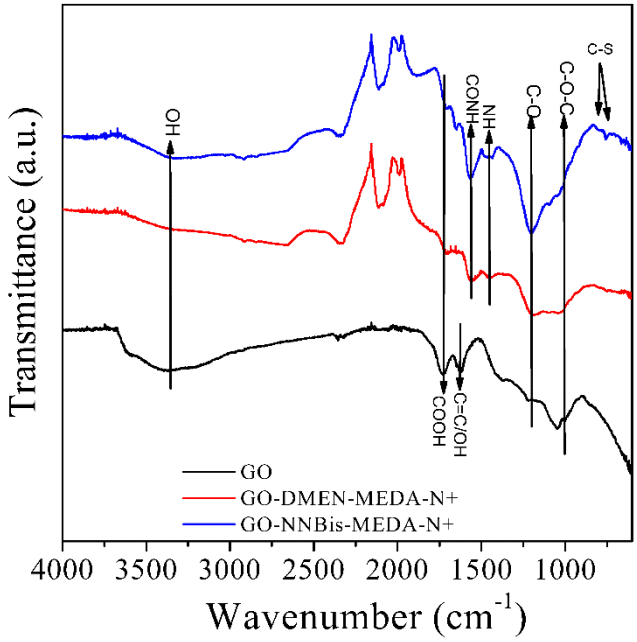

Figure 6.2 Caractérisation ATR-FTIR de GO, GO-DMEN-MEDA-N^+ et GO-NNBis-MEDA-N^+.

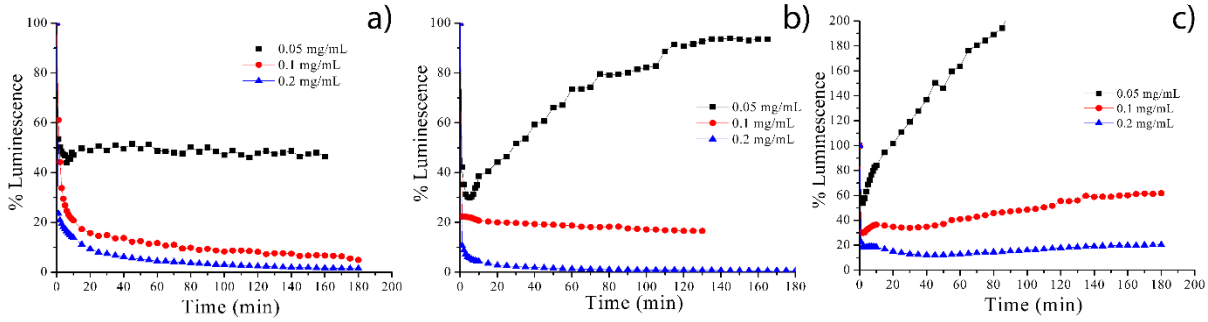

Figure 6.3 Luminescence characterization of: a) GO, b) GO-DMEN-MEDA-N^+ and c) GO-NNBis-MEDA-N^+.

L'activité antibactérienne des matériaux à base d'GO multi-fonctionnalisés a été évaluée chez *E. coli* par mesure de la bioluminescence (Figure 6.3). La bactérie *E. coli* MG1655 a été

[46] Li, J.; et al. *Compos. Part A Appl. Sci. Manuf.* 2017, 101, 115–122.

utilisée comme bactérie modèle en présence de GO, GO-DMEN-MEDA-N^+ et GO-NNBis-MEDA-N^+. La figure 6.3 montre les résultats de l'activité antibactérienne des trois matériaux à trois concentrations différentes. L'OG a montré un effet bactériostatique à des concentrations de 0,05 mg / mL car après 2 h, la réponse de luminescence était pratiquement constante. Lorsque la concentration de l'OG augmentait, une diminution de la réponse de luminescence était détectée. A partir d'une concentration de 0,1 mg / mL, 80% des bactéries ont été tuées après 15 min d'incubation. Dans le cas de GO-DMEN-MEDA-N^+ et GO-NNBis-MEDA-N^+, tous deux ont réduit la réponse de luminescence, mais ensuite, la luminescence a augmenté à nouveau lorsque des concentrations de 0,05 mg / mL ont été utilisées. Cependant, lorsque la concentration des matériaux a été augmentée, on a observé une diminution de la luminescence d'environ 80% après 1 h d'incubation. Le GO-DMEN-MEDA-N^+ a obtenu une réduction de 80% de la luminescence à 0,1 mg / mL de concentration en 20 min, tandis qu'une concentration de 0,2 mg / mL a produit une réduction de 95% de la luminescence dans les 10 premières min.

Conclusions

Il a été rapporté les premières tentatives de développement de matériaux d'oxyde de graphène multi-fonctionnalisés en utilisant les différents groupes fonctionnels de l'OG. Les époxydes, acides carboxyliques et alcènes de l'GO peuvent être fonctionnalisés par des voies chimiques orthogonales. Les résultats d'ATR-FTIR ont apporté une conclusion partielle sur la double fonctionnalisation réussie. Cependant, une caractérisation supplémentaire, en spectroscopie XPS et Raman spécifique, est nécessaire pour corroborer la fonctionnalisation. Le GO-DMEN-MEDA-N^+ a présenté une meilleure activité antibactérienne par rapport l'OG à des concentrations de 0,2 mg / mL. Cela pourrait être attribué aux charges positives générées après la fonctionnalisation chimique. Le matériau GO-NNBis-MEDA-N^+ n'a pas montré d'amélioration significative de l'activité antibactérienne. Cela pourrait être associé à une faible insertion de molécules NNBis sur les couches d'OG et au changement de morphologie des couches d'OG après la fonctionnalisation chimique.

RÉSUMÉ

L'oxyde de graphène (GO) est une nan ostructure de carbone qui a suscité un grand intérêt en raison de sa grande surface, sa polyvalence chimique mais aussi, GO présente des propriétés optiques, électriques et thermiques intéressantes. La fonctionnalisation chimique de GO est une étape critique pour développer des matériaux multi-fonctionnalisés pour une large gamme d'applications. Cependant, la chimie complexe et large de GO est un inconvénient lors de la fonctionnalisation, en raison la présence de différents groupes fonctionnels peuvent réagir simultanément, limitant les possibilités de multi-fonctionnaliser le GO. D'une manière générale, la fonctionnalisation GO a été réalisée sur des groupements époxyde et acide carboxylique car ils présents en forte ‘concentration’ dans les couches GO, et parce que la chimie des époxydes et acides carboxyliques est bien connue. Néanmoins, les deux groupes fonctionnels peuvent réagir simultanément en présence d’un nucléophile dans la réaction perdant leur orthogonalité lors de la fonctionnalisation. De man ière alternative, des groupes alcènes apparaissent dans le réseau graphitique pendant l'oxydation du graphite. La réactivité de ce dernier groupe fonctionnel a été étudiée mais avec l'inconvénient d'utiliser des conditions ‘dures’ conduisant à une réduction de GO. Le GO étant utilisé comme plate-forme pour une large gamme de molécules, il est nécessaire d'explorer la chimie du GO pour tirer pleinement parti de ses groupes fonctionnels. Par conséquent, différentes stratégies doivent être étudiées pour créer des matériaux à base d’oxyde de graphène multi-fonctionnalisés qui peuvent élargir la gamme d'applications possibles. Motivé par cette idée, cette thèse apporte un éclairage et une meilleure compréhension de la fonctionnalisation chimique de GO, en se concentrant sur les époxydes, les acides carboxyliques et les groupes alcènes. En explorant de nouvelles voies pour la fonctionnalisation GO, il serait possible de créer des matériaux GO avec une double fonctionnalisation qui peuvent améliorer ses performances pour une large gamme d'applications. Grâce aux voies chimiques générées dans cette thèse, nous avons développé les premières tentatives de nouveaux matériaux d'oxyde de graphène multi-fonctionnalisés contenant des charges positives pour améliorer l'activité antibactérienne du GO d'origine.

MOTS CLÉS

Chimie d l'oxyde de graphène, Fonctionnalisation, Matériaux hybrides, Matériaux synergiques, Matériaux antibactériennes

ABSTRACT

Graphene oxide (GO) is a carbon nanostructure that has attracted a great interest due to its great surface area, chemical versatility but also, GO exhibits interesting optical, electrical, and thermal properties. The chemical functionalization of GO is a critical step to develop multi-functionalized materials for a wide range of applications. However, the complex and wide chemistry of GO is a drawback during the functionalization, due to different functional groups can react simultaneously, wasting the possibility to multi-functionalize the GO. Generally, GO functionalization has been carried out on epoxide and carboxylic acid groups since they constitute the strongest concentration in GO layers, and because the chemistry of epoxides and carboxylic acids is well-known. Nonetheless, both functional groups can react simultaneously with a nucleophile in the reaction losing orthogonality during the functionalization. Alternatively, alkene groups arise in the graphitic lattice leading during the graphite oxidation. This last functional group has been tried to explore but with disadvantage of using extreme conditions leading to GO reduction. Since GO has been used as a platform for a wide range of molecules, it is necessary to explore the chemistry of the GO to take full advantage of its functional groups. Therefore, different strategies must be studied to create multi-functionalized graphene materials which can increase the range of possible applications. Motivated by this idea, this thesis brings insights and better understandings in the chemical functionalization of GO, focusing on the epoxides, carboxylic acids, and alkene groups. By exploring new pathways for the GO functionalization, it would be possible to create GO materials with dual functionalization that can improve its performance for a wide range of applications. Through the chemical routes generated in this thesis, it was developed the first attempts of novel multi-functionalized graphene oxide materials containing positive charges to improve the antibacterial performance of pristine GO.

KEYWORDS

Graphene oxide chemistry, Functionalization, Hybrid materials, Synergistic materials, antibacterial materials